2007

Investigation of the impact of environmental conditions on field welding of precast concrete connections

Jason Andrew Zimpfer
Lehigh University

Zimpfer, Jason Andrew

Investigation of the Impact of Environmental Conditions on Field Welding of...

September 2007

Investigation of the Impact of Environmental Conditions on Field Welding of Precast Concrete Connections

by

Jason Andrew Zimpfer

A Thesis

Presented to the Graduate and Research Committee

Of Lehigh University

In Candidacy for the Degree of

Master of Science

in

The Department of Civil and Environmental Engineering

Lehigh University

September 2007

This thesis is accepted and approved in partial fulfillment of the requirements for the Master of Science.

7/27/07

Date

Thesis Advisor

Co-Advisor

Co-Advisor

Chairperson of Department

Acknowledgements

The authors would like to acknowledge the Precast/Prestressed Concrete Institute (PCI) for financial and technical support of this project. The guidance provided by the PCI technical advisory committee members Tom D'Arcy (Chair), Michael Hudgins, Harry Gleich, Rick Martel, Greg Gibbons, Aaron Vnuk, Franc Genoese, Al Williams, and Anant Dabholkar is gratefully acknowledged. The advice and assistance given by the PCI Erectors Committee is also acknowledged. The authors would additionally like to express appreciation for material donations from High Concrete Structures, Inc. and Metromont Corporation. More specifically, appreciation is expressed to Karen Laptas and Cheryl Lantz of High Concrete and Harry Gleich of Metromont for their helpfulness in obtaining materials for the testing program.

Table of Contents

List of Tables

List of Figures

Abstract

This study investigated the impact of wind, humidity, temperature, and surface moisture conditions on the quality of field welding of precast concrete connections. The connections are typical of precast concrete construction and use the shielded metal arc welding (SMAW) process. The study focused on ASTM A36, Type 304 Stainless Steel, and ASTM A36 Galvanized steel plates. Weld surfaces and cross-sections were examined visually and with optical microscopy. The results of the inspections were compared to acceptable limits for various weld discontinuities in accordance with the AWS D1.1 and AWS D1.6 codes. In addition, strength tests were performed on some of the welded connections to assess the impact of environmental conditions on strength.

It was found from inspection of welds made under wind up to 35 mph, temperatures as low as -10°F [-23.3°C], and under wet conditions, that the SMAW process resulted in good quality welds. In general, acceptable welds were fabricated under the variety of environmental conditions examined. Various types of discontinuities were observed in the study and are presented, but the presence of the discontinuities observed in the experimental program was not found to cause a significant reduction in the transverse shear strength of the welds tested in the second phase of this study.

Based on the results presented in this report, 1/4-in. fillet welds made on 3/8-in. thick ASTM A36 and 3/16-in. welds made on type 304 stainless steel plate using E7018-H4R and E308-16 electrodes, respectively, can be performed under the following environmental conditions as long as the welder is able to create a weld meeting the AWS profile requirements:

- In wind up to 35MPH in the vicinity of the weld.
- In an ambient temperature of 0°F and above, without preheat.

- In high humidity conditions, up to 100% relative humidity.

SMAW electrodes should be stored, handled, and used in accordance with manufacturer guidelines and AWS D1.1 requirements. It is not recommended to perform welds when water from precipitation can enter the weld pool. It is recommended that galvanizing be removed in the area of welds made on galvanized plates, consistent with the American Galvanizers Association recommendations.

1 Project Overview

Erection of precast concrete structures requires welding to be performed in the field under a variety of wind, humidity, and temperature conditions. Current American Welding Society (AWS) specifications either restrict or are unclear about the conditions under which welds can be made in the field. A research program sponsored by the Precast/Prestressed Concrete Institute (PCI) was conducted to investigate the impacts of environmental conditions on the quality of field welded precast concrete connections.

The research program investigated the quality of welded connections made under various environmental conditions. Welds were made under a variety of temperature, humidity, and wind conditions simulating those conditions encountered in precast concrete construction. Three steel types used in precast construction, namely, ASTM A36, ASTM A36 Galvanized, and Type 304 Stainless Steel, were examined. The study focused on 1/4-in. fillet welds produced with the shielded metal arc welding (SMAW) process. The SMAW process is the most common field welding process used in precast construction.

The study used physical inspection (visual, microscopic) and destructive testing of the welded specimens. The inspection (Phase 1) evaluation was carried out to determine whether welds made under the given conditions were adequate in quality, using AWS D1.1 standards as an assessment guide. The destructive (Phase 2) testing was designed to confirm the adequacy, from a strength perspective, of welds made under base conditions (71°F, 35% RH, 0 mph wind) and other conditions which had the potential to cause defects in the welds. The influence of flaws observed during the inspection of Phase 2 specimens on weld strength was studied.

To assist in the development of the research program, an advisory committee was formed by PCI. The members of the committee represent engineers and precast concrete building erectors

familiar with the current state of the practice. In addition, two advisory meetings were held with the PCI Erectors Committee to provide additional guidance to the project scope.

This report is organized as follows. First, background on weld discontinuities, their cause, and the impact they have on the integrity of a weld is outlined. In addition, the potential link between environmental conditions and weld quality is examined through a literature survey. Then, the experimental program is presented in detail along with all the Phase 1 results. These results are presented in a standardized form to allow for direct comparison of test results from one environmental condition to another. A detailed discussion of the Phase 1 study is presented following the results. The Phase 2 research program, including test results and discussion, follows. The conclusions from these two phases are then presented, followed by recommendations.

2 Background on Weld Discontinuities

Adverse environmental conditions can affect the quality of structural steel welds made in the field. To date, however, no concise summary of the impact of adverse environmental conditions on the field welding of precast concrete connections has been made. The safety and reliability of precast construction and the efficiency and cost of erecting precast structures depends on high quality field welds made under various conditions.

The use of precast concrete construction techniques provides many benefits. Precast operations are often performed in an environmentally controlled facility which allows for year round production of building and bridge members of high quality. Speed of construction is increased since members can be prefabricated rather than cast on site. Erection of precast structures often requires welded joints between steel plates embedded in precast components. Often a few welds are made to provide stability to the component being erected. The remaining welds are performed at a later time to provide a full load path of adequate strength. Construction schedules often require that welds be made in adverse environmental conditions. Depending on the location of the construction site and the time of year, the environmental conditions can vary widely. Conditions across the country range from warm, dry, and calm conditions to -75°F temperatures in McGrath, Alaska[1], *average* annual humidity over 90%RH through several states[2], and *average* monthly wind speeds in excess of 15 mph in Dodge City, Kansas,[3] with gusts well in excess of the average in many parts of the country.

The present investigation focused on the effects of temperature, wind speed, humidity, and surface moisture (liquid water or ice on the steel plate surfaces) on simulated field welding. During the investigation, the exposure of welding electrodes to moisture before they were used was added as an additional environmental variable. The investigation focused on the most common field welding process, shielded metal arc welding (SMAW). SMAW, or "stick

welding" as it is commonly called, is known to produce sound welds under relatively poor environmental conditions. In this investigation, the welds were limited to ¼ in. fillet welds made in the flat, horizontal position, simulating the common field welded precast connection shown in Figure 2.1, which is a connection between a precast double tee and a precast inverted tee.

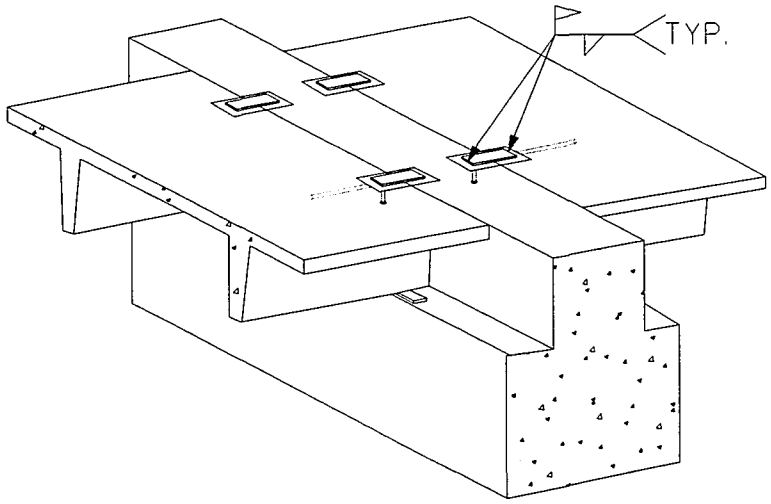

Figure 2.1: Typical Precast Connection Representative of Experimental Connection

2.1 Allowable Welding Conditions

A review of current codes was conducted to develop a matrix of test parameters. The primary code that was reviewed was the American Welding Society (AWS) structural welding codes: AWS D1.1/D1.1M:2006 *Structural Welding Code – Steel* and AWS D1.6:1999 *Structural Welding Code – Stainless Steel.* The AWS structural welding codes specify proper welding procedures which have been shown to lead to welds of sufficient quality and strength. When deviating from these pre-qualified procedures, a welding procedure specification, or WPS, is necessary to outline the procedure to be used. Further, a performance qualification record (PQR) is required to demonstrate that welds made with the procedure are sound metallurgically

and mechanically. The tests required to obtain approval of a WPS are outlined in the AWS structural welding codes, and these tests must be performed at an accredited AWS testing facility.

In order to make sounds welds, the AWS D1.1 code not only prescribes welding procedures but also outlines the allowable environmental conditions under which welds can be made. The D1.1 code provides a summary of unacceptable environmental conditions for welding in Section 5.12.2:

> "Welding shall not be done (1) when the ambient temperature (temperature in immediate vicinity of weld) is below 0°F [-20°C], or (2) when surfaces are wet or exposed to rain, snow, or (3) high wind velocities, or (4) when welding personnel are exposed to inclement conditions."[4]

In accordance with D1.1, preheat is required for ASTM A36 base metal with thickness between 1/8 inch and 3/4-in. welded with low-hydrogen electrodes using the SMAW process, when the base metal temperature is 32°F [0°C] or below. If the base metal temperature is below 32°F [0°C], the base metal must be preheated to at least 70°F [20°C].[4]

For conditions with high wind speeds, a suitable shelter must be used to protect the weld.[4] High wind speed is defined as 5 mph (8 km/h) for the GMAW, GTAW, EGW, and FCAW-G processes. These processes use a gas shield and thus require a low wind condition to maintain the shield. Since the SMAW process does not use a gas shield, a wind speed limit is not prescribed by AWS.

The AWS D1.6:1999 code for stainless steels similarly states that welding should not be performed on surfaces that are wet or in wind that would adversely effect the shielding

properties of the process being used in the welding procedure.[5] There is no quantification in the AWS D1.6 code regarding what wind speed would affect the shielding process.

The American Petroleum Institute (API) has similar environmental restrictions within its document, *Welded Steel Tanks for Oil Storage.*[6] With respect to wind, API does not allow field welds during periods of high wind unless the welder and weld are sheltered adequately. With respect to moisture, API forbids welding when surfaces are wet from any form of precipitation or when precipitation is falling. Lastly, with respect to temperature, API requires preheat if the ambient temperature is between 0°F [-18°C] and 32°F [0°C], and welding is forbidden if the temperature is below 0°F [-18°C].[6]

To summarize, current welding codes prohibit welding when the ambient temperature is under 0°F [-18°C] and permit welding, with preheating, between 0°F [-18°C] and 32°F [0°C]. Further, wind conditions are limited ambiguously for the SMAW process, which has no quantified maximum wind speed associated with it. Lastly, there are no restrictions on ambient moisture, but welding is prohibited when surfaces are wet. Table 2-1 is a summary of the restrictions on environmental conditions placed on field welding by the API, AWS D1.1, and AWS D1.6 codes.

Table 2-1: Summary of Restrictions on Environmental Conditions for Field Welding

Code	API	AWS D1.1	AWS D1.6
Wind	No field welding during periods of high wind unless shielded.	No welding under high wind sppeds; no wind speed limit stated for SMAW.	No welding in wind that would adversely impact shielding properties of weld.
Humidity/Moisture	No welding when surfaces are wet from precipitation or if precipitation is falling.	No welding when surfaces are wet, exposed to rain or snow.	No welding on wet surfaces.
Temperature	Preheat required if ambient temperature between 0°F and 32°F. No welding below 0°F.	Preheat required if base metal temperature below 32°F. No welding when ambient temperature is below 0°F.	No restriction listed; preheat must remove moisture from joint at a minimum.

2.2 Electrode Exposure

The exposure of standard carbon steel electrodes (E70XX) to ambient humidity is limited by AWS D1.1 to four hours outside of a hermetically sealed container or holding oven. Electrodes that have been wet are prohibited from use. AWS D1.1 also states that certain electrodes with the supplemental designation "R" (such as the E7018-H4R electrodes used in this study) have been approved for nine hours of exposure to the ambient environment[4], as reported in AWS A5.1.

AWS D1.6 states that electrodes for stainless steel welding using the SMAW process can be kept in hermetically sealed containers provided they are re-closed immediately after opening. Otherwise, the electrodes must be stored in a holding oven at 250°F [121°C] [5] (i.e. the same as required by D1.1). A maximum exposure time is not defined, perhaps because welds made on

austenitic stainless steels are not susceptible to hydrogen cracking caused by exposure of electrodes to moisture prior to welding.[16]

2.3 Welding Through Galvanization

Connection plates used in precast concrete elements are often galvanized to limit the potential for corrosion. In many cases, welding of these galvanized plates is needed to create a load path through the structural system. Welding through the galvanization is often requested by erectors to simplify construction.

Welding through a galvanized zinc coating requires the zinc coating to be melted and/or vaporized. The melting point of zinc, the primary component of galvanized coatings, is approximately 788°F [419.7°C], and the temperature at which zinc vaporizes is approximately 1665°F [907°C]. The melting point of steel is approximately 2500°F [1510°C], and the arc temperature in the SMAW process can be as hot as 10,500°F [5800°C]. As a result, it is possible that some of the zinc coating is vaporized as the arc approaches. It has been reported[7] that it is possible to weld through a galvanized coating without impacting weld strength.

The PCI Design Handbook states in Section 6.7.1.1 that, "Welding of hot-dip galvanized steel requires thorough removal of galvanizing material and following qualified welding procedures."[8] This PCI recommendation is based on the information provided in *The Procedure Handbook on Arc Welding*[9] and *Design and Typical Details of Connections for Precast and Prestressed Concrete.*[10] The Design Handbook further states that if the galvanizing material is not removed, a pre-qualified welding procedure must be submitted. Approval of these welding procedures is contingent on the inspecting agency overseeing the project.

The AWS indirectly specifies that galvanizing should be removed. For example, AWS D1.1 states in Section 5.15, "...Surfaces to be welded and surfaces adjacent to a weld, shall also be

free from loose or thick scale, slag, rust, moisture, grease, and other foreign material that would prevent proper welding or produce objectionable fumes." Welding through galvanization produces zinc oxides (a known health hazard[11]) as the coating is vaporized. Thus the presence of galvanization, or a "foreign material," and the generation of zinc oxides, or "objectionable fumes," precludes welding through galvanization according to AWS D1.1.

The American Galvanizers Association (AGA) suggests that all zinc galvanizing in the area of a weld be removed prior to welding. The AGA document states that removal can be made through grinding or burning, but the coating should be removed at least one to four inches from either side of the weld zone and on both sides of the work piece.[12] In contradiction to the AGA recommendations, a review of the *AWS D19.0, Welding Zinc Coated Steel* [13] indicates that acceptable methods have been developed where galvanization can be left in place prior to welding. Section 6 of the AWS D19.0 provides detailed specifications on how to use the SMAW process to weld galvanized plates. It is recommended that, "a slower travel speed than normal and a slight whipping motion of the electrode,"[13] be used to produce sound welds. This report was last edited in 1972 and may not represent current welding standards. These specialized techniques were not followed in the experimental program. Instead, standard welding procedures for non-galvanized plate were used.

The issue of welding through zinc galvanization, therefore, does not appear to be settled when considering research, current practice, and codes and standards. Problems with arc stability may be encountered by welding through the irregular zinc coating. The zinc coating, when vaporizing, can create porosity if gases become trapped in the weld joint between two coated surfaces. Additionally, if zinc is present in solution in the molten weld pool, it creates an increased potential for weld cracking. Zinc compounds have a lower solidification (melting)

temperature, and the solidification and cooling of these zinc compounds are restrained by already solidified steel.

Despite the lack of clarity and consistency in the documents discussed in this section, welding through galvanization is nevertheless part of construction practice. A recent survey published by PCI,[14] reports that 70% of reporting PCI Producer Members remove galvanizing on plates before welding, and 73% remove galvanizing on reinforcement before welding. In addition, 63% of the respondents have developed an associated Welding Procedure Specification (WPS) for welding galvanized components. To assess the quality of welds conducted through galvanization, galvanized plates were included in the study.

2.4 Weld Discontinuities

Fillet welds are susceptible to a variety of discontinuities which can affect the strength and integrity of the welded joint. The discontinuities (or flaws) will be briefly summarized in this section. Welding discontinuities are often divided into three main categories, namely those related to (1) procedure, (2) design, or (3) metallurgical behavior. The following is a summary of the causes and impacts of various discontinuities, based on this categorization.

Procedure-related discontinuities are related to the procedure used by the welder in making the weld. The procedure-related discontinuities are further categorized into geometric and non-geometric. The main geometric discontinuities are: profile irregularities, surface irregularities or ripples, incomplete penetration, and lack of fusion. Non-geometric discontinuities include: arc strikes, spatter, and slag inclusions. All procedure-related discontinuities are affected by the technique of the welder, but environmental conditions can potentially impact the presence or severity of such discontinuities. It is difficult to separate the contributions of welder technique and environmental conditions in creating discontinuities.

Metallurgical discontinuities are related to the properties of the weld and base metals. This includes slag inclusions, porosity, crack formation, and heat affected zone discontinuities. The formation of these flaws can be related to the environmental conditions under which the weld is produced. The sensitivity to the environment and the implication of these flaws on the strength and integrity of a weld are discussed in detail in the subsequent subsections.

Design discontinuities are related to errors by the design engineer. These can include improper specification of the weld size, type, or electrode. For example, an improperly specified weld size or type can induce stress concentrations. Such design issues are unrelated to present study.

2.4.1 Weld Profile Irregularities

Profile irregularities include undercut, concavity or convexity, and overlap. These irregularities are illustrated in Figure 2.2. Undercut can be caused by improper welding techniques such as improper electrode angle or weaving technique or by a welding current that is too high.[15] It commonly occurs parallel to the junction of weld metal and base metal at the top of the profile as shown in Figure 2.2. Undercut can reduce the strength of the weld when it creates a sharp or deep notch in the profile resulting in a stress concentration. Convexity and concavity are specific forms of oversized or undersized welds, respectively. Convexity is measured as the perpendicular distance from the weld face of a typical ¼-in. profile to the outermost dimension of the convex weld face. Convexity is limited by AWS D1.1 to 1/8-in. in the case of ¼-in. fillet welds, and it is limited to 1/16-in. in the case of 3/16-in. fillet welds. Concavity is detrimental in its reduction of weld area and strength, but weld passes can be added to increase weld size to a sufficient level. Poor surface appearance is generally caused by improper technique or lack of adherence to the welding procedure specified.[16]

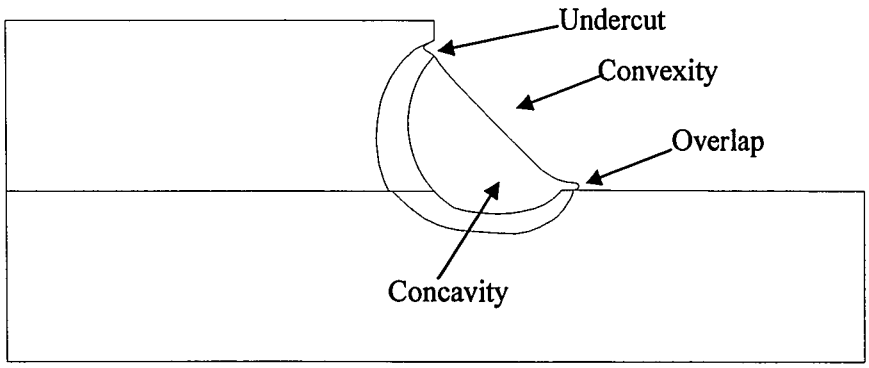

Figure 2.2: Welding Discontinuities

For field welds, it is possible that profile irregularities may be directly impacted by wind or moisture and indirectly by the effect of environmental conditions on the welder. Oversized welds are not inherently harmful to weld quality or strength but may interfere with assembly geometry and may produce excessive distortion of the welded plates.

Overlap is also usually caused by improper procedure or improper preparation of the base metal.[16] Improper surface preparation can lead to overlap due to interference of surface oxides with the fusion process if they are not removed in a cleaning process prior to welding.

Weld profile irregularities also include surface irregularities. Surface irregularities or ripples can be caused by improper technique or by excessive wind acting on the molten weld pool. It should be noted, however, that varying widths of weld height, depressions, non-uniformity of weld ripples, and other surface irregularities are not actually classified as weld discontinuities.[16] In the case of the present study, however, it is important to determine the effects of the environmental conditions on the surface condition of the weld.

2.4.2 Incomplete Penetration/Incomplete Fusion

Incomplete penetration and fusion can produce unsound welds. Incomplete penetration refers to the inadequacy of the penetration of the weld metal into the base metal at the root of the weld.

It is typically caused by insufficient welding heat or poor control of the welding arc. Incomplete fusion is a lack of fusion between the weld metal and the base metal along one or more of the joint boundaries; it can result from improper preparation of the base metal prior to welding (insufficient cleaning) or insufficient welding current.[16]

2.4.3 Arc Strikes and Spatter

Non-geometric, procedure-related discontinuities include arc strikes and spatter. Arc strikes are extraneous locations on the base metal where an arc is struck at which surface pores or cracks can form as the molten base metal cools. Arc strikes are caused by welder error and are generally the result of accidental contact of the electrode with the base metal. Poor visibility due to smoke and vapor formation is a common cause of arc strikes. This occurred in the experimental program due to smoke and vapor formation under some of the environmental conditions in the study. Spatter is molten metal deposited in a location other than the weld joint. This typically appears as bead-like protrusions on the base metal surface around the weld and is not of particular interest from a structural standpoint.

2.4.4 Slag Inclusions

Slag inclusions are nonmetallic solid materials that become trapped in the weld metal or at the interface of the weld metal and base metal. These discontinuities generally result from faulty technique or a rapid solidification rate which traps slag in the weld pool. With proper welder technique and under proper welding conditions, molten slag should rise to the surface of the molten weld metal providing a protective layer as the weld metal cools.[16] Slag inclusions affect weld strength by reducing the cross-sectional area of the weld metal and subsequently reducing the weld strength. Slag inclusions are of concern when they have large dimensions. These discontinuities will also lead to regions of stress concentration.

2.4.5 Porosity

Porosity is a metallurgical discontinuity that appears on the weld face and on the cross-section of a weld. Porosity is, in a general sense, caused by the presence of gases in a greater concentration than their solubility limit when the weld metal solidifies. Hydrogen, oxygen, and nitrogen are the only gases considered soluble in the weld metal. Hydrogen, however, is the primary cause of porosity in most welds. Hydrogen can enter the molten weld pool through the cellulose constituents of the electrode coating or through dissociation of water. Water can be present on the electrode, the base metal, or in the air surrounding the weld.[17] Porosity has a variety of appearances. The main types are uniformly scattered, clustered, linear, and piping (elongated). Scattered porosity represents pores of various sizes distributed more or less uniformly through the weld metal. Clustered porosity describes groups of pores clustered together and separated by porosity-free weld metal. Linear porosity is porosity occurring in a repetitious pattern, typically associated with the root of the weld and found in conjunction with a lack of fusion or penetration. Finally, piping porosity describes elongated (tubular) cavities caused by continued entrapment of gas at the solidifying interface.

Porosity reduces the cross sectional area of the weld which has a direct reduction in the strength. Since porosity typically forms in the shape of a gas bubble, the resulting void shape is smooth. The issue of porosity has been the subject of many papers and studies (e.g., references 18, 19, 20, 21, 22, 23, 24), and there is information available that demonstrates the effect of porosity on strength. Research has shown that scattered, unaligned, unclustered porosity has little impact on the static yield strength, the ultimate strength, and the ductility of welds from "slow bend" tests when in a quantity less than 5% of the cross-sectional area and in some cases up to 7%.[25]

2.4.6 Cracking

Cracks in the weld or base metal are a serious discontinuity from a structural integrity viewpoint. The presence of cracks increases the propensity for abrupt weld fracture by inducing large stress concentrations at the tip of the crack. The AWS code therefore provides no allowance for cracks of any kind in welds. However, the inspection for cracks in fillet welds is limited to a visual inspection of the weld surface in the field. For the development of a welding procedure specification (WPS), visual observation of three etched sections from a standard test specimen (see Figure 3.15) is required. No microscopic examination of the etched section specimens is prescribed by D1.1; therefore, only those cracks detectable by visual examination of surfaces or etched section specimens are of consequence in the AWS inspection criteria. While other NDE techniques exist (radiographic, magnetic particle, ultrasonic, etc.), they are not required for approval of a fillet weld WPS. Furthermore, depending on crack orientation and location, these NDE techniques may not detect cracks within a weld. For these reasons, cracks of concern according to AWS inspection include only those that are detectable by visual inspection techniques (i.e., with the naked eye). For visual identification, a minimum crack length of approximately 1/32-in. is needed. For the purposes of this paper, the term "micro-crack" refers to a crack-like discontinuity of length less than approximately 1/32-in., while the term "crack" refers to those with a length greater than approximately 1/32-in., or those which are visible to the naked eye.

Cracking of the weld can occur during the solidification process as well as hours or days after the weld has been completed. Cracks that form during solidification are called "hot cracks". Cracks can form at elevated temperatures during solidification due to stresses generated from chemical constituents with different solidification temperatures. Crack formation during solidification is exacerbated by concave weld profiles which are not strong enough to withstand

the stresses. In addition, contaminants from poorly cleaned weld surfaces or the chemical properties of the weld or base metal can lead to various rates of solidification and stress development.[17] This crack formation often occurs at the root of the weld since it is the last place to cool during solidification, and hot cracks form between grains in the weld microstructure. The cooled metal regions around the root of the weld provide restraint of the cooling contraction of this area, sometimes causing cracks to form at the root.

Cracks often form after the weld has been completed and has cooled due to the presence of hydrogen in the weld. During welding, hydrogen can be introduced to the weld pool from various sources including moisture on plate surfaces or electrodes. The diffused hydrogen trapped in the weld deposit builds pressure within micro-sized voids in the steel, initiating cracking. Since hydrogen may take time to pool in the microstructure, the crack may form hours to weeks after the weld is completed. This typically occurs below 100°C after the weld has cooled. Due to the cause and the age at which this type of crack forms, it is also referred to as delayed cracking, cold cracking, or hydrogen assisted cracking. This type of crack is likely to form in the regions where there are discontinuties such as pores or inclusions since hydrogen will have a tendency to pool in voids during solidification.[17] In addition, they may form in the coarse-grained HAZ, or the region of highest hardness and lowest ductility which occurs in a narrow strip of the HAZ adjacent to the weld metal. Hydrogen cracks, in addition to propagating along grain boundaries, can also propagate through grains in the weld microstructure.

Cracks are further classified as longitudinal, along the weld axis, or transverse, perpendicular to the weld axis. These classifications are subdivided into throat, root, crater, toe, and underbead cracks. Examples of a transverse throat crack, root crack, toe crack, and underbead crack are shown in Figure 2.3.

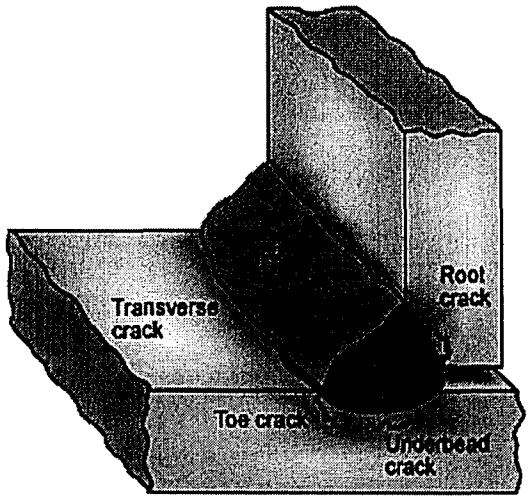

Figure 2.3: Crack Types[26]

Throat cracks are generally hot cracks and form on the face of the weld, running longitudinally. Root cracks can be hot or cold cracks, but these cracks originate in the root of the weld and run longitudinally. Crater cracks are generally star shaped and form in the crater than is often present at the end of a weld bead if the arc is not terminated properly. Toe cracks are typically cold cracks and initiate normal to the base metal surface and propagate from the toe of the weld where there are high residual stresses. Finally, under bead cracks are generally cold cracks which form in the heat-affected zone (HAZ). These cracks are typically short, and can occur when hydrogen is present and there are high residual stresses.[16]

The HAZ cracking behavior of a weld is determined largely by three factors: restraint, the amount of hydrogen present, and the steel microstructure. Further, cracking is influenced by localized imperfections or stress concentrations. Because of the significance of cracking to weld quality and its importance in this study, a summary of the causes and impacts of cracking on weld quality is provided below.

HAZ crack susceptibility is sensitive to the percentage of carbon present in the base metal. The level of carbon has a direct impact on the microstructure of the weld. To address this issue,

ASTM A36[27] prescribes a maximum carbon content of 0.25%, (for plate thickness less than 3/4-in.). A high carbon content has a hardening effect on steel and can lead to a crack-susceptible steel microstructure, increasing the likelihood of cracking.

Stainless steel 304, however, is not affected by cracks that form as a result of microstructure hardening (cold cracks). This is due to the austenitic microstructure of the steel and the fact that it is not hardenable on cooling into martensite, which is necessary for cold cracking to occur. The carbon content of the stainless steel used, therefore, is not as important as the carbon content of conventional carbon steel (e.g. A36 steel).

Restraint is also a key factor in enabling cracks to form. As the molten metal in the weld pool cools, it contracts and tends to distort the base plates if they are not properly restrained. If a high degree of restraint is provided (embedded anchored plates, thick base plates, etc.), the molten weld metal is restrained as it attempts to contract, and high tensile stresses develop. A brief discussion of the relevance of restraint is given in Section 3.1 of the report, where the test setup used in the study is described.

2.5 Discontinuity Summary

In summary, the main discontinuities of concern are: profile irregularities (convexity, concavity, undercut, and surface irregularities), incomplete fusion, slag inclusions, porosity, and cracking. Cracking is the discontinuity of greatest concern since it can lead to premature weld failure as a result of stress concentrations. Each of these discontinuities is investigated in the present study and is related to environmental conditions under which the welds are made.

3 Experimental Research Program

To evaluate fillet welds made under adverse environmental conditions, a two phase experimental research program was conducted. In the first phase, a large number of welds were made and inspected using visual techniques. In the second phase, welds were made under a select set of conditions and examined through destructive testing to assess the effect of environmental conditions on the strength. This chapter describes each phase.

3.1 Phase 1 Test Setup

The test setup was based on a connection similar to the double tee to inverted tee connection shown in Figure 2.1. The Phase 1 test specimen consisted of three plates (PL6x4x3/8), including two base plates and one cover plate, oriented in a horizontal position as shown in Figure 3.1. The base plates were recessed in a 4 in. thick concrete block to simulate the embedment of plates typical of precast construction with the goal of matching the thermal heat sink properties present in typical precast connection. The embedded plates were clamped at each of the four corners to simulate the restraint of a precast plate connection. The cover plate was held stationary as shown by a single, unobtrusive hold down point in the plate's center. The restraint of the base plates allows residual stresses to develop due to restraint of cooling contraction of the weld metal; therefore the restraint enables crack formation. As previously discussed in Section 2.4, cracking behavior is also dependent upon a crack-susceptible steel microstructure (high hardenability), as well as the amount of hydrogen present.

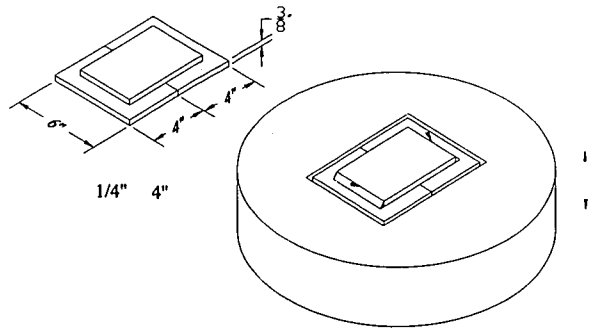

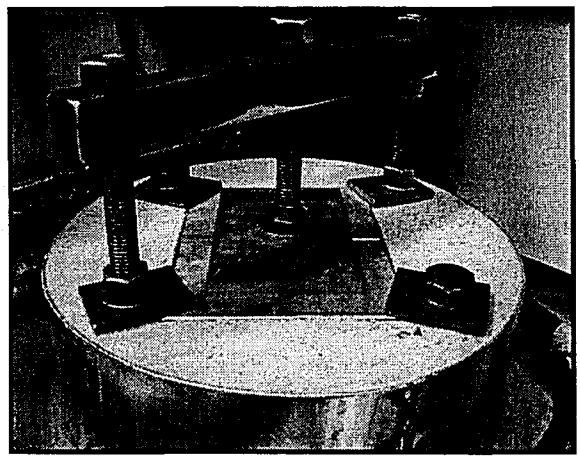

Figure 3.1: Test specimen configuration

It should be noted that the concrete block depicted in Figure 3.2 was used for the fabrication of several of the initial stainless steel specimens. This original block (Figure 3.2) allowed significant warping of the base plates (see Figure 3.3) during cooling of the weld and was deemed unsatisfactory because it did not provide sufficient restraint to the plates.

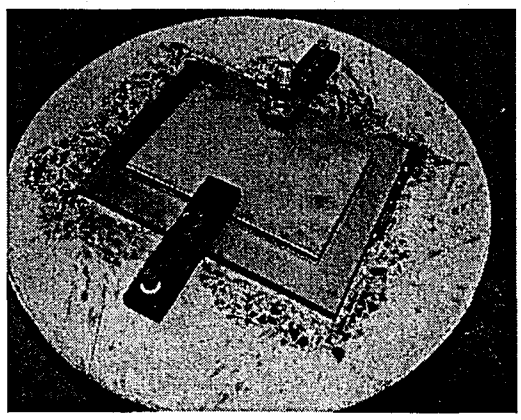

Figure 3.2: Original Concrete Test Block

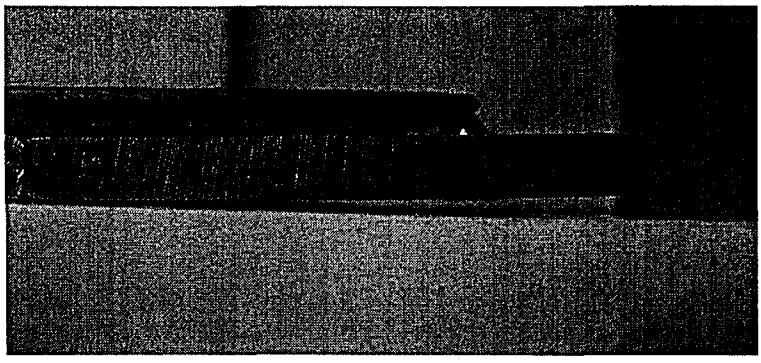

Figure 3.3: Warped Specimen

The block seen in Figure 3.1 was designed and used for the rest of the welds to provide adequate restraint. As discussed in the previous chapter, the stainless steel specimens were not susceptible to delayed or hydrogen-related cracking, and consequently, the stainless specimens welded using the original block were not remade.

3.2 Types of Base Metal

The experimental program included ASTM A36 non-galvanized, ASTM A36 Galvanized, and Stainless Steel Type 304. Two types of A36 were examined, one with a moderate carbon content and another with a relatively high carbon content. This variation allowed for an assessment of the effect of carbon content on cracking behavior.

The sensitivity carbon content has on crack formation can be summarized using the Graville diagram, presented in Figure 3.4. Steel materials lying in Zone I are unlikely to crack except in the case of high levels of hydrogen and high restraint. Zones II and III represent a greater likelihood of cracking in the weld, and AWS provides methods to be used to determine the minimum energy input or the preheat. As shown in Figure 3.4, the classification of steels presented in the Graville diagram is dependent on both the carbon content and the carbon equivalent.

The carbon equivalent, a measure of the propensity for cracking as a weighted average of several chemical elements, was calculated for each of the carbon steels used in the study. The carbon equivalent (CE) is calculated using the carbon equivalent formula presented in AWS D1.1, Section I5.1 (Equation 1).

$$CE = C + \frac{(Mn + Si)}{6} + \frac{(Cr + Mo + V)}{5} + \frac{(Ni + Cu)}{15} \qquad \text{Equation 1}$$

To study the effect of carbon content, steel with high carbon content was sought. Most readily available ⅜-in A36 steel plate has a moderate carbon content, and obtaining A36 steel with a high carbon content proved difficult. Steel plate was donated to the project by High Concrete Structures, Inc. (A36 non-galvanized, A36 galvanized, and Stainless 304). The material originated from two different manufacturers, Steel Dynamics® (Roanoke Bar Division) and Pennsylvania Steel Company. Mill certificates were obtained for each metal type, and additionally, a sample of each of the metal types was sent to Laboratory Testing Inc. of Hatfield, PA for independent chemical analysis. A spectrographic analysis was performed on each of the samples, and the results of the independent analyses were compared to mill certificate values. The non-galvanized A36 plates had a carbon content of 0.13%. The CE for this A36 steel plate was calculated to be 0.330, while the CE for the galvanized A36 steel is 0.319.

Since this A36 steel had a relatively low carbon content, the sensitivity to cracking was low. A small amount of high carbon A36 plate material was obtained, however, from Metromont Corporation. The material originated from two heats of steel manufactured by Nucor Steel. The carbon equivalent of one heat was 0.420 and 0.397 for the second heat. The plates from both of these heats should display an increase in their propensity for cracking, as compared with the A36 steel with a moderate carbon content. The carbon content and CE are important

variables in predicting cracking behavior, and because of uncertainty in chemical composition of embedded steel in precast elements, caution should be exercised in controlling other factors which might cause cracking.

The carbon content and carbon equivalent of all of the carbon steel plates are plotted on Figure 3.4 to provide a means of comparison of the steels with regard to their sensitivity to cracking.

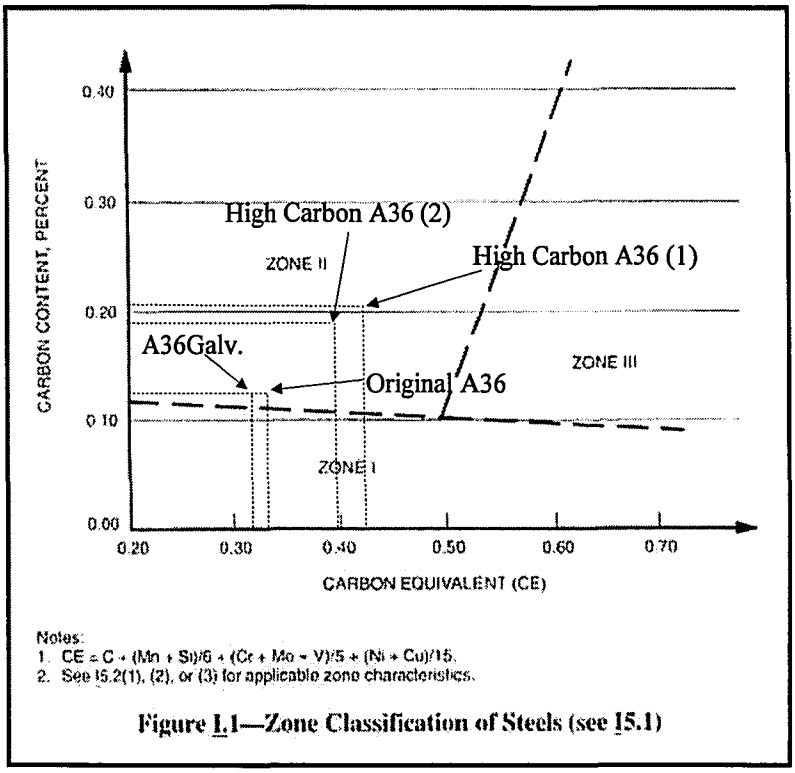

Figure 3.4: AWS Steel Carbon Classification[4]

As can be seen in Figure 3.4, all steel materials used in the project are in Zone II, meaning that there is some risk of cracking if energy input and/or preheat is not used.

Detailed chemical compositions for each plate material used in the project are summarized along with the test results for each plate material type in Sections 4.1, 5.1, 6.1.

3.3 Environmental Chamber

The welding was performed in an environmentally controlled chamber. (Figure 3.5). The chamber, Model 518, was purchased from Electro-Tech Systems, Inc., of Glenside, Pa. The chamber was modified to accommodate the extreme temperatures of the test program by adding ¾-in. foam insulation, and the walls and insulation of the chamber were protected by installing aluminum sheeting over the interior surfaces except for the upper viewing window and acrylic door. A centrifugal blower was mounted on the chamber floor as seen in Figure 3.5 to simulate wind transverse to the weld axis.

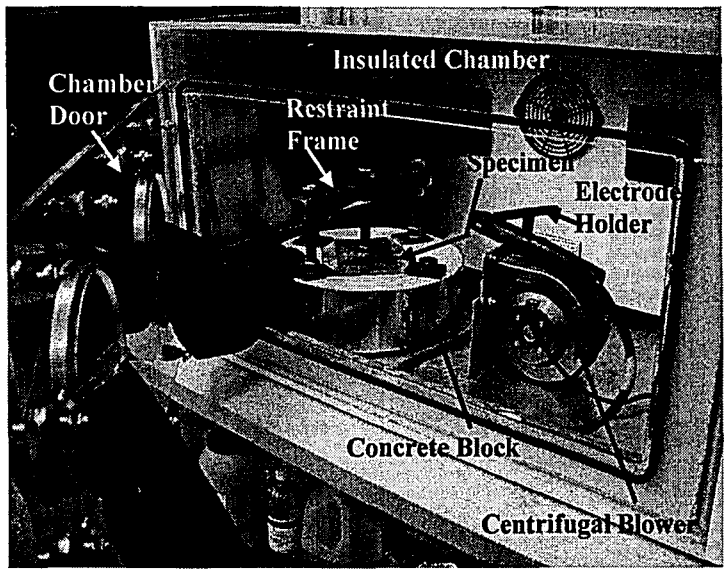

Figure 3.5: Environmental Control Chamber

Within the chamber, the ambient temperature and relative humidity were controlled, with the ability to create temperatures as low as -18°F [-27.8°C] and relative humidity from approximately 35%RH to 100%. Wind was simulated with a variable powered centrifugal blower with air flow in a direction transverse to the fillet weld (normal to weld axis). The fan was configured to achieve wind speeds ranging from 0 to 35 mph at the weld, with the wind being applied at a nominal distance of 6-in. from the fillet weld. Airflow remained

unobstructed by the welder during welding, as can be seen in the right most image of Figure 3.6, where the welding is underway and the fan orifice can be seen.

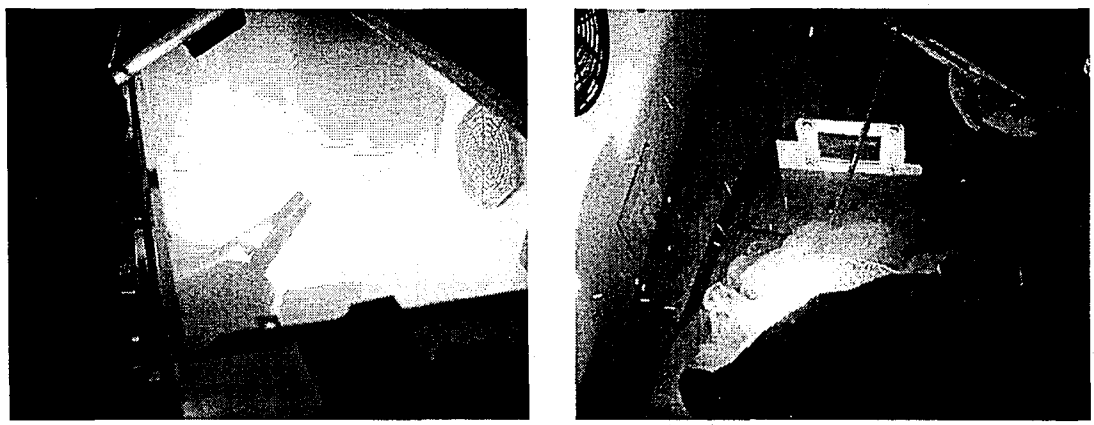

Figure 3.6: Welding Process

3.4 Environmental Condition Measurements

For each test specimen, measurements of environmental conditions were made and recorded inside the chamber to verify the wind speed, humidity, and temperature. Relative humidity was measured in the chamber using a handheld Kestrel® 3000 Pocket Weather Meter, which has a measurement range of 0.0 to 100.0 %RH and an accuracy of ±3 %RH. The readings were taken near the center of the chamber at approximately the mid-height of the chamber. Relative humidity, or RH, was used as a basis of measurement and is defined as the ratio of the partial pressure of water vapor in the air to the saturation vapor pressure in the air at a given temperature.

The temperature was measured using a thermocouple or temperature probe, and temperatures were recorded in the air in the vicinity of the weld, as well as on the surface of the steel at the weld joint and on the concrete surface about 1-in. away from the plate recess. The wind was recorded using the same handheld weather meter used for the humidity readings. The weather meter had an anemometer that measured wind speed in mph to an accuracy of ±3% of the

reading taken and over a range of 0.8 to 135 mph. The wind speed was measured approximately 6-in. from the opening of the blower at the height of the blower opening. This height also corresponded to the location of the weld bead, such that the anemometer was rested on the plate at the weld joint oriented perpendicular to the airflow.

3.5 Welding Electrodes

Welding electrodes typical of precast concrete building erection were used in the experimental program. For the ASTM A36 and A36 Galvanized steel, E7018-H4R electrodes were used in accordance with AWS D1.1. Electrodes were stored and used in accordance with the restrictions found in AWS D1.1, except in the cases where the exposure of electrodes to moisture was studied. Specifically, the E7018-H4R electrodes were purchased in hermetically sealed containers, stored in a holding oven held at a nominal temperature of 250°F after the containers were opened, and not exposed to the environment for a time exceeding 9 hours, the limit for E70XXR electrodes according to AWS D1.1.

The electrodes used for the A36 and A36 galvanized welds were 5/32-in. diameter, E7018-H4R electrodes, with a nominal ultimate strength of 70 ksi. The weld metal yield and tensile strengths are typically determined from an all-weld-metal tensile coupon extracted from a large multi-pass weld. The supplemental –"H4R" designation comes from AWS A5.1-91 and indicates a hydrogen level and moisture resistance. The "H4" designation indicates that the electrodes met the requirement of 4mL average diffusible hydrogen content in 100 g of deposited weld metal when tested in the "as-received" condition. The "R" designation indicates electrodes that pass the absorbed moisture test after exposure to an environment of 80°F (26.7°C) and 80% relative humidity for a period of 9 hours.

For the type 304 stainless steel, 1/8-in. E308-16 electrodes were chosen at the beginning of the study for the purpose of producing 1/4-in. fillet welds in a single pass. For the first sets of welds made on the 304 stainless steel plates, the 1/8-in. electrode consistently produced 3/16-in. welds. This was not the intended weld size, but a 3/16-in. weld is an acceptable weld size for the 3/8-in. plate thickness used in the study, according to AWS D1.1. The weld size was measured after the specimens were cross-sectioned. Therefore, these welds were included in the study even though the majority of the stainless steel welds had a size of 3/16-inch. Rather than repeat any of the stainless steel welds with a larger electrode, the remainder of the stainless steel welds were made using the same 1/8-in. electrodes, and the data was analyzed with respect to a 3/16-in. weld instead of a 1/4-in. weld.

In addition, two specimens were welded with a full 1/4-in. weld size on 304 stainless steel plate materials, using the 1/8-in. electrode. This was accomplished by reducing the travel speed to deposit more filler metal in the weld joint. This was done to determine whether the environmental effects would have had a greater (or lesser) impact on the larger sized welds. It was assumed that the environmental parameter that would most alter the weld quality when the size was increased was wind speed, which might impact the weld profile. Therefore, a base specimen with a 1/4-in. weld was made with no wind at 71°F, and 50%RH, and a second specimen was made at 71°F, 95%RH and 35mph wind condition.

3.6 Welding Setup

All welds were performed using the dominant hand of the welder to produce consistent and high-quality welds, to the extent that it was possible under the prevailing conditions.

The welding setup used a constant current welding power source. Grounding was provided directly to the restraint clamp which was in contact with the plates as shown in Figure 3.7.

Figure 3.7: Welding Electrical Ground

Noting the voltage and current of the welding power source during the welding process and measuring the travel time for a given weld, the welding energy input was calculated for several of the weld tests using the following formula:

$$H = EI / v \qquad \text{Equation 2}$$

H is the energy input [J/in.], E is the voltage [Volt], I is the current [Amp], and v is the travel speed of the weld [in./sec]. The data for representative welds for each type of base metal is shown in Table 3-1.

Figure 3.7: Welding Electrical Ground

Noting the voltage and current of the welding power source during the welding process and measuring the travel time for a given weld, the welding energy input was calculated for several of the weld tests using the following formula:

$$H = EI / v \qquad \text{Equation 2}$$

H is the energy input [J/in.], E is the voltage [Volt], I is the current [Amp], and v is the travel speed of the weld [in./sec]. The data for representative welds for each type of base metal is shown in Table 3-1.

Table 3-1: Representative Weld Energy Inputs				
Metal Type	Current, I [Amp]	Voltage, E [Volts]	Travel Speed, v [in./sec]	Energy Input, H [kJ/in.]
A36 Moderate Carbon Steel	165	24	0.089	45
A36 Moderate Carbon Steel	160	24	0.080	48
A36 Moderate Carbon Steel	160	24	0.098	39
A36 Moderate Carbon Steel	160	19	0.089	34
A36 Moderate Carbon Steel	160	20	0.076	42
A36 High Carbon Steel	170	22	0.089	42
A36 High Carbon Steel	165	24	0.107	37
A36 Galvanized Steel	160	24	0.095	40
Type 304 Stainless Steel	140	25	0.114	31
Type 304 Stainless Steel	123	29	0.111	32
Type 304 Stainless Steel	123	29	0.108	33
Type 304 Stainless Steel	123	29	0.111	32

The energy input for the 1/4-in. A36 steel welds ranged from 33-48 kJ/in. For the A36 Galvanized welds, the energy input ranged from 41-48 kJ/in. For the smaller 3/16-in. type 304 stainless steel welds, the energy input ranged from 30-33 kJ/in. The lower energy input for the stainless steel welds reflects the smaller weld size used for those welds.

3.7 Phase 1 Program

The test matrix for the Phase 1 welded specimens was formulated through correspondence with the PCI project advisory committee and by review of AWS D1.1 limitations on welding in various environmental conditions. Three temperature levels were chosen. The standard room temperature of 71°F [22°C] was chosen as the base condition for the study. The second level

corresponds to the temperature below which preheat is required by AWS D1.1 (32°F [0°C]), and the third temperature was selected as one sufficiently below 32°F [0°C] but practically achievable, and one below which welding would rarely take place in the field (-10°F [-23°C]).

The humidity values were chosen to represent a low level of moisture, an average level, and a level of humidity at or near saturation. The values were thus set originally at 0, 50, and 100%RH, but due to challenges of achieving these values within the environmental chamber, the values were adjusted to more practical levels of 35%, 50%, and 95%RH. The low humidity level proved difficult to achieve in some cases, and the time necessary to decrease the chamber humidity below approximately 40%RH made 35%RH the lowest practical value. In a survey of relative humidity data from the Northeast Regional Climate Center[2], it was found that of 274 major U.S. cities, only 41 ever experienced at least one month with an average humidity less than 35%RH. Because of the rarity of such low humidity conditions and the fact that the low humidity conditions are more favorable welding conditions, the low humidity level was changed to 35%RH. Additionally, a "surface wet" condition was added to the matrix so the effects of liquid or frozen water on the plate surface could be investigated. The surface wet condition was achieved by misting using a spray bottle, or for one of the stainless steel specimens (SS-88) by droplet moisture as opposed to mist.

Finally, the wind speed levels were chosen as 0, 5, 10, 20, and 35 mph, with the lower bound of 5 mph being the limit for most welding processes in AWS D1.1. The upper bound, 35 mph, was chosen as the highest wind speed in which a welder would likely be operating and the maximum wind speed at the weld location. The 10 and 20 mph wind speed conditions were chosen to provide adequate data to quantify the effects of wind on the welds.

The combinations of materials and environmental conditions investigated in the Phase 1 study are summarized in the test matrix Table 3-2.

Table 3-2: Phase 1 Test Matrix

Specimen ID*	Base Material	Temp. [°F]	Relative Humidity [%RH]	Wind Speed [mph]	Electrode Condition**	Plate Surface Condition†
36-1	ASTM A36	72.0	41.0	0	AWS D1.1	Dry
36-3	ASTM A36	72.5	98.2	0	AWS D1.1	Dry
36-6	ASTM A36	76.6	94.3	20	AWS D1.1	Dry
36-7	ASTM A36	73.6	97.8	34.7	AWS D1.1	Dry
36-8	ASTM A36	78.3	92.4	0	AWS D1.1	Wet
36-14	ASTM A36	39.0	75.5	20	AWS D1.1	Dry
36-15	ASTM A36	31.0	100.0	32.4	AWS D1.1	Dry
36-22	ASTM A36	-5.0	99.9	21.3	AWS D1.1	Dry
36-23	ASTM A36	-13.0	100.0	27	AWS D1.1	Dry
36-17(95)(1)	ASTM A36	72.9	92.0	0	~4%	Dry
36-17(95)(2)	ASTM A36	77.1	88.6	0	~4%	Dry
36-C1	ASTM A36 High-Carbon(1)	-6.0	100.0	0	AWS D1.1	Dry
36-C2	ASTM A36 High-Carbon(1)	-4.0	66.7	0	AWS D1.1	Dry
36-PC1*	ASTM A36	88.9	43.4	0	AWS D1.1	1 Wet /1 Dry
36-PC2*	ASTM A36	91.1	50.0	0	AWS D1.1	1 Wet /1 Dry
36-PC3*	ASTM A36	91.9	28.8	0	AWS D1.1	Dry
36-PC4*	ASTM A36	84.5	50.0	0	AWS D1.1	Wet
36-PC5*	ASTM A36	15	85.3	0	AWS D1.1	Wet (Ice)
36-PC6*	ASTM A36 High-Carbon(2)	74.2	17.6	0	AWS D1.1	Wet
36G-25	ASTM A36 Galv.	73.0	43.0	4.3	AWS D1.1	Dry
36G-33(1)	ASTM A36 Galv.	36.0	28.5	3	AWS D1.1	Dry
36G-33(2)	ASTM A36 Galv.	20	33.6	3	AWS D1.1	Dry
36G-17(95)	ASTM A36 Galv.	77.3	84.6	3	~4%	Dry
SS-73	Stainless Steel 304	73.0	35.7	0	AWS D1.6	Dry
SS-74	Stainless Steel 304	73.7	47.7	0	AWS D1.6	Dry
SS-75	Stainless Steel 304	77.0	100	0	AWS D1.6	Dry
SS-76	Stainless Steel 304	71.4	100	5.1	AWS D1.6	Dry
SS-77	Stainless Steel 304	74.8	95.7	10.1	AWS D1.6	Dry
SS-78	Stainless Steel 304	75.5	94.8	20.1	AWS D1.6	Dry
SS-79	Stainless Steel 304	75.8	90.9	33.2	AWS D1.6	Dry
SS-82	Stainless Steel 304	45.5	48.8	0	AWS D1.6	Dry
SS-83	Stainless Steel 304	35.6	99.2	0	AWS D1.6	Dry
SS-84	Stainless Steel 304	43.4	100.0	5.1	AWS D1.6	Dry

Table 3-2: Phase 1 Test Matrix (continued)						
Specimen ID*	Base Material	Temp. [°F]	Relative Humidity [%RH]	Wind Speed [mph]	Electrode Condition**	Plate Surface Condition†
SS-85	Stainless Steel 304	39.8	100.0	10	AWS D1.6	Dry
SS-86	Stainless Steel 304	37.2	100.0	19.3	AWS D1.6	Dry
SS-87	Stainless Steel 304	33.8	100.0	33.1	AWS D1.6	Dry
SS-88	Stainless Steel 304	35.7	99.9	~15	AWS D1.6	Wet
SS-89	Stainless Steel 304	-4.6	24.7	0	AWS D1.6	Dry
SS-90	Stainless Steel 304	-5.0	49.5	0	AWS D1.6	Dry
SS-91	Stainless Steel 304	-5.4	100.0	0	AWS D1.6	Dry
SS-92	Stainless Steel 304	-2.2	95.5	5.5	AWS D1.6	Dry
SS-93	Stainless Steel 304	-2.4	93.0	10	AWS D1.6	Dry
SS-94	Stainless Steel 304	-3.0	100.0	20.6	AWS D1.6	Dry
SS-95	Stainless Steel 304	-1.2	100.0	26-27	AWS D1.6	Dry
SS-96	Stainless Steel 304	-2.0	99.9	0	AWS D1.6	Wet
SS-4(100)	Stainless Steel 304	73	96.7	0	4 HR.‡	Dry
SS(1/4)-35	Stainless Steel 304	73	94.6	32	AWS D1.6	Dry
SS(1/4)-0	Stainless Steel 304	78	45.4	0	AWS D1.6	Dry

*Specimens which were not sectioned according to standard procedure, but were welded for the purpose of examining for porosity and cracking behavior and inspected as needed for these purposes.
**Electrodes were stored and used in accordance with provisions outlined in AWS D1.1 Welding Code for carbon steel electrodes and AWS D1.6 for stainless steel electrodes. 4%, when used, refers to the approximate percent moisture in electrode by weight. (17 hr. exposure at >80%RH).
† Wet indicates that the surface was intentionally wetted prior to welding.
‡ Refers to exposure of E308-16 electrodes for 4 hours to moist environment (within AWS D1.6 limits).

3.7.1 Evaluation Procedure

In Phase 1, the welds were made as summarized in Table 3-2. The completed welds were left intact for at least 24 hours to allow for the potential development of cold cracking. After 24 hours, the welds were sectioned as shown in Figure 3.8.

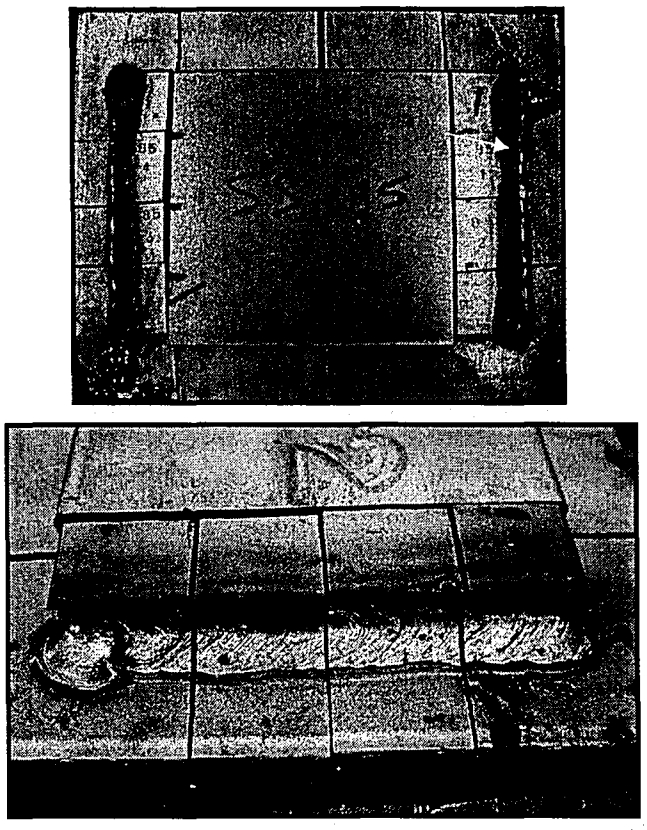

Figure 3.8: Specimen Sectioning

First, the outer faces of the center cut sections (as viewed in the right-hand image of Figure 3.8) were polished up to a grit of 1200, buffed with a 0.3μm particle solution, and etched using an appropriate acid etching agent (2-3% NITAL for the A36 steel and A36 Galvanized steel specimens, Marble's reagent for the stainless steel specimens). The final product was a clean surface with a clear view of the weld cross section, as illustrated in Figure 3.9.

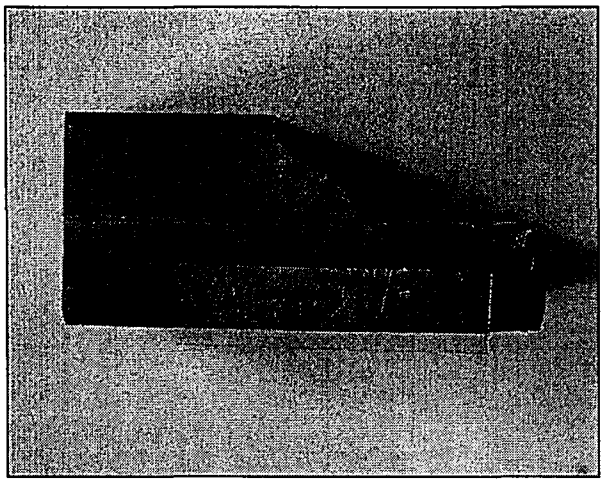

Figure 3.9: Polished A36 Cross Section

The cross sections were examined and photographed. Weld size and profile measurements were made to determine if the AWS code profile requirements were met. Additionally, slag inclusions, undercut, porosity, cracking, and root and joint fusion were examined for comparison to AWS code requirements.

3.7.2 Inspection Methods

Welds were inspected with a variety of methods to assess their quality, measure discontinuities, and ascertain properties of the welds. The first method of inspection was a visual observation of the weld surface and surrounding base metal. This observation determined if there were surface pores, cracks, or profile irregularities. An optical microscope was used to closely examine surfaces of the welds made on A36 steel to investigate the possibility of cracking on the weld face (the surface of a weld is shown in the right image of Figure 3.8) or base metal around the weld. A magnifying glass and digital caliper were used to quantify the dimensions of surface pores.

After the welds were sectioned and polished, the cross-sections of the welds were inspected by observation with the naked eye and a magnifying glass, by measurements made on photographs

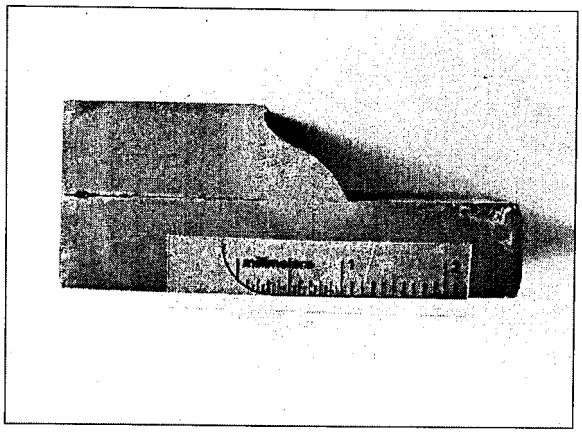

Figure 3.9: Polished A36 Cross Section

The cross sections were examined and photographed. Weld size and profile measurements were made to determine if the AWS code profile requirements were met. Additionally, slag inclusions, undercut, porosity, cracking, and root and joint fusion were examined for comparison to AWS code requirements.

3.7.2 Inspection Methods

Welds were inspected with a variety of methods to assess their quality, measure discontinuities, and ascertain properties of the welds. The first method of inspection was a visual observation of the weld surface and surrounding base metal. This observation determined if there were surface pores, cracks, or profile irregularities. An optical microscope was used to closely examine surfaces of the welds made on A36 steel to investigate the possibility of cracking on the weld face (the surface of a weld is shown in the right image of Figure 3.8) or base metal around the weld. A magnifying glass and digital caliper were used to quantify the dimensions of surface pores.

After the welds were sectioned and polished, the cross-sections of the welds were inspected by observation with the naked eye and a magnifying glass, by measurements made on photographs

taken of each cross section, and microscopically with a Nikon Optiphot microscope. When quantifiable flaws were observed, they were measured using the magnifying glass and a digital caliper. The largest dimensions of pores and inclusions were measured, and undercut was quantified as the distance from a line passing through the original plate edge to the tip of the undercut, in cross section (Figure 2.2). Discontinuities were further investigated under the microscope where their properties could be more closely examined, and cracks that were not visible to the naked eye were observed using microscopy. Discontinuities were measured when appropriate and recorded. The acceptability of the weld profiles, as determined from the section photographs, was also recorded.

3.7.3 Evaluation Criteria

In Phase 1, the welds were examined visually to determine acceptability. Welds were required to meet the profile requirements of AWS D1.1 (Figure 3.10), and such determinations were made using scaled measurements taken on cross-section photographs. A weld profile was deemed unacceptable if:

- Either of the leg lengths was found to be under the required weld size.
- The throat dimension was less than the required throat dimension as calculated by multiplying the leg size by 0.707.
- The convexity was greater than 1/8-in. for 1/4-in. welds, or 1/16-in. for 3/16-in. welds.
- The throat dimension at any point on the weld face fell below the required profile shape, depicted in Figure 3.10.

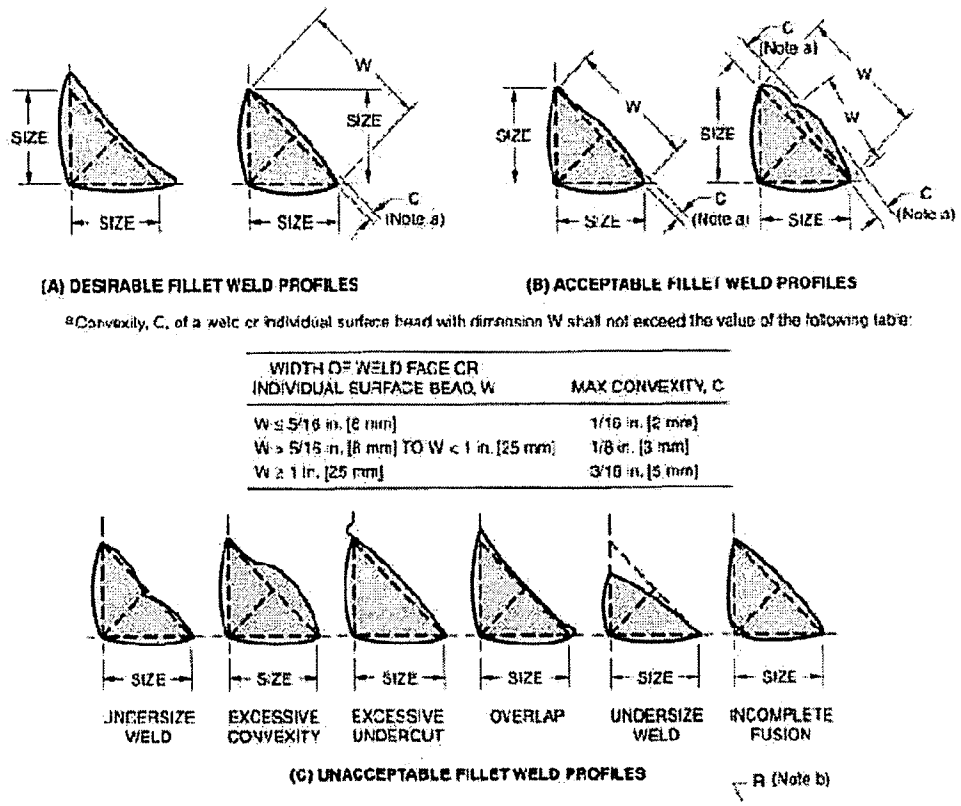

Figure 3.10: AWS Weld Profile Acceptance Figure[4]

It is noted that these acceptability levels were more stringent than AWS D1.1 provisions, which allow 3/16-in. welds to be undersized by 1/16-in. and 1/4-in. welds to be undersized by 3/32-in. (AWS D1.1:Table 6.1). However, AWS 1.1 allows the undersized portion to be as much as 10% of the weld length. Because profile measurements were made accurately at only four points along the weld length where the sections were taken, a more stringent undersize requirement was incorporated into the profile inspection criteria. It should also be noted that this profile measurement technique could not be applied in the field due to its destructive nature, but it nonetheless provides a consistent basis for determining whether welds made in the study were undersized at standard locations along each weld. In a field inspection, weld size should

be determined through the use of a fillet weld gage, as demonstrated in Figure 3.11. The figure illustrates the measurement of a concave weld using the gage with three points. The middle point of the gage must touch the weld face for the weld to have an adequate throat dimension. The leg length is determined using the black tick-mark on the gage, as shown in Figure 3.11. A weld with adequate leg length but an undersized concave throat is shown in (A). A convex weld with adequate leg length and throat is shown in (B).

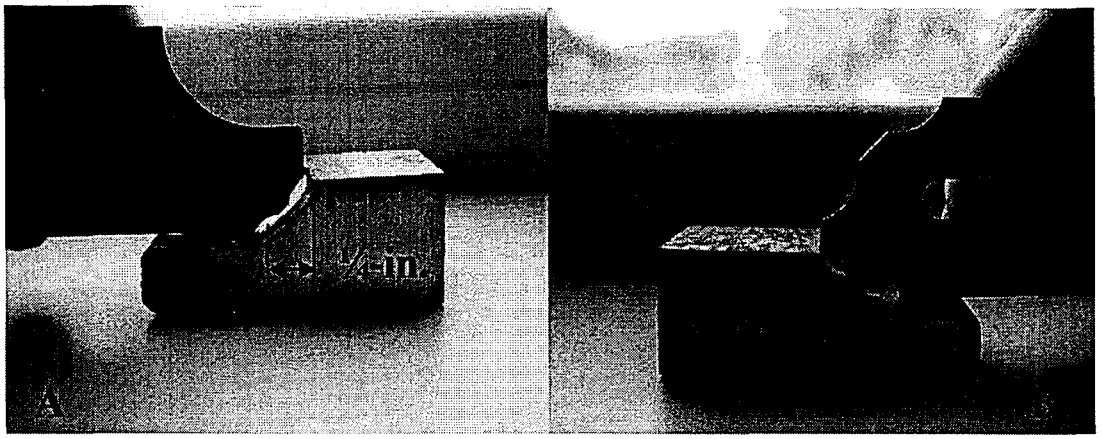

Figure 3.11: Fillet Weld Gage—Concave Measurement (A), Convex Measurement (B)

Because profile measurements were only made at two locations where sections were cut, a "profile index" was established to quantify the regularity of the weld surface and profile along the length of the weld. The index assigns a 0, 1, or 2 based on a qualitative assessment of the overall weld appearance. A value of 0 for a "good" weld represents a weld with a smooth surface, no excessive ripples, and a consistent throat dimension along the length. A value of 1 for a "fair" weld represents a weld with moderate changes in throat dimension or the presence of some ripples in the weld surface. A value of 2 for a "poor" weld indicates that the weld was extremely irregular in the throat dimension, had a weld surface with deep ripples, or had significant melting along the top edge of the cover plate. A typical sample corresponding to each of the profile indices is shown in Figure 3.12, Figure 3.13, and Figure 3.14

be determined through the use of a fillet weld gage, as demonstrated in Figure 3.11. The figure illustrates the measurement of a concave weld using the gage with three points. The middle point of the gage must touch the weld face for the weld to have an adequate throat dimension. The leg length is determined using the black tick-mark on the gage, as shown in Figure 3.11. A weld with adequate leg length but an undersized concave throat is shown in (A). A convex weld with adequate leg length and throat is shown in (B).

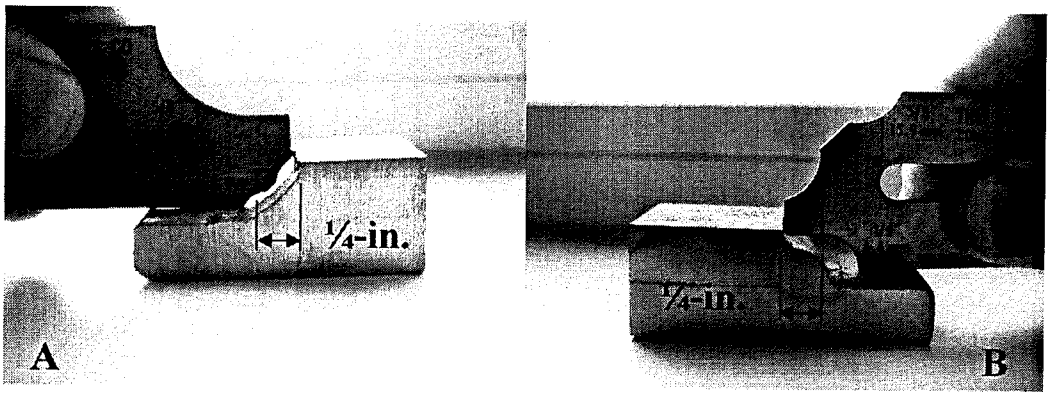

Figure 3.11: Fillet Weld Gage—Concave Measurement (A), Convex Measurement (B)

Because profile measurements were only made at two locations where sections were cut, a "profile index" was established to quantify the regularity of the weld surface and profile along the length of the weld. The index assigns a 0, 1, or 2 based on a qualitative assessment of the overall weld appearance. A value of 0 for a "good" weld represents a weld with a smooth surface, no excessive ripples, and a consistent throat dimension along the length. A value of 1 for a "fair" weld represents a weld with moderate changes in throat dimension or the presence of some ripples in the weld surface. A value of 2 for a "poor" weld indicates that the weld was extremely irregular in the throat dimension, had a weld surface with deep ripples, or had significant melting along the top edge of the cover plate. A typical sample corresponding to each of the profile indices is shown in Figure 3.12, Figure 3.13, and Figure 3.14

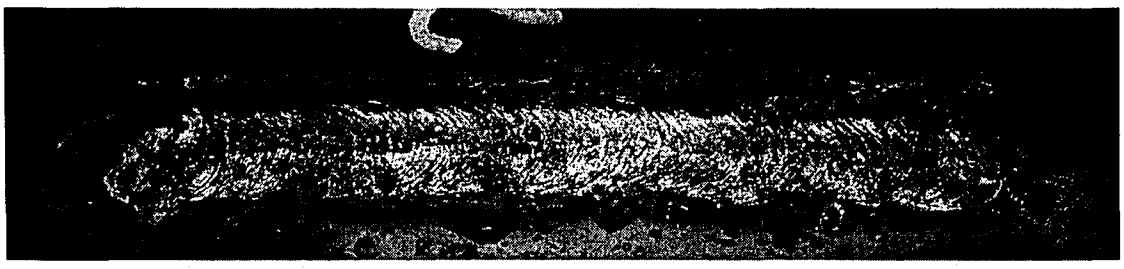

Figure 3.12: Example of Weld Classified as "Good" (1)

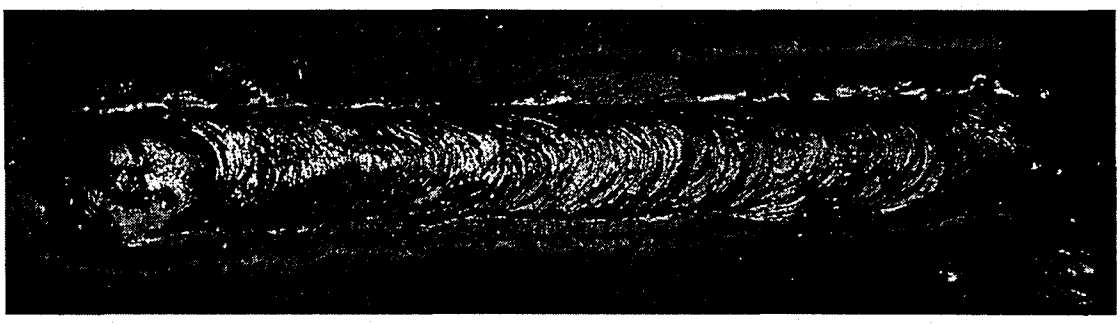

Figure 3.13: Example of Weld Classified as "Fair" (1)

Figure 3.14: Example of Weld Classified as "Poor" (2)

In accordance with AWS D1.1, no cracks, regardless of size, are acceptable, and welds susceptible to cracking were examined under a microscope to look for the presence of cracks. If cracks were found, their location and nature were noted, and in most cases, microscopic images were taken and are shown with the description of their respective specimens in Chapters 4,5, and 6. It is noted that, as discussed in Section 2.4.6, AWS D1.1 does not call for microscopic evaluation of etched specimens, but the microscopic evaluation was performed to thoroughly catalog all weld discontinuities. The crack-like discontinuities observed on a microscopic level

would not be detectable by standard weld inspection techniques and do not necessarily constitute a means for concern with regard to weld strength. Such cracks are called "micro-cracks" in this study, while cracks visible without a microscope are called "cracks." The "micro-crack" and "crack" designations correspond to weld lengths less than 1/32-in. or greater than 1/32-in, respectively. This issue was investigated in the strength tests of Phase 2.

The weld surfaces and cross-sections were also examined visually to determine the presence and severity of porosity. The presence and size of pores observed on the weld surfaces and cross-sections were noted and recorded. As discussed in Section 2.4.5, it has been shown through past research that porosity below 5% of the weld cross-sectional area will not affect the static tensile strength. The percentage of cross-section porosity was quantified when it was observed and noted in the specimen summaries. The direct measurement of cross section porosity in this study was limited to the measurement of those pores that appeared in the sections, which were cut at predetermined locations along the weld length. An additional acceptance criteria for porosity is found in Section 4.30.2.3 of AWS D1.1 and states: "Fillet welds...shall have: ...(e) for porosity 1/32-in. [1 mm] or larger, accumulated porosity not exceeding ¼-in. [6 mm]." This criteria refers to the macroetch test specimen used for qualification testing of a welder, which is cut from a 5/16-in. fillet weld on a T-joint, as shown below in Figure 3.15.

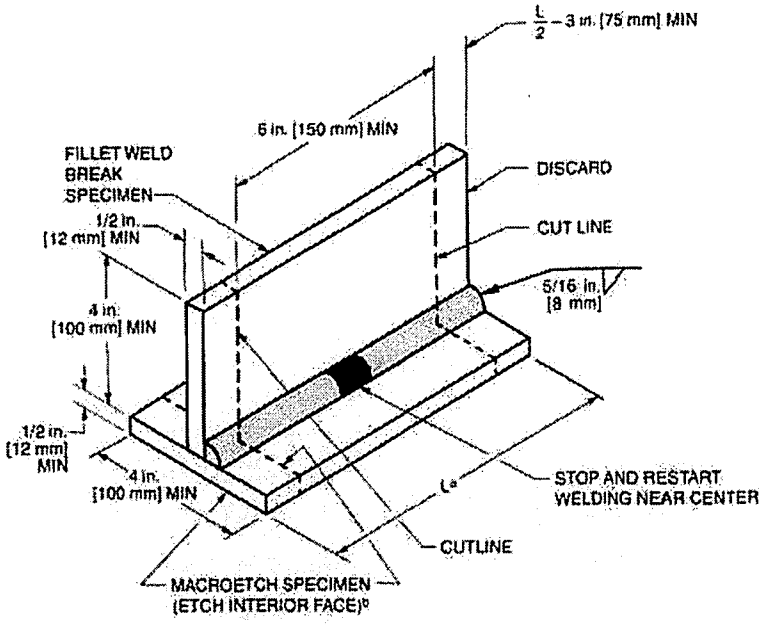

[a] L = 8 in. [200 mm] min welder, 15 in. [380 mm] min (welding operator).
[b] Either end may be used for the required macroetch specimen. The other end may be discarded.

Figure 4.37—Fillet Weld Break and Macroetch Test Plate—Welder or Welding Operator Qualification—Option 1 (see 4.28 or 4.25)

Figure 3.15: Fillet Weld Macroetch Test Specimen for Welder Qualification[4]

Two porosity-related acceptance criteria based on external visual inspection are noted in Table 6.1 of AWS D1.1. Table 6.1 (8)(A), for the case of a statically loaded non-tubular connection, states: "...for fillet welds, the sum of the visible piping porosity 1/32 in. [1 mm] or greater in diameter shall not exceed 3/8 in. [10 mm] in any linear inch of weld and shall not exceed 3/4 in. [20 mm] in any 12 in. [300 mm] length of weld." Table 6.1 (8)(B), for the case of a cyclically loaded, non-tubular connection, states, "The frequency of piping porosity in fillet welds shall not exceed one in each 4 in. [100 mm] of weld length and the maximum diameter shall not exceed 3/32 in. [2.5 mm]."

Cyclic load is defined as "load, within the elastic range, of frequency and magnitude sufficient to initiate cracking and progressive failure (fatigue)."[4] Fillet welds in the types of connections

used in precast building structures are not often subjected to fatigue loading conditions. However, precast members in bridge applications may be subjected to fatigue loading conditions. In cases where fatigue is a concern, extra care should be taken to ensure the acceptance criteria for discontinuities in welds under cyclic loading are met. *The present study assumes that the welds are statically loaded.*

Weld cross sections were examined for the presence of slag inclusions. The size and shape of each inclusion is discussed with the description of each specimen. It is generally accepted that slag inclusions reduce the tensile strength in proportion to their projected area. The size and nature of the inclusion is important to the strength. Linearly aligned discontinuities such as inclusions appear to have a greater impact on static tensile properties than widely separated ones. AWS D1.1, Section 4.30.2.3(3) states,

> "Fillet welds...shall have: ...(f) No accumulated slag, the sum of the greatest dimensions of which shall not exceed 1/4 in. [4 mm]."

This acceptance criteria refers to the aforementioned macroetch test (5/16-in. weld) used in welder qualification, and the associated specimen in shown as Figure 3.15. Additionally, Section 4.30.4.1 of AWS D1.1 refers to the fillet weld break test (the same test specimen as the macroetch test specimen shown in Figure 3.15) and states,

> "...The broken specimen shall pass if...(2) The fillet weld, if fractured, has a fracture surface showing complete fusion to the root of the joint and no inclusion or porosity larger than 3/32 in. [2.5 mm] in greatest dimension, and (3) The sum of the greatest dimensions of all inclusions and porosity shall not exceed 3/8 in. [10 mm] in the 6 in [150 mm] long specimen."[4]

Undercut is limited to 1/32 in. [1 mm] in all portions of the AWS D1.1 code where it is discussed, and this was therefore used as the standard of acceptability for measurements of undercut taken from the specimens. Lastly, fusion of weld metal and base metal were visually inspected to ensure that all portions of the weld cross section exhibited thorough fusion to the base metal.

With regard to fusion, AWS prescribes that thorough fusion shall exist between all layers of weld metal in a multi-pass weld and between the weld metal and the base metal. For the single-pass fillet welds of this study, the etched profiles were used to determine whether there was complete fusion between the weld metal and the base metal.

In summary, the evaluation criteria used for each weld are based on the AWS code acceptance criteria. Table 3-3 summarizes the AWS code acceptance criteria for each type of discontinuity for the plate thickness used and the fillet weld size prescribed. The criteria used in the research program are compared to the visual and macroetch inspection techniques described in AWS D1.1 and D1.6. The criteria listed are for statically loaded, non-tubular, welded connections.

Table 3-3: Evaluation Criteria Summary

Discontinuity Type	AWS Visual Inspection	AWS Macroetch Specimens (5/16-in. fillet weld)	Test Program Evaluation Criteria
Profile	Profiles in conformance with D1.1 Section 5.24, namely must meet criteria in Figure 3.10 above; weld may be undersized by 1/32-in. for no more than 10% of weld length.	Fusion to root of joint, minimum leg size shall meet specified size, profiles shall conform to intended detail, with none of the variations prohibited in 5.24 (Figure 3.10 above).	Profiles in conformance with Figure 3.10 as measured from cross sections.
Cracks	Any crack, regardless of size or location, is unacceptable.	No cracks are permitted when macroetch specimen is inspected visually.	Visible cracks (>1/32-in.) on macroetch specimens are unacceptable. Micro-cracks are noted when observed under the microscope but do not disqualify the weld.
Porosity	Sum of visible piping porosity 1/32-in. or greater in diam. shall not exceed 3/8-in. in any linear in. of weld or ¾-in. in any 12-in. length of weld.	For porosity 1/32-in. or larger, accumulated porosity shall not exceed ¼-in.	Porosity summed on all cross sections and compared toAWS macroetch criteria (previous column); sum of visible piping porosity measured for each weld, compared to visual inspection criteria.
Slag Inclusions	n/a	Sum of greatest dimensions shall not exceed ¼-in.	Sum of greatest dimensions taken on each polished section, compared to AWS macroetch criteria (previous column).
Undercut	Undercut shall not exceed 1/32-in., with the exception that undercut shall not exceed 1/16-in. in an accumulated length of 2-in. in any 12-in.	Undercut shall not exceed 1/32-in.	Undercut measured on each polished section, must be less than 1/32-in.
Incomplete Fusion	Thorough fusion is required between weld metal and base metal.	Thorough fusion is required between weld metal and base metal.	Thorough fusion is required between weld metal and base metal.

Each weld fabricated as part of the research program is examined according to the test program criteria presented in Table 3-3.

3.8 Phase 2 Program

The Phase 2 testing was designed to provide a reasonable means of predicting and measuring the transverse shear strength of welds performed under base conditions (71°F, 35% RH, 0 mph wind) and to investigate the strength of a small number of welds made under adverse environmental conditions. The Phase 2 test specimens were welded in the environmental chamber and subjected to conditions similar to the Phase 1 test specimens. The specimen was modified by offsetting the top plate. This was done to accommodate the necessary grip length in the tensile testing machine and to ensure failure of the specimens through the weld metal, rather than the base metal. The Phase 2 specimen had one 4 in. x 6 in. cover plate lapped over one 4 in. x 6 in. base plate, with both plates oriented in the same direction such that the weld metal was deposited along the six inch plate length, as seen in Figure 3.16. Restraint was maintained using the edge clamps as in Phase 1.

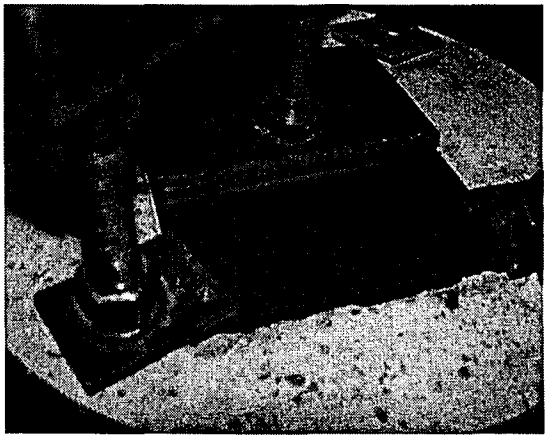

Figure 3.16: Phase 2 Strength Test Specimen in Concrete Block

The welded specimens were cut in half in a direction perpendicular to the weld axis, and each half was further cut to yield two pieces with a reduced weld length of one inch, as shown in Figure 3.17.

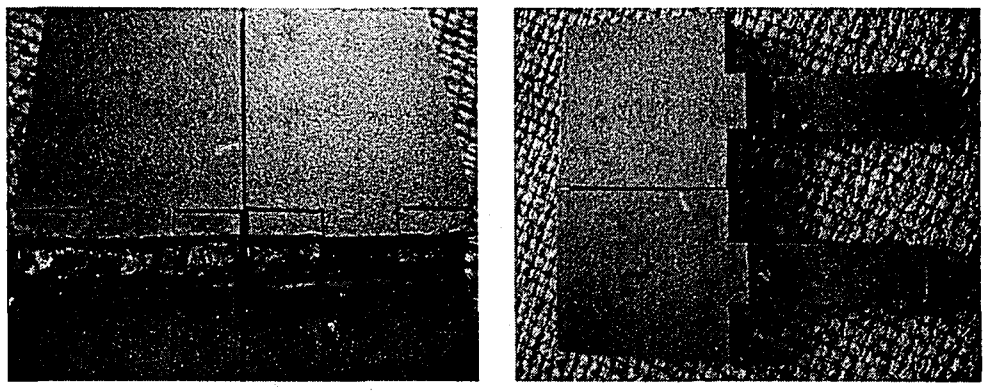

Figure 3.17: Cut Test Specimen

The strength testing of the weld was conducted using a 60 kip universal testing machine. The start and stop portions of the weld were not included in the tested specimen since these portions typically contain a disproportionately high level of pores or other discontinuities and do not represent the majority of the weld. This is standard practice when testing fillet welds, as seen in Figure 3.15 for the case of the fillet weld break test specimen. Finally, a bolt was placed through holes drilled in the cover plate of these two halves, as well as through a central 3/4-in. plate, which served as a grip for the testing machine through which load could be applied concentrically and equally to the welds on either side of the central 3/4-in. plate (Figure 3.18).

The welded specimens were cut in half in a direction perpendicular to the weld axis, and each half was further cut to yield two pieces with a reduced weld length of one inch, as shown in Figure 3.17.

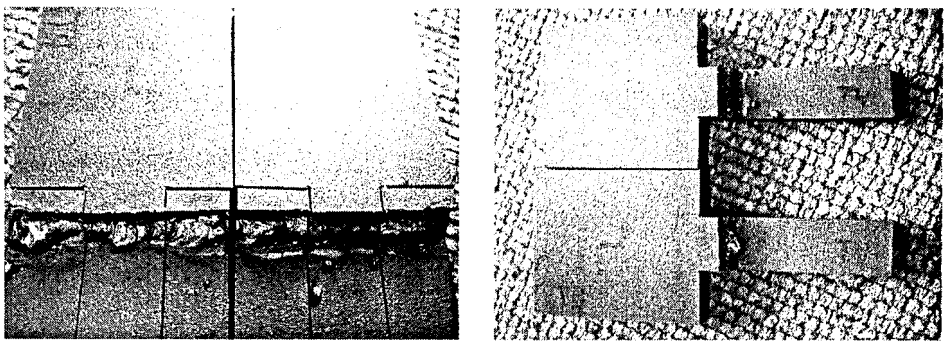

Figure 3.17: Cut Test Specimen

The strength testing of the weld was conducted using a 60 kip universal testing machine. The start and stop portions of the weld were not included in the tested specimen since these portions typically contain a disproportionately high level of pores or other discontinuities and do not represent the majority of the weld. This is standard practice when testing fillet welds, as seen in Figure 3.15 for the case of the fillet weld break test specimen. Finally, a bolt was placed through holes drilled in the cover plate of these two halves, as well as through a central 3/4-in. plate, which served as a grip for the testing machine through which load could be applied concentrically and equally to the welds on either side of the central 3/4-in. plate (Figure 3.18).

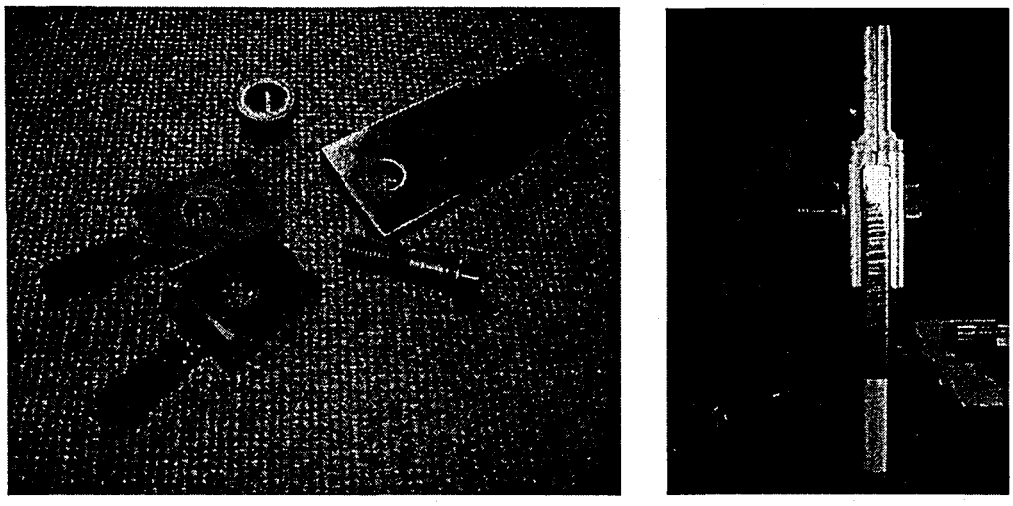

Figure 3.18: Complete Phase 2 Strength Test Specimen

Testing of the resulting Phase 2 strength test specimen loaded the one inch weld segments in transverse shear, as the diagram of the complete test specimen (Figure 3.19) shows. The testing machine and test specimen are shown in Figure 3.20.

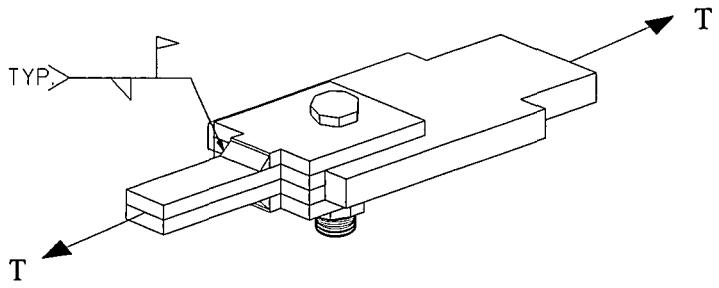

Figure 3.19: Phase 2 Strength Test Specimen Detail

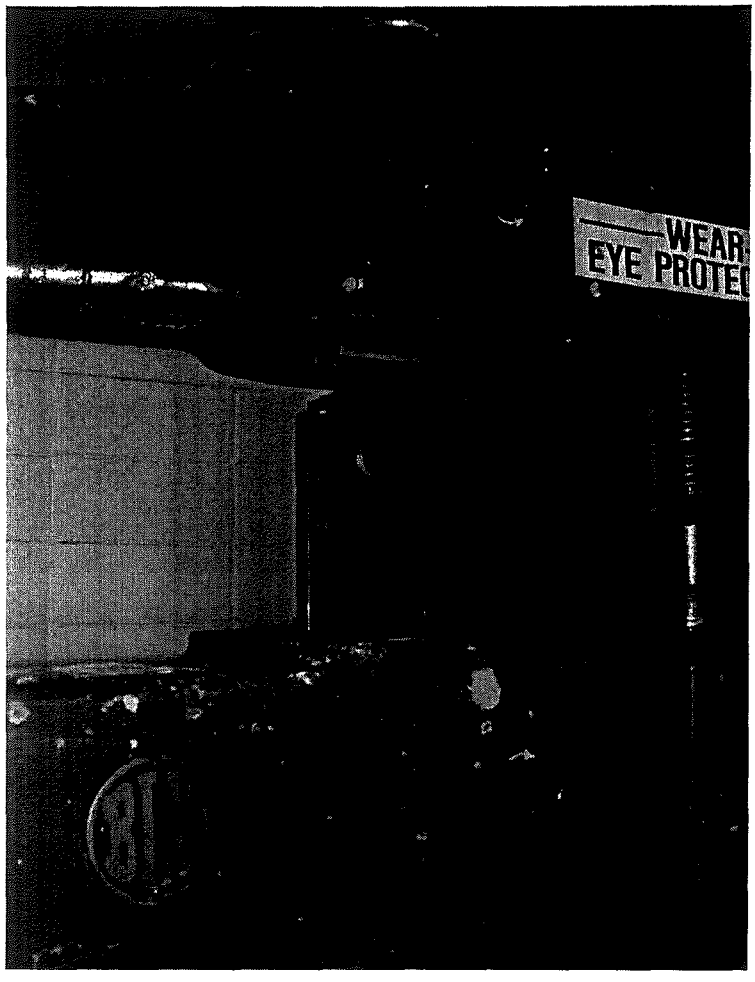

Figure 3.20: Tensile Test Apparatus and Loaded Specimen

Strength test specimens welded under base conditions (nominally 71°F, 35% RH, 0 mph) were tested using the low carbon A36 and high carbon A36 steel plate. The nominal failure load of a given weld was predicted using a modified version of the AISC weld strength equation[28]:

$$P = 0.6F_{EXX} \cdot T \cdot l \cdot 1.5 \qquad \text{Equation 3}$$

where P is the predicted failure load [kips] of a single weld, F_{EXX} is the *nominal* weld metal tensile strength [ksi], T is the minimum measured weld throat dimension [in.], and l is the

measured length of the weld [in.]. The factor of 1.5 is a multiplication factor included in the expression because the shear loading is transverse, increasing the strength by 50% as compared to longitudinal shear loading (i.e. loading in the direction of the weld axis), as described in Section J2.4 of the AISC Specifications for Structural Steel Buildings[28].

The conditions under which the five test specimens were welded are presented in Table 3-4.

Table 3-4: Phase 2 Test Matrix

ID	Base Material	Temp. [°F]	Relative Humidity %RH	Wind Speed [mph]	Electrode Condition	Plate Surface Condition
T-1	ASTM A36 (Orig.)	84	15.4	0	AWS D1.1*	Dry
T-2	ASTM A36 High Carbon(2)	77.9	26.4	0	AWS D1.1	Dry
T-3	ASTM A36 High Carbon(2)	-15.4	73	0	AWS D1.1	Dry
T-4	ASTM A36 High Carbon(1)	72	32.3	0	AWS D1.1	Wet**
T-5	ASTM A36 High Carbon(2)	72.7	19.3	0	AWS D1.1	Wet

*AWS D1.1 indicates proper storage of electrodes according to AWS D1.1 specifications.
** Wet indicates intentional application of liquid moisture to thoroughly wet all plate surfaces.

The predicted failure loads of the specimens are calculated as described in Chapter 8 subsequently, and the predicted loads are then compared to the measured test data.

4 A36 Phase 1 Specimens

The first set of Phase 1 tests examines the sensitivity of fillet welds made on ASTM A36[27] carbon steel under varying environmental conditions. Due to the possibility of corrosion, this material is commonly used under conditions where long term exposure to moisture is not a concern.

As previously discussed, higher carbon levels in the base metal increases the potential for cold cracking in the weld or HAZ of the base metal. The ASTM A36 specification permits a carbon content of up to 0.25% by weight for plates up to ¾ in. [20 mm] thick. This thickness represents the upper bound for plates used in precast concrete construction.

Two types of A36 material were examined, one with a high carbon level and the other with a moderate level. The carbon levels were chosen relative to the A36 steel material currently available in the market. A survey of 6 steel plate producers around the country was conducted. 78 mill certificates for A36 steel thin angle and plate material (1/4-in., 3/8-in.) were obtained and tabulated. The survey of mill certificate values indicated a maximum carbon content of 0.22% by weight, a minimum of 0.10% and an average of 0.18%. The standard deviation was 0.04.

The moderate carbon A36 material used in the study contained a carbon content of 0.13% and a carbon equivalent (CE) of 0.330 as determined by the independent chemical analysis of the plate material. The higher carbon A36 material came from two separate heats of steel, one with a carbon content of 0.21% and CE of 0.425, and the other with a carbon content of 0.19% and CE of 0.397. The chemical and material properties of these A36 steel plates are presented in Table 4-1, Table 4-2 and Table 4-3.

4.1 Carbon Steel Base Metal Material Properties

The moderate carbon A36 plate was supplied as 6-in. x 3/8-in. bar stock. Plates were pre-cut to the required size of ⅜-in. x 4-in. x 6-in and arranged and welded in accordance with the procedure described in Section 3.1. The A36 specimens were restrained at the four corners of the base plates and on the cover plate as shown in Figure 4.1.

The moderate carbon A36 plate material was obtained as a donation through High Concrete Structures, Inc. The plate material came from the Durrett Sheppard Steel Co., originating from the Roanoke Bar Division of Steel Dynamics®. The chemical composition of the steel and the mechanical properties were obtained from the mill certificate for the steel used. An additional independent chemical analysis was made by Laboratory Testing, Inc., of Hatfield, PA. The values of the chemical composition from the independent analysis and from the mill certificate are summarized in Table 4-1 with the computed carbon equivalent (AWS formulation), along with the mechanical properties of the material.

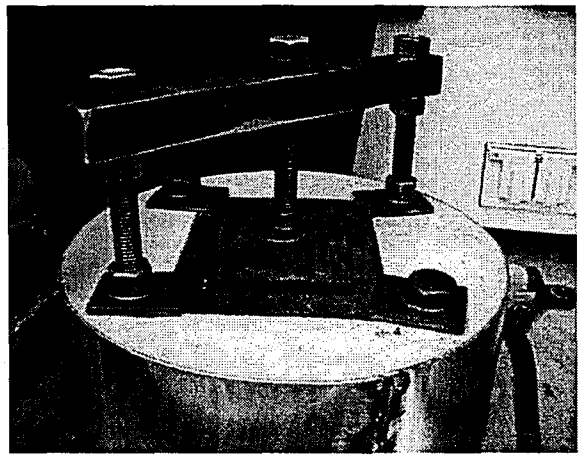

Figure 4.1: A36 Steel Specimen in Setup

Table 4-1: A-36 Material Data

Heat Number						JF3653				
Manufacturer						Steel Dynamics®-Roanoke Bar Division				
Applicable Specimens						36-XX, 36-PC1 through 36-PC5				
Specifications										
ASTM A36-04			ASME SA36QQS741D			ASTM A709-00A GR36				
Chemical Composition [%]-Independent Chemical Analysis Values										
C	Mn	P	S	Si	Cr	Ni	Nb	Cu	V	Mo	CE
0.13	0.74	0.010	0.026	0.13	0.087	0.084	0.001	0.33	0.002	0.05	0.330
Chemical Composition [%]-Mill Certificate Values										
C	Mn	P	S	Si	Cr	Ni	Nb	Cu	V	Mo	CE
0.12	0.84	0.010	0.026	0.15	0.09	0.09	0.002	0.38	0.003	0.02	0.339
Mechanical Properties										
Mill Cert Test Number			Yield Stress [ksi]			Ultimate Stress [ksi]			Elongation [%-8-in.]	
1			44.6			65.9			31.9	
2			43.2			65.3			34.4	

The high carbon A36 plate material was obtained as a donation through Metromont Corporation. The plate material came from the Nucor Bar Mill Group, Darlington Division. The chemical composition of the steel and the mechanical properties were obtained from the mill certificate for the steel used. An additional independent chemical analysis was completed by Laboratory Testing, Inc., of Hatfield, PA. The values of the chemical composition from the independent analyses and from the mill certificates are summarized in Table 4-2 and Table 4-3, along with the mechanical properties of the materials.

Table 4-2: High Carbon A-36 Material Data-Heat 1										
Heat Number				767625						
Manufacturer				NUCOR Bar Mill Group-Darlington Division						
Applicable Specimens				36-CX						
Specifications										
ASTM A36			ASME SA36(250)				ASTM A709 GR36(250)			
Chemical Composition [%]-Independent Chemical Analysis Values										
C	Mn	P	S	Si	Cr	Ni	Cu	V	Mo	CE
0.21	0.73	0.02	0.04	0.15	0.12	0.11	0.43	0.002	0.04	0.425
Chemical Composition [%]-Mill Certificate Values										
C	Mn	P	S	Si	Cr	Ni	Cu	V	Mo	CE
0.21	0.74	0.010	0.040	0.17	0.16	0.10	0.36	0.004	0.02	0.429
Mechanical Properties										
Mill Cert Test Number			Yield Stress [ksi]				Ultimate Stress [ksi]			
1			52				76			
2			53				76			

Table 4-3: High Carbon A-36 Material Data-Heat 2										
Heat Number				770217						
Manufacturer				NUCOR Bar Mill Group-Darlington Division						
Applicable Specimens				36-PC6						
Specifications										
ASTM A36			ASME SA36(250)				ASTM A709 GR36(250)			
Chemical Composition [%]-Independent Chemical Analysis Values										
C	Mn	P	S	Si	Cr	Ni	Cu	V	Mo	CE
0.19	0.68	0.02	0.02	0.14	0.14	0.08	0.45	0.003	0.03	0.397
Chemical Composition [%]-Mill Certificate Values										
C	Mn	P	S	Si	Cr	Ni	Cu	V	Mo	CE
0.22	0.71	0.010	0.040	0.15	0.14	0.10	0.41	0.005	0.02	0.430
Mechanical Properties										
Mill Cert Test Number			Yield Stress [ksi]				Ultimate Stress [ksi]			
1			52				74			
2			52				75			

4.2 Carbon Steel Weld Material Properties

The SMAW electrode used for the A36 steel weld specimens was E7018-H4R, shown in Figure 4.2. This rod is readily available and used in field welding processes for precast construction. It is a low-hydrogen rod which, in the field, helps to prevent hydrogen related

discontinuities, such as porosity and cold cracking by preventing significant absorption of moisture by the flux coating of the rod.

The electrodes used in this study were 5/32-in. E7018-H4R Code-Arc® electrodes, manufactured by The Lincoln Electric Company. Mill data was obtained for the general electrode type from a Certificate of Conformance for the Code-Arc® 7018 MR electrodes, meeting specifications AWS A5.1-91 and ASME SFA-5.1, with tests completed February 26, 2004. The data provided indicated that the ultimate strength of the weld metal is 77,900 psi, and the yield strength is 63,600 psi. The elongation is listed as 32%, and the average Rockwell Hardness (B) is 87.

The electrodes were stored at approximately 250°F in a holding oven in close proximity to the environmental chamber and were removed prior to use for the test specimens. The electrodes were typically exposed to the ambient environment for approximately one half hour to one hour before use. The E7018-H4R electrodes may be exposed to a moist environment for up to nine hours before they must be returned to a holding oven. If exposed to a moist environment for less than nine hours, they may be kept in a holding oven at 250°F for four hours and re-issued. The electrodes were therefore handled according to AWS D1.1 standards as described in Section 3.1[4] except for cases where electrodes were intentionally exposed to a moist environment prior to testing, in which case they were exposed in the environmental chamber as shown in

Figure 4.2.

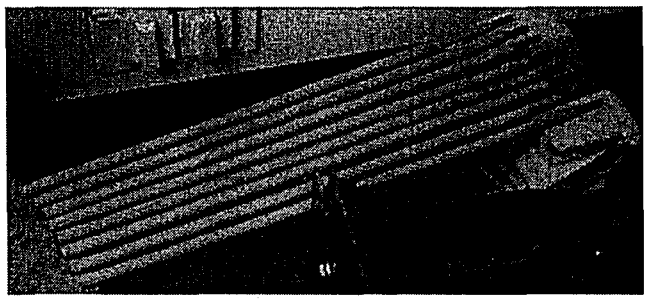

Figure 4.2. E-7018 H4R Electrodes

4.3 Specimen Performance Evaluation

The results for each ASTM A36 welded specimen are described in the following sections. Each specimen description includes a table summarizing the nominal environmental conditions from the test matrix as well as the measured conditions prior to welding. Images of the weld specimen, weld beads, and four cross-sections are shown, and descriptions of the weld surface condition and cross section flaws are noted. The weld surface condition is noted below the image of each weld in the specimen descriptions using the profile index discussed in Section 3.7.3. Additionally, when of specific interest, microscopic images of discontinuities are presented with accompanying descriptions of the discontinuities. When microscopic images are included, a yellow box on a cross-section image denotes the area included in the associated microscopic image.

4.4 Specimen 36-1: Base Condition

This specimen was subjected to the environmental conditions shown in Table 4-4 in the environmental chamber at the time of welding.

Table 4-4: Environmental Conditions – Specimen 36-1					
Specimen: 36-1	Air Temp.	Concrete Temp.	Steel Temp.	Rel. Humidity	Wind Speed
	°F	°F	°F	%RH	[mph]
Nominal Values	71	71	71	35	0
Measured Values	71	72	72	41	0

The welded specimen is shown in Figure 4.3. Photographs of each of the two welds are presented along with an overview photo of the entire specimen. Sections were taken at four locations from the specimen and polished to examine the quality of the weld. These photos are also included.

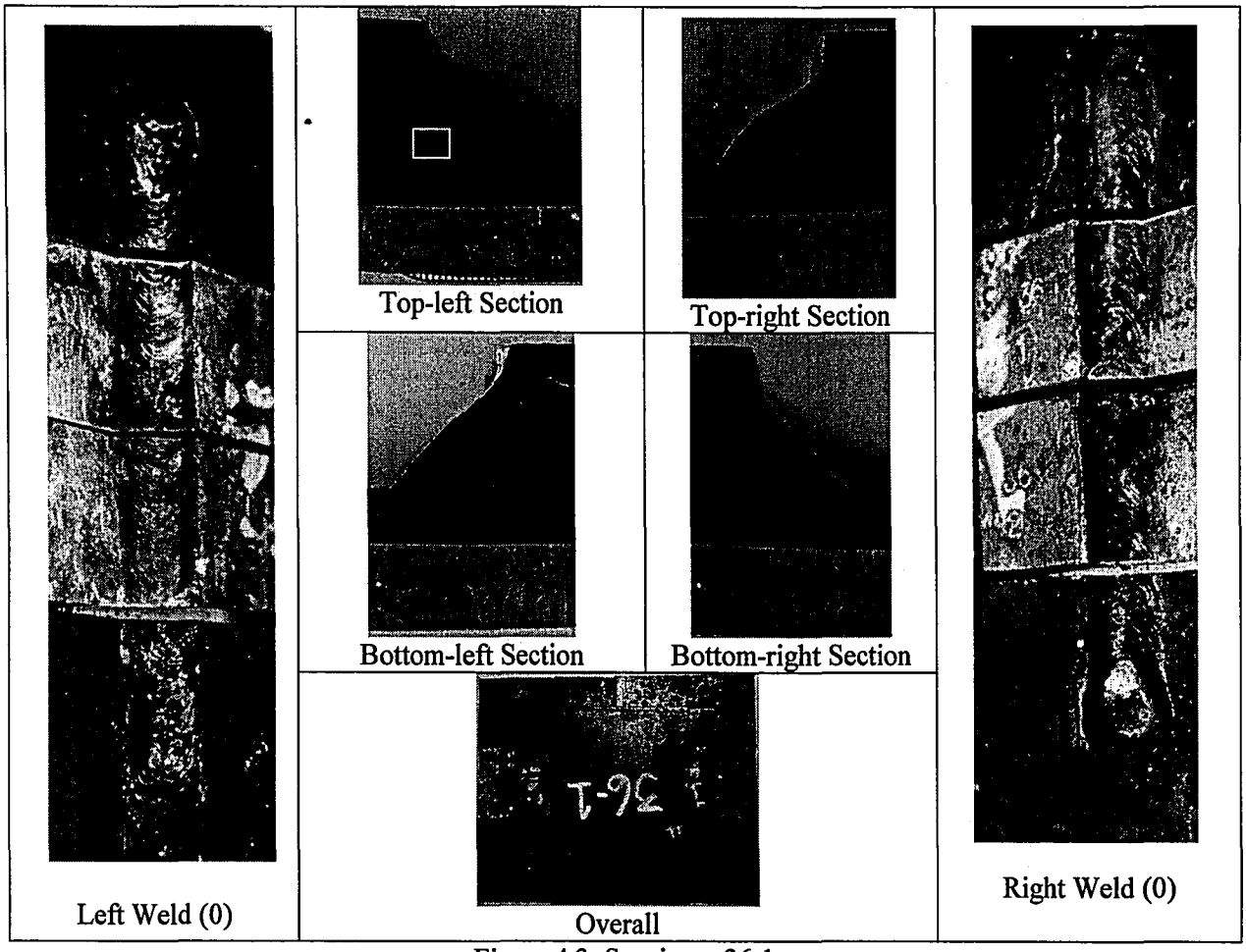

Figure 4.3: Specimen 36-1

4.4.1 Visual Observation Summary

From an external perspective, the ends of the right and left welds both exhibit some edge-melt (a condition named for the apparent melting of the top edge of the cover plate, as seen in the bottom of the right-most image above). The weld surface condition is noted below the images of the right weld and left weld in Figure 4.3, as is the case for all specimen descriptions which follow. All but one of the sections (bottom-right) met the full 1/4-in. size requirements.

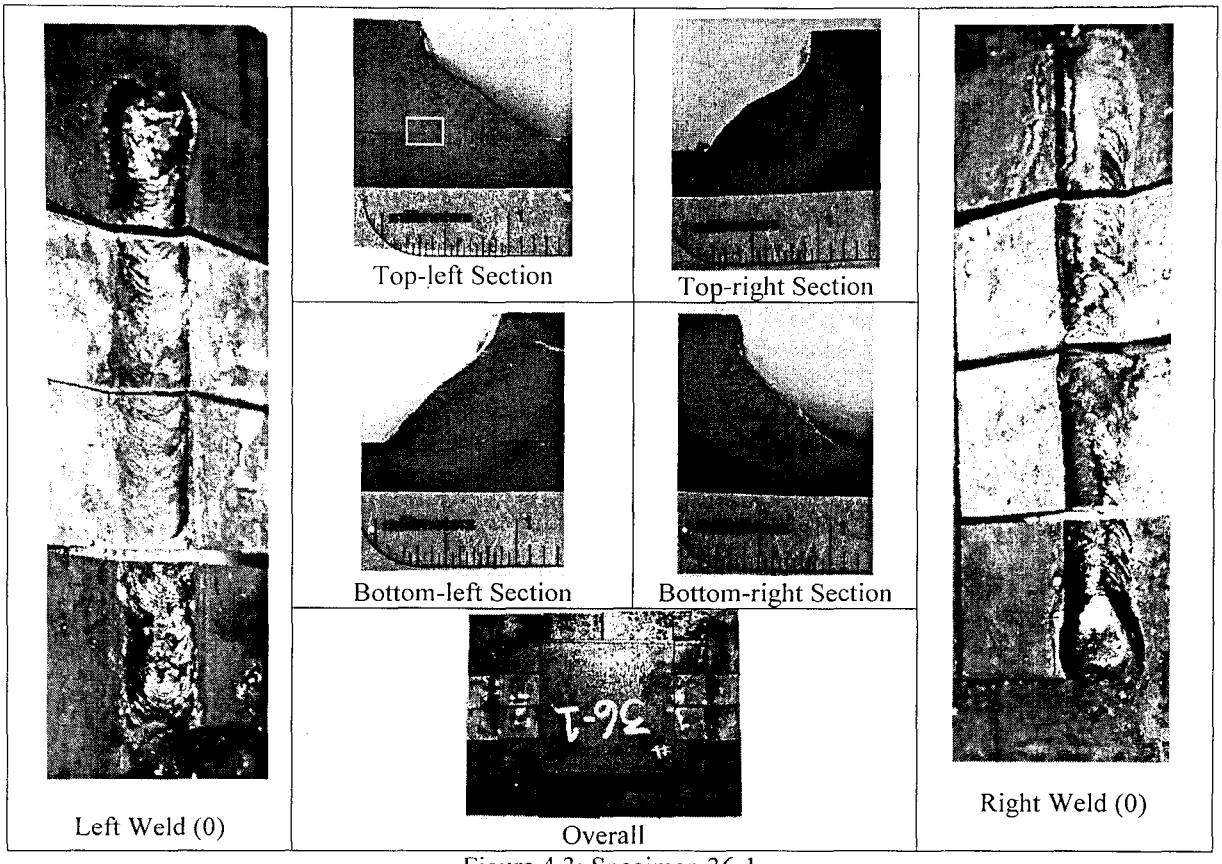

Figure 4.3: Specimen 36-1

4.4.1 Visual Observation Summary

From an external perspective, the ends of the right and left welds both exhibit some edge-melt (a condition named for the apparent melting of the top edge of the cover plate, as seen in the bottom of the right-most image above). The weld surface condition is noted below the images of the right weld and left weld in Figure 4.3, as is the case for all specimen descriptions which follow. All but one of the sections (bottom-right) met the full 1/4-in. size requirements.

4.4.2 Microscopy Observation Summary

The top left section showed a small amount of micro-cracking at the root, and Figure 4.4 shows the micro-cracking observed at the root of the weld. There appears to be some solidification micro-cracking protruding from the root of the weld, as well as a fusion line discontinuity leading to a pore at the lower right of the image.

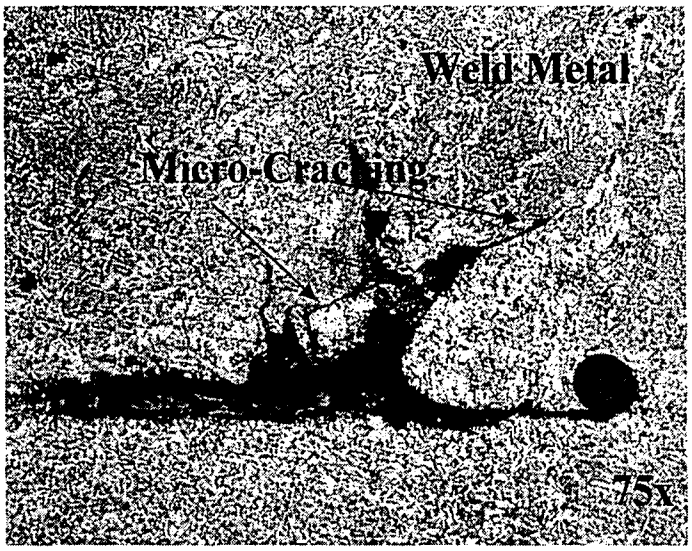

Figure 4.4: Micro-Cracking in Specimen 36-1, Top-left Section

4.5 Specimen 36-3: Warm, High Humidity, No Wind

This specimen was subjected to the environmental conditions shown in Table 4-5 in the environmental chamber at the time of welding.

Table 4-5: Environmental Conditions – Specimen 36-3

Specimen: 36-3	Air Temp.	Concrete Temp.	Steel Temp.	Rel. Humidity	Wind Speed
	°F	°F	°F	%RH	[mph]
Nominal Values	71	71	71	95	0
Measured Values	70.5	73.1	72.5	98.2	0

The welded specimen is shown in Figure 4.5. Photographs of each of the two welds are presented along with an overview photo of the entire specimen. Sections were taken at four

locations from the specimen and polished to examine the quality of the weld. These photos are also included.

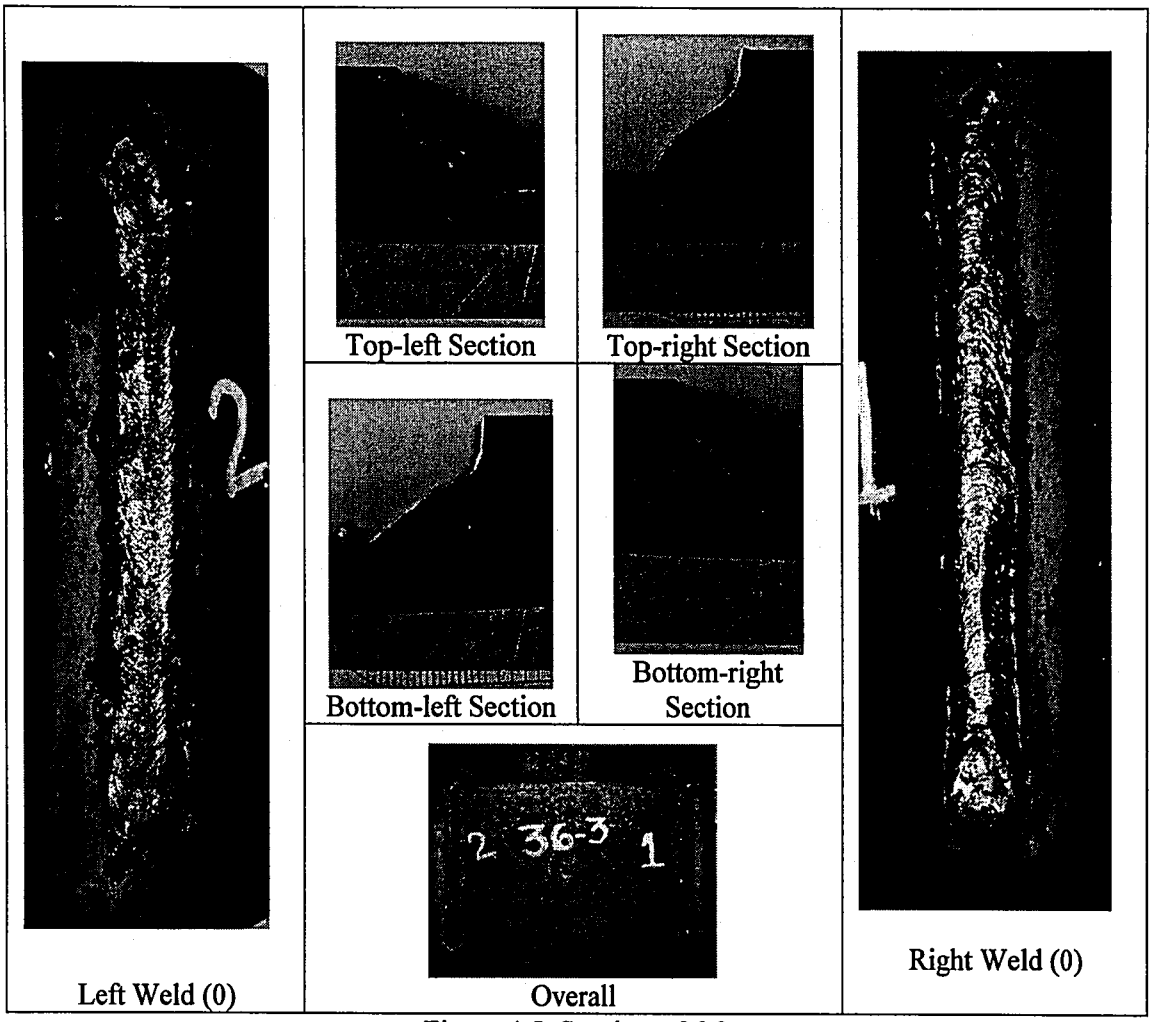

Figure 4.5: Specimen 36-3

4.5.1 Visual Observation Summary

The end of the right weld displays a small amount of edge-melt, but neither of the welds had any observed pores or undercut. The bottom-left section had a very small inclusion (.014-in.) near the root of the weld, and all four sections had slightly convex profiles; however, convexity was well within acceptable limits for all sections. The top-right section was the only section that met the full 1/4-in. profile requirements.

locations from the specimen and polished to examine the quality of the weld. These photos are also included.

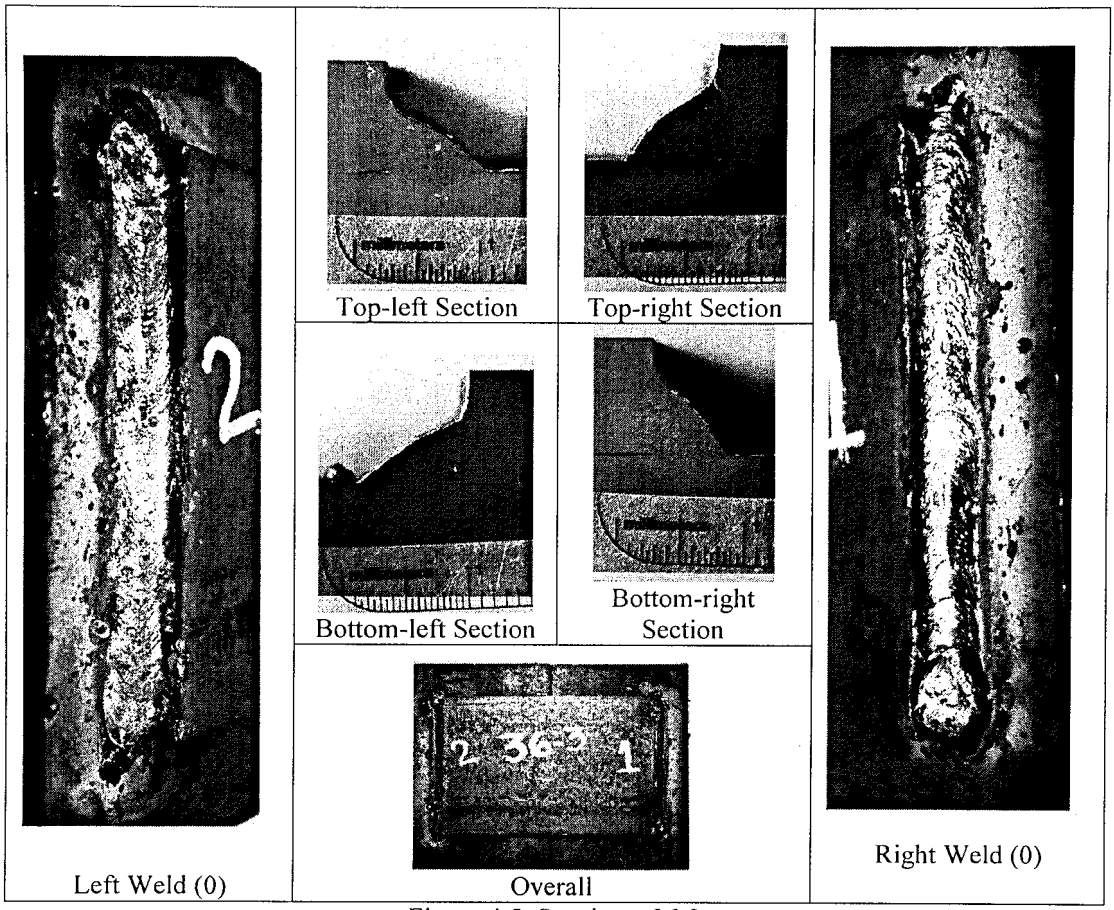

Figure 4.5: Specimen 36-3

4.5.1 Visual Observation Summary

The end of the right weld displays a small amount of edge-melt, but neither of the welds had any observed pores or undercut. The bottom-left section had a very small inclusion (.014-in.) near the root of the weld, and all four sections had slightly convex profiles; however, convexity was well within acceptable limits for all sections. The top-right section was the only section that met the full 1/4-in. profile requirements.

4.6 Specimen 36-6 Warm, High Humidity, 20 mph Wind

This specimen was subjected to the environmental conditions shown in Table 4-6 in the environmental chamber at the time of welding.

Table 4-6: Environmental Conditions – Specimen 36-6					
Specimen: 36-6	Air Temp.	Concrete Temp.	Steel Temp.	Rel. Humidity	Wind Speed
	°F	°F	°F	%RH	[mph]
Nominal Values	71	71	71	95	20
Measured Values	71.2	81.8	76.6	94.3	20

The welded specimen is shown in Figure 4.6. Photographs of each of the two welds are presented along with an overview photo of the entire specimen. Sections were taken at four locations from the specimen and polished to examine the quality of the weld. These photos are also included.

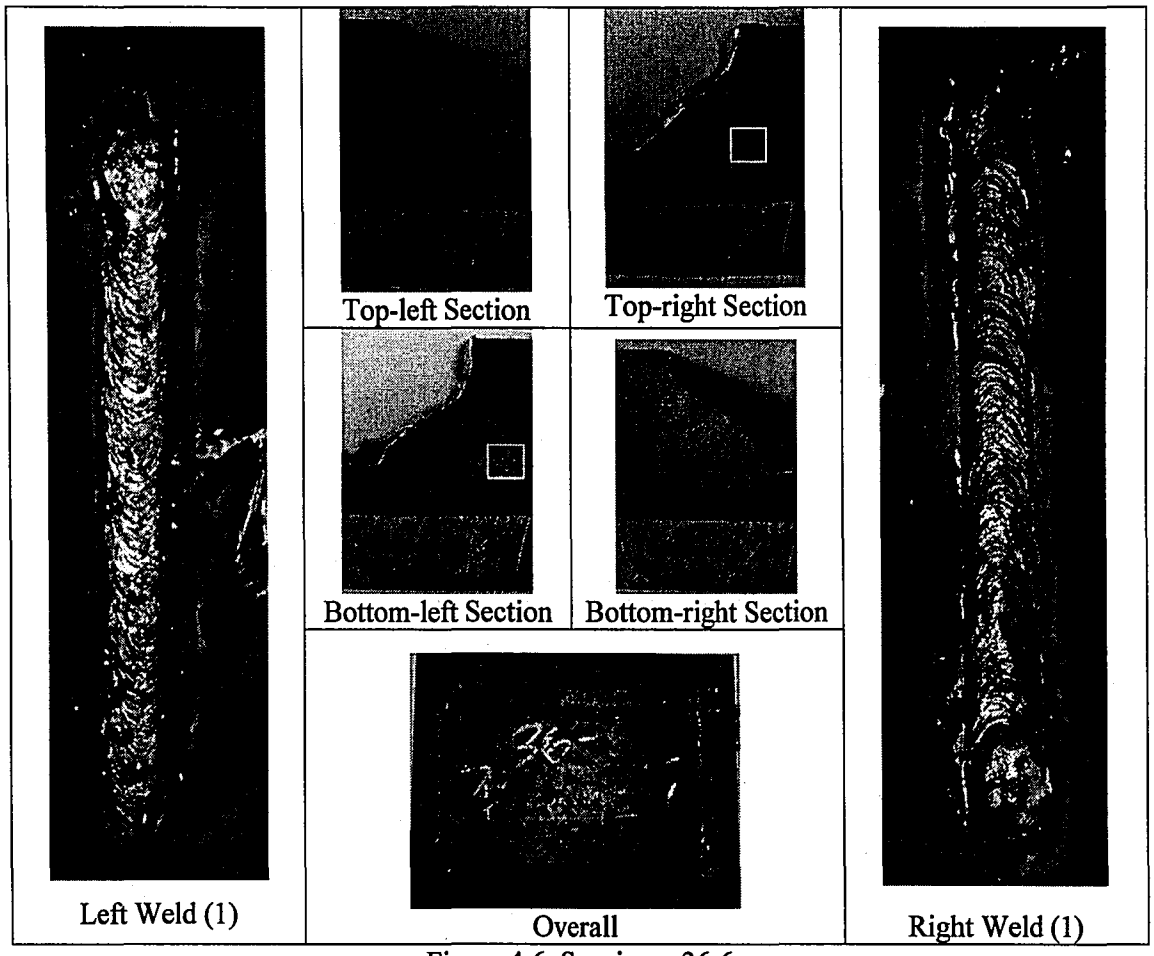

Figure 4.6: Specimen 36-6

4.6.1 Visual Observation Summary

There were no notable surface flaws on either of the welds. The top-right section had a skew to the vertical leg of the weld, and all three remaining sections had convex profiles, and all but the top-left section met ¼-in. profile requirements. The top left section had a root slag inclusion (.042-in.). The top-right, bottom-right, and bottom-left sections had discontinuities along the horizontal fusion line, and microscopic images of the two of these discontinuities are shown in 4.6.2. These discontinuities represent small segments exhibiting incomplete fusion at the root and are visible without microscopy at approximately 1/32-in. in length.

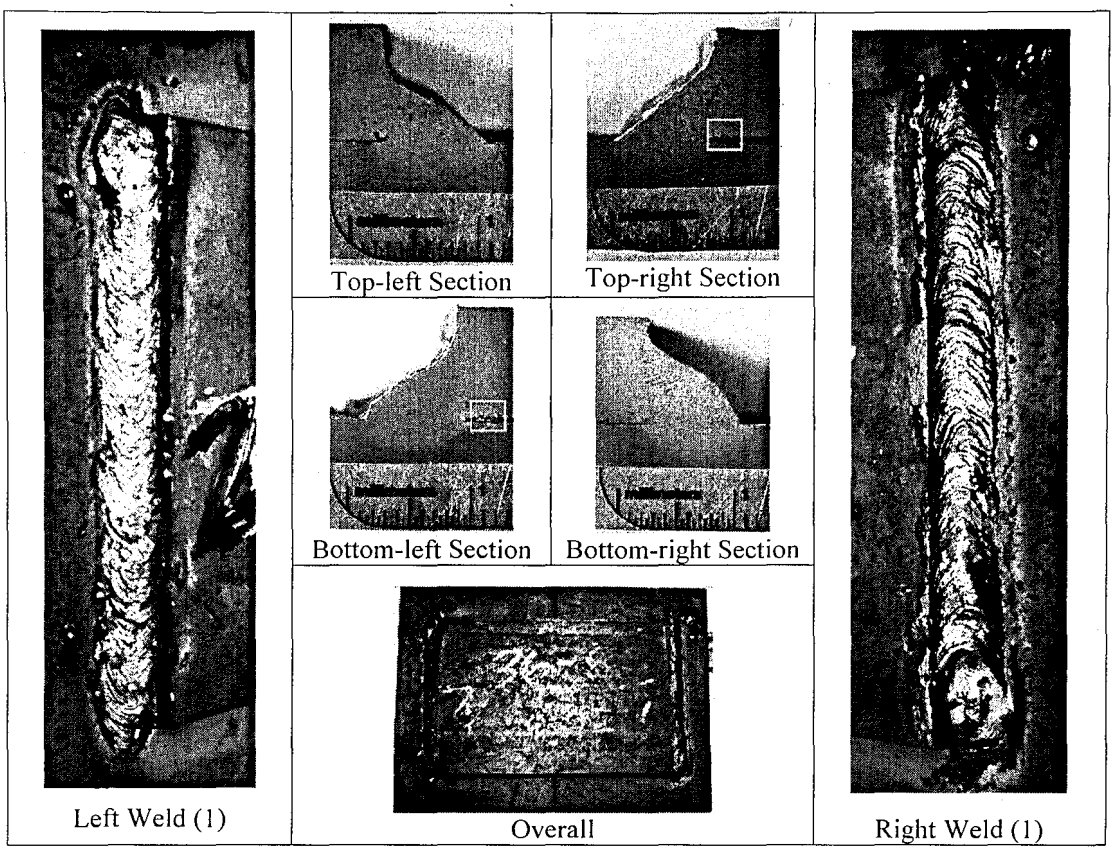

Figure 4.6: Specimen 36-6

4.6.1 Visual Observation Summary

There were no notable surface flaws on either of the welds. The top-right section had a skew to the vertical leg of the weld, and all three remaining sections had convex profiles, and all but the top-left section met ¼-in. profile requirements. The top left section had a root slag inclusion (.042-in.). The top-right, bottom-right, and bottom-left sections had discontinuities along the horizontal fusion line, and microscopic images of the two of these discontinuities are shown in 4.6.2. These discontinuities represent small segments exhibiting incomplete fusion at the root and are visible without microscopy at approximately 1/32-in. in length.

4.6.2 Microscopy Observation Summary

The following images show two of the sections from Specimen 36-6 and are taken near the root of the sections. They each show a lack of fusion between weld metal and base metal, with a portion of the heat affected zone (HAZ) still below the discontinuity. The HAZ formed as a result of heat transfer around the incomplete fusion without actually fusing the weld metal and base metal.

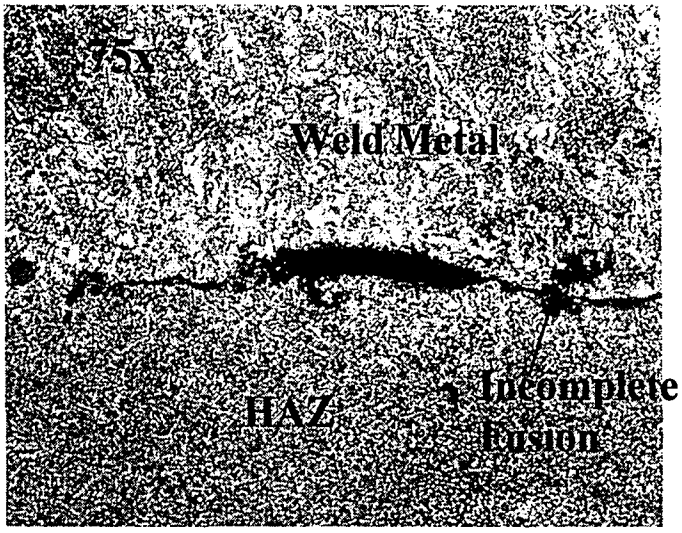

Figure 4.7: Incomplete Fusion-Specimen 36-6, Top-right Section

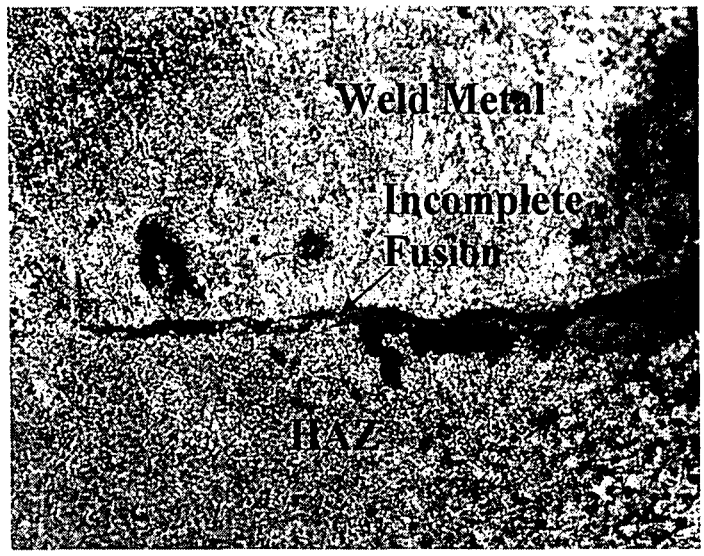

Figure 4.8: Incomplete Fusion-Specimen 36-6, Bottom-left Section

4.7 Specimen 36-7 Warm, High Humidity, 35 mph Wind

This specimen was subjected to the environmental conditions shown in Table 4-7 in the environmental chamber at the time of welding.

Table 4-7: Environmental Conditions – Specimen 36-7

Specimen: 36-7	Air Temp.	Concrete Temp.	Steel Temp.	Rel. Humidity	Wind Speed
	°F	°F	°F	%RH	[mph]
Nominal Values	71	71	71	95	35
Measured Values	70.8	74.7	73.6	97.8	34.7

The welded specimen is shown in Figure 4.9. Photographs of each of the two welds are presented along with an overview photo of the entire specimen. Sections were taken at four locations from the specimen and polished to examine the quality of the weld. These photos are also included.

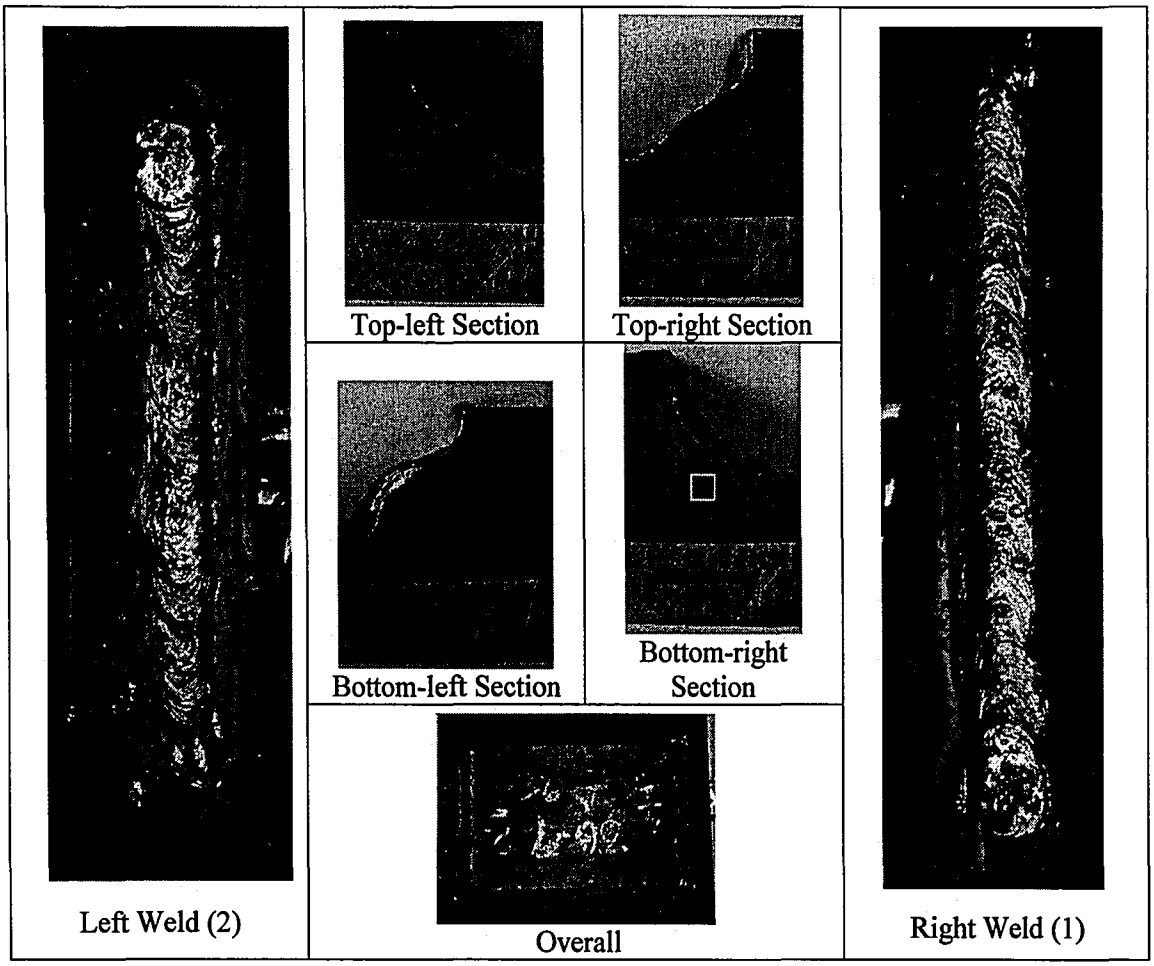

Figure 4.9: Specimen 36-7

4.7.1 Visual Observation Summary

The right weld had a relatively short vertical leg, with the bottom-right section below the 1/4-in. profile requirements. The bottom-right and both left sections had convex profiles, with the top-left profile also not meeting ¼-in. requirements. The left weld had a fair amount of edge-melt along the weld, some of which could be categorized as mild undercut (.012-in.). There was a small root inclusion in each of the top and bottom right sections (.013-in., .017-in.). The bottom-right section also had a root crack, shown in 4.7.2. Also notable is the fact that the welding chamber became extremely foggy during welding, making visibility quite difficult and thereby likely reducing the quality of the weld.

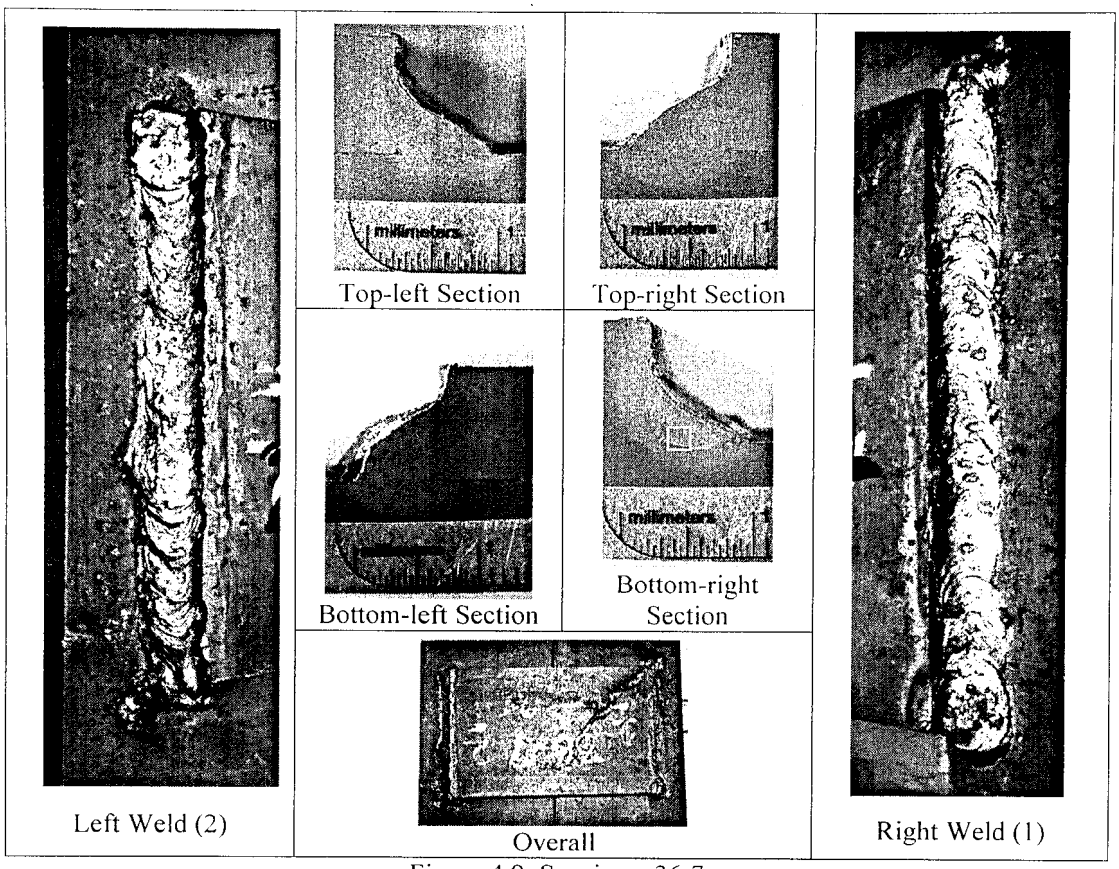

Figure 4.9: Specimen 36-7

4.7.1 Visual Observation Summary

The right weld had a relatively short vertical leg, with the bottom-right section below the 1/4-in. profile requirements. The bottom-right and both left sections had convex profiles, with the top-left profile also not meeting ¼-in. requirements. The left weld had a fair amount of edge-melt along the weld, some of which could be categorized as mild undercut (.012-in.). There was a small root inclusion in each of the top and bottom right sections (.013-in., .017-in.). The bottom-right section also had a root crack, shown in 4.7.2. Also notable is the fact that the welding chamber became extremely foggy during welding, making visibility quite difficult and thereby likely reducing the quality of the weld.

4.7.2 Microscopy Observation Summary

The bottom-right section of Specimen 36-7 displays a root crack, which is shown below in Figure 4.10 and is notable upon close visual examination without microscopy. Notable is the fact that this crack formed directly along the boundary between the HAZ and weld metal, and the region with the highest hardness is the coarse-grained HAZ, located immediately to the left of this boundary as viewed in Figure 4.10. Additionally, this crack formed between other discontinuities.

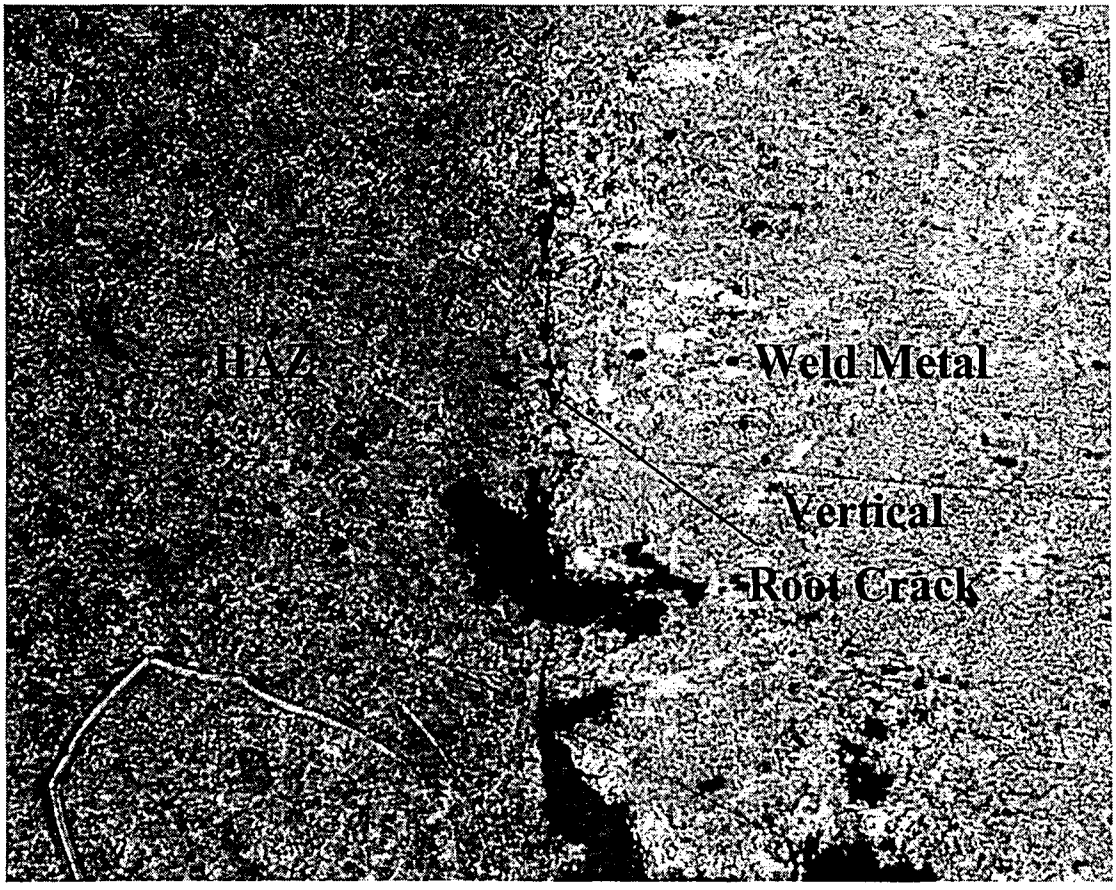

Figure 4.10: Vertical Root Crack-Specimen 36-7, Bottom-right Section

4.8 Specimen 36-8: Warm, Surface Wet, No Wind

This specimen was subjected to the environmental conditions shown in Table 4-8 in the environmental chamber at the time of welding.

Table 4-8: Environmental Conditions – Specimen 36-8					
Specimen: 36-8	Air Temp.	Concrete Temp.	Steel Temp.	Rel. Humidity	Wind Speed
	°F	°F	°F	%RH	[mph]
Nominal Values	71	71	71	Surface Wet	0
Measured Values	72.1	83.8	78.3	92.4-surf. misted	0

The welded specimen is shown in Figure 4.11. Photographs of each of the two welds are presented along with an overview photo of the entire specimen. Sections were taken at four locations from the specimen and polished to examine the quality of the weld. These photos are also included.

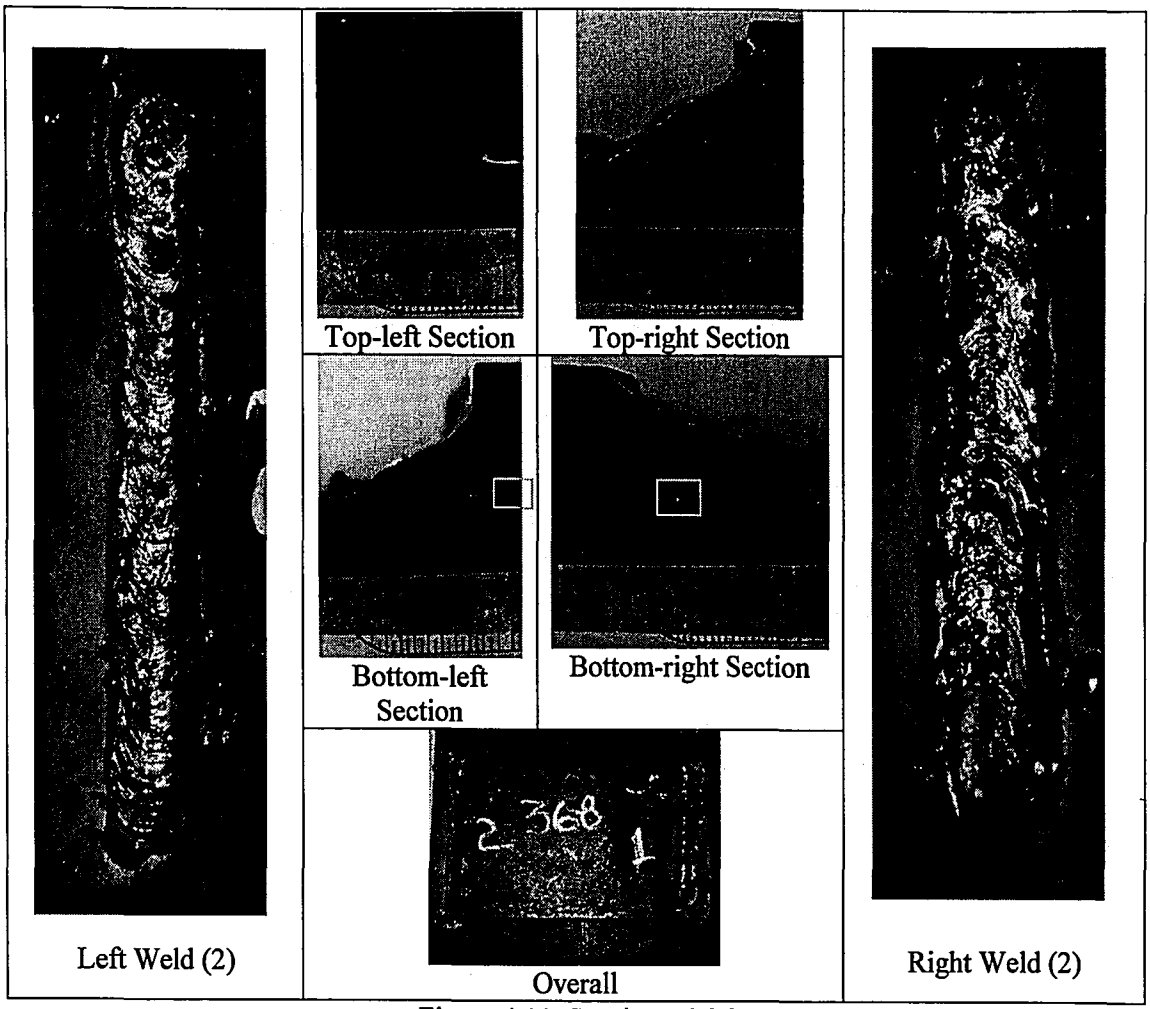

Figure 4.11: Specimen 36-8

4.8.1 Visual Observation Summary

The right weld contained three surface pores (.031-in., .062-in., .037-in.) and had severe edge-melt. The left weld contained two surface pores (.069-in., .064-in.) and exhibited end edge-melt. The bottom-right section exhibited severe edge-melt and bulging toward the horizontal leg, as well as a root inclusion (.035-in.) and what appears to be two much smaller inclusions (.004-in., .004-in.) near the root. Undercut can be seen in both the top-right and top-left sections (.023-in., .034-in.). Due to profile irregularities, none of the sections met the 1/4-in. profile requirements.

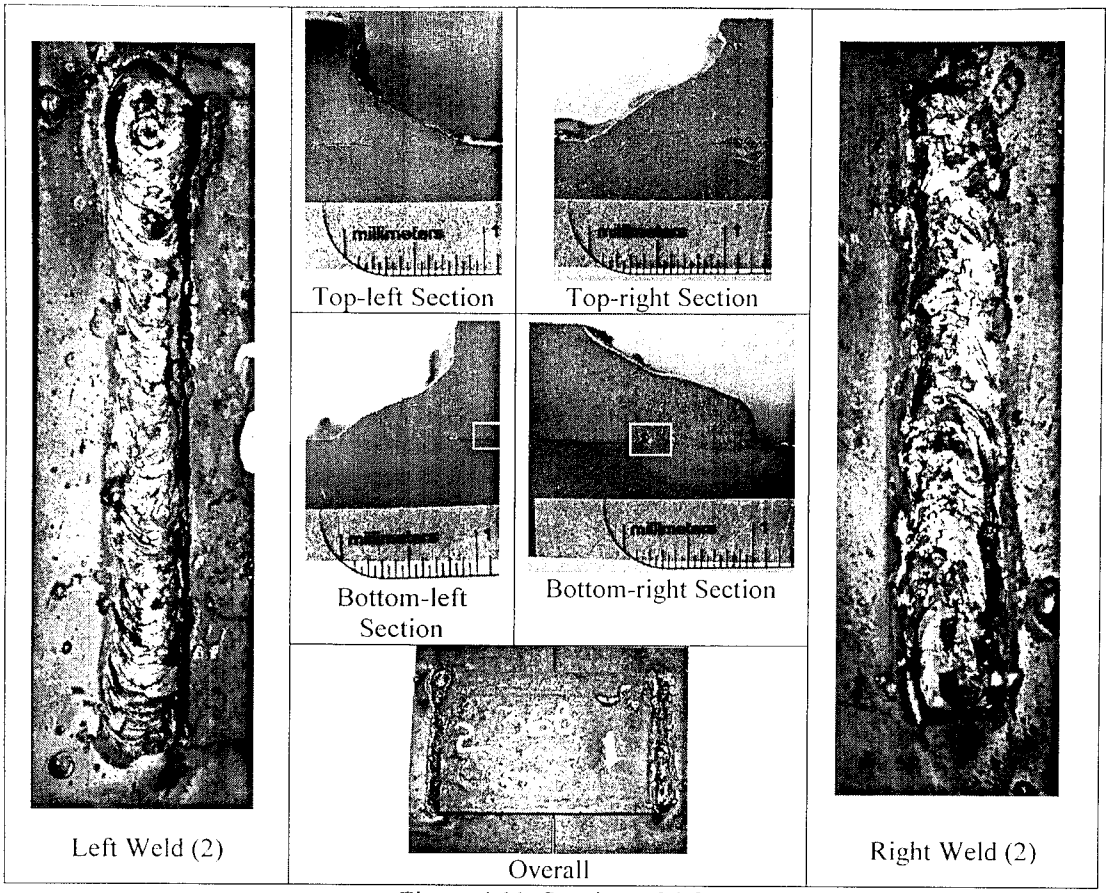

Figure 4.11: Specimen 36-8

4.8.1 Visual Observation Summary

The right weld contained three surface pores (.031-in., .062-in., .037-in.) and had severe edge-melt. The left weld contained two surface pores (.069-in., .064-in.) and exhibited end edge-melt. The bottom-right section exhibited severe edge-melt and bulging toward the horizontal leg, as well as a root inclusion (.035-in.) and what appears to be two much smaller inclusions (.004-in., .004-in.) near the root. Undercut can be seen in both the top-right and top-left sections (.023-in., .034-in.). Due to profile irregularities, none of the sections met the 1/4-in. profile requirements.

4.8.2 Microscopy Observation Summary

The bottom-right section displayed incomplete fusion at the root, and the bottom-left section exhibited micro-cracking at the root. It should be noted that the visibility was severely limited due to steam caused by welding over moist surface. Figure 4.12 depicts a lack of fusion for a segment of weld at the root with associated micro-cracking through other local discontinuities. Micro-cracks at the root of the bottom-left section can be seen in Figure 4.13. It can again be observed that the micro-cracking formed between local discontinuities.

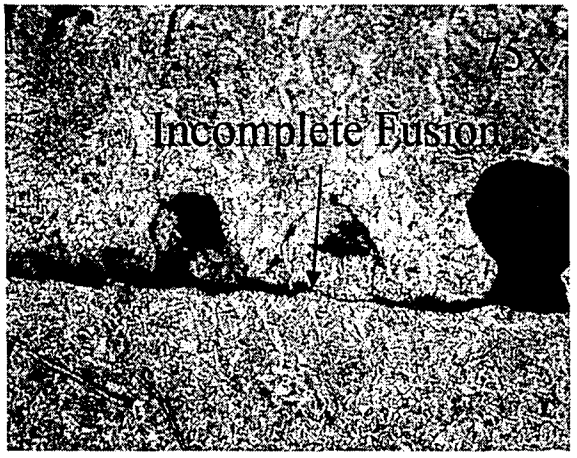

Figure 4.12: Incomplete Fusion in Specimen 36-8, Bottom-right section

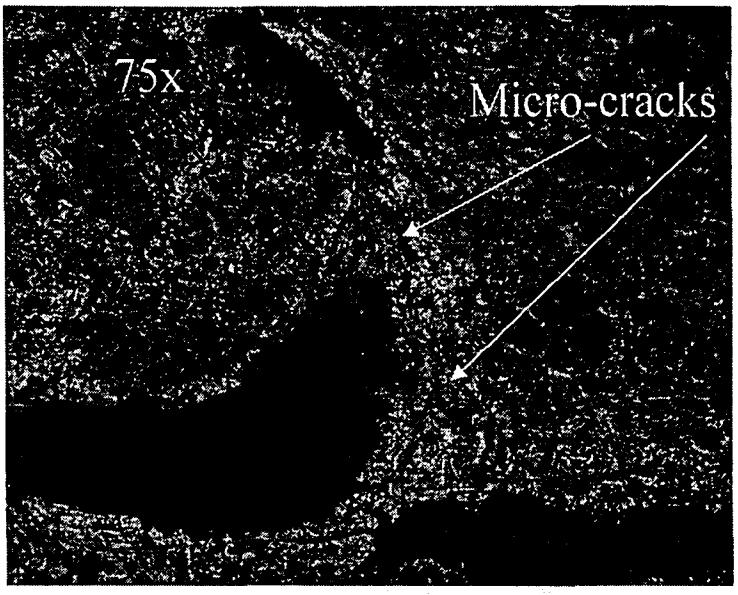

Figure 4.13: Micro-cracking in Specimen 36-8, Bottom-left Section

4.9 Specimen 36-14: 32°F, High Humidity, 20 mph Wind

This specimen was subjected to the environmental conditions shown in Table 4-9 in the environmental chamber at the time of welding.

Table 4-9: Environmental Conditions – Specimen 36-14					
Specimen: 36-14	Air Temp.	Concrete Temp.	Steel Temp.	Rel. Humidity	Wind Speed
	°F	°F	°F	%RH	[mph]
Nominal Values	32	32	32	95	20
Measured Values	30	44	39	75.5	20

The welded specimen is shown in Figure 4.14. Photographs of each of the two welds are presented along with an overview photo of the entire specimen. Sections were taken at four locations from the specimen and polished to examine the quality of the weld. These photos are also included.

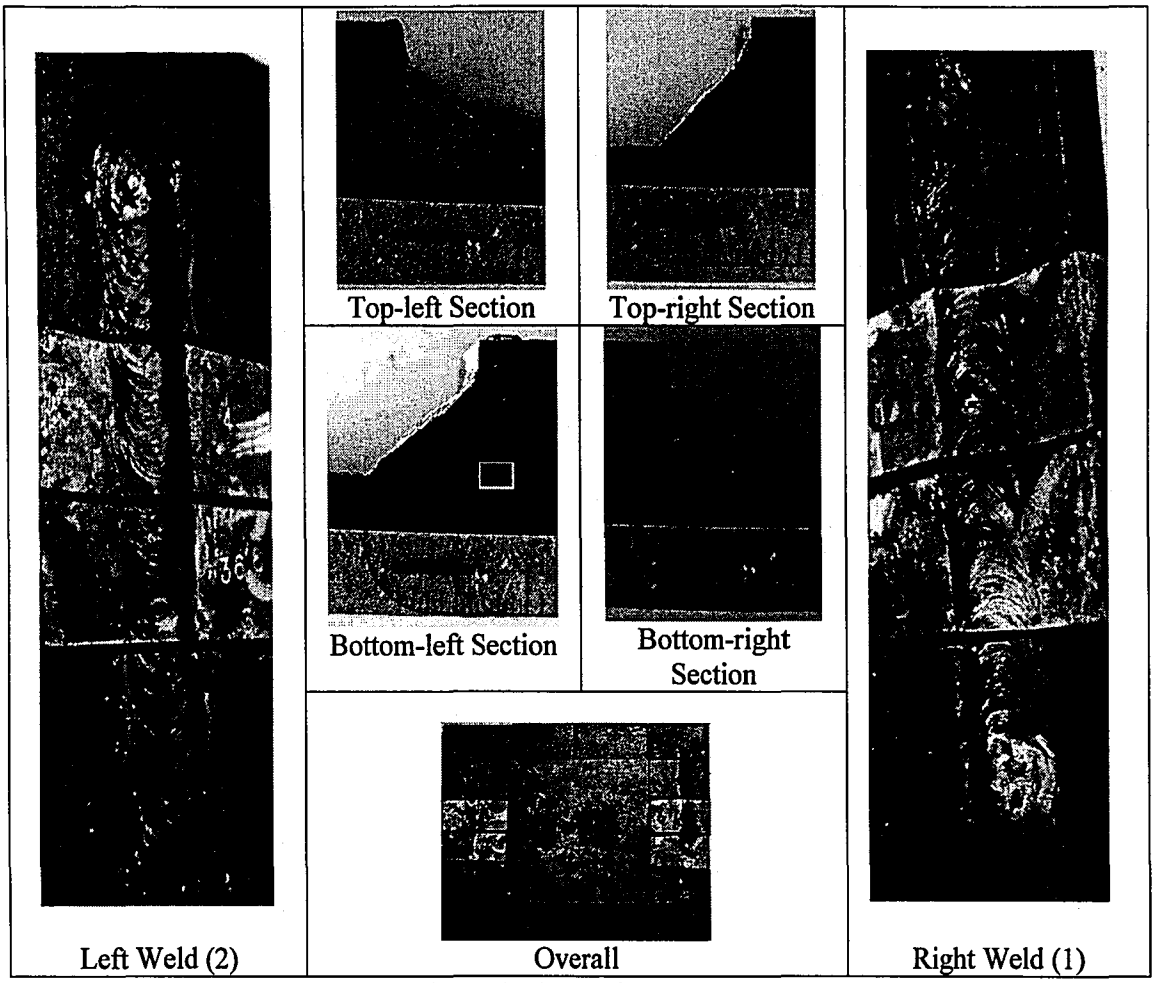

Figure 4.14: Specimen 36-14

4.9.1 Visual Observation Summary

The right weld had some edge-melt, and both weld surfaces had a slight amount of choppiness likely caused by wind. There was one small slag inclusion (.02-in.) at the root and two pores (.028-in., .020-in.) near the weld face in the top-left section (comprising 1.5% of the weld area), and a small inclusion (.025-in.) in the bottom-right section. Leg and throat dimensions satisfied the 1/4-in. profile requirements for all sections, although the top-left section had a profile which fell slightly below the proper 1/4-in. profile shape, rendering it unacceptable.

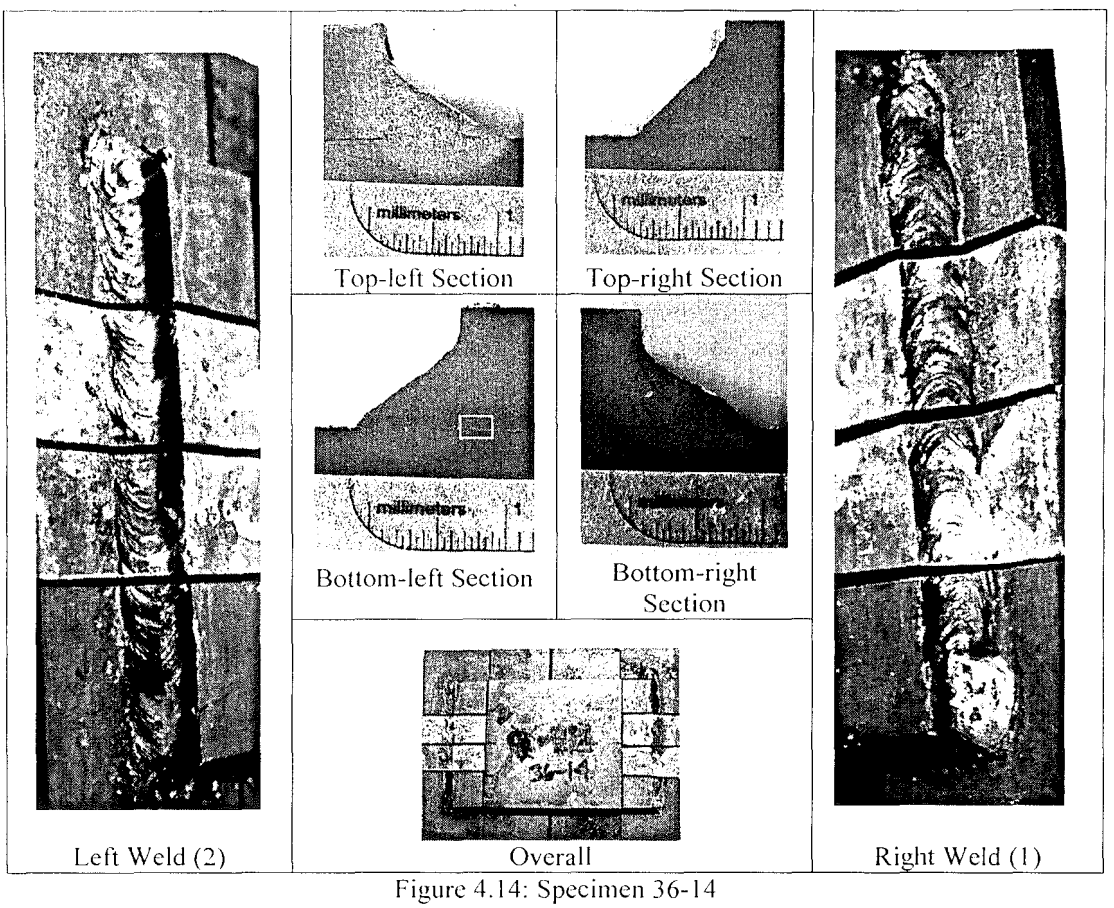

Figure 4.14: Specimen 36-14

4.9.1 Visual Observation Summary

The right weld had some edge-melt, and both weld surfaces had a slight amount of choppiness likely caused by wind. There was one small slag inclusion (.02-in.) at the root and two pores (.028-in., .020-in.) near the weld face in the top-left section (comprising 1.5% of the weld area), and a small inclusion (.025-in.) in the bottom-right section. Leg and throat dimensions satisfied the 1/4-in. profile requirements for all sections, although the top-left section had a profile which fell slightly below the proper 1/4-in. profile shape, rendering it unacceptable.

4.9.2 Microscopy Observation Summary

The bottom-left section displays micro-cracking at its root. The environmental chamber had a good deal of fog during welding, limiting visibility. The micro-cracking in the bottom-left section passes through discontinuities near the root of the section. These micro-cracks are shown in Figure 4.15 in the microscopic image taken of the section. It appears that the slag inclusions which were connected by the micro-cracks played some role in increasing the likelihood of micro-cracking locally.

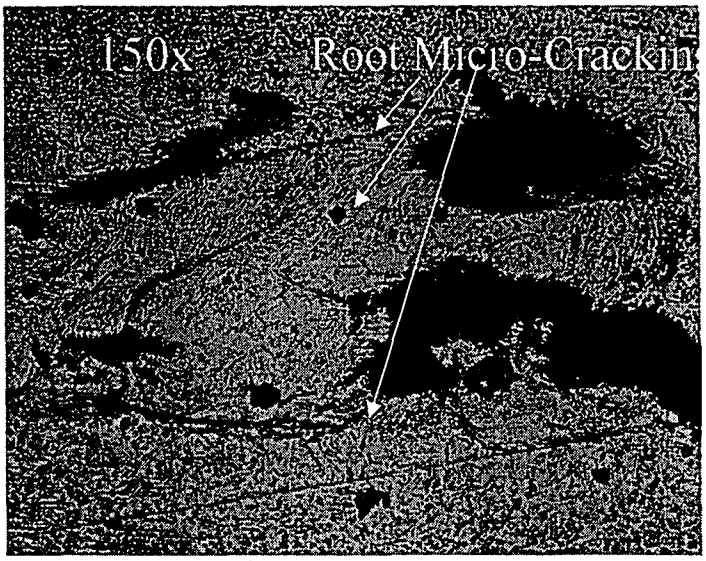

Figure 4.15: Root Micro-Cracking in Specimen 36-14-Bottom-left Section

4.10 Specimen 36-15: 32°F, High Humidity, 35 mph Wind (Delayed Removal)

This specimen was subjected to the environmental conditions shown in Table 4-10 in the environmental chamber at the time of welding.

Table 4-10: Environmental Conditions – Specimen 36-15					
Specimen: 36-15	Air Temp.	Concrete Temp.	Steel Temp.	Rel. Humidity	Wind Speed
	°F	°F	°F	%RH	[mph]
Nominal Values	32	32	32	95	35
Measured Values	25	35	31	100.0	32.4

The welded specimen is shown in Figure 4.16. Photographs of each of the two welds are presented along with an overview photo of the entire specimen. Sections were taken at four locations from the specimen and polished to examine the quality of the weld. These photos are also included.

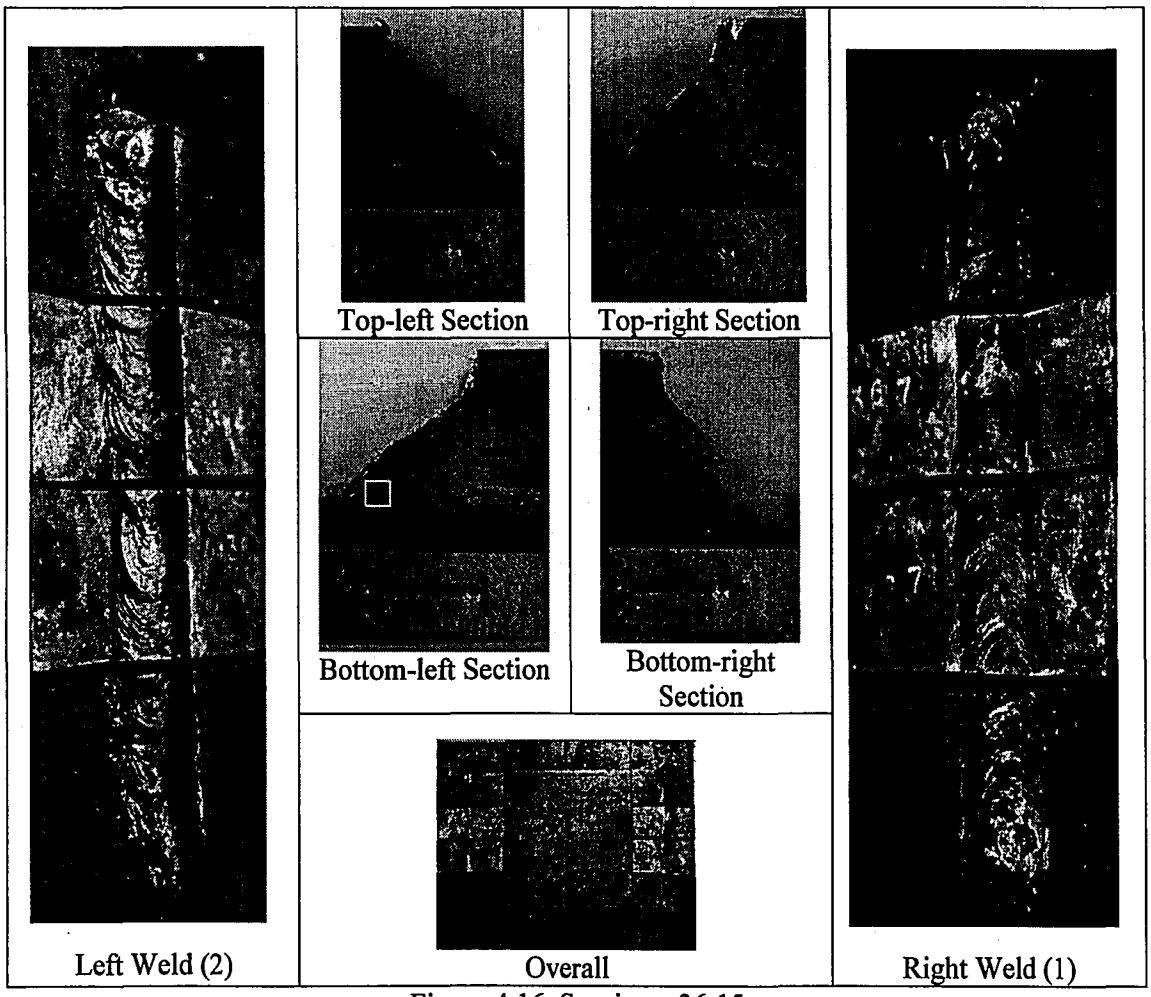

Figure 4.16: Specimen 36-15

Table 4-10: Environmental Conditions – Specimen 36-15					
Specimen: 36-15	Air Temp.	Concrete Temp.	Steel Temp.	Rel. Humidity	Wind Speed
	°F	°F	°F	%RH	[mph]
Nominal Values	32	32	32	95	35
Measured Values	25	35	31	100.0	32.4

The welded specimen is shown in Figure 4.16. Photographs of each of the two welds are presented along with an overview photo of the entire specimen. Sections were taken at four locations from the specimen and polished to examine the quality of the weld. These photos are also included.

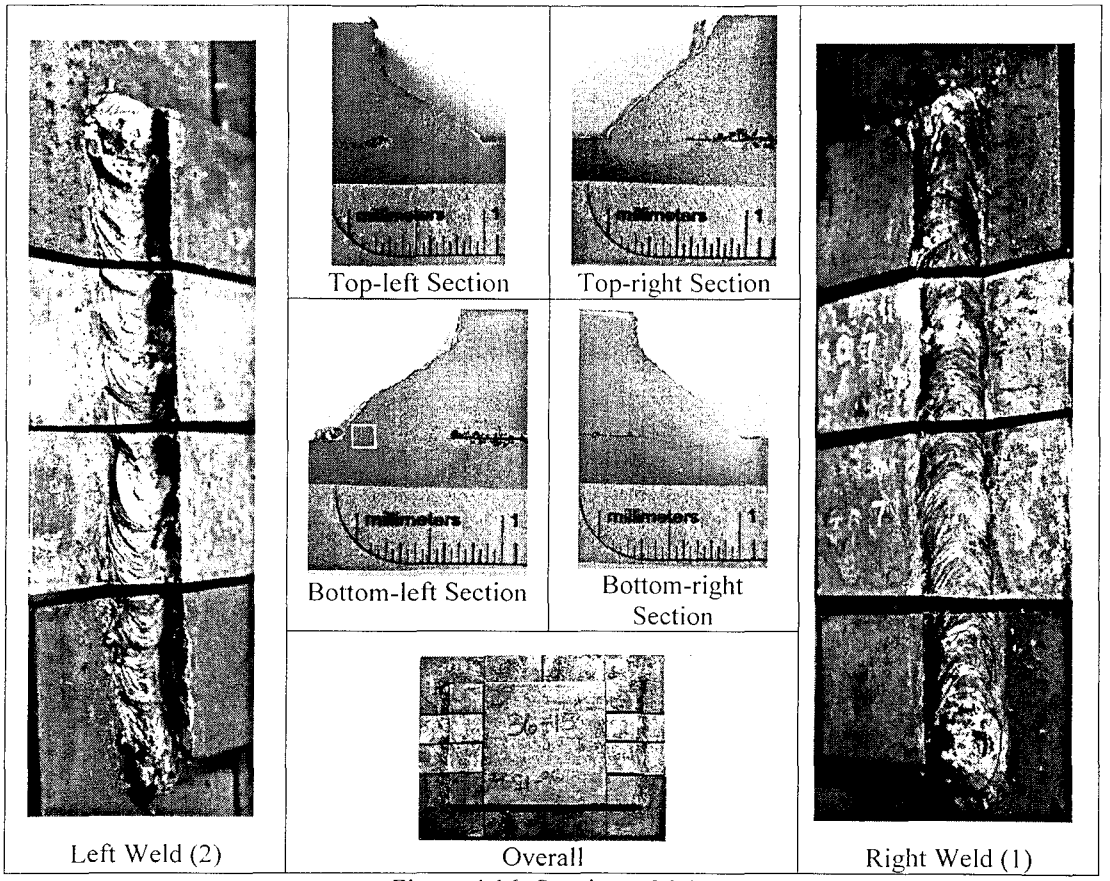

Figure 4.16: Specimen 36-15

4.10.1 Visual Observation Summary

Both welds had an erratic and choppy surface, and the right weld exhibited some edge-melt, resulting from the high wind speed. Some skew to the vertical leg of the weld was observed in the top-left section, again a result of high wind speed. All sections had a root inclusion, and starting from the top-right and moving clockwise, the largest dimensions of the each inclusion were .017-in., .033-in., .039-in., .015-in. All welds except the top-left section met the 1/4-in. profile requirements.

4.10.2 Microscopy Observation Summary

The bottom-left section exhibited a toe micro-crack, as depicted in Figure 4.17. This specimen remained restrained in the concrete block for a period of at least 24 hours prior to removal. Toe cracks are often cold cracks, forming normal to the plate boundary and in the HAZ as a result of hydrogen embrittlement and shrinkage strains. It is interesting to note that this specimen was fully restrained for 24 hours prior to removal from the concrete block and likely developed shrinkage strains that promoted this type of micro-cracking.

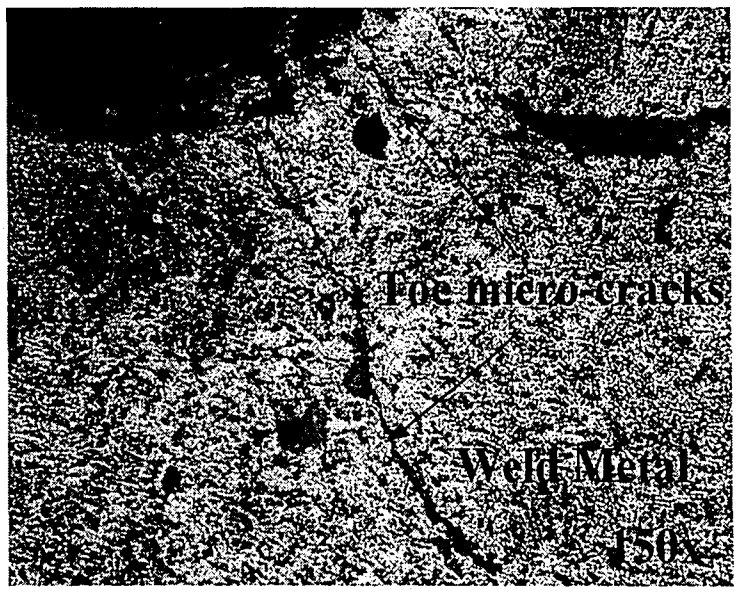

Figure 4.17: Toe Micro-Cracking in Specimen 36-15-Bottom-left Section

4.11 Specimen 36-22: -10°F, High Humidity, 20 mph Wind

This specimen was subjected to the environmental conditions shown in Table 4-11 in the environmental chamber at the time of welding.

Table 4-11: Environmental Conditions – Specimen 36-22					
Specimen: 36-22	Air Temp.	Concrete Temp.	Steel Temp.	Rel. Humidity	Wind Speed
	°F	°F	°F	%RH	[mph]
Nominal Values	-10	-10	-10	95	20
Measured Values	-5	5	-5	99.9	21.3

The welded specimen is shown in Figure 4.18. Photographs of each of the two welds are presented along with an overview photo of the entire specimen. Sections were taken at four locations from the specimen and polished to examine the quality of the weld. These photos are also included.

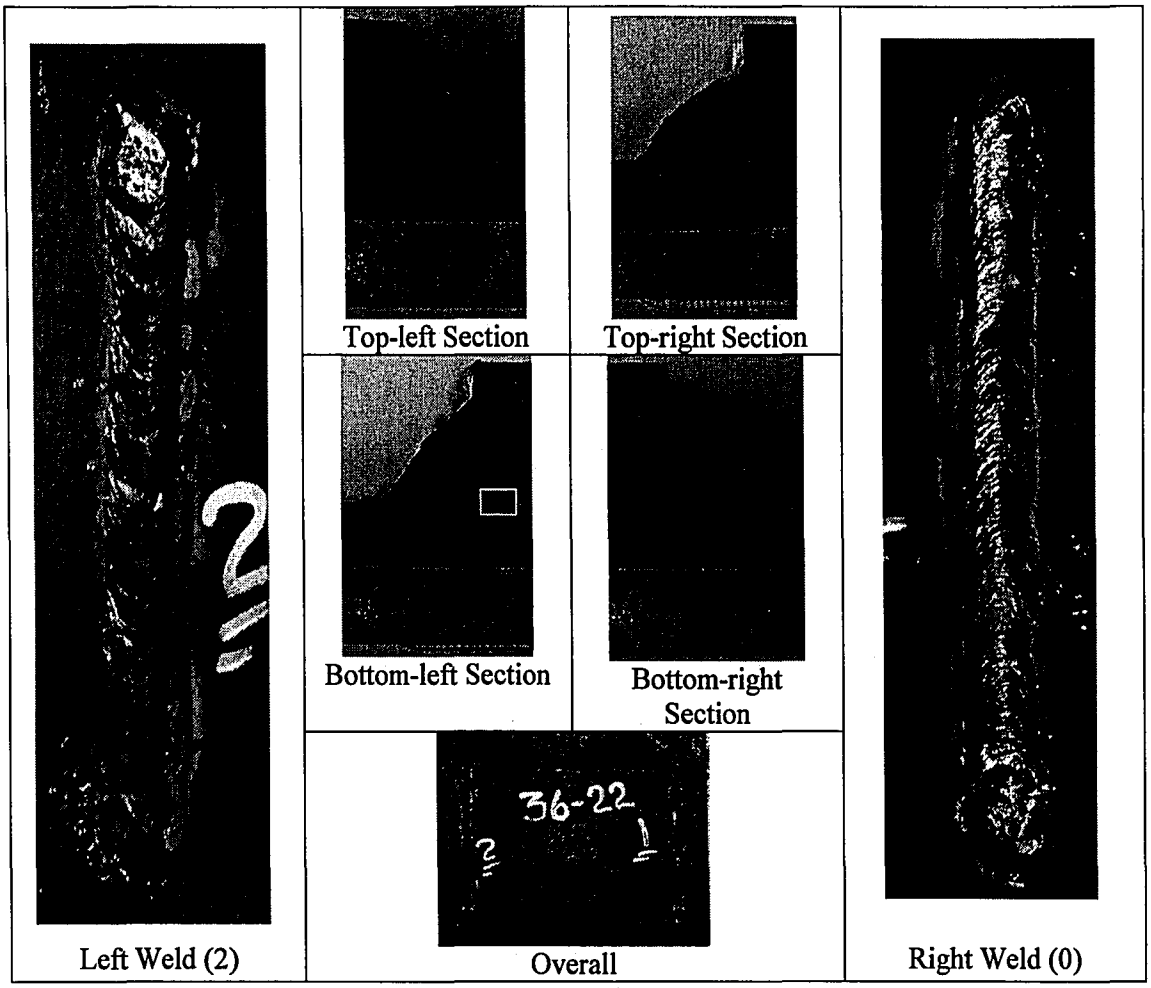

Figure 4.18: Specimen 36-22

4.11.1 Visual Observation Summary

Both welds from this specimen exhibited no notable surface flaws or profile flaws except slight convexity in the profile of the right weld. The bottom-right section was below the 1/4-in. profile requirements, but the remaining three welds satisfied the 1/4-in. profile requirements.

4.11.2 Microscopy Observation Summary

The bottom-left section exhibited incomplete fusion as well as very small micro-cracks that appeared to connect the non-fused plate edge with a slag inclusion above the tip of the non-fused segment. The incomplete fusion found in the bottom-left section of Specimen 36-22 is

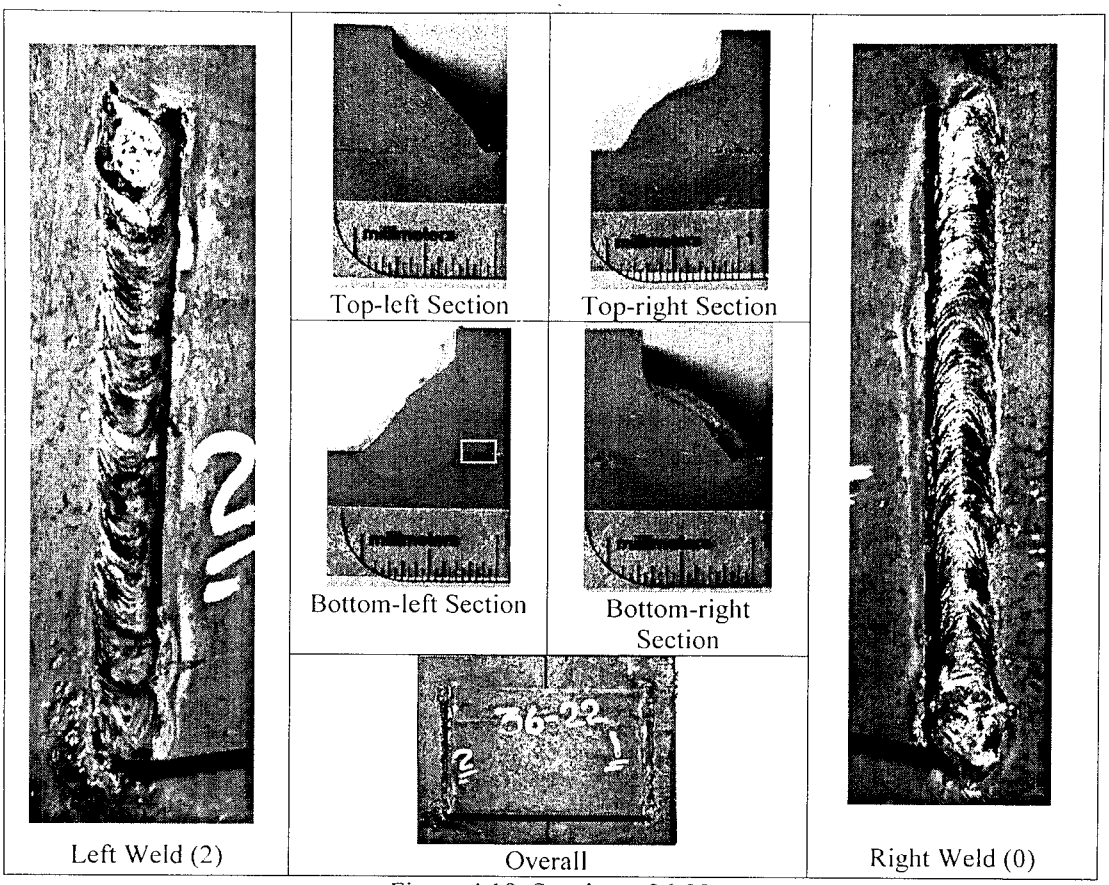

Figure 4.18: Specimen 36-22

4.11.1 Visual Observation Summary

Both welds from this specimen exhibited no notable surface flaws or profile flaws except slight convexity in the profile of the right weld. The bottom-right section was below the 1/4-in. profile requirements, but the remaining three welds satisfied the 1/4-in. profile requirements.

4.11.2 Microscopy Observation Summary

The bottom-left section exhibited incomplete fusion as well as very small micro-cracks that appeared to connect the non-fused plate edge with a slag inclusion above the tip of the non-fused segment. The incomplete fusion found in the bottom-left section of Specimen 36-22 is

depicted in Figure 4.19, and the connecting micro-cracking to the slag inclusion can be seen on the left side of the image above the tip of the non-fused segment.

Figure 4.19: Incomplete Fusion and Micro-Cracking in Specimen 36-22, Bottom-left Section

4.12 Specimen 36-23: -10°F, High Humidity, 35 mph Wind (Delayed Removal)

This specimen was subjected to the environmental conditions shown in Table 4-12 in the environmental chamber at the time of welding.

Table 4-12: Environmental Conditions – Specimen 36-23

Specimen: 36-23	Air Temp.	Concrete Temp.	Steel Temp.	Rel. Humidity	Wind Speed
	°F	°F	°F	%RH	[mph]
Nominal Values	-10	-10	-10	95	35
Measured Values	-4	7	-13	100	27-29*

*Maximum fan output at subzero temperatures yields from 27-29 mph.

The welded specimen is shown in Figure 4.20. Photographs of each of the two welds are presented along with an overview photo of the entire specimen. Sections were taken at four

locations from the specimen and polished to examine the quality of the weld. These photos are also included.

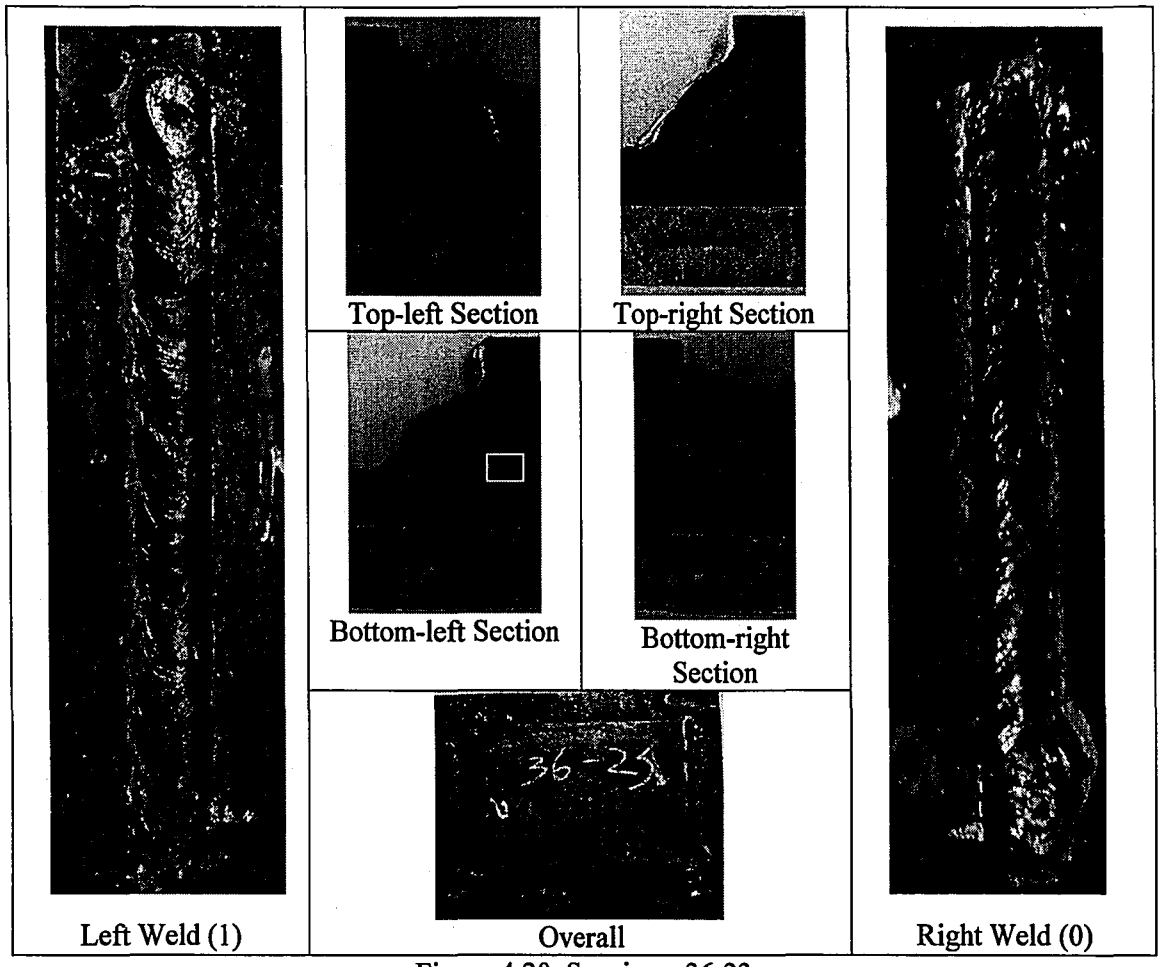

Figure 4.20: Specimen 36-23

4.12.1 Visual Observation Summary

Neither weld exhibited any notable surface flaws, although each profile was convex, with the top-left profile having the greatest convexity. All sections, however, were within AWS limitations for convexity, less than 3/32-in. There was a small amount of undercut in the bottom-right section (.017-in.). The top-right, bottom-right, and bottom-left profiles were below the ¼-in. profile requirements.

locations from the specimen and polished to examine the quality of the weld. These photos are also included.

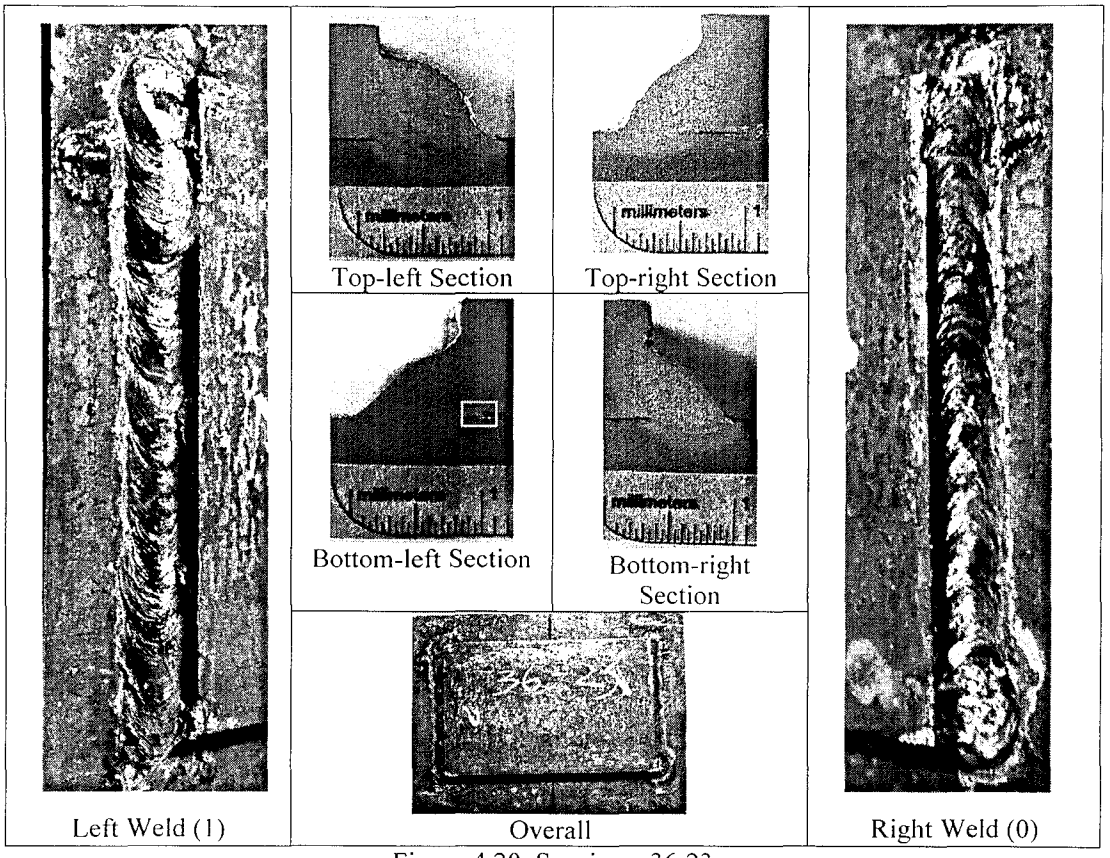

Figure 4.20: Specimen 36-23

4.12.1 Visual Observation Summary

Neither weld exhibited any notable surface flaws, although each profile was convex, with the top-left profile having the greatest convexity. All sections, however, were within AWS limitations for convexity, less than 3/32-in. There was a small amount of undercut in the bottom-right section (.017-in.). The top-right, bottom-right, and bottom-left profiles were below the ¼-in. profile requirements.

4.12.2 Microscopy Observation Summary

The bottom-left section exhibited root micro-cracking, as did the top-left section. This specimen remained restrained for a period of almost 72 hours prior to removal from the concrete block. The root micro-cracking observed in the bottom-left section of the specimen is shown in Figure 4.21. The small segment exhibiting incomplete fusion (Figure 4.21) springs from the root along the boundary between the weld metal and HAZ, and the thinner micro-crack appears to propagate through local discontinuities.

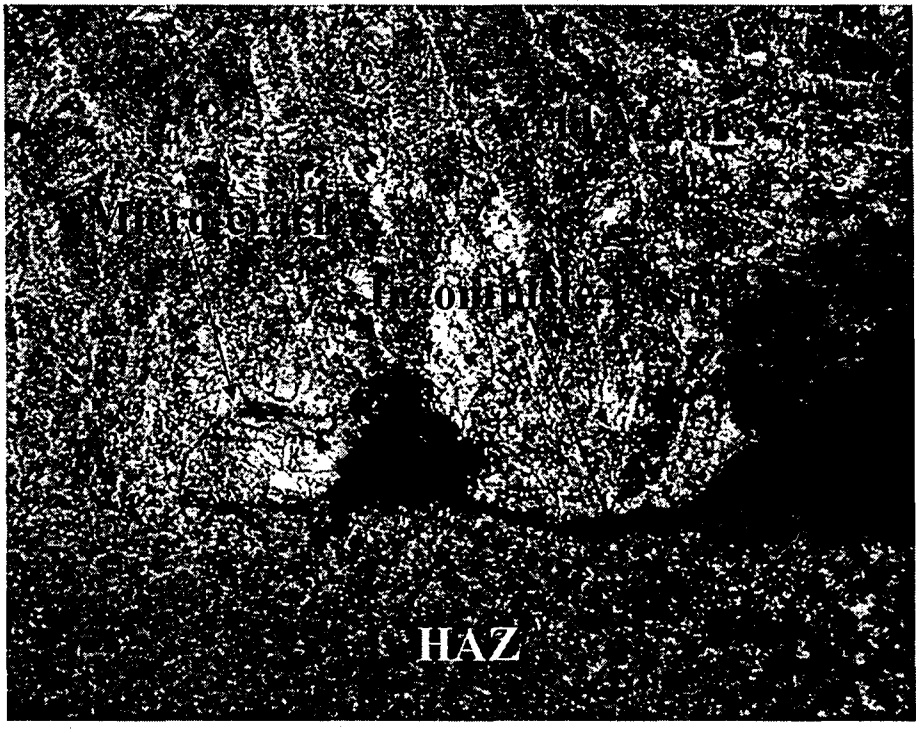

Figure 4.21: Incomplete Fusion, Root Micro-cracking in Specimen 36-23, Bottom-left Section

4.13 Specimen 36-17HR(1): Warm, High Humidity, No Wind, 17 hr. electrode exposure

This specimen was subjected to the environmental conditions shown in Table 4-13 in the environmental chamber at the time of welding. The electrodes were also exposed to 95% RH,

71°F for approximately 17 hours prior to welding. This resulted in a moisture content in the electrode of 4% by weight.

Table 4-13: Environmental Conditions – Specimen 36-17HR(1)					
Specimen: 36-17HR(1)	Air Temp. °F	Concrete Temp. °F	Steel Temp. °F	Rel. Humidity %RH	Wind Speed [mph]
Nominal Values	71	71	71	95	0
Measured Values	71.2	72.5	72.9	92	0

The welded specimen is shown in Figure 4.22. Photographs of each of the two welds are presented along with an overview photo of the entire specimen. Sections were taken at four locations from the specimen and polished to examine the quality of the weld. These photos are also included.

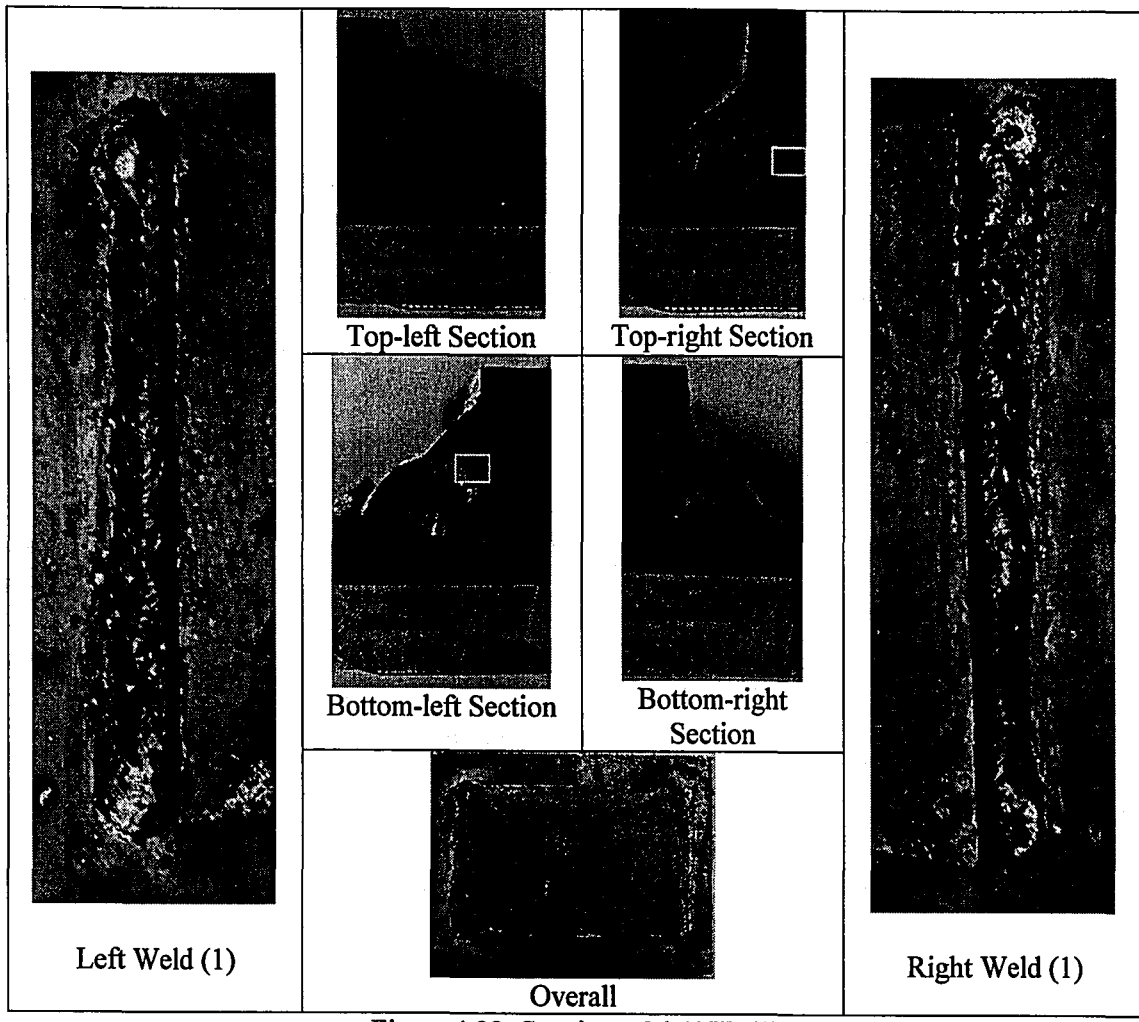

Figure 4.22: Specimen 36-17HR(1)

4.13.1 Visual Observation Summary

The right weld had a slightly choppy profile and contained three surface pores at the start position with diameters of .047-in., .040-in., and .020-in. and three surface pores located approximately 1-in. from the start position of the weld with diameters of .05-in., .072-in., and .029-in. Approximately 1 1/2-in. length of the right weld was undersized as determined using a standard fillet gage. The left weld was full size and contained three large surface pores (.077-in., .074-in., .058-in.), and the beginning of the weld was not well aligned in the joint. Two slag inclusions were present in the center of the top-right profile (.017-in., .036-in.), as well as a

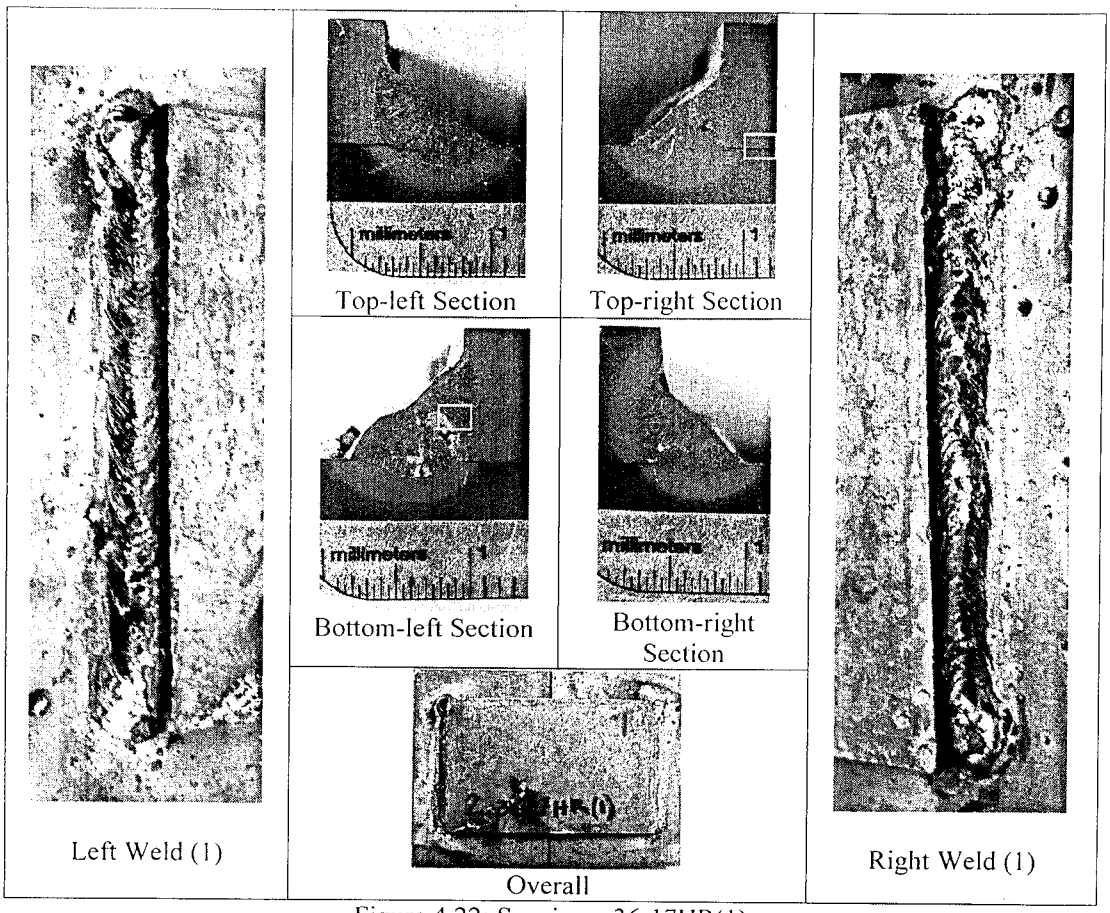

Figure 4.22: Specimen 36-17HR(1)

4.13.1 Visual Observation Summary

The right weld had a slightly choppy profile and contained three surface pores at the start position with diameters of .047-in., .040-in., and .020-in. and three surface pores located approximately 1-in. from the start position of the weld with diameters of .05-in., .072-in., and .029-in. Approximately 1 1/2-in. length of the right weld was undersized as determined using a standard fillet gage. The left weld was full size and contained three large surface pores (.077-in., .074-in., .058-in.), and the beginning of the weld was not well aligned in the joint. Two slag inclusions were present in the center of the top-right profile (.017-in., .036-in.), as well as a

small root slag inclusion (.027-in.) in the bottom-right section. Two large piping pores were located in the center of the bottom-left section (.102-in., 0.052-in.), comprising 8.74% of the weld area in cross-section. Three of the four profiles were below the 1/4-in. profile requirements (top-right, bottom-right, top-left).

4.13.2 Microscopy Observation Summary

The following microscopic images show some of the flaws found in the sections of these welds. Figure 4.23 shows the head of a piping pore which is oriented as seen in the bottom-left section photo above, originating near the root of the weld and growing toward the weld face. This is likely a result of the introduction of moisture from the moist electrode into the weld pool where the dissolved hydrogen introduced by the moisture did not escape from the weld before solidification occurred, forming this elongated pore. The top-right section possessed what appears to be a small hot micro-crack projecting from the fusion line at the root of the weld. The second image, Figure 4.24 shows this micro-crack.

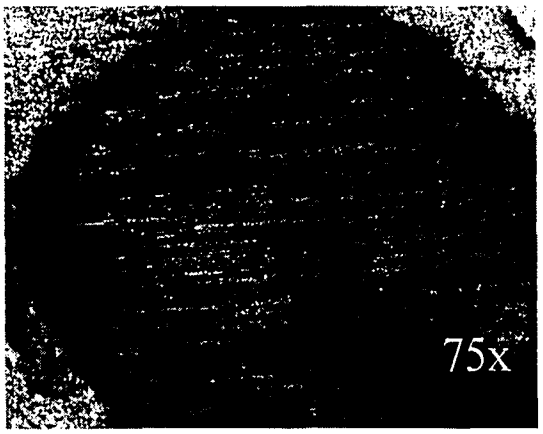

Figure 4.23: Head of Piping Pore (Bottom-left Section)

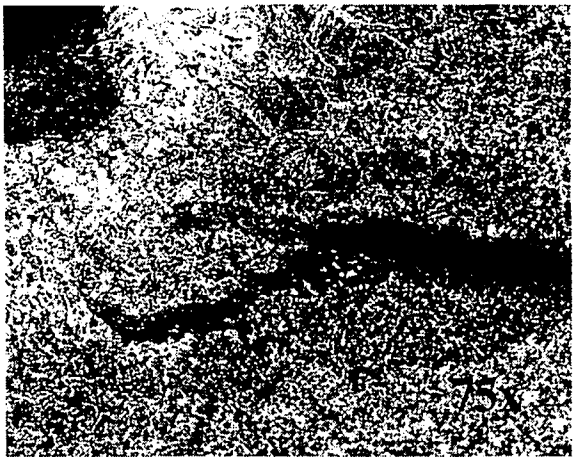

Figure 4.24: Hot Micro-Crack at Root of Top-right Section

4.14 Specimen 36-17HR(2): Warm, High Humidity, No Wind, 17 hr. electrode exposure

This specimen was subjected to the environmental conditions shown in Table 4-14 in the environmental chamber at the time of welding. The electrodes were also exposed to 95% RH, 71°F for approximately 17 hours prior to welding. This resulted in a moisture content in the electrode of 4% by weight.

Table 4-14: Environmental Conditions – Specimen 36-17HR(2)

Specimen: 36-17HR(2)	Air Temp.	Concrete Temp.	Steel Temp.	Rel. Humidity	Wind Speed
	°F	°F	°F	%RH	[mph]
Nominal Values	71	71	71	95	0
Measured Values	72.6	82.7	77.1	88.6	0

The welded specimen is shown in Figure 4.25. Photographs of each of the two welds are presented along with an overview photo of the entire specimen. Sections were taken at four locations from the specimen and polished to examine the quality of the weld. These photos are also included.

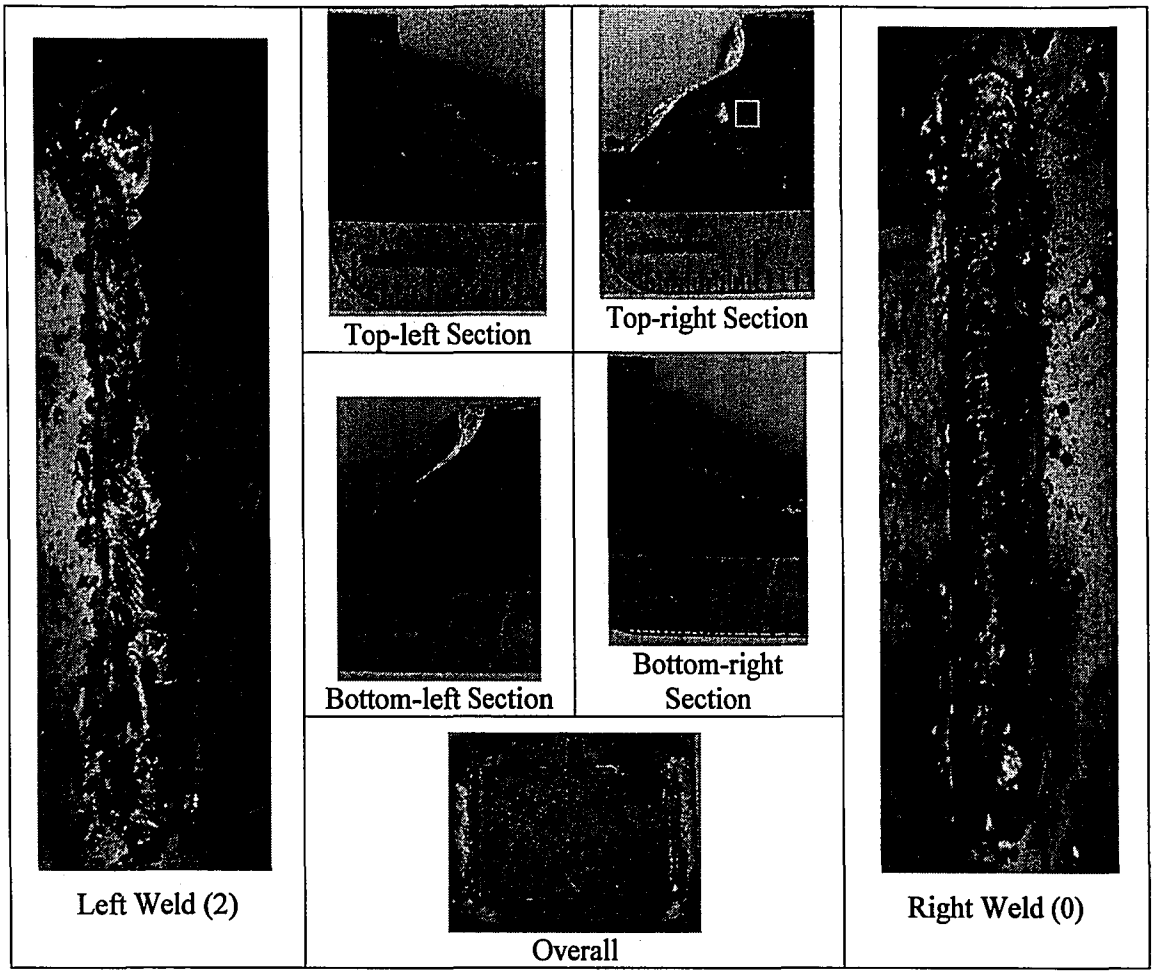

Figure 4.25: Specimen 36-17HR(2)

4.14.1 Visual Observation Summary

The right weld contained two surface pores (.051-in., .039-in.) near the start of the weld and had no undercut or edge-melt. The left weld had one small pore (.044-in.) and edge-melt at the beginning and end of the weld. The top-right profile had what appears to be an irregularly shaped pore near the center (.050-in., comprising 3.0% of the weld area in cross-section) and had a convex profile, as well as a small root inclusion (.024-in.). The bottom-left section had a convex profile and a minute pore (.005-in., 0% of weld area). The bottom-left section had a bulge in profile toward the horizontal leg, displayed some edge-melt, and had a slag inclusion at the root (.030-in.). The top-left profile contained a small (0.024-in.) slag inclusion near the

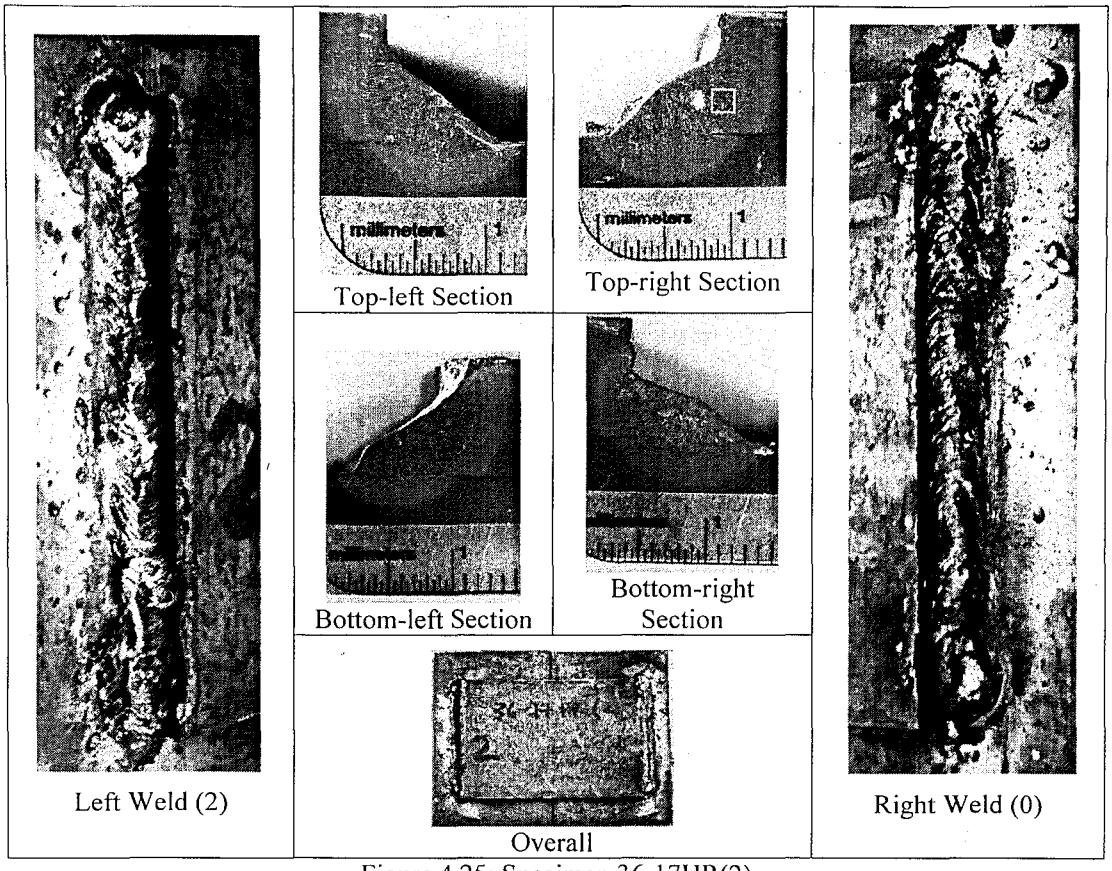

Figure 4.25: Specimen 36-17HR(2)

4.14.1 Visual Observation Summary

The right weld contained two surface pores (.051-in., .039-in.) near the start of the weld and had no undercut or edge-melt. The left weld had one small pore (.044-in.) and edge-melt at the beginning and end of the weld. The top-right profile had what appears to be an irregularly shaped pore near the center (.050-in., comprising 3.0% of the weld area in cross-section) and had a convex profile, as well as a small root inclusion (.024-in.). The bottom-left section had a convex profile and a minute pore (.005-in., 0% of weld area). The bottom-left section had a bulge in profile toward the horizontal leg, displayed some edge-melt, and had a slag inclusion at the root (.030-in.). The top-left profile contained a small (0.024-in.) slag inclusion near the

root. The top-right, bottom-right, and top-left profiles fell below the 1/4-in. profile requirements.

4.14.2 Microscopy Observation Summary

The following image (Figure 4.26) shows a microscopic view of one portion of a gas pore found in the top-right section above. Although the shape of the pore is not rounded, as would be expected from a typical pore, the edges are rather smooth and uncharacteristic of a slag inclusion, and the boundary of the shape appears to be one caused by hydrostatic pressure, rather than the usually rough and random shape of a typical slag inclusion, indicating that this was most likely a large gas pore trapped near the center of the weld profile in the weld metal.

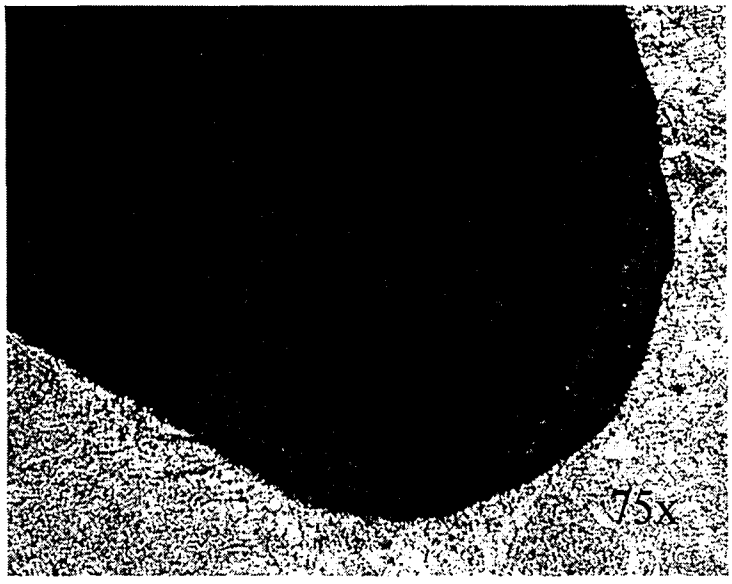

Figure 4.26: Portion of Pore in Specimen 36-17HR(2), Top-right Section

4.15 Specimen 36-C1: -10°F, High Humidity, No Wind, High Carbon Steel

This specimen was subjected to the environmental conditions shown in Table 4-15 in the environmental chamber at the time of welding. Plates were pre-cooled in an insulated box with

liquid nitrogen prior to welding, but plates did not come into contact with liquid nitrogen at any time.

Table 4-15: Environmental Conditions – Specimen 36-C1					
Specimen: 36-C1	Air Temp.	Concrete Temp.	Steel Temp.	Rel. Humidity	Wind Speed
	°F	°F	°F	%RH	[mph]
Nominal Values	-10	-10	-10	95	0
Measured Values	-9.8	22.9	-6	100	0

The welded specimen is shown in Figure 4.27. Photographs of each of the two welds are presented along with an overview photo of the entire specimen. Sections were taken at four locations from the specimen and polished to examine the quality of the weld. These photos are also included.

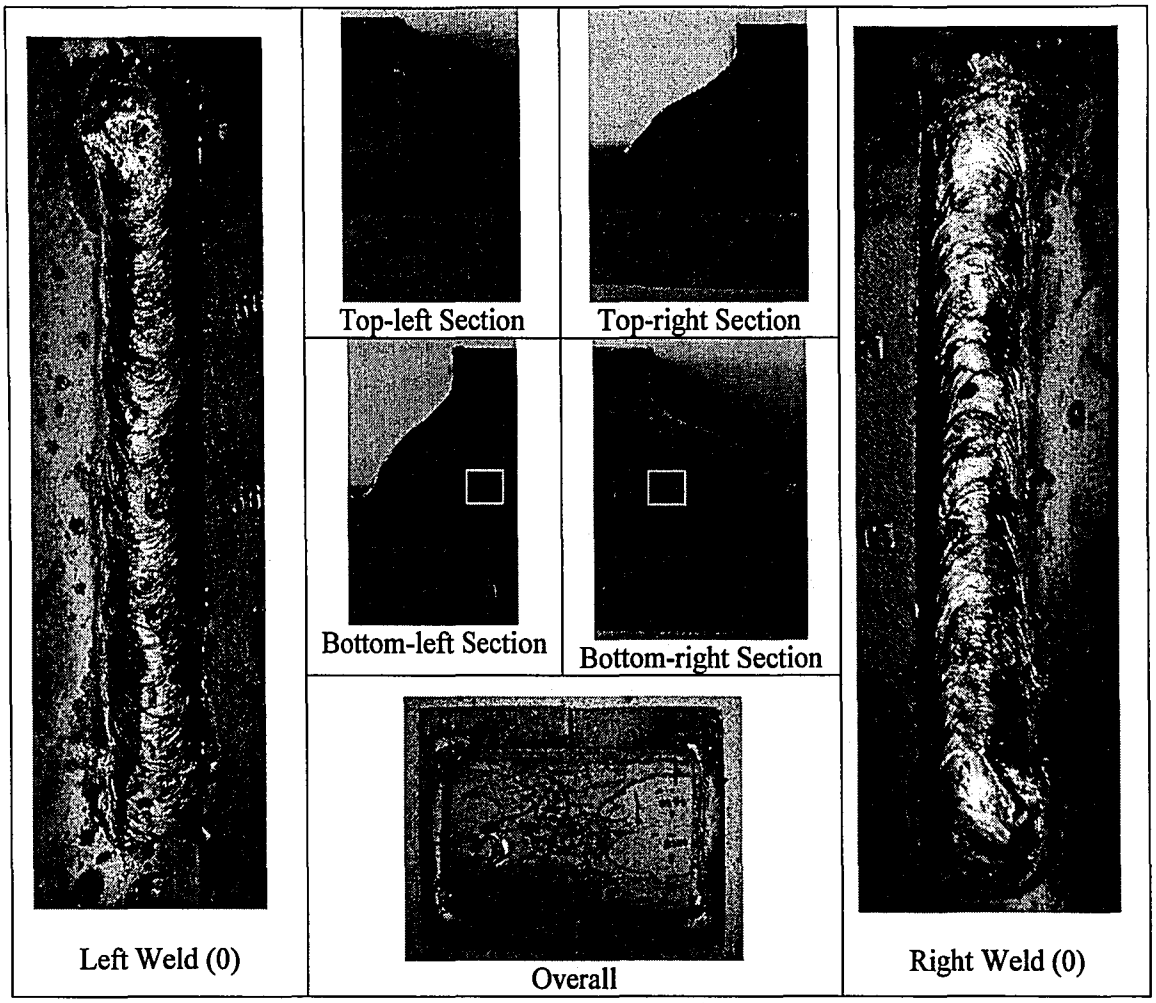

Figure 4.27: Specimen 36-C1

4.15.1 Visual Observation Summary

The right weld was oversized but had no pores, undercut, or edge-melt. The profile was fairly regular over the length. The left weld was slightly undersized for roughly 3/8-in., had minimal edge-melt at its beginning, but had no pores or undercut. The only section flaws observed were crack-like in nature and occurred at the roots of the bottom-right and bottom-left sections with associated incomplete fusion. All sections satisfy the 1/4-in. profile requirements except the bottom-right section which, due to curvature, falls just below the full profile at one location along the weld face.

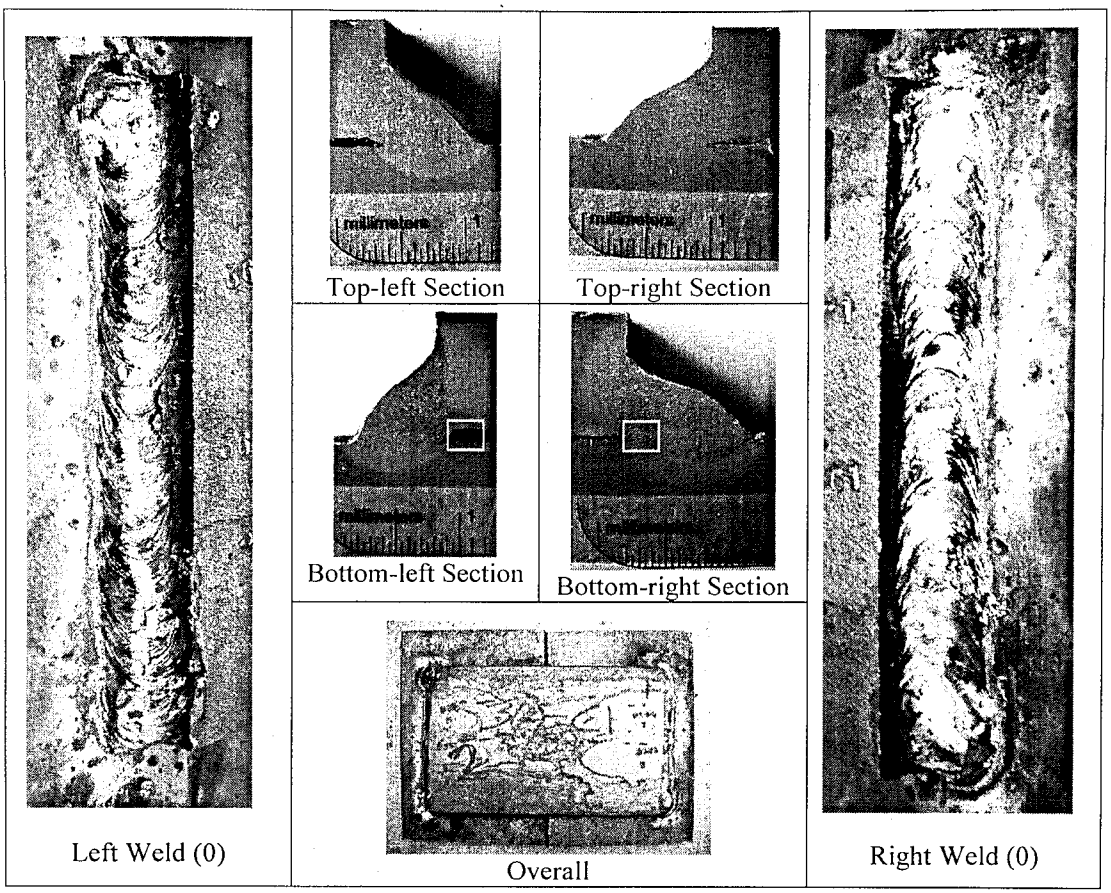

Figure 4.27: Specimen 36-C1

4.15.1 Visual Observation Summary

The right weld was oversized but had no pores, undercut, or edge-melt. The profile was fairly regular over the length. The left weld was slightly undersized for roughly 3/8-in., had minimal edge-melt at its beginning, but had no pores or undercut. The only section flaws observed were crack-like in nature and occurred at the roots of the bottom-right and bottom-left sections with associated incomplete fusion. All sections satisfy the 1/4-in. profile requirements except the bottom-right section which, due to curvature, falls just below the full profile at one location along the weld face.

4.15.2 Microscopy Observation Summary

The discontinuities shown in Figure 4.28 and Figure 4.29 occurred along the fusion line and extend along the boundary between the weld metal and coarse-grained HAZ. The bottom image also shows a connecting micro-crack between the non-fused segment and a small slag inclusion above it.

Figure 4.28: Micro-Cracking and Incomplete Fusion in Specimen 36-C1, Bottom-right Section

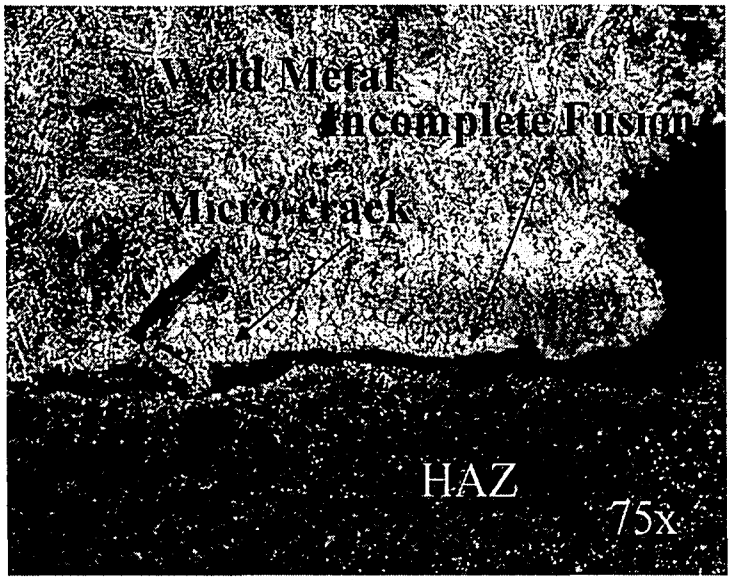

Figure 4.29: Micro-Cracking and Incomplete Fusion in Specimen 36-C2, Bottom-left Section

4.16 Specimen 36-C2: -10°F, High Humidity, No Wind, High Carbon Steel (Delayed Removal)

This specimen was subjected to the environmental conditions shown in Table 4-16 in the environmental chamber at the time of welding. Plates were pre-cooled in an insulated box with liquid nitrogen prior to welding, but plates did not come into contact with liquid nitrogen at any time.

Table 4-16: Environmental Conditions – Specimen 36-C2

Specimen: 36-C2	Air Temp.	Concrete Temp.	Steel Temp.	Rel. Humidity	Wind Speed
	°F	°F	°F	%RH	[mph]
Nominal Values	-10	-10	-10	95	0
Measured Values	-5.3	20.7	-4**	66.7*	0

*Ambient humidity measurement seemed questionable as similar moisture was present following the welding of specimen 36-C1, which had 100%RH.

**Temperature of cover plate approximately 10° cooler; temperature shown is from recessed plate.

The welded specimen is shown in Figure 4.30. Photographs of each of the two welds are presented along with an overview photo of the entire specimen. Sections were taken at four locations from the specimen and polished to examine the quality of the weld. These photos are also included.

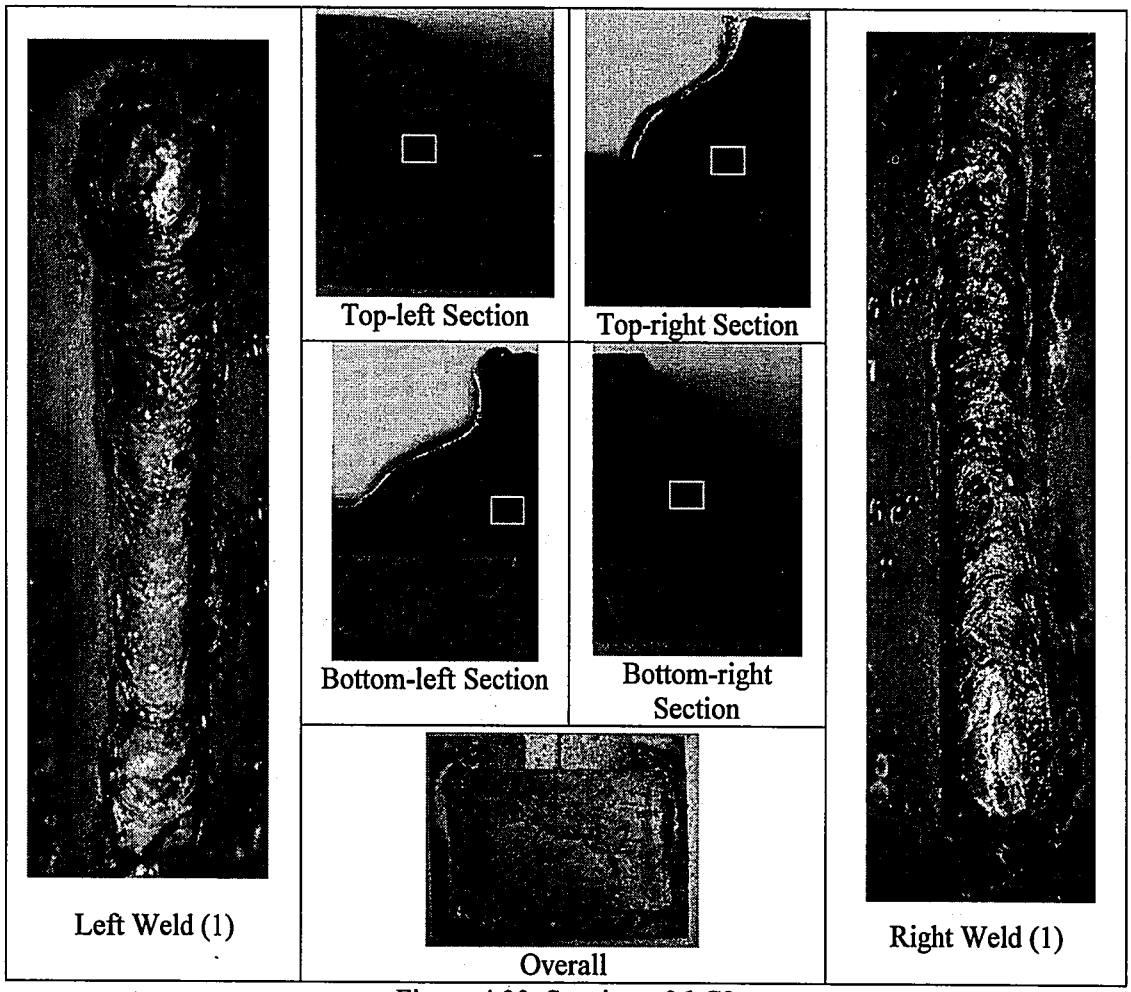

Figure 4.30: Specimen 36-C2

4.16.1 Visual Observation Summary

The right weld was undersized for approximately the beginning 1/2-in. and showed undercut, and edge-melt was also present near the weld start. The weld was otherwise choppy but had no observable surface pores. The left weld had some spatter at the beginning and had a pore (.027-

The welded specimen is shown in Figure 4.30. Photographs of each of the two welds are presented along with an overview photo of the entire specimen. Sections were taken at four locations from the specimen and polished to examine the quality of the weld. These photos are also included.

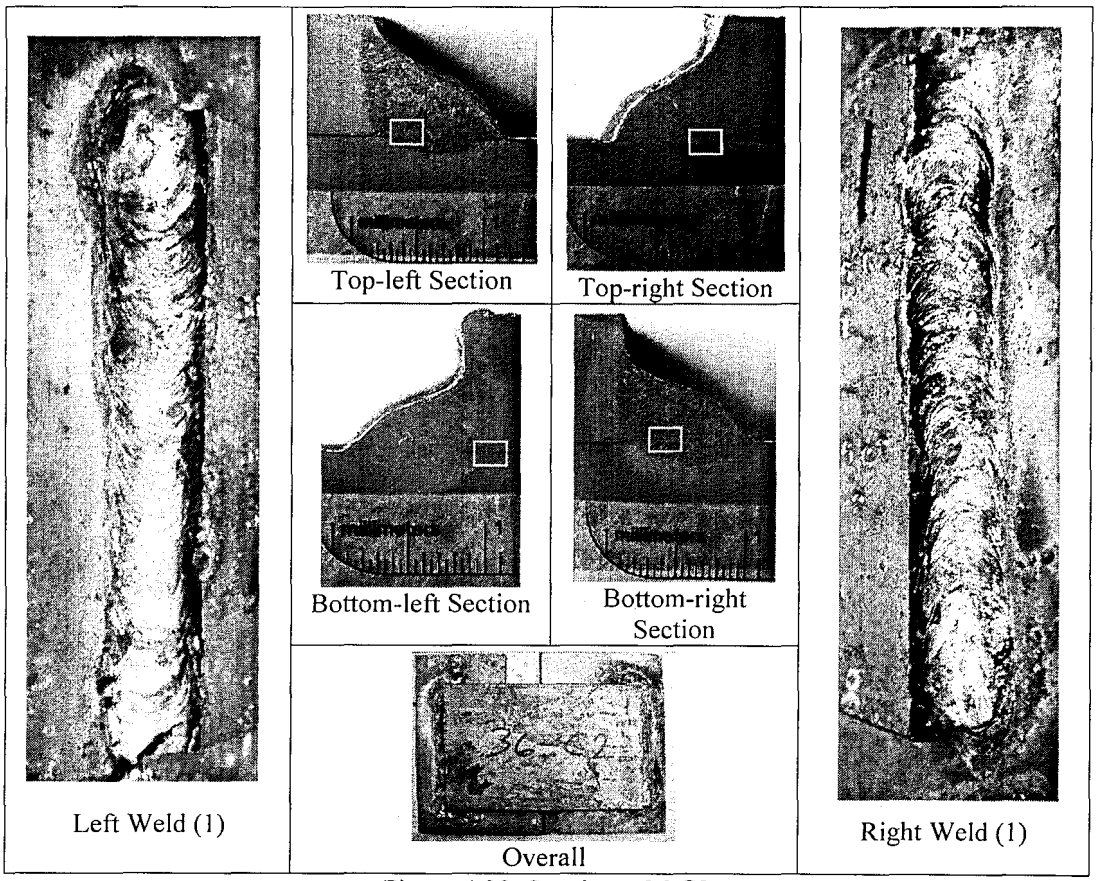

Figure 4.30: Specimen 36-C2

4.16.1 Visual Observation Summary

The right weld was undersized for approximately the beginning 1/2-in. and showed undercut, and edge-melt was also present near the weld start. The weld was otherwise choppy but had no observable surface pores. The left weld had some spatter at the beginning and had a pore (.027-

in.) in an edge-melt region on the top edge of the cover plate. There was no undercut, but the weld was somewhat irregular in size for the latter half of the weld. The top-right section exhibited incomplete fusion along the horizontal leg, and the top-left section had a small slag inclusion (.016-in.) at the root. All four profiles did not meet the 1/4-in. profile requirements as a result of excessive curvature of the weld face near the vertical leg, causing the profiles to fall below the required throat dimension at those areas. The specimen remained restrained for more than 24 hours prior to removal from the chamber.

4.16.2 Microscopy Observation Summary

The bottom-right, bottom-left, and top-left sections exhibited some form of cracking, and microscopy images below show the cracks. The four figures shown are images from the root of each cross section for Specimen 36-C2. Figure 4.31 is an example of incomplete fusion from the root of the top-right section, and Figure 4.32 shows micro-cracking at the root of the bottom-right section. In the case of Figure 4.33, there is a small micro-crack protruding vertically from the small non-fused segment at the root of the bottom-left section. In Figure 4.34, several small connecting micro-cracks can be observed between the small inclusions at the root of the weld.

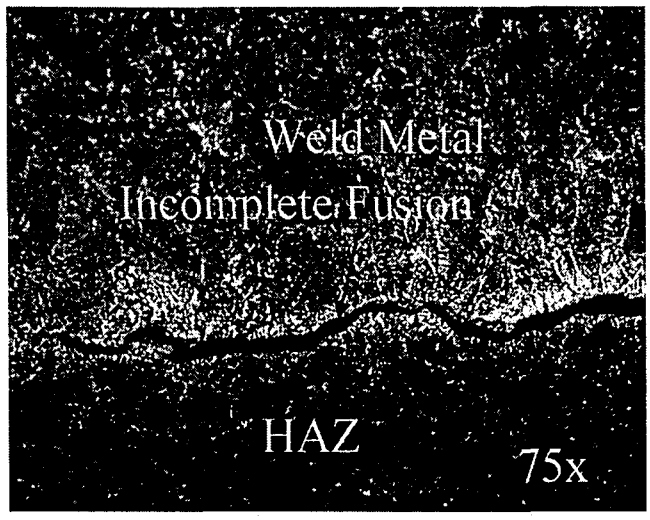

Figure 4.31: Incomplete Fusion in Specimen 36-C2-Top-right Section

Figure 4.32: Micro-Cracking in Specimen 36-C2-Bottom-right Section

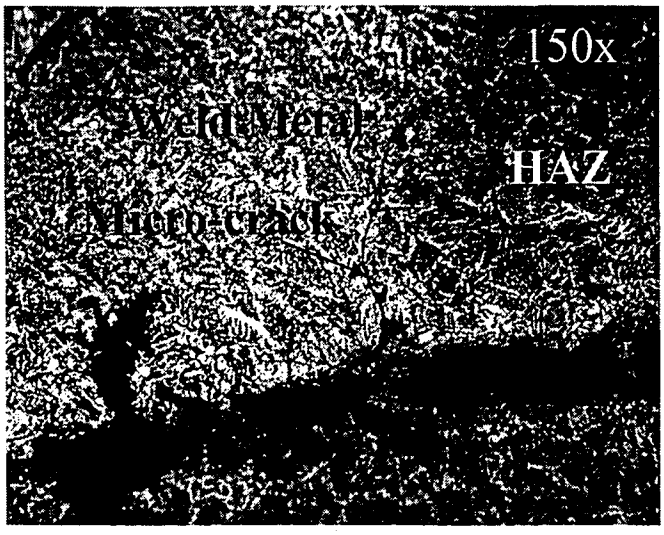

Figure 4.33: Micro-cracking in Specimen 36-C2-Bottom-left Section

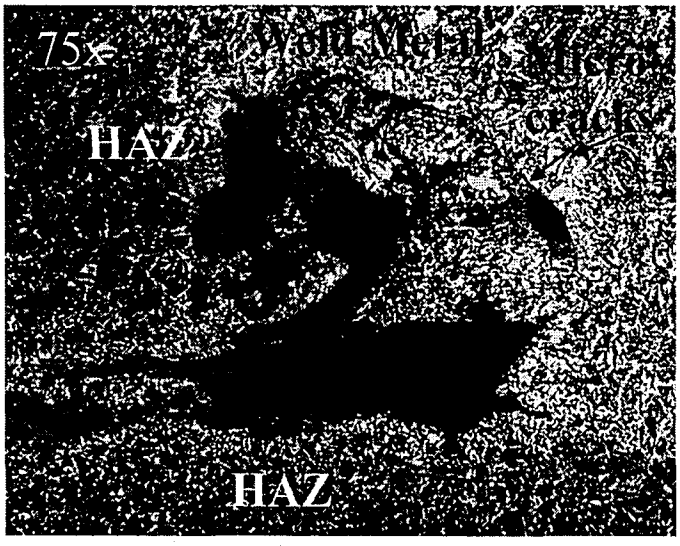

Figure 4.34: Micro-Cracking in Specimen 36-C2-Top-left Section

4.17 Porosity Check Specimens: 36-PC1—36-PC6

As discussed previously welding is prohibited when plate surfaces are wet. To assess this condition, several specimens were welded to examine the effects of surface moisture on the

porosity of fillet welds. Plate surfaces were wet using a spray bottle, as shown below in Figure 4.35.

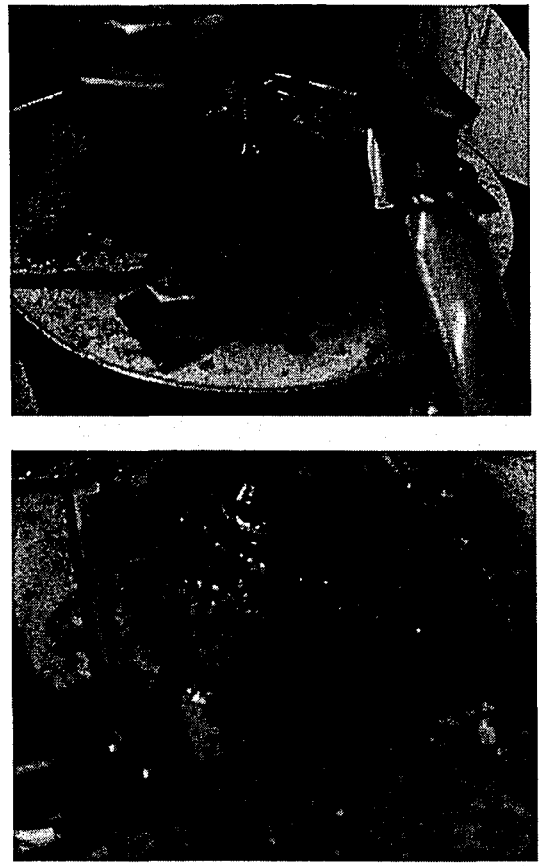

Figure 4.35: Wetting Process and Surface Wet Plate Assembly

The top surfaces of the base plates were wet prior to placement of the cover plate, and after its placement, the assembly was again sprayed to wet the joint. In the case of Specimen PC-4, water was actually poured into the recess in the concrete block such that placement of the base plates caused water to overflow from the recess. Additionally, water was poured over the assembly prior to welding.

All of the porosity-check specimens were carried out on A36 plate material. Specimens 36-PC1 to PC4 were fabricated from the moderate carbon A36 plate material. 36-PC5 and 36-PC6 were fabricated using the second heat of high carbon plate, namely the plate with material properties

summarized in Table 4-3. The first four specimens were welded at room temperature and were examined solely for the presence of porosity on the weld surface, or piping porosity that reached the surface. Additionally, specimen 36-PC4 was sectioned in several locations to investigate whether subsurface porosity was being generated but was not manifesting itself on the weld surface.

The fifth and sixth specimens were designed to combine the potential impact of wetness and high carbon content in the steel on both porosity and cracking. In the case of specimen 36-PC5, an attempt was made to weld through an ice coating produced by wetting plates which were pre-cooled with liquid nitrogen such that a layer of ice formed on all of the plate surfaces, as seen in Figure 4.36. The ice coating provided resistance to the striking of the arc, and furthermore, poor visibility resulting from steam made welding quite difficult in the environmental chamber. The first weld was not able to be completed due to a lack of visibility, as discussed later, and the second weld was completed immediately after the first weld was terminated.

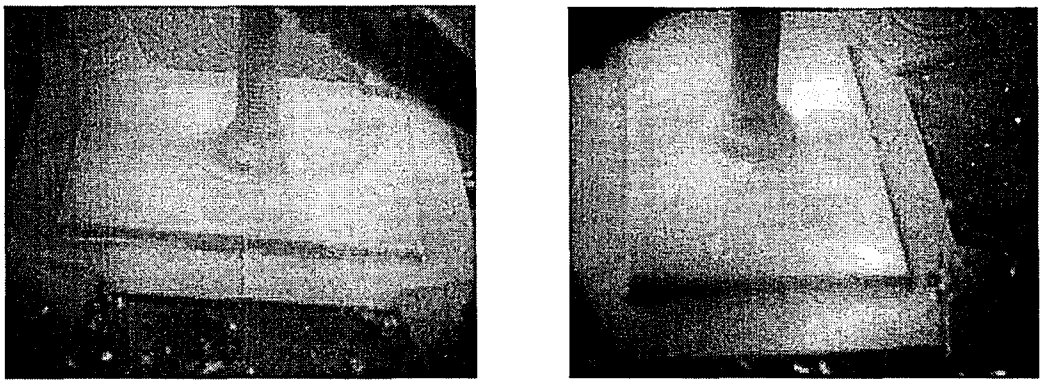

Figure 4.36: Images of Ice-Coated Specimen PC-5 in Chamber

The final porosity-check specimen, 36-PC6, was made using the high carbon A36 steel at room temperature and thoroughly wet. The specimen was, however, left restrained for at least 24 hours prior to its removal from the chamber to allow for potential cracking to occur due to

shrinkage restraint. Specimen 36-PC6 was sectioned thoroughly to investigate the presence of subsurface porosity or cracking.

The conditions during welding of the porosity-check specimens are summarized in Table 4-17, and images of the welds are shown in Figure 4.37 through Figure 4.42.

Table 4-17: Porosity-Check Specimen Fabrication Summary

Specimen ID	Base Metal	Steel Temperature [°F]	Relative Humidity [%RH]	Wind [mph]	Weld 1	Weld 2	Notes
PC-1	Moderate Carbon A36	88.9	43.4	0	Wet	Dry	†
PC-2	Moderate Carbon A36	91.1	50.0	0	Wet	Dry	†
PC-3	Moderate Carbon A36	91.9	28.8	0	Dry	Dry	--
PC-4	Moderate Carbon A36	84.5	50.0	0	Wet	Wet	Inundated
PC-5	High Carbon A36	15*	85.3	0	Ice	Ice	No visibility Weld 1
PC-6	High Carbon A36	74.2	17.6	0	Wet	Wet	Delayed Removal

* Plate temperature was approximately -20°F prior to wetting, but warmer water created ice and actually "warmed" outer plate surface. 15°F was taken from exposed surface without ice coating.

† A small amount of wetness may have seeped into welds on the half of the plates not intentionally wetted.

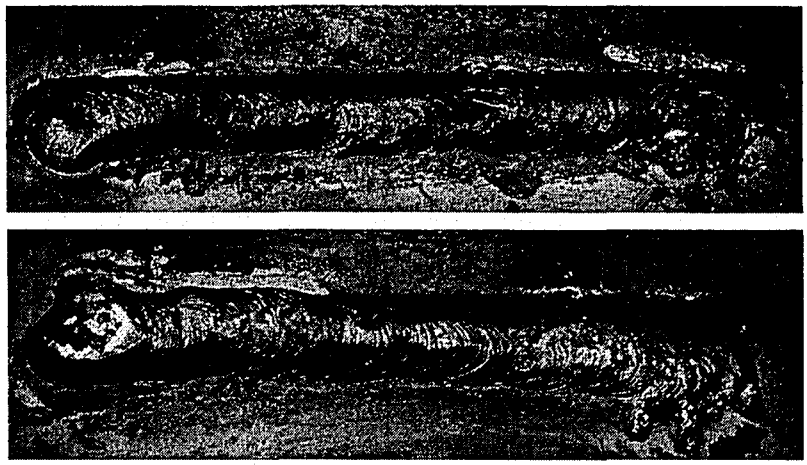

Figure 4.37: Specimen PC-1—Top Image-Weld 1(Wet), Bottom Image-Weld 2(Dry)

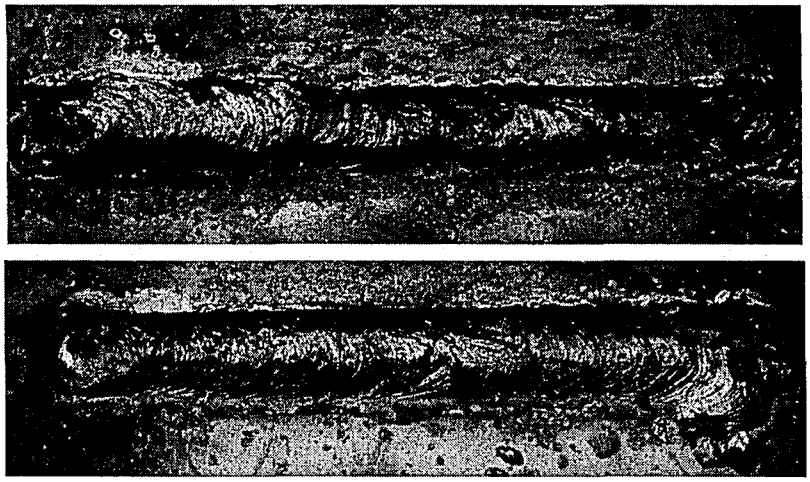

Figure 4.38: Specimen PC-2—Top Image-Weld 1(Wet), Bottom Image-Weld 2(Dry)

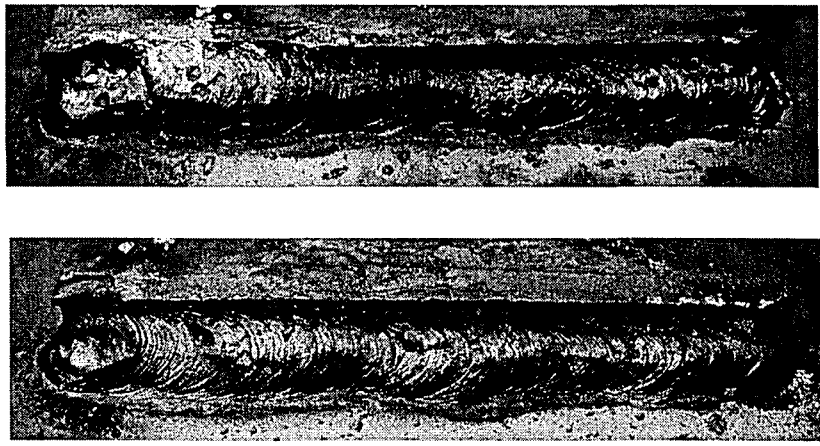

Figure 4.39: Specimen PC-3—Top Image-Weld 1(Dry), Bottom Image-Weld 2(Dry)

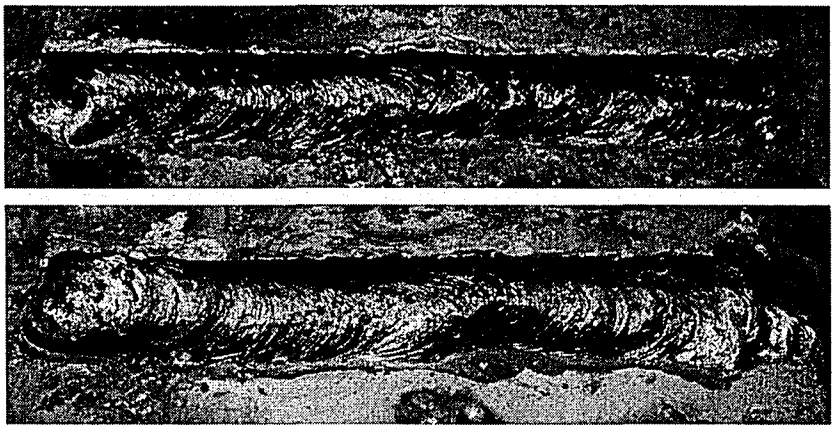

Figure 4.40: Specimen PC-4—Top Image-Weld 1(Wet), Bottom Image-Weld 2(Wet)

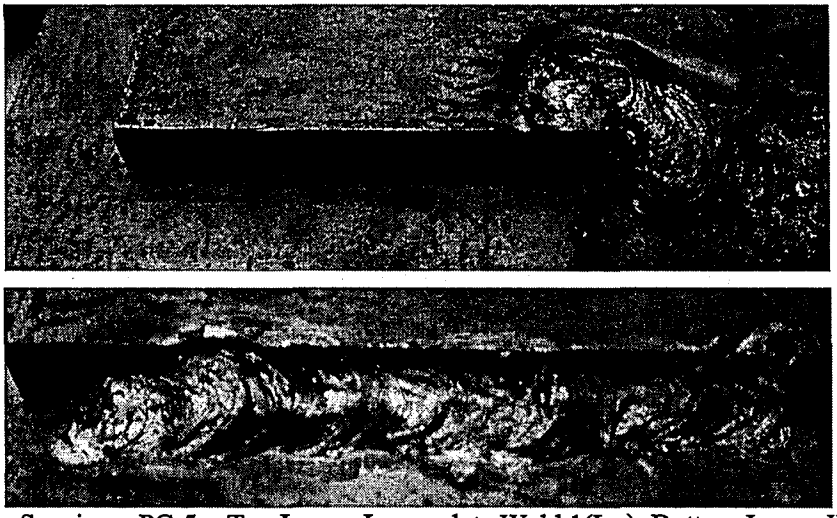

Figure 4.41: Specimen PC-5—Top Image-Incomplete Weld 1(Ice), Bottom Image-Weld 2(Ice)

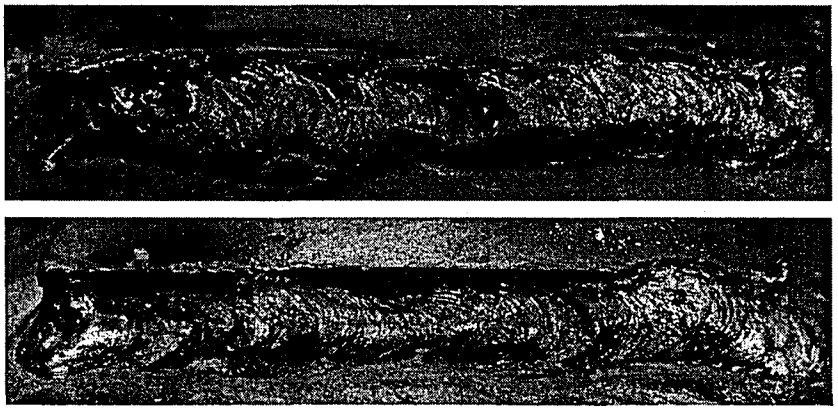

Figure 4.42: Specimen PC-6—Top Image-Weld 1(Wet), Bottom Image-Weld 2(Wet)

The welds made through surface wetness did not have significant amounts of piping porosity. In one instance (Weld 2, Specimen PC-5) a single piping pore was observed near the start position of the weld. The weld appearance is poor in most cases due to the generation of steam which limited visibility during welding.

From a porosity perspective, the welds made through surface wetness are satisfactory according to requirements of AWS D1.1, as referenced in Section 2.4.5. It was observed visually by the welder at the time of welding that the moisture on the plate surface was being driven off ahead of the weld bead such that the surface wetness was not likely entering the weld, but was evaporating as the weld bead progressed.

Because Specimen PC-6 was thoroughly wet and remained restrained for 24 hours prior to removal, it was theorized that it might contain cracks as a result of the moisture. As discussed previously, the hydrogen from moisture can dissociate into hydrogen which becomes dissolved in the weld pool. If the hydrogen does not escape from the solidifying weld pool, it can become trapped in voids in the microstructure and exert pressure which initiates cracking. Furthermore, the specimen was restrained for 24 hours, and such restraint is also known to promote cracking as it restrains cooling contraction and allows the weld to develop thermal shrinkage strains. The specimen was therefore sectioned and polished in much the same way as Phase 1 specimens and was examined for cracks under the microscope. The polished cross-sections are presented below in Figure 4.43.

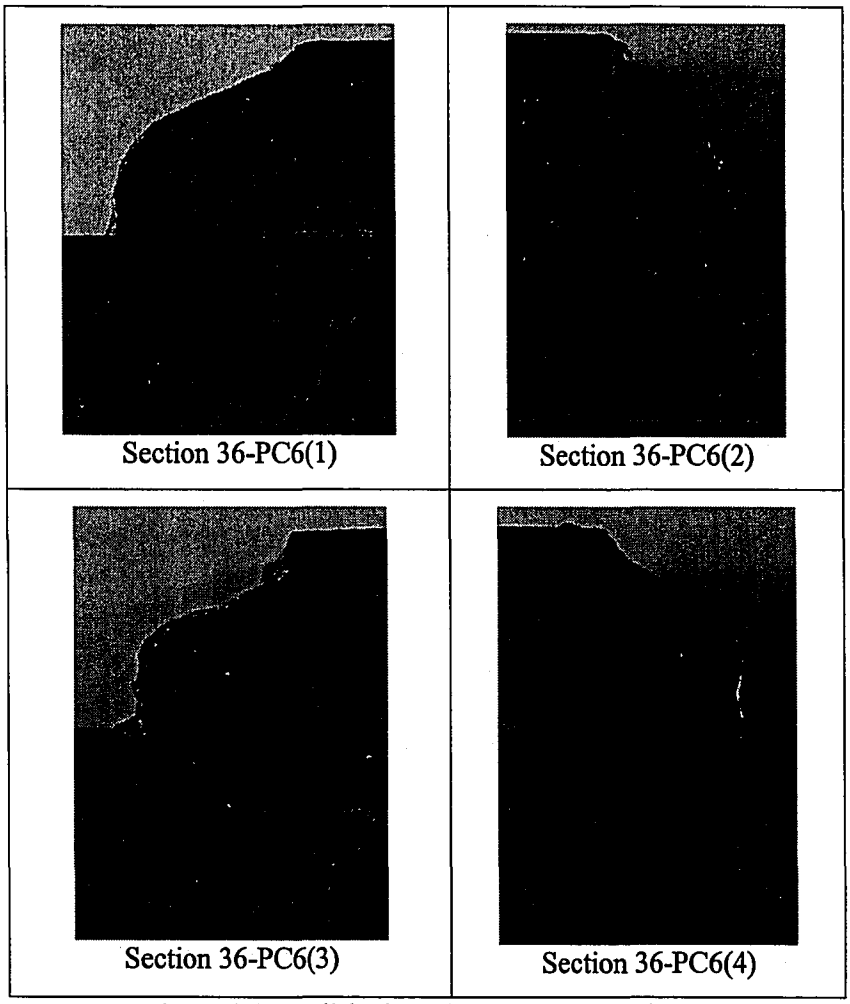

Figure 4.43: Polished Sections-Specimen 36-PC6

The profiles are each extremely convex. This may be a result of poor visibility due to steam generated by welding through the moisture, or it may be related to arc instability due to the surface wetness. Sections PC6(1) and PC6(4) each contain small inclusions at the root. However, no porosity is observed in any section, consistent with the surface observations in which no piping porosity was observed on the weld surface either.

Micro-cracks were observed in PC-6(2) that are connecting micro-cracks in the vicinity of the slag inclusion at the root of the weld in this section (Figure 4.44).

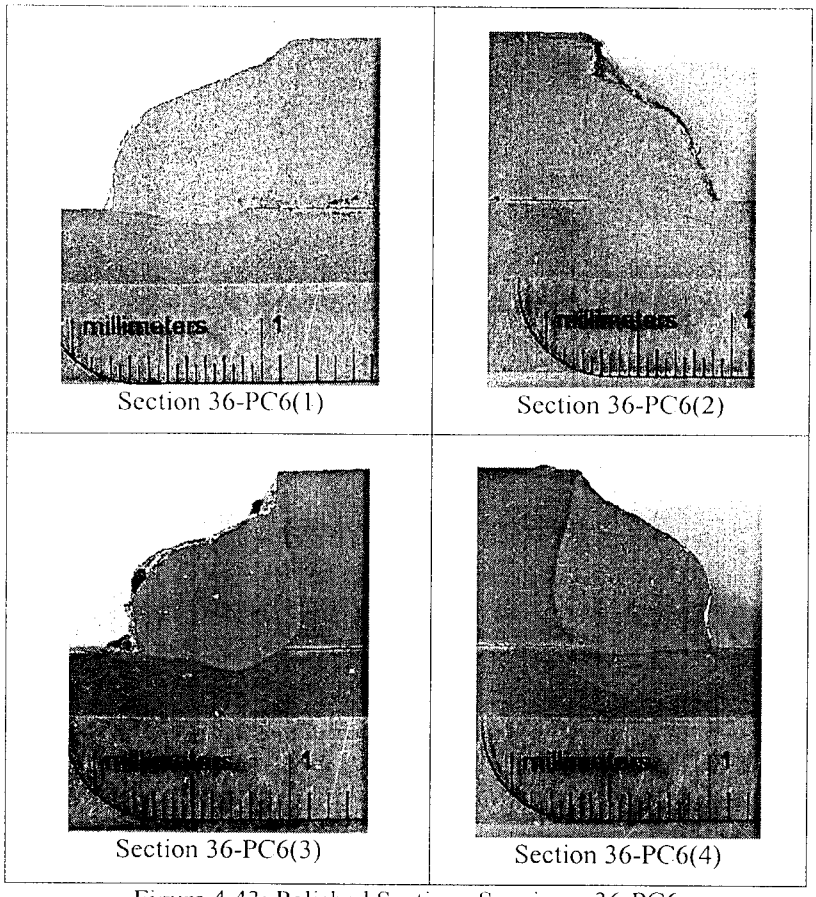

Figure 4.43: Polished Sections-Specimen 36-PC6

The profiles are each extremely convex. This may be a result of poor visibility due to steam generated by welding through the moisture, or it may be related to arc instability due to the surface wetness. Sections PC6(1) and PC6(4) each contain small inclusions at the root. However, no porosity is observed in any section, consistent with the surface observations in which no piping porosity was observed on the weld surface either.

Micro-cracks were observed in PC-6(2) that are connecting micro-cracks in the vicinity of the slag inclusion at the root of the weld in this section (Figure 4.44).

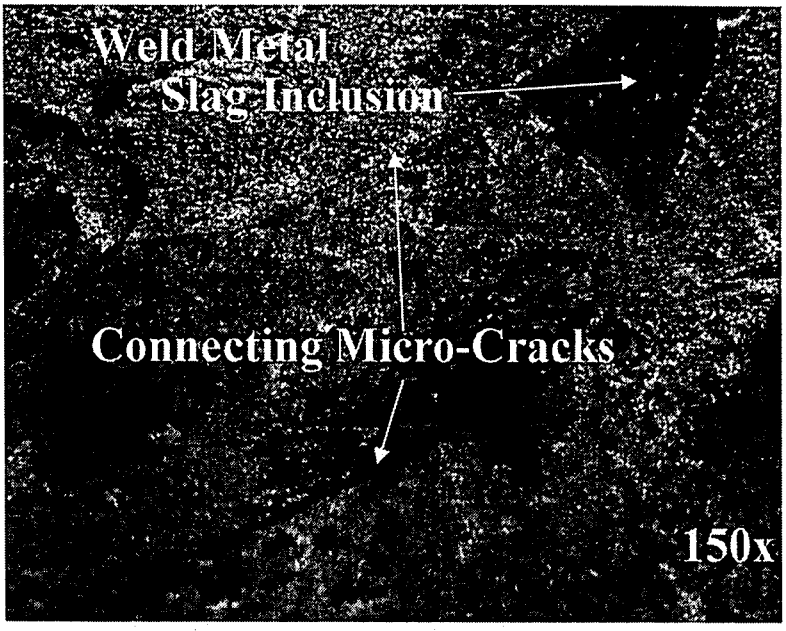

Figure 4.44: Connecting Micro-Cracks in Specimen 36-PC6, Section PC6(2)

Micro-cracks were also observed in section PC-6(4) at the toe and the root. An image of the toe micro-cracking is shown in Figure 4.45.

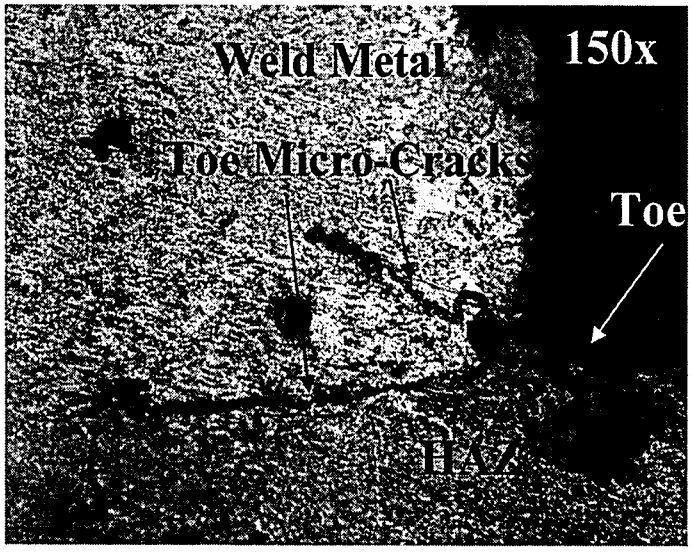

Figure 4.45: Toe Micro-Cracks in Specimen 36-PC6, Section PC-6(4)

4.18 Hardness Measurements

The cold cracking behavior of welds is tied to the hardness of the heat-affected zone (HAZ). Cracking will tend to occur in areas of higher hardness where the ductility is low. For this reason, hardness measurements were taken on several specimens made with A36 plate material and are presented in this section. Hardness can be measured using various scales, but the Vickers microhardness test was used for this study, as it has the capacity to measure the hardness of points at close intervals and measure the hardness across the various regions of the HAZ.[16] The test is performed using a pyramid shaped diamond indenter which is pressed into the specimen with a given load over a prescribed time duration (10 seconds in this case). The indentation is then measured using a microscope, and the dimensions of the indentation are used to calculate the hardness on the Vickers scale.

The Vickers microhardness test procedure is conducted as follows. A polished cross section is placed on the Leco M-400-G1 Microhardness Tester platform, and the 10X magnification microscope is used to roughly locate an area where weld hardness testing is desired, typically at the weld metal/HAZ boundary. The specimen is then magnified to 55X and the weld metal/HAZ boundary is brought into the center of view. From this location, calibrated dials are used to move the specimen five intervals of 0.5mm on a line orthogonal to the HAZ boundary, progressing into the region of weld metal. At this point, the indenter is dropped into the specimen in a process controlled by the machine, and a load of 1.0 kg is applied for a duration of ten seconds. The indenter is then raised, and the 55X microscope is used to position calibrated lines in the viewfinder on the horizontal boundaries of the diamond indentation. The measurement in microns corresponding to the distance between the lines in the viewfinder is recorded and stored by the machine. The second (vertical) dimension of the diamond indentation is recorded, and the hardness is automatically computed by the test machine. This

value is recorded, and the specimen is moved exactly 0.5mm toward the boundary. The indenter is again dropped into the specimen, and the process is repeated until the indenter measures the hardness at the HAZ boundary. At this point, three measurements are taken, one in the original line of measurements, and one on either side of the first measurement, spaced 0.5mm away. The measurements again resume on the original line of indentations until the desired number of readings are taken or until the hardness values level out, indicating solely base metal is being indented. The number of hardness measurements taken on a given section ranged from 11 to 15. A figure illustrating the indentations is presented below as Figure 4.46.

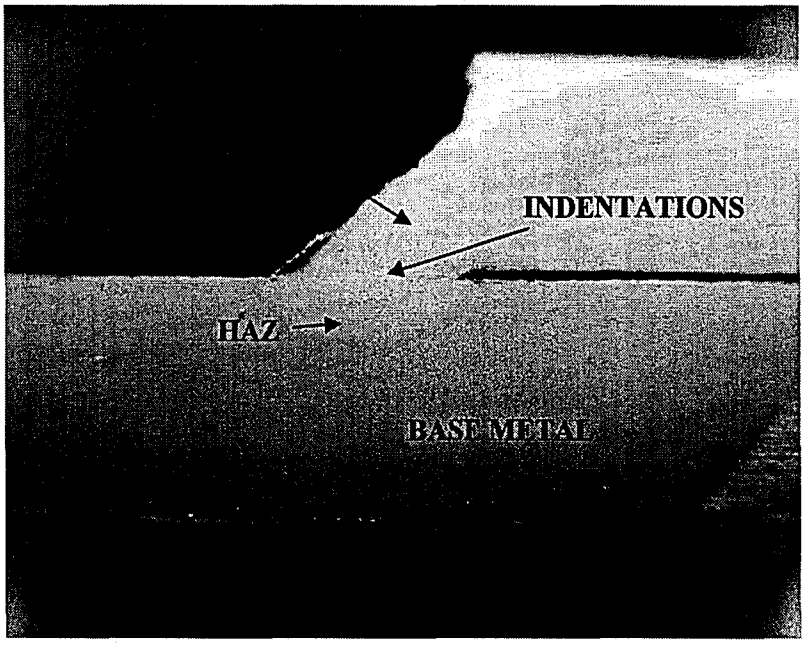

Figure 4.46: Vickers Microhardness Test Specimen

The hardness across the weld cross-section is controlled by the steel microstructure created during the welding and subsequent cooling process. Depending on the cooling rate and the carbon content of the base metal, martensite may form in the HAZ, increasing hardness and crack susceptibility. The hardness of the HAZ is therefore a good indicator of the amount of martensite present and the cold cracking potential. Cold cracking rarely occurs when hardness

value is recorded, and the specimen is moved exactly 0.5mm toward the boundary. The indenter is again dropped into the specimen, and the process is repeated until the indenter measures the hardness at the HAZ boundary. At this point, three measurements are taken, one in the original line of measurements, and one on either side of the first measurement, spaced 0.5mm away. The measurements again resume on the original line of indentations until the desired number of readings are taken or until the hardness values level out, indicating solely base metal is being indented. The number of hardness measurements taken on a given section ranged from 11 to 15. A figure illustrating the indentations is presented below as Figure 4.46.

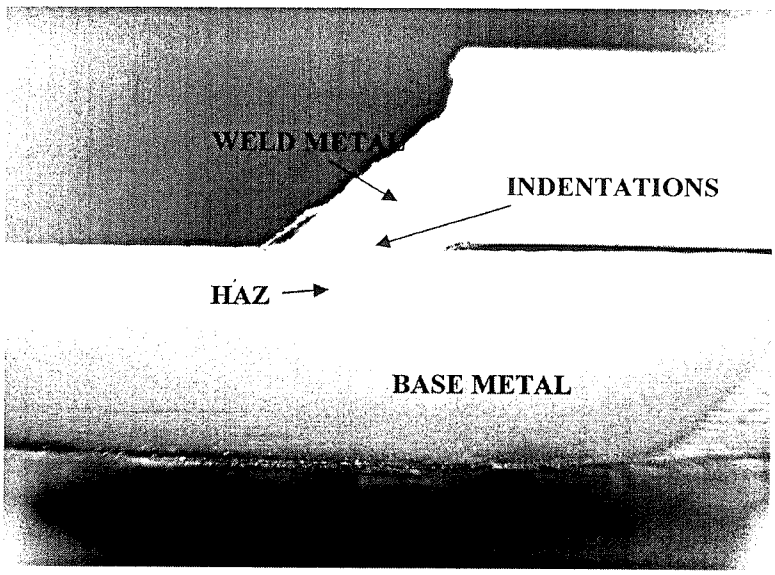

Figure 4.46: Vickers Microhardness Test Specimen

The hardness across the weld cross-section is controlled by the steel microstructure created during the welding and subsequent cooling process. Depending on the cooling rate and the carbon content of the base metal, martensite may form in the HAZ, increasing hardness and crack susceptibility. The hardness of the HAZ is therefore a good indicator of the amount of martensite present and the cold cracking potential. Cold cracking rarely occurs when hardness

is below a Vickers hardness of 265 HV but is common when the Vickers hardness approaches 470 HV.[16] Preheating of the base plates is used as a precaution against a cooling rate that may be too high, allowing martensite to form in the HAZ. Preheat *was not* used in this study.

Microhardness tests were performed on five specimens. These were:

1. Specimen 36-6, Moderate carbon A36 steel – 76.6°F, 94.3%RH, 20 mph wind
2. Specimen 36-7, Moderate carbon A36 steel – 73.6°F, 97.8%RH, 34.7 mph wind
3. Specimen 36-22, Moderate carbon A36 steel – -5.0°F, 99.9%RH, 21.3 mph wind
4. Specimen 36-C1, High carbon A36 steel – -6.0°F, 100%RH, 0 mph wind
5. Specimen 36-C2, High carbon A36 steel – -4.0°F, 66.7%RH, 0 mph wind

Specimens welded at a lower ambient temperature have a higher likelihood to form martensite in the HAZ due to the increased cooling rate. In addition, steels with a higher carbon equivalent have a higher likelihood to form martensite in the HAZ.[16]

The values from the hardness measurements for all five specimens listed above are depicted graphically in Figure 4.47. The approximate crack-susceptibility threshold of 265 HV is indicated on the figure, as well as the approximate zones (weld metal, HAZ, and base metal) for the tested specimens.

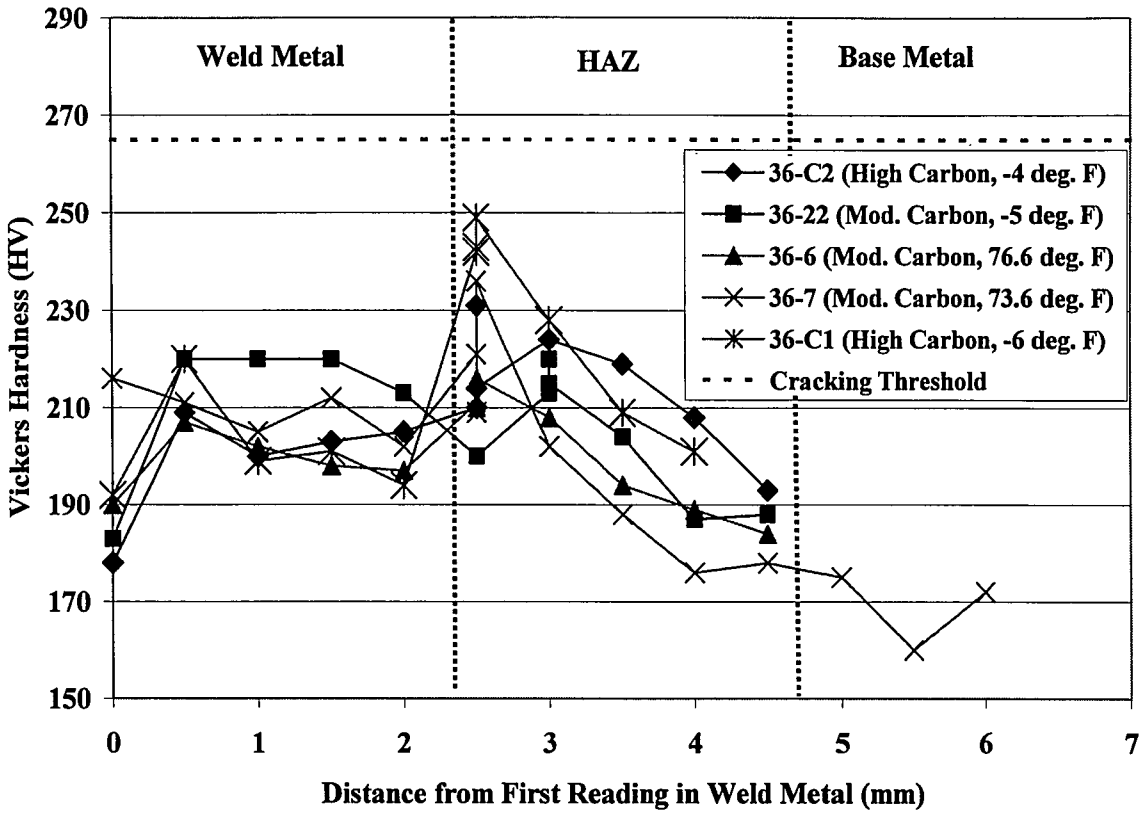

Figure 4.47: Plot of Vickers Hardness From Microhardness Tests

It can be seen from Figure 4.47 that the peak values of the hardness in the specimens tested are consistent in magnitude at approximately 215-250 HV. This suggests that the welding and cooling processes were similar for the different specimens.

The final metallurgical structure (and hardness) of a weld zone is dependent largely on the cooling rate, which is in turn affected by initial plate temperature. For the plate thickness used in this study, the expression used to calculate cooling rate is given by Equation 4.[16]

$$R = 2 \cdot \pi \cdot k \cdot \rho C \cdot (\frac{h}{H_{net}})^2 \cdot (T_c - T_o)^3 \qquad \text{Equation 4}$$

where R is the cooling rate at the weld center line [°C/s], k is the thermal conductivity of the steel [0.028 J/mm*s*°C], ρC is the volumetric specific heat of the base metal [0.0044 J/mm^3*°C], h is the base metal thickness [mm], H_{net} is the ratio of energy input [J/mm] to travel speed [mm/s], T_c is the temperature at which the cooling rate is calculated, and T_o is the initial temperature of the base metal. When calculating the cooling rate at a temperature, T_c, of roughly 550°C [1020°F], and using average energy input and travel speeds for A36 steel (from Section 3.6), the difference in cooling rates for steel with an initial plate temperature of -10°F [-23.33°C] versus 71°F [21.6°C] is calculated to be approximately 25%.

Although the cooling rate is affected by the initial plate temperature, the results of the hardness measurements do not indicate that there is a significant increase in hardness between welds made on plate with an initial temperature of -10°F [-23.33°C] versus 71°F [21.6°C]. The similarity of the peak hardness values suggests that the cooling rate in the case of those specimens welded in sub-zero temperatures was not sufficiently high to form a microstructure with hardness above the cracking threshold (265 HV).

The welds made on higher carbon steel at low temperatures (-6°F and -4°F), namely Specimens 36-C1 and 36-C2, while having slightly higher peak values (10% higher on average compared to moderate carbon samples), do not appear to be approaching hardness levels that are associated with cold cracking.

5 A36 Galvanized Phase 1 Specimens

To protect steel connections from corrosion the exposed plate materials are often galvanized. AWS D1.1 and the PCI Design Handbook (see Section 2.3) require the galvanization to be removed in the vicinity of the weld prior to welding. Failure to perform this step could result in a poor weld due to the low melting point of the zinc galvanization. To verify this possibility and to assess if other negative conditions would occur, a series of galvanized plates were welded *without removal* of galvanization. A limited number of conditions were evaluated.

5.1 A36 Galvanized Steel Material Properties

The A36 steel used for the galvanized plate specimens had properties given in Table 5-1. Plates were pre-cut to the required size of ⅜-in. x 4-in. x 6-in and hot-dip galvanized, such that all faces and edges were coated. Plates were arranged and welded in accordance with the welding setup procedure described in Section 3.1. The A36 Galvanized specimens were restrained at the four corners of the base plates and across the cover plate as shown in Figure 5.1.

Figure 5.1: A36 Galvanized Specimen in Setup During Welding

The A36 Galvanized plate materials were donated by High Concrete Structures, Inc. The plate material came from the Durrett Sheppard Steel Co., originating from the Roanoke Bar Division of Steel Dynamics®. The chemical composition of the steel and the mechanical properties were obtained from the mill certificate for the steel used. An additional independent chemical analysis was completed by Laboratory Testing, Inc., of Hatfield, PA. The values of the chemical composition from the independent analysis and from the mill certificate are summarized in Table 5-1 with the computed carbon equivalent, along with the mechanical properties of the metal.

Table 5-1: A36 Galvanized Material Data

Heat Number				JF3289							
Manufacturer				Steel Dynamics®-Roanoke Bar Division							
Applicable Specimens				36G-25, 36G-33(1), 36-G33(2), 36G-17HR							
Specification											
ASTM A36-04				ASME SA36QQS741D				ASTM A709-00A GR36			
Chemical Composition [%]-Independent Chemical Analysis Values											
C	Mn	P	S	Si	Cr	Ni	Nb	V	Cu	Mo	CE
0.13	0.66	0.007	0.025	0.21	0.068	0.080	0.001	0.002	0.24	0.042	0.319
Chemical Composition [%]-Mill Certificate Values											
C	Mn	P	S	Si	Cr	Ni	Nb	V	Cu	Mo	CE
0.13	0.73	0.007	0.021	0.22	0.07	0.08	0.002	0.002	0.29	0.02	0.331
Mechanical Properties											
Test		Yield Stress [ksi]			Ultimate Stress [ksi]			Elongation [%-8-in.]			
1		46.4			67.8			30.6			
2		46.5			67.5			31.3			

5.2 A36 Galvanized Weld Material Properties

E7018-H4R SMAW electrodes were used for all welds. This is the same electrode used for the non-galvanized A36 steel specimens. The material description and properties are discussed in Section 4.2.

5.3 Specimen Performance Evaluation

The results for each ASTM A36 Galvanized welded specimen are described in the following sections. Each specimen description includes a table summarizing the nominal environmental conditions from the test matrix as well as the measured conditions prior to welding. Images of the weld specimen, weld beads, and four cross-sections are shown, and descriptions of the weld surface condition and cross section flaws are noted. The weld surface condition is noted below the image of each weld in the specimen descriptions using the profile index discussed in Section 3.7.3. Additionally, when of specific interest, microscopic images of discontinuities are presented with accompanying descriptions of the discontinuities. When microscopic images are included, a yellow box on a cross-section image denotes the area included in the associated microscopic image.

5.4 Specimen 36G-25: Base Condition

This specimen was subjected to the environmental conditions shown in Table 5-2 in the environmental chamber at the time of welding. A side door was opened in the chamber through which an exhaust system removed fumes.

Table 5-2: Environmental Conditions – Specimen 36G-25

Specimen: 36G-25	Air Temp.	Concrete Temp.	Steel Temp.	Rel. Humidity	Wind Speed
	°F	°F	°F	%RH	[mph]
Nominal Values	71	71	71	35	0
Measured Values	72	72	73	43.0	4.3*
*Exhaust system created draft over weld joint with wind speed of approximately 4.3 mph.					

The welded specimen is shown in Figure 5.2. Photographs of each of the two welds are presented along with an overview photo of the entire specimen. Sections were taken at four locations from the specimen and polished to examine the quality of the weld. These photos are also included.

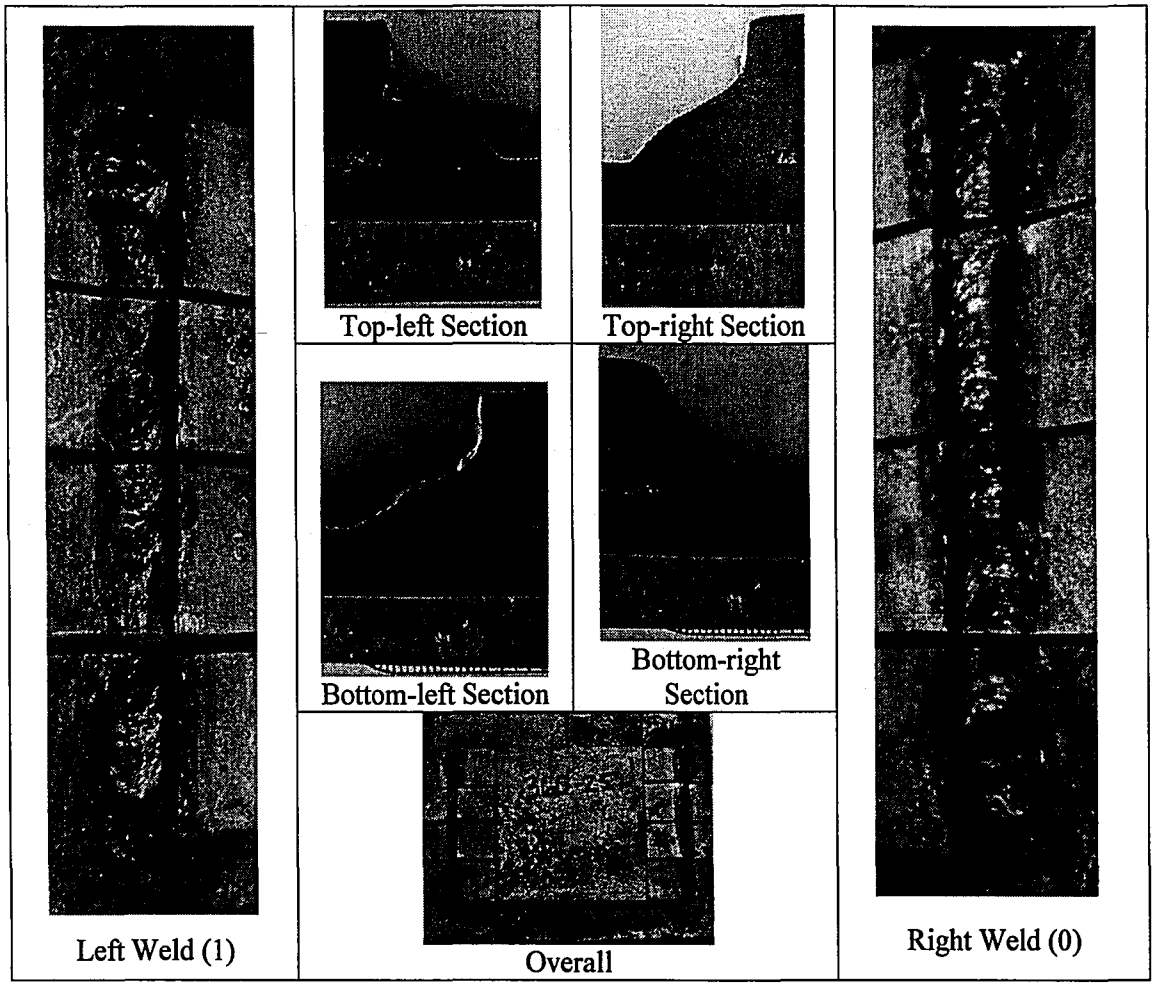

Figure 5.2: Specimen 36G-25

5.4.1 Visual Observation Summary

Both welds had a satisfactory appearance from a surface perspective, with some slightly erratic size changes along the length. The top-left section exhibited slight undercut (.022-in.), and the bottom-right, bottom-left, and top-left profiles had short vertical legs, failing to meet the full 1/4-in. profile requirements. The specimen remained restrained until cooled to room temperature.

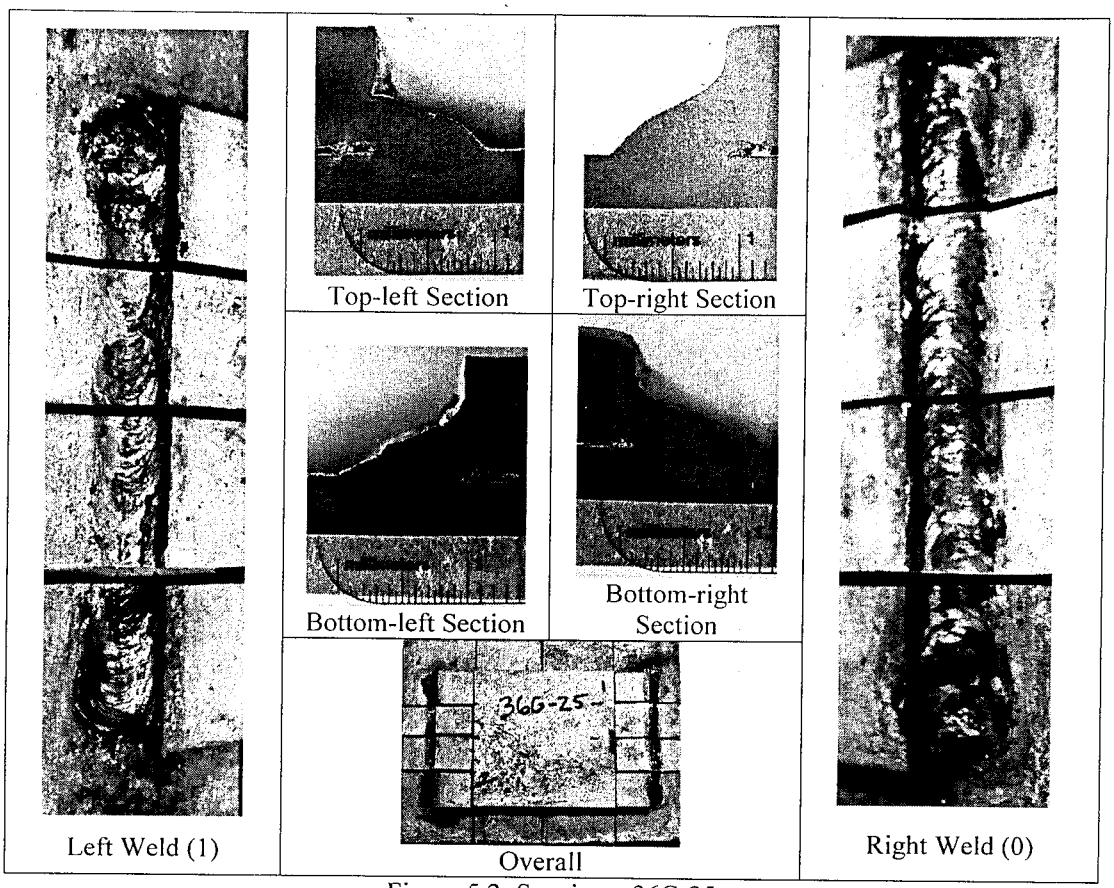

Figure 5.2: Specimen 36G-25

5.4.1 Visual Observation Summary

Both welds had a satisfactory appearance from a surface perspective, with some slightly erratic size changes along the length. The top-left section exhibited slight undercut (.022-in.), and the bottom-right, bottom-left, and top-left profiles had short vertical legs, failing to meet the full 1/4-in. profile requirements. The specimen remained restrained until cooled to room temperature.

5.5 Specimen 36G-33(1): 32°F, Low Humidity, Low Wind

This specimen was subjected to environmental conditions outdoors at the time of welding. Plates were pre-cooled with liquid nitrogen, and visibility and zinc fume problems were avoided by welding outdoors. The specific conditions for the weld are detailed in Table 5-3.

Table 5-3: Environmental conditions – Specimen 36G-33(1)

Specimen: 36G-33(1)	Air Temp.	Concrete Temp.	Steel Temp.	Rel. Humidity	Wind Speed
	°F	°F	°F	%RH	[mph]
Nominal Values	32	32	32	35	0
Measured Values	38.8	54.2	36	28.5	3-5

The welded specimen is shown in Figure 5.3. Photographs of each of the two welds are presented along with an overview photo of the entire specimen. Sections were taken at four locations from the specimen and polished to examine the quality of the weld. These photos are also included.

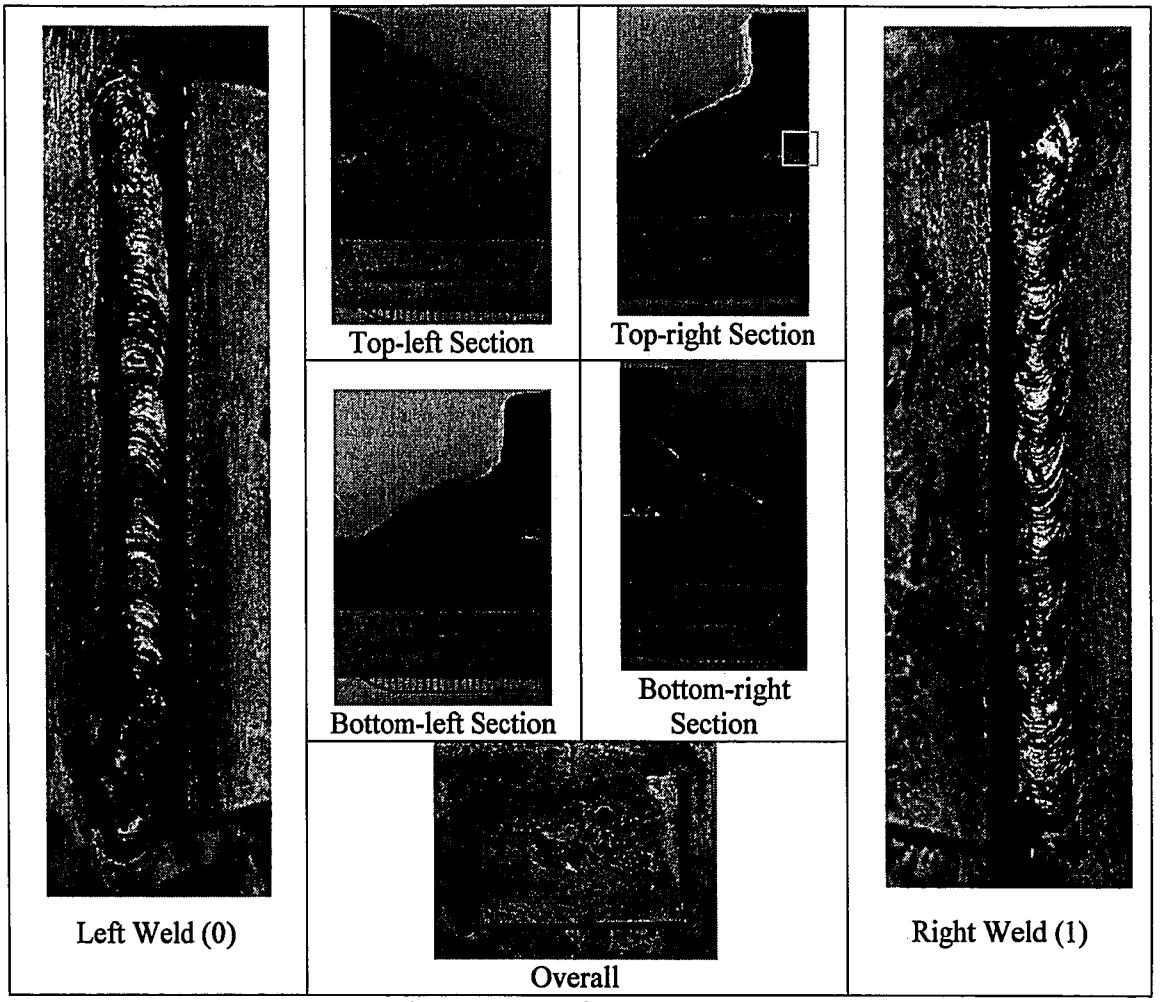

Figure 5.3: Specimen 36G-33(1)

5.5.1 Visual Observation Summary

The right weld had a skew to the horizontal leg, contained no pores in the surface or in the sections, and had a small amount of undercut. The left weld also had a short vertical leg and no pores in the surface or in the sections. The top-right, bottom-left, and top-left profiles exhibited convexity and undercut (.035-in., unacceptable) can be seen in the vertical leg of the bottom-right section. None of the sections satisfy the 1/4-in. profile requirements. A small root crack was observed in the top-right section and is presented in more detail in Section 5.5.2.

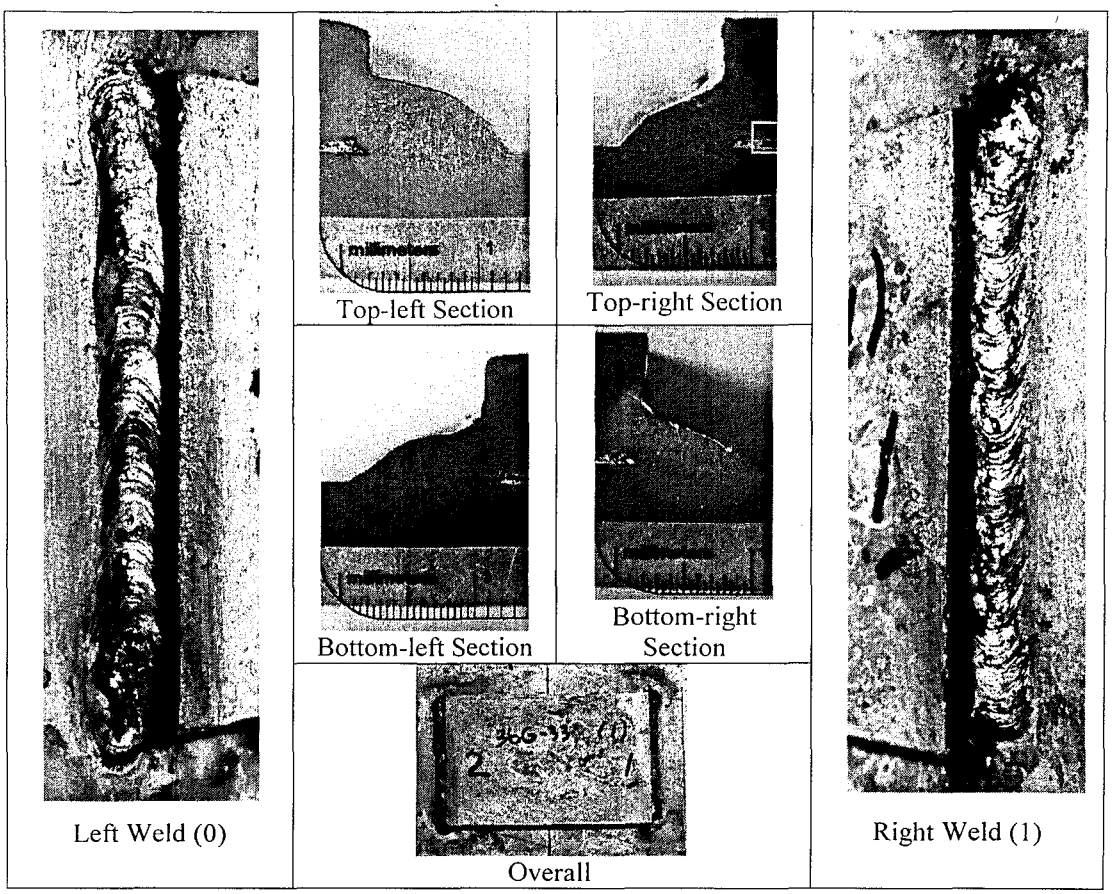

Figure 5.3: Specimen 36G-33(1)

5.5.1 Visual Observation Summary

The right weld had a skew to the horizontal leg, contained no pores in the surface or in the sections, and had a small amount of undercut. The left weld also had a short vertical leg and no pores in the surface or in the sections. The top-right, bottom-left, and top-left profiles exhibited convexity and undercut (.035-in., unacceptable) can be seen in the vertical leg of the bottom-right section. None of the sections satisfy the 1/4-in. profile requirements. A small root crack was observed in the top-right section and is presented in more detail in Section 5.5.2.

5.5.2 *Microscopy Observation Summary*

The small root crack observed in the top-right section originates at the interface between weld metal and the material wedged in the gap between the base plates and cover plates. The rough galvanized plate surfaces, in general, caused larger gaps than uncoated steel surfaces, resulting in material trapped in the plate gap. Wedged material in the gap between the base plates and cover plate caused a stress concentration that permitted this crack to form. As a result of some leaching and local discoloration around the crack, the crack is identifiable without the aid of microscopy, although its size may not be in excess of approximately 1/32-in., the threshold of the micro-crack designation.

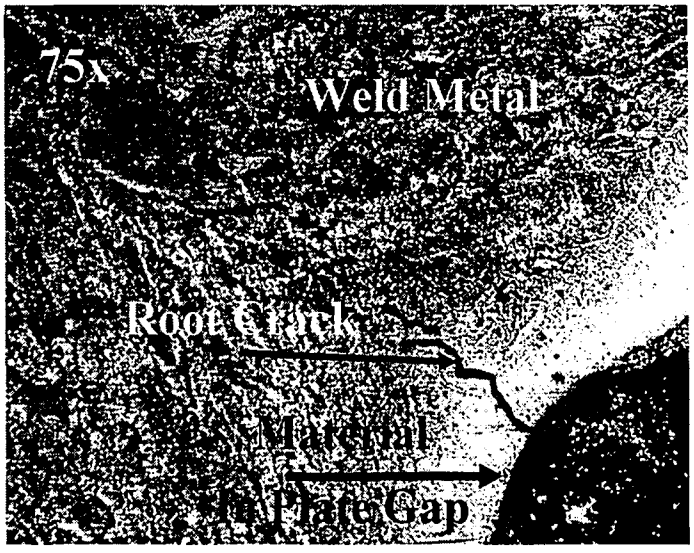

Figure 5.4: Root cracking in Specimen 36G-33(1)-Top-right Section

5.6 Specimen 36G-33(2): 32°F, Low Humidity, Low Wind (Delayed Removal)

This specimen was subjected to environmental conditions outdoors at the time of welding. Plates were pre-cooled with liquid nitrogen, and visibility and zinc fume problems were avoided by welding outdoors. The specific conditions for the weld are detailed in Table 5-4.

Table 5-4: Environmental conditions – Specimen 36G-33(2)					
Specimen: 36G-33(2)	Air Temp.	Concrete Temp.	Steel Temp.	Rel. Humidity	Wind Speed
	°F	°F	°F	%RH	[mph]
Nominal Values	32	32	32	35	0
Measured Values	37	61	20	33.6	3

The welded specimen is shown in Figure 5.5. Photographs of each of the two welds are presented along with an overview photo of the entire specimen. Sections were taken at four locations from the specimen and polished to examine the quality of the weld. These photos are also included.

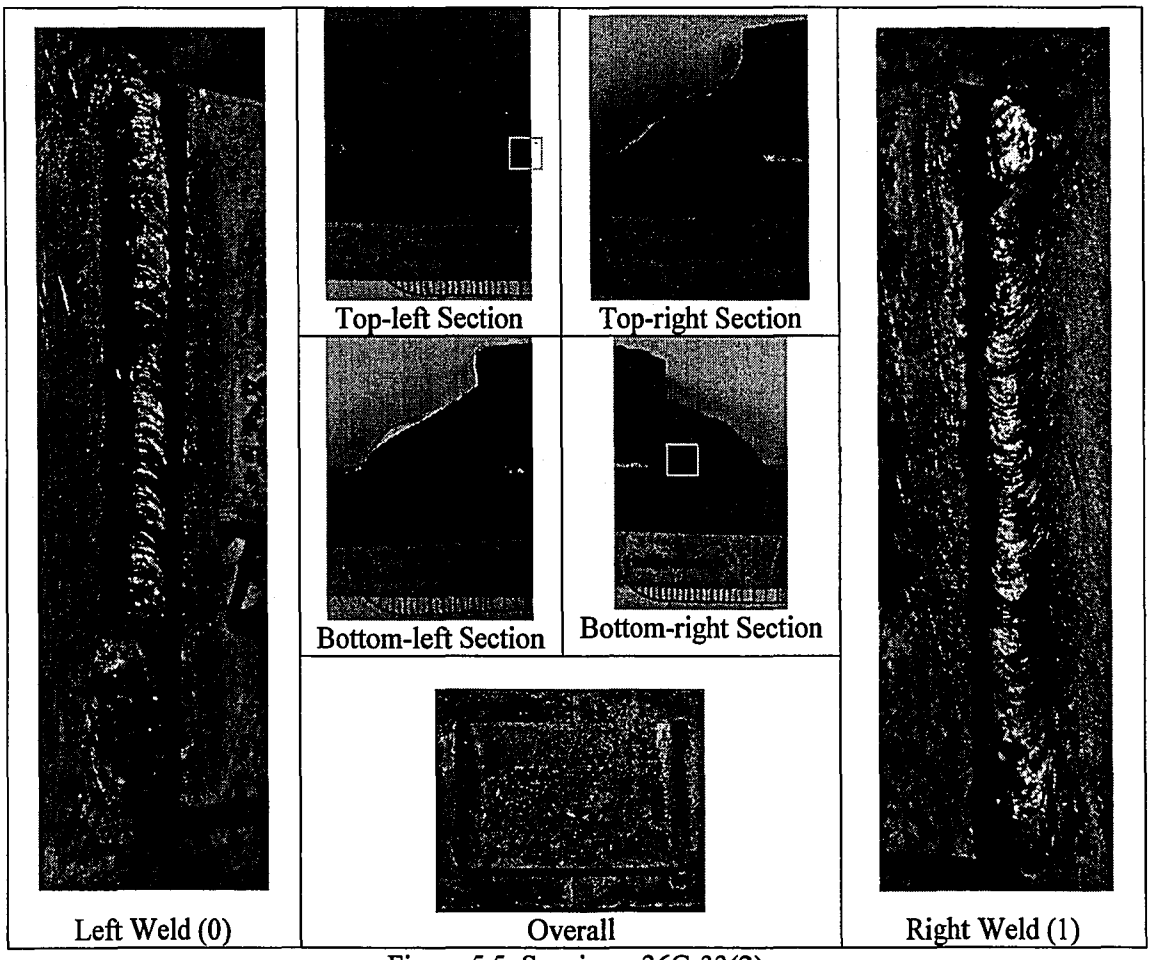

Figure 5.5: Specimen 36G-33(2)

Table 5-4: Environmental conditions – Specimen 36G-33(2)					
Specimen: 36G-33(2)	Air Temp.	Concrete Temp.	Steel Temp.	Rel. Humidity	Wind Speed
	°F	°F	°F	%RH	[mph]
Nominal Values	32	32	32	35	0
Measured Values	37	61	20	33.6	3

The welded specimen is shown in Figure 5.5. Photographs of each of the two welds are presented along with an overview photo of the entire specimen. Sections were taken at four locations from the specimen and polished to examine the quality of the weld. These photos are also included.

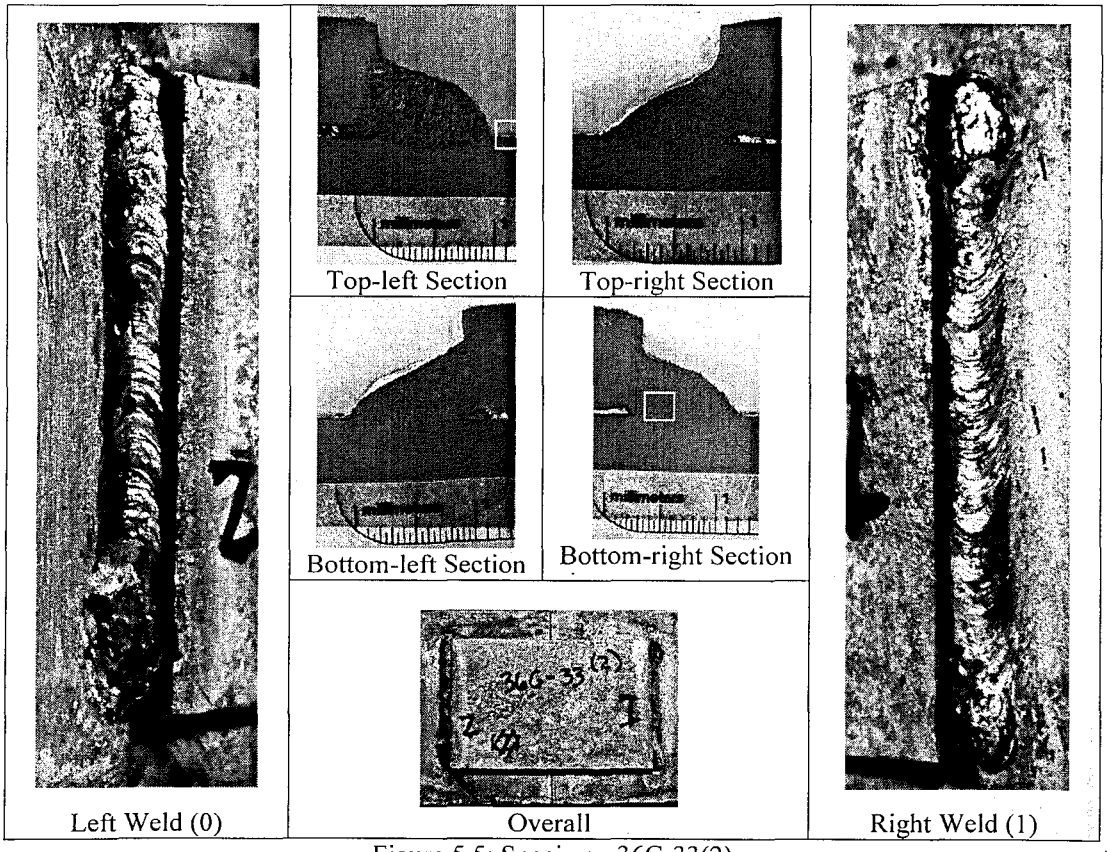

Figure 5.5: Specimen 36G-33(2)

5.6.1 Visual Observation Summary

The right and left welds had no notable discontinuities, although the left weld had somewhat erratic size changes. The bottom-right and top-left profiles were convex, bulging toward the horizontal leg, and the bottom-left profile exhibited similar skew to the horizontal leg. All profiles had sufficient leg length and throat dimensions to meet the 1/4-in. profile requirements; however, the top-left profile had unacceptable convexity (.126-in.), and all four sections did not meet the 1/4-in. profile requirements.

5.6.2 Microscopy Observation Summary

The bottom-right and bottom-left sections had root micro-cracks, while the top-left section had a toe micro-crack. Plates remained restrained for 24 hours prior to removal from the test block. The bottom-left and bottom-right sections exhibit micro-cracks like the one shown in Figure 5.6. These appear to be solidification hot micro-cracks that are likely the result of low solidification temperature zinc compounds being present in solution in the weld pool. As the weld cooled, the root was the last place to cool. The low solidification (melting) temperature zinc compounds solidified late, and the solidified steel around the root restrained the cooling contraction there, allowing a small micro-crack to open at a 45 degree angle. The micro-crack discontinuities seen in the toe vicinity of the top-left section may be a result of stress imposed by the restraint of the specimen for 24 hours due to delayed removal. These are likely cold micro-cracks, related to the presence of hydrogen. The micro-crack discontinuities are not detectable by visual inspection, and due to their small size, it is unlikely that these types of discontinuities would influence the strength of the weld.

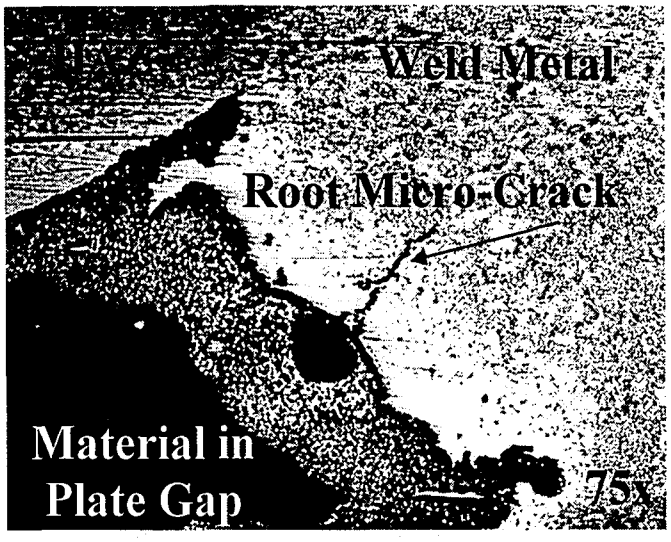

Figure 5.6: Root Micro-Crack in Specimen 36G-33(2)-Bottom-right Section

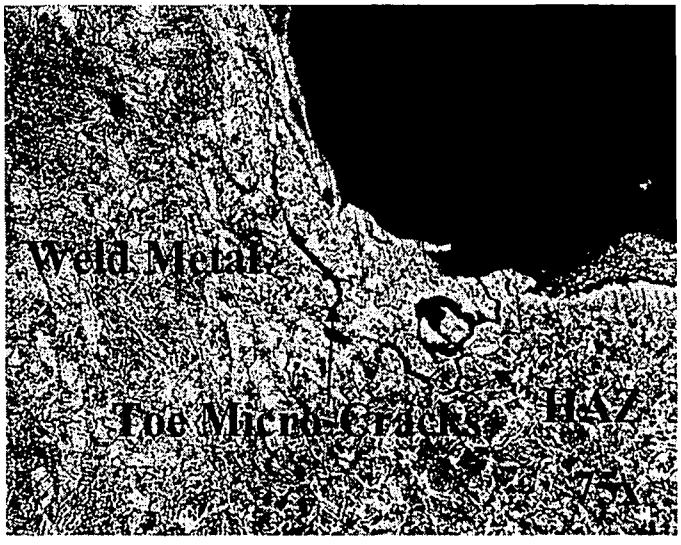

Figure 5.7: Toe Micro-Cracking in Specimen 36G-33(2)-Top-left Section

5.7 Specimen 36G-17HR: Warm, High Humidity, Low Wind, 17 hr. electrode exposure

This specimen was subjected to environmental conditions in the environmental chamber at the time of welding. The electrodes were also exposed to 95% RH, 71°F for approximately 17 hours prior to welding, and the resulting moisture content of the electrodes was 4% by weight. The specific conditions for the weld are detailed in Table 5-5.

Table 5-5: Environmental conditions – Specimen 36G-17HR					
Specimen: 36G-17HR	Air Temp.	Concrete Temp.	Steel Temp.	Rel. Humidity	Wind Speed
	°F	°F	°F	%RH	[mph]
Nominal Values	71	71	71	95	0
Measured Values	74.8	88.1	77.3	84.6	3-4

The welded specimen is shown in Figure 5.8. Photographs of each of the two welds are presented along with an overview photo of the entire specimen. Sections were taken at four locations from the specimen and polished to examine the quality of the weld. These photos are also included.

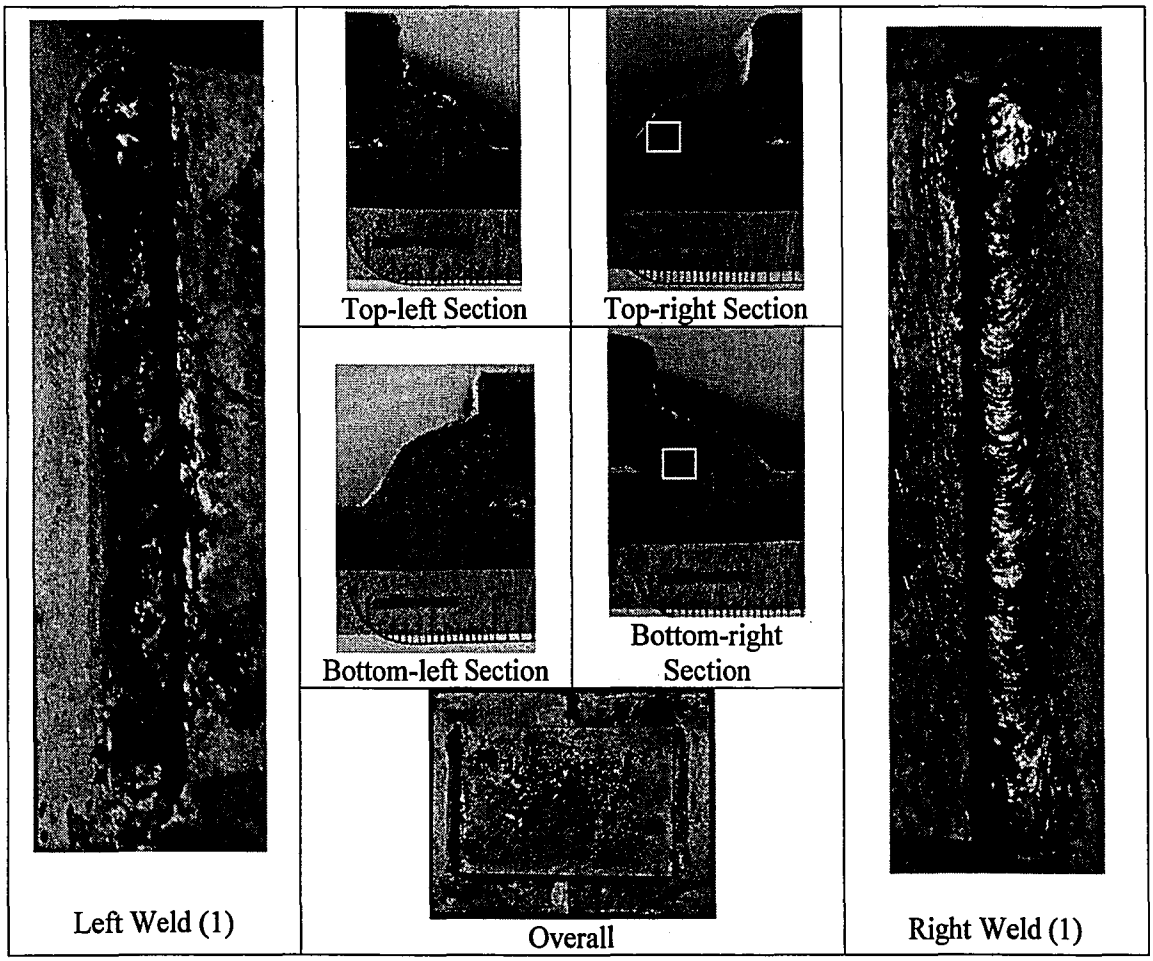

Figure 5.8: Specimen 36G-17HR

Table 5-5: Environmental conditions – Specimen 36G-17HR					
Specimen: 36G-17HR	Air Temp.	Concrete Temp.	Steel Temp.	Rel. Humidity	Wind Speed
	°F	°F	°F	%RH	[mph]
Nominal Values	71	71	71	95	0
Measured Values	74.8	88.1	77.3	84.6	3-4

The welded specimen is shown in Figure 5.8. Photographs of each of the two welds are presented along with an overview photo of the entire specimen. Sections were taken at four locations from the specimen and polished to examine the quality of the weld. These photos are also included.

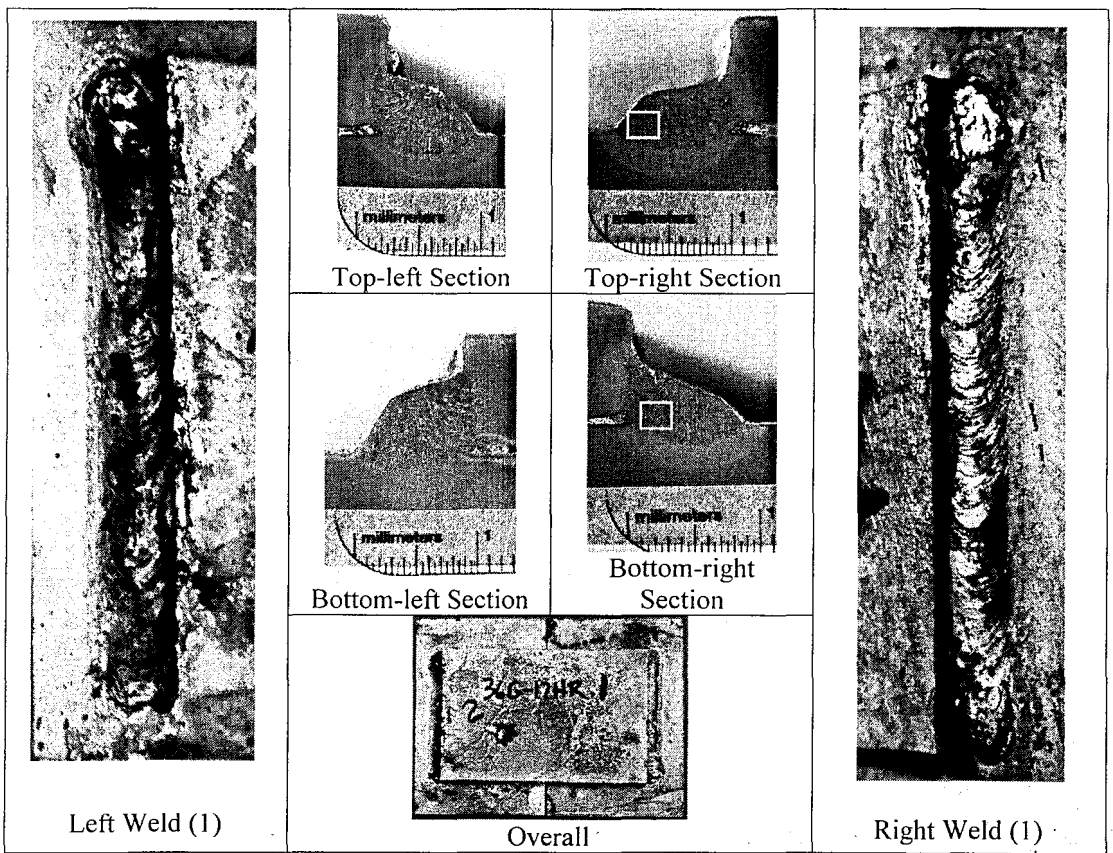

Figure 5.8: Specimen 36G-17HR

5.7.1 Visual Observation Summary

The right weld had significant skew to the horizontal leg and an undersized vertical leg. The left weld had some slightly irregular size changes along its length but had no notable flaws otherwise. All profiles were of a convex nature, particularly the bottom-left section (.11-in. convexity, less than allowable 1/8-in.). The top-right section had what may be a very small pore or slag inclusion (.008-in.), and the only section meeting the 1/4-in. profile requirements was the bottom-left section.

5.7.2 Microscopy Observation Summary

The top-right section had a small toe micro-crack, and the bottom-right section had a sizable [5/64-in.] crack protruding from the root. The following two images show the toe micro-crack and root crack from these two sections. The micro-crack shown in Figure 5.9 is likely a cold micro-crack (hydrogen related) based upon its location at the toe of the weld and its jagged appearance. It is extremely short, however, making it difficult to determine its type or cause. Figure 5.10 shows what appears to be a hot crack based upon its location and progression toward the surface of the weld. This crack is distinguishable without the aid of microscopy and is approximately 5/64-in. in length. This crack was caused by the solidification process which left the area around the root in the molten state while the remaining metal cooled around it and restrained its cooling contraction. This crack was also likely related to the low solidification temperature of zinc compounds from the galvanizing in solution with the solidifying steel. The steel cooled and solidified more rapidly than the zinc, providing restraint to the shrinkage of the solidifying and cooling zinc compounds and potentially resulting in a crack like that of Figure 5.10.

Figure 5.9: Toe Micro-Crack in Specimen 36G-17HR-Top-right Section

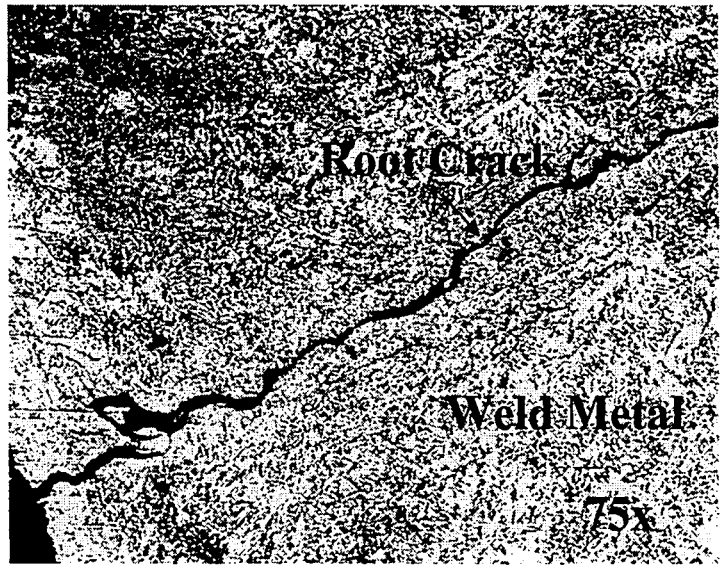

Figure 5.10: Hot Crack at Root of Specimen 36G-17HR-Bottom-right Section

6 Type 304 Stainless Steel Phase 1 Specimens

For locations where corrosion is a major concern, stainless steel connection plates are used in precast structures. While stainless steel is expensive in comparison to conventional carbon steels, it provides significant improvements in weldability relative to galvanized carbon steel. To assess the performance of fillet welds made on stainless steel plates, a commonly used grade of stainless steel was used in the study.

6.1 Stainless Steel Material Properties

The stainless steel used for the welded plate specimens consisted of Type 304 material with properties given in Table 6-1. Plates were pre-cut to the required size of ⅜-in. x 4-in. x 6-in and arranged and welded in accordance with the welding setup procedure described in Section 3.1. The stainless steel specimens SS-73—SS-88 were welded while restrained at the middle of the plate and unrestrained at the ends as shown in Figure 6.1(A) in the original test setup, described in Section 3.1. The remaining specimens, SS-89-SS-96, SS-4HR, SS-1/4(X), were welded using the test setup shown in the Figure 6.1(B).

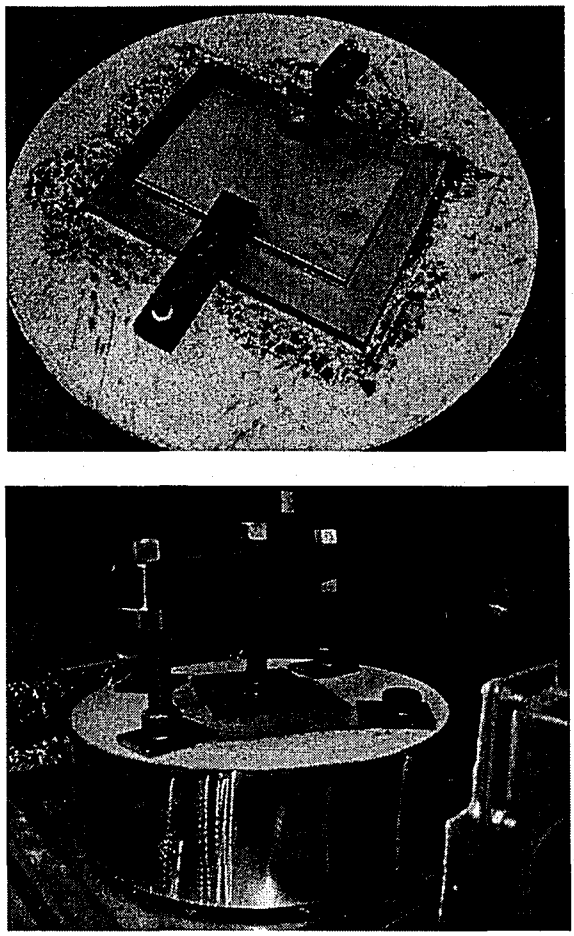

Figure 6.1: Stainless Steel Specimen in Setup: Original (A), Modified(B)

The stainless steel plate material was donated by High Concrete Structures, Inc. The plate material originated from the Pennsylvania Steel Company (PSC). The chemical composition of the steel and the mechanical properties were obtained from the mill certificate provided with the steel shipment. An additional independent chemical analysis was completed by Laboratory Testing, Inc., of Hatfield, PA. The values of the chemical composition from the independent analysis are summarized in Table 6-1, along with material properties from the mill certificate. The same material was used for all Phase 1 stainless steel specimens.

Table 6-1: Stainless Steel Material Data									
Heat Number				85C6					
Manufacturer				Pennsylvania Steel Company					
Applicable Specimens				SS-73 through SS-96, SS-4HR, SS-1/4X					
Specification									
ASME SA A240-01			ASTM A276-02A COND.A			MILS 5059D AMEND3			
ASTM A167-99			ASTM A479/A479M-02, S2.1			QQ-763E COND.A			
ASTM A240/A240M-02			ASTM A480/A480M-01			QQ-S-766D COND.A			
ASME SA 276-01			ASTM A484/A484M-00TB 5			ASME SA 479-01.S2.1			
Chemical Composition [%]-Independent Chemical Analysis Values									
C	Mn	P	S	Si	Cr	Ni	N	Cu	Mo
0.05	1.83	0.024	0.004	0.34	18.57	8.24	--	0.33	0.33
Chemical Composition [%]-Mill Certificate Values									
C	Mn	P	S	Si	Cr	Ni	N	Cu	Mo
.052	1.875	.031	.002	.308	18.650	8.169	.058	.349	.312
Mechanical Properties									
Hardness		Yield Stress @ 0.2%		Ultimate Stress		Elongation			
RB		[ksi]		[ksi]		%-2-in.			
84.50		50.02		91.14		48.96			

6.2 Stainless Weld Material Properties

The SMAW electrode used for the stainless steel weld specimens was the E308-16 rod. This is a titania-coated stainless steel electrode recommended for all applications when welding is in the flat position. The electrodes used are 1/8-in. E308-16, manufactured by MG Welding Products. Table 6-2 summarizes typical electrode data from a mill certificate of this electrode type by MG Welding Products. The stainless electrodes were stored and used according to the specifications on AWS D1.6, as described in Section 3.1.

Table 6-2: Stainless Electrode Properties										
Chemical Composition [%]-Typical Mill Certificate Values										
C	Mn	Si	S	P	Ni	Cr	Mo	Cu	Cb	Fe
0.029	0.61	0.67	0.016	0.018	10.34	19.58	0.10	0.05	0.03	Balanc
Specification/Classification										
AWS 5.4/ASME SFA5.4 ClassE308-16						CWB W48-01 Class E308-16				
Mechanical Properties										
Ultimate Stress [ksi]						Elongation [%]				
84-85						35				

6.3 Specimen Performance Evaluation

The results for each Type 304 Stainless Steel welded specimen are described in the following sections. Each specimen description includes a table summarizing the nominal environmental conditions from the test matrix as well as the measured conditions prior to welding. Images of the weld specimen, weld beads, and four cross-sections are shown, and descriptions of the weld surface condition and cross section flaws are noted. The weld surface condition is noted below the image of each weld in the specimen descriptions using the profile index discussed in Section 3.7.3. Additionally, when of specific interest, microscopic images of discontinuities are presented with accompanying descriptions of the discontinuities. When microscopic images are included, a yellow box on a cross-section image denotes the area included in the associated microscopic image.

6.4 Specimen SS-73: Base Condition

This specimen was subjected to the conditions summarized in Table 6-3 in the environmental chamber at the time of welding.

Table 6-3: Environmental Conditions – Specimen SS-73					
Specimen: SS-73	Air Temp.	Concrete Temp.	Steel Temp.	Rel. Humidity	Wind Speed
	°F	°F	°F	%RH	[mph]
Nominal Values	71	71	71	35	0
Measured Values	70.0	72.7	73.0	35.7	0

The welded specimen is shown in Figure 6.2. Photographs of each of the two welds are presented along with an overview photo of the entire specimen. Sections were taken at four locations from the specimen and polished to examine the quality of the weld. These photos are also included.

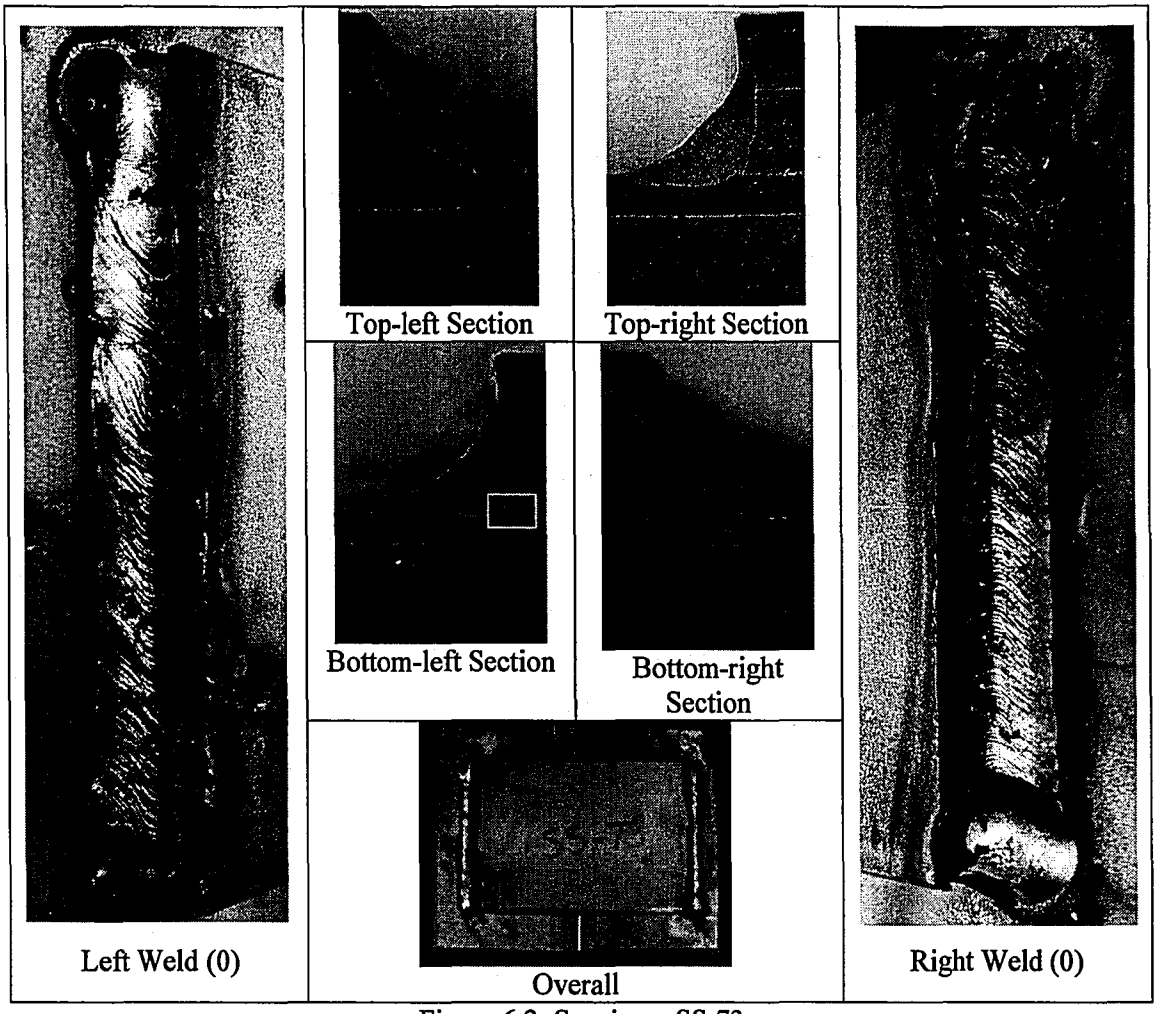

Figure 6.2: Specimen SS-73

6.4.1 Visual Observation Summary

One small surface pore was located near the start position of the right weld (.038-in.). A root slag inclusion (.029-in.) was found in the bottom-left cross section (further magnified in Figure 6.3), and the top-right and top-left cross sections also contained small inclusions at their roots (.004, .013-in.). All sections except the bottom-right met the 3/16-in. profile requirements.

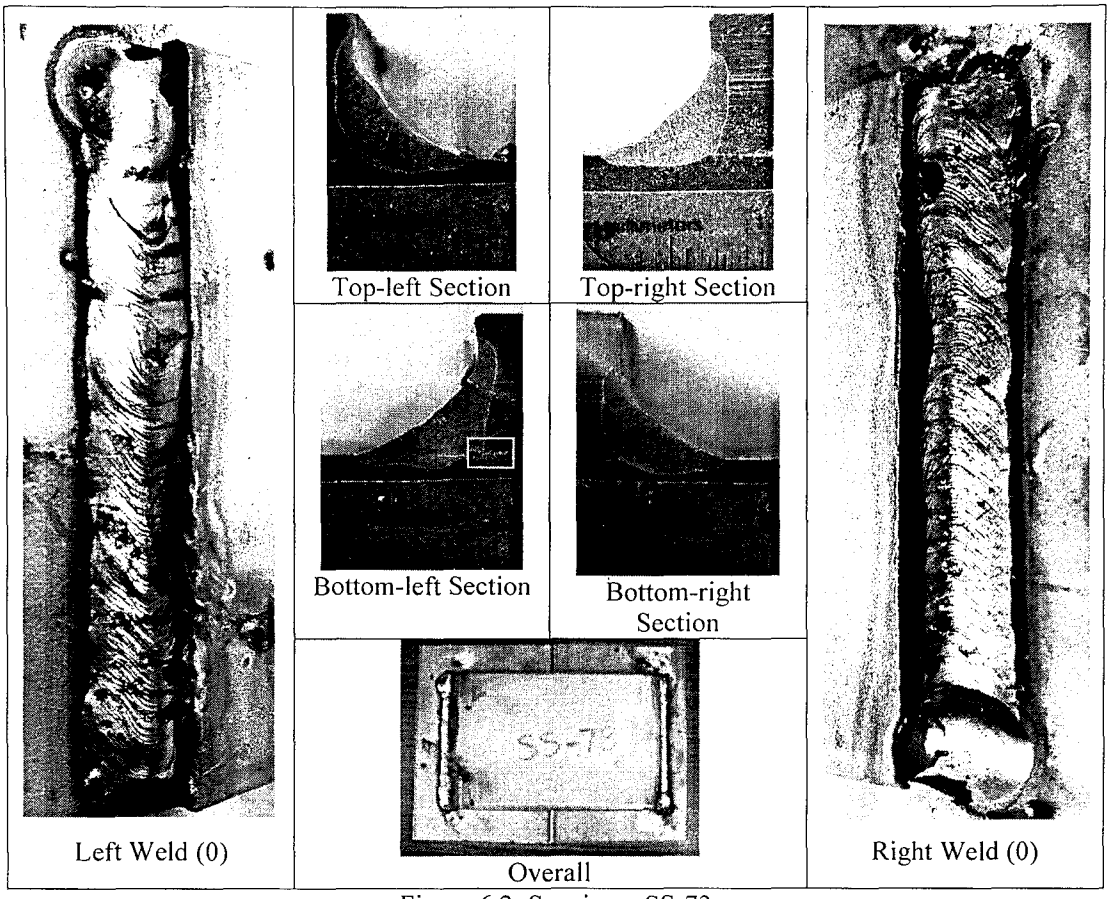

Figure 6.2: Specimen SS-73

6.4.1 Visual Observation Summary

One small surface pore was located near the start position of the right weld (.038-in.). A root slag inclusion (.029-in.) was found in the bottom-left cross section (further magnified in Figure 6.3), and the top-right and top-left cross sections also contained small inclusions at their roots (.004, .013-in.). All sections except the bottom-right met the 3/16-in. profile requirements.

6.4.2 Microscopy Observation Summary

The only discontinuity found in the cross sections taken from sample SS-73 was located at the root of the bottom-left cross-section. The discontinuity is a slag inclusion, and a microscopic image (75x) of the slag inclusion is shown in Figure 6.3.

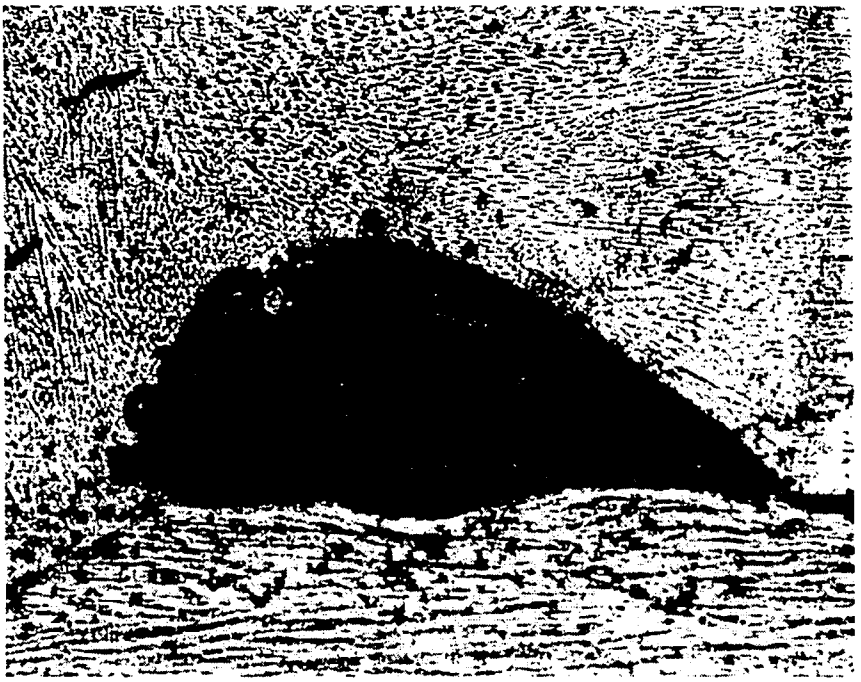

Figure 6.3: Slag Inclusion-Specimen SS-73, Bottom-left section

6.5 Specimen SS-74: Warm, Moderate Humidity, No Wind

This specimen was subjected to the conditions summarized in Table 6-4 at the time of welding.

Table 6-4: Environmental Conditions – Specimen SS-74					
Specimen: SS-74	Air Temp.	Concrete Temp.	Steel Temp.	Rel. Humidity	Wind Speed
	°F	°F	°F	%RH	[mph]
Nominal Values	71	71	71	50	0
Measured Values	72.7	73.4	73.7	47.7	0

The welded specimen is shown in Figure 6.4. Photographs of each of the two welds are presented along with an overview photo of the entire specimen. Sections were taken at four

locations from the specimen and polished to examine the quality of the weld. These photos are also included.

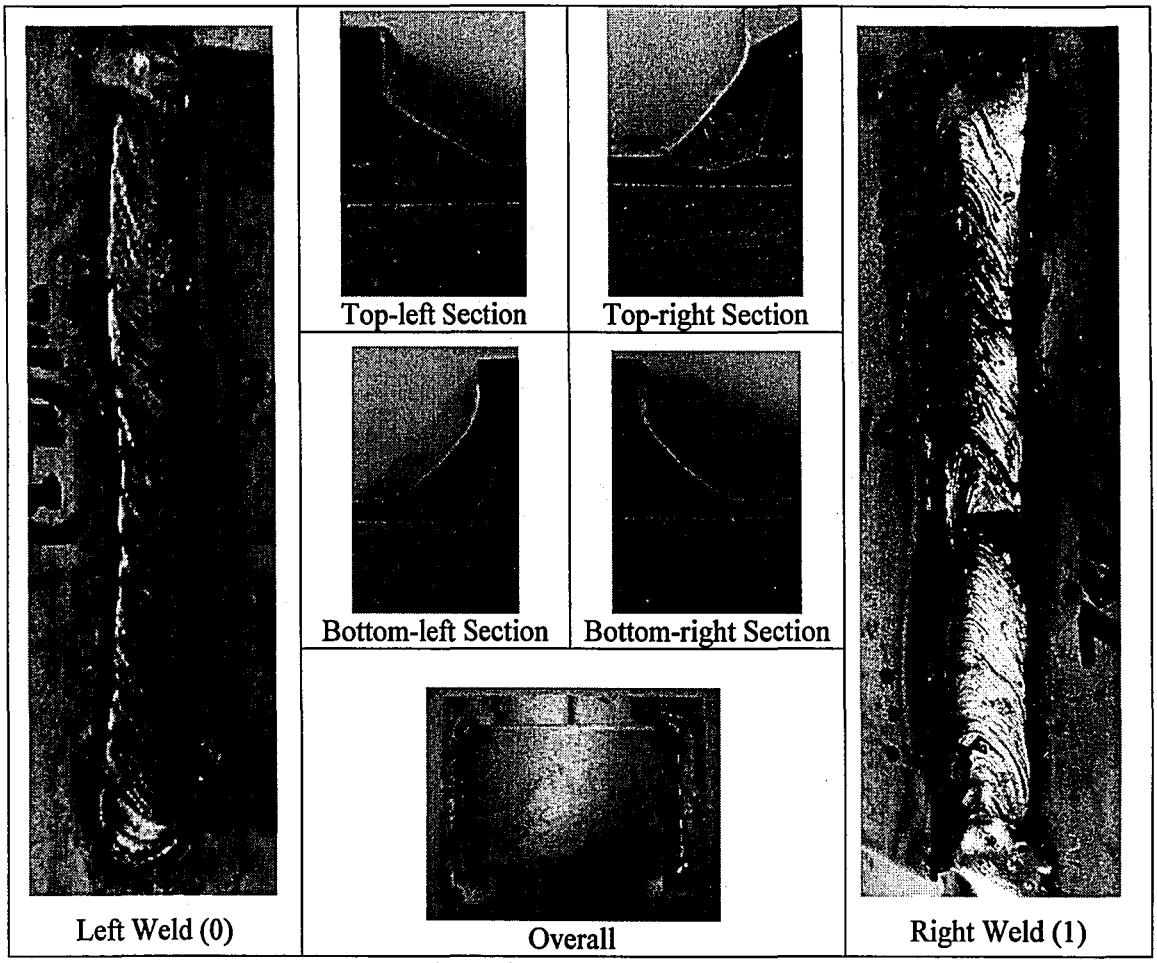

Figure 6.4: Specimen SS-74

6.5.1 Visual Observation Summary

The right weld had a surface discontinuity which constituted an abrupt change in surface geometry but did not appear to be related to the ambient conditions. The left weld did not have any notable surface flaws. The top-left section had a short vertical leg as well as unusually deep penetration at the root of the weld. The top-right, bottom-right, and bottom-left sections contained very small slag inclusions at their roots (.006-in., .011-in., .007-in.). Additionally, the

locations from the specimen and polished to examine the quality of the weld. These photos are also included.

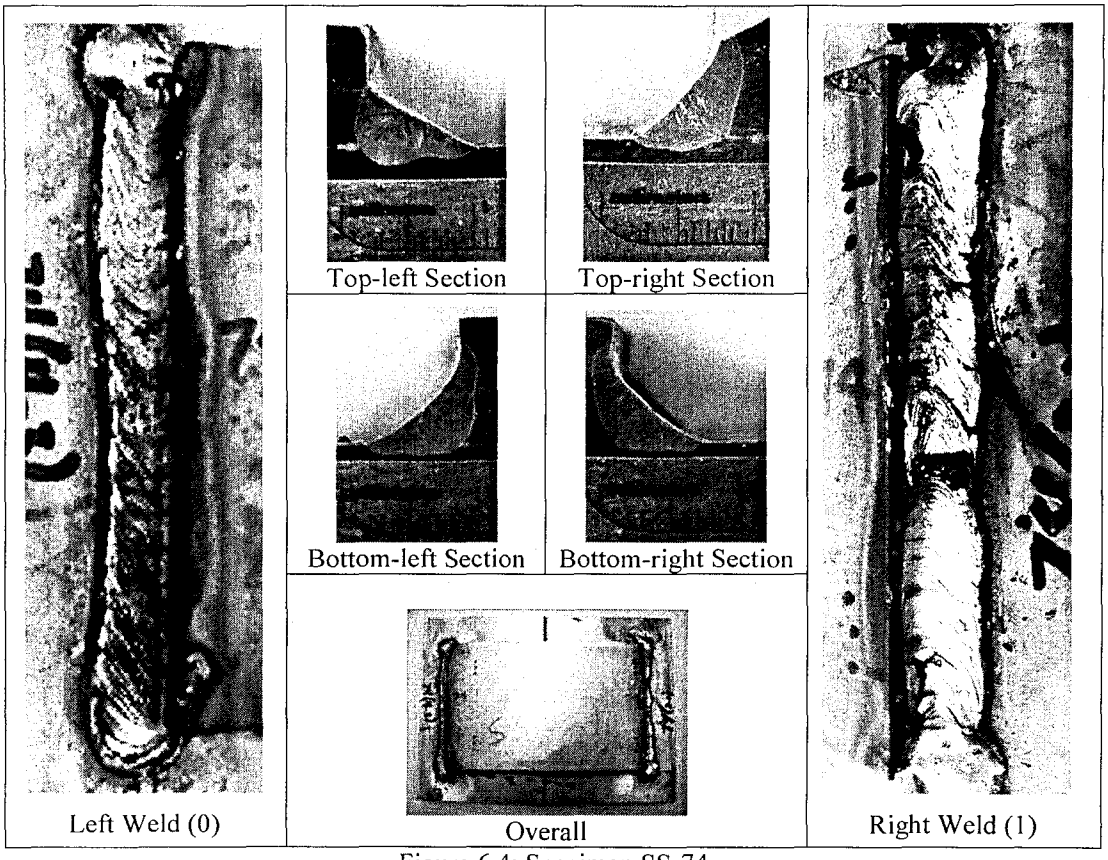

Figure 6.4: Specimen SS-74

6.5.1 Visual Observation Summary

The right weld had a surface discontinuity which constituted an abrupt change in surface geometry but did not appear to be related to the ambient conditions. The left weld did not have any notable surface flaws. The top-left section had a short vertical leg as well as unusually deep penetration at the root of the weld. The top-right, bottom-right, and bottom-left sections contained very small slag inclusions at their roots (.006-in., .011-in., .007-in.). Additionally, the

top-right section exhibited a small amount of undercut (.013-in.). All four sections met the 3/16-in. profile requirements.

6.6 Specimen SS-75: Warm, High Humidity, No Wind

This specimen was subjected to conditions summarized in Table 6-5 at the time of welding.

Table 6-5: Environmental Conditions – Specimen SS-75

Specimen: SS-75	Air Temp.	Concrete Temp.	Steel Temp.	Rel. Humidity	Wind Speed
	°F	°F	°F	%RH	[mph]
Nominal Values	71	71	71	95	0
Measured Values	72.6	76.4	77	100	0

The welded specimen is shown in Figure 6.5. Photographs of each of the two welds are presented along with an overview photo of the entire specimen. Sections were taken at four locations from the specimen and polished to examine the quality of the weld. These photos are also included.

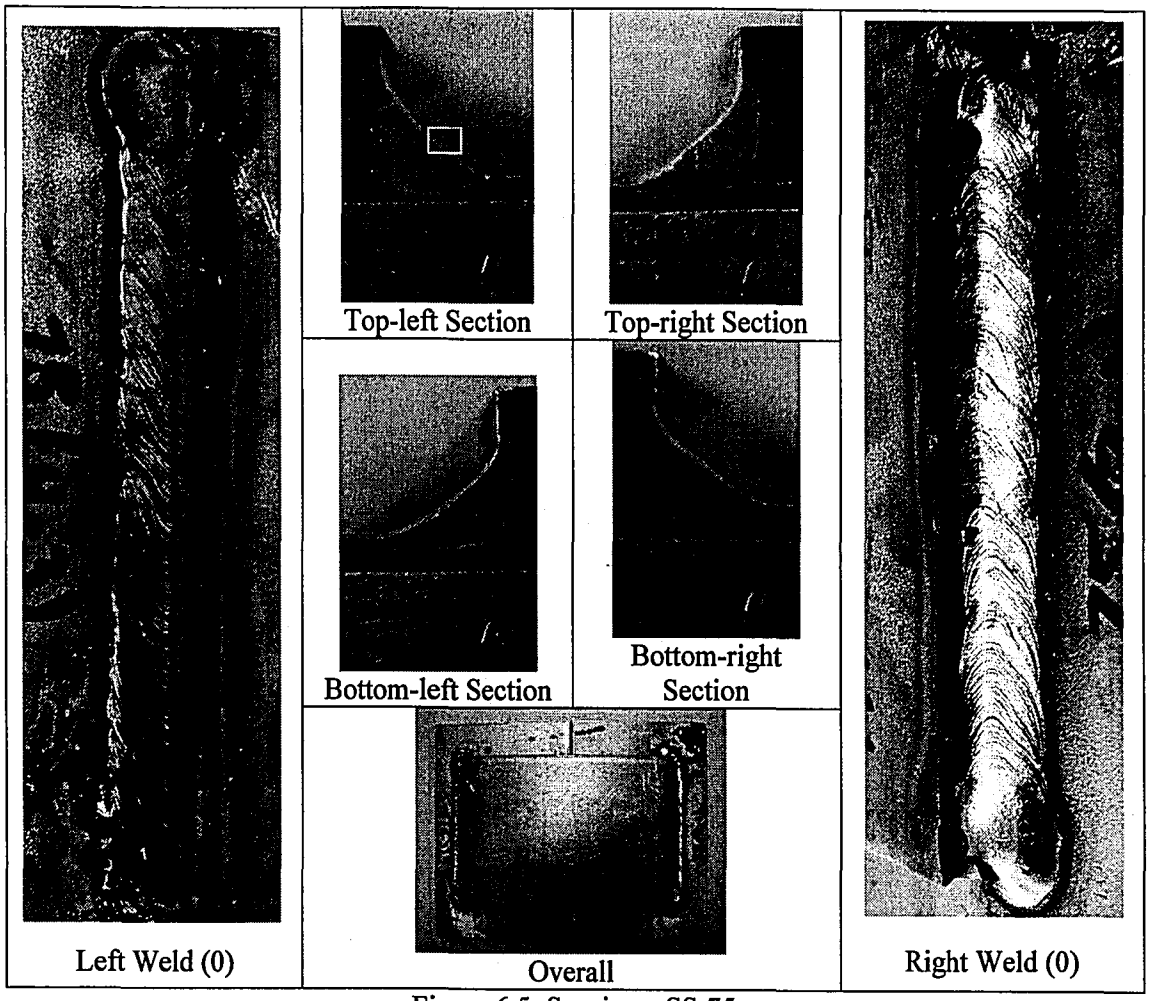

Figure 6.5: Specimen SS-75

6.6.1 Visual Observation Summary

The right weld had some stray-arcing as well as edge-melt at the beginning, while the left weld had a small amount of edge-melt at the end. In general, all welds and profiles were virtually discontinuity free, except a small slag inclusion at the root of the bottom-left section (.002-in.). All four sections met 3/16-in. profile requirements. Visibility was severely limited by intense fog in the chamber during welding.

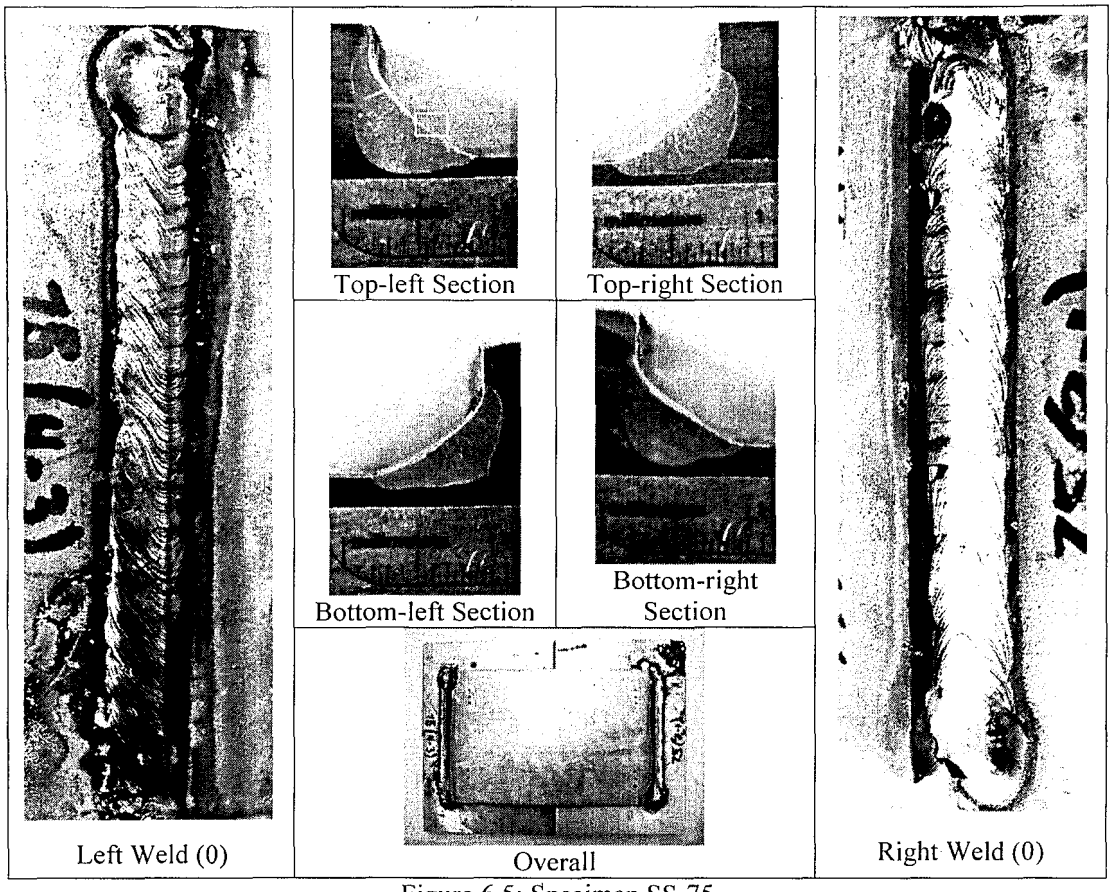

Figure 6.5: Specimen SS-75

6.6.1 Visual Observation Summary

The right weld had some stray-arcing as well as edge-melt at the beginning, while the left weld had a small amount of edge-melt at the end. In general, all welds and profiles were virtually discontinuity free, except a small slag inclusion at the root of the bottom-left section (.002-in.). All four sections met 3/16-in. profile requirements. Visibility was severely limited by intense fog in the chamber during welding.

6.6.2 *Microscopy Observation Summary*

The top-left section had a linear discontinuity that may be a portion of a hot crack near the weld face, further magnified in Figure 6.6. The crack-like discontinuity in the top-left section is shown in Figure 6.6 as viewed under the optical microscope at 75x magnification. The nature of the discontinuity is indicative of a hot micro-crack, although its general location and shape are not characteristic of typical micro-cracks observed in the study.

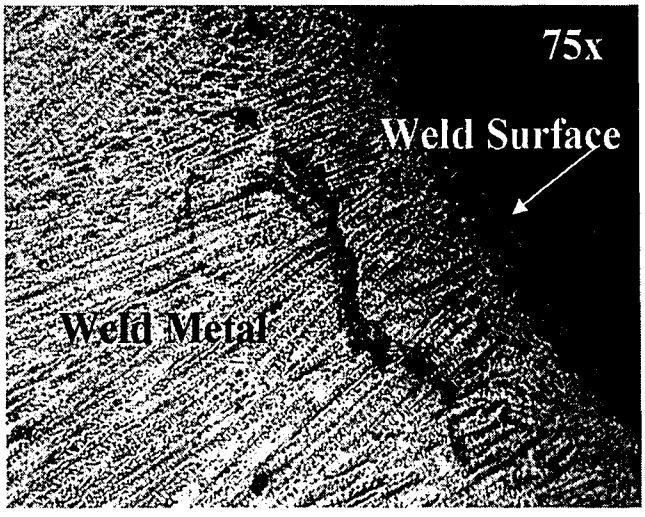

Figure 6.6: Crack-like Discontinuity in Specimen SS-75, Top left Section

6.7 ***Specimen SS-76: Warm, High Humidity, 5 mph Wind***

This specimen was subjected to conditions summarized in Table 6-6 at the time of welding.

Table 6-6: Environmental Conditions – Specimen SS-76					
Specimen: SS-76	Air Temp.	Concrete Temp.	Steel Temp.	Rel. Humidity	Wind Speed
	°F	°F	°F	%RH	[mph]
Nominal Values	71	71	71	95	5
Measured Values	72.6	76.4	71.4	100	5.1

The welded specimen is shown in Figure 6.7. Photographs of each of the two welds are presented along with an overview photo of the entire specimen. Sections were taken at four locations from the specimen and polished to examine the quality of the weld. These photos are also included.

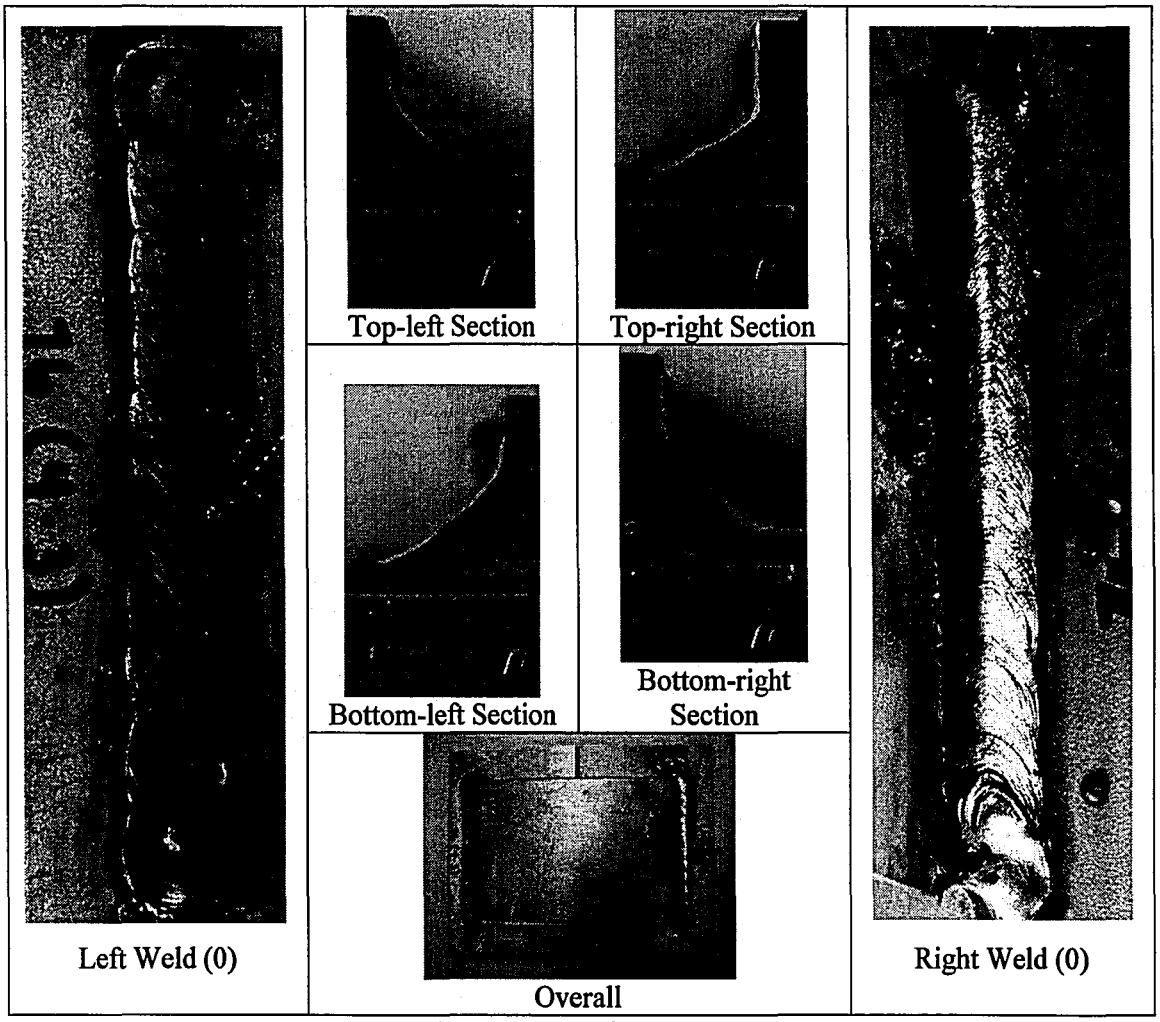

Figure 6.7: Specimen SS-76

6.7.1 Visual Observation Summary

The right weld was undersized at the beginning and tapered to a larger weld profile toward the end, although no discontinuities existed on the surface. The left weld had one surface pore at the beginning (.056-in.). The top-right and top-left sections were both quite small, and the top-

The welded specimen is shown in Figure 6.7. Photographs of each of the two welds are presented along with an overview photo of the entire specimen. Sections were taken at four locations from the specimen and polished to examine the quality of the weld. These photos are also included.

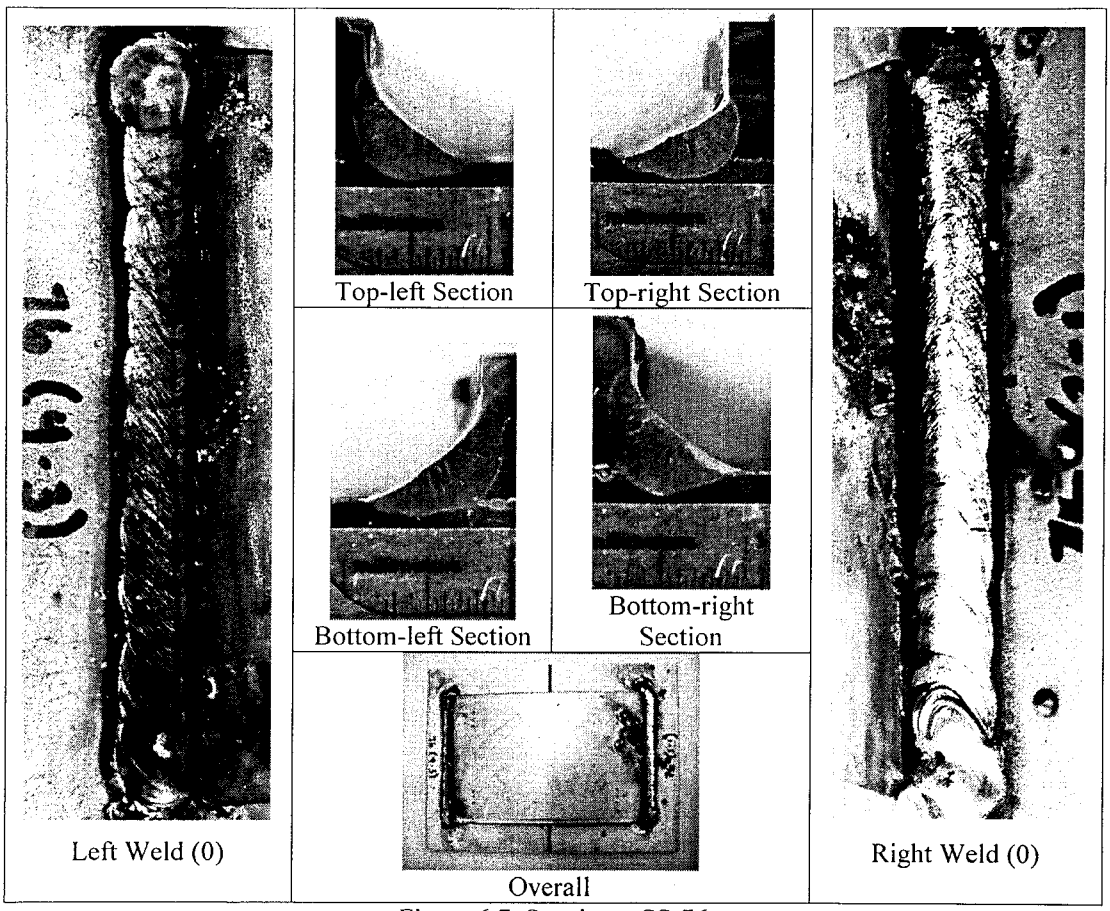

Figure 6.7: Specimen SS-76

6.7.1 Visual Observation Summary

The right weld was undersized at the beginning and tapered to a larger weld profile toward the end, although no discontinuities existed on the surface. The left weld had one surface pore at the beginning (.056-in.). The top-right and top-left sections were both quite small, and the top-

right section did not meet the 3/16-in. profile requirements. Visibility was severely limited by intense fog in the chamber during welding.

6.8 Specimen SS-77: Warm, High Humidity, 10 mph Wind

This specimen was subjected to conditions summarized in Table 6-7 at the time of welding.

Table 6-7: Environmental Conditions – Specimen SS-77					
Specimen: SS-77	Air Temp.	Concrete Temp.	Steel Temp.	Rel. Humidity	Wind Speed
	°F	°F	°F	%RH	[mph]
Nominal Values	71	71	71	95	10
Measured Values	72.8	73.1	74.8	95.7	10.1

The welded specimen is shown in Figure 6.8. Photographs of each of the two welds are presented along with an overview photo of the entire specimen. Sections were taken at four locations from the specimen and polished to examine the quality of the weld. These photos are also included.

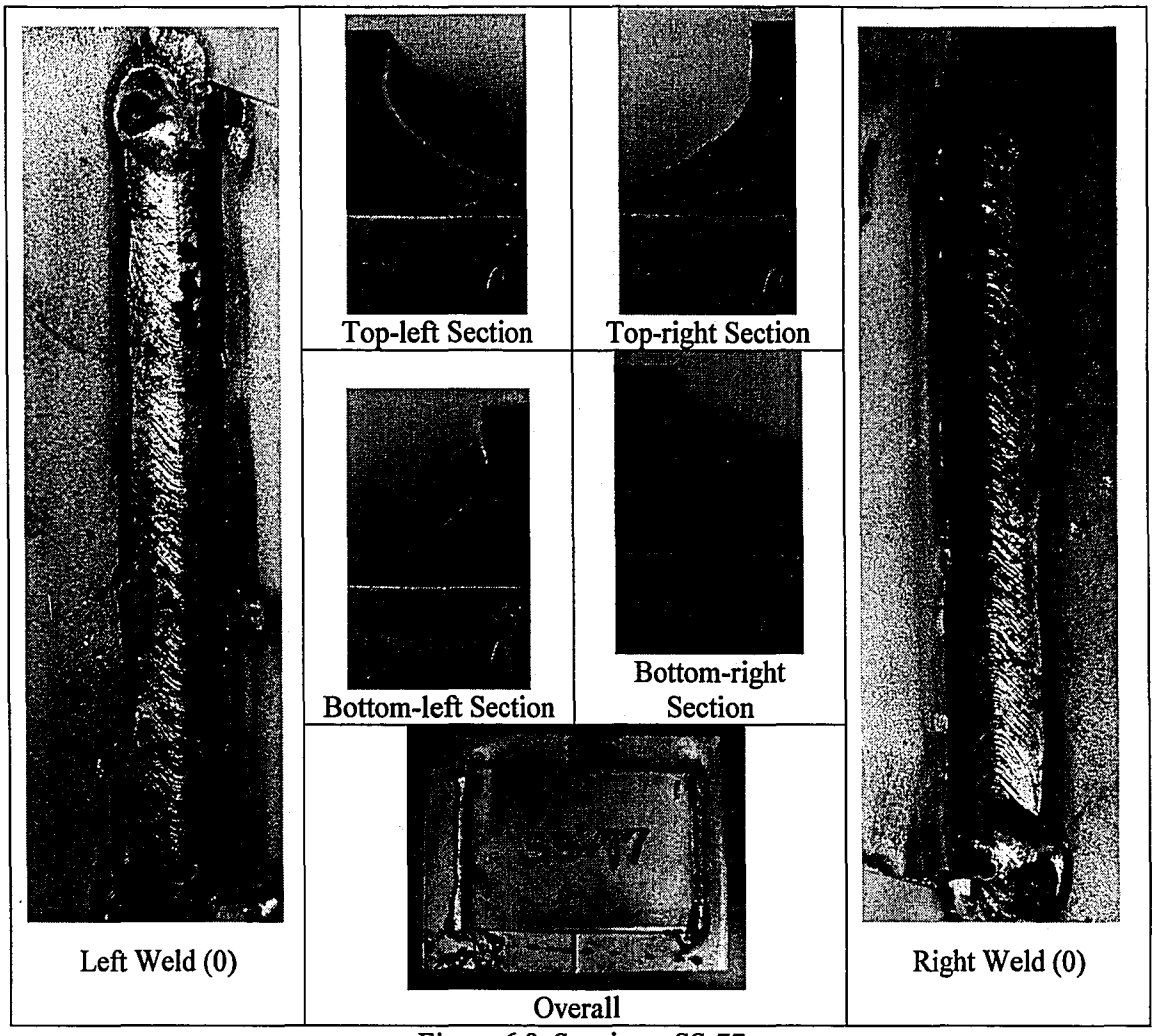

Figure 6.8: Specimen SS-77

6.8.1 Visual Observation Summary

The right weld had one surface pore (.046-in.) located approximately 1-in. from the beginning of the weld and edge-melt at the end of the weld. The left weld becomes rather small at its end but possesses no surface discontinuities. All sections had rather concave profiles, and the bottom-left section exhibited a small amount of undercut (.014-in.). All sections fell below the 3/16-in. profile requirements based upon their concavity.

6.9 Specimen SS-78: Warm, High Humidity, 20 mph Wind

This specimen was subjected to conditions summarized in Table 6-8 at the time of welding.

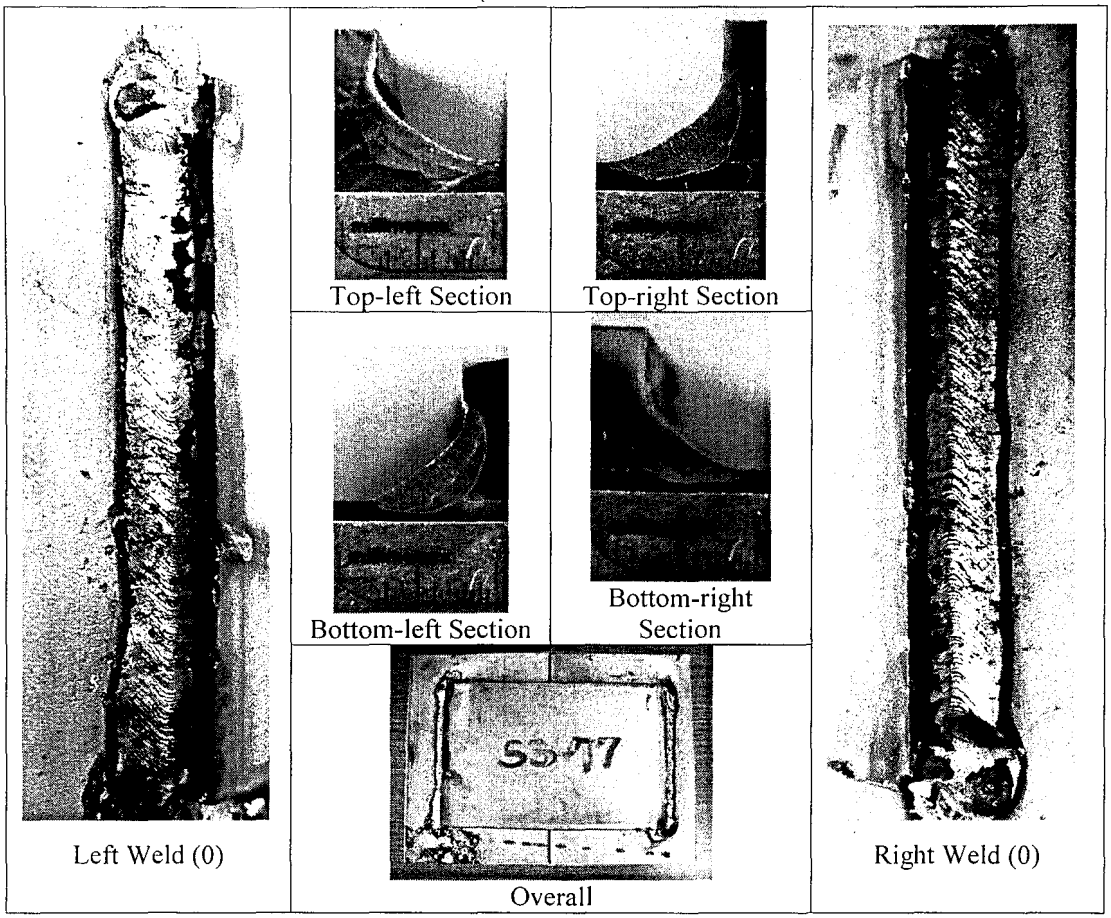

Figure 6.8: Specimen SS-77

6.8.1 Visual Observation Summary

The right weld had one surface pore (.046-in.) located approximately 1-in. from the beginning of the weld and edge-melt at the end of the weld. The left weld becomes rather small at its end but possesses no surface discontinuities. All sections had rather concave profiles, and the bottom-left section exhibited a small amount of undercut (.014-in.). All sections fell below the 3/16-in. profile requirements based upon their concavity.

6.9 Specimen SS-78: Warm, High Humidity, 20 mph Wind

This specimen was subjected to conditions summarized in Table 6-8 at the time of welding.

Table 6-8: Environmental Conditions – Specimen SS-78					
Specimen: SS-78	Air Temp.	Concrete Temp.	Steel Temp.	Rel. Humidity	Wind Speed
	°F	°F	°F	%RH	[mph]
Nominal Values	71	71	71	95	20
Measured Values	74.0	75.1	75.5	94.8	20.1

The welded specimen is shown in Figure 6.9. Photographs of each of the two welds are presented along with an overview photo of the entire specimen. Sections were taken at four locations from the specimen and polished to examine the quality of the weld. These photos are also included.

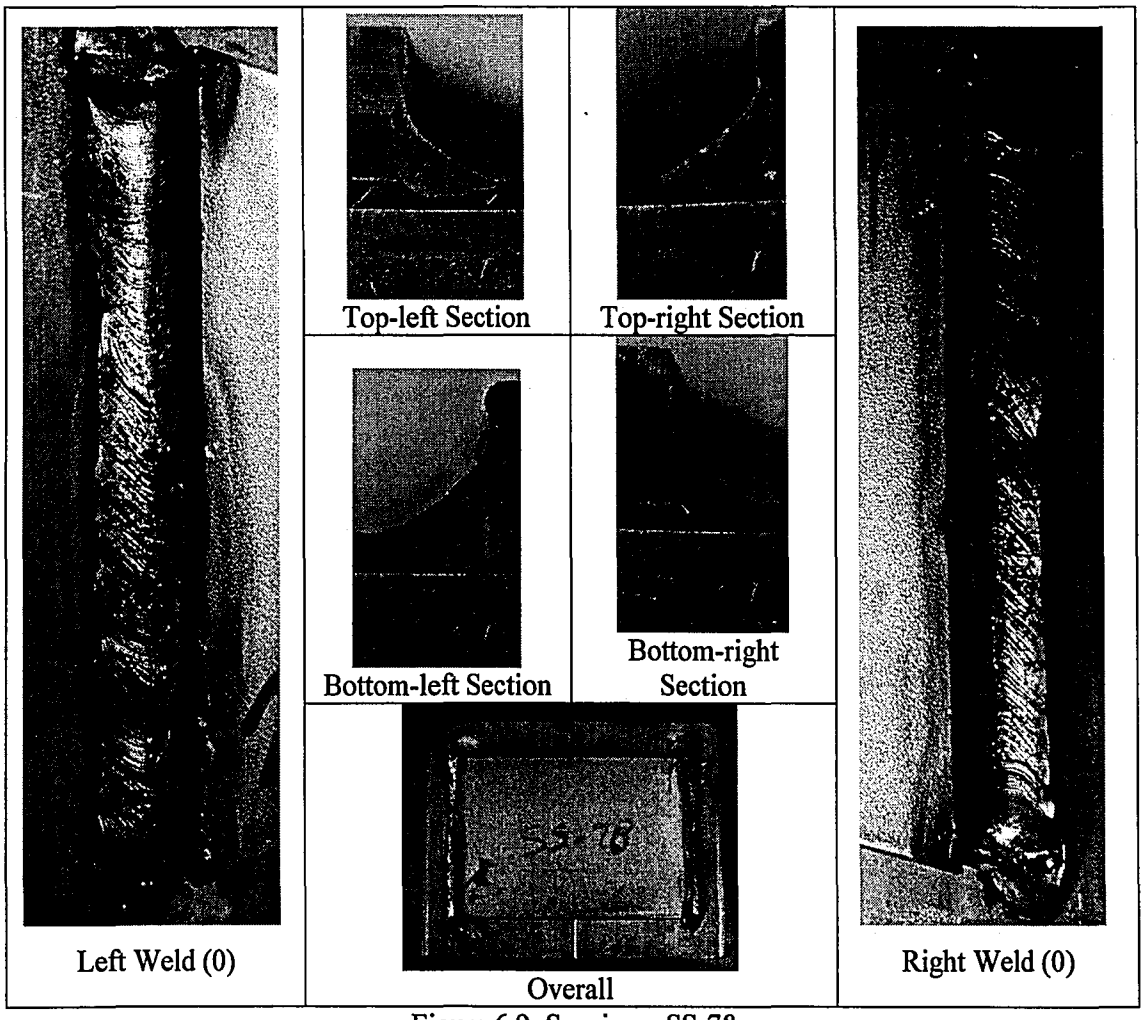

Figure 6.9: Specimen SS-78

Table 6-8: Environmental Conditions – Specimen SS-78					
Specimen: SS-78	Air Temp.	Concrete Temp.	Steel Temp.	Rel. Humidity	Wind Speed
	°F	°F	°F	%RH	[mph]
Nominal Values	71	71	71	95	20
Measured Values	74.0	75.1	75.5	94.8	20.1

The welded specimen is shown in Figure 6.9. Photographs of each of the two welds are presented along with an overview photo of the entire specimen. Sections were taken at four locations from the specimen and polished to examine the quality of the weld. These photos are also included.

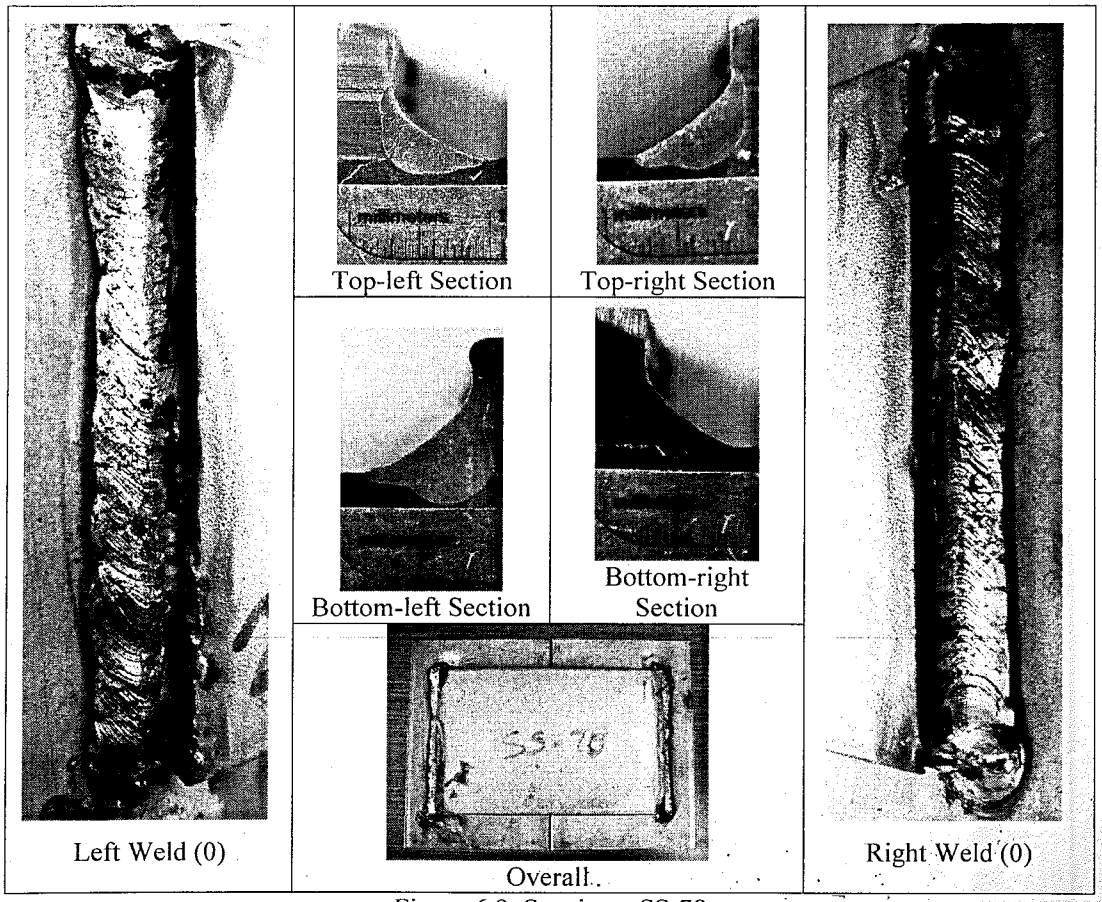

Figure 6.9: Specimen SS-78

6.9.1 Visual Observation Summary

No notable flaws were observed on the surfaces of these welds. All sections were rather small in profile, and the bottom left section had unusually deep root penetration, corresponding to an area of the weld with relatively long leg lengths. The top-right, bottom-right, and top-left sections each had a slag inclusion at the root with a size of approximately .008-in. The top-left section did not meet the 3/16-in. profile requirements.

6.10 Specimen SS-79: Warm, High Humidity, 35 mph Wind

This specimen was subjected to conditions summarized in Table 6-9 at the time of welding.

Table 6-9: Environmental conditions – Specimen SS-79

Specimen:SS-79	Air Temp.	Concrete Temp.	Steel Temp.	Rel. Humidity	Wind Speed
	°F	°F	°F	%RH	[mph]
Nominal Values	71	71	71	95	35
Measured Values	76.8	77.4	75.8	90.9	33.2

The welded specimen is shown in Figure 6.10. Photographs of each of the two welds are presented along with an overview photo of the entire specimen. Sections were taken at four locations from the specimen and polished to examine the quality of the weld. These photos are also included.

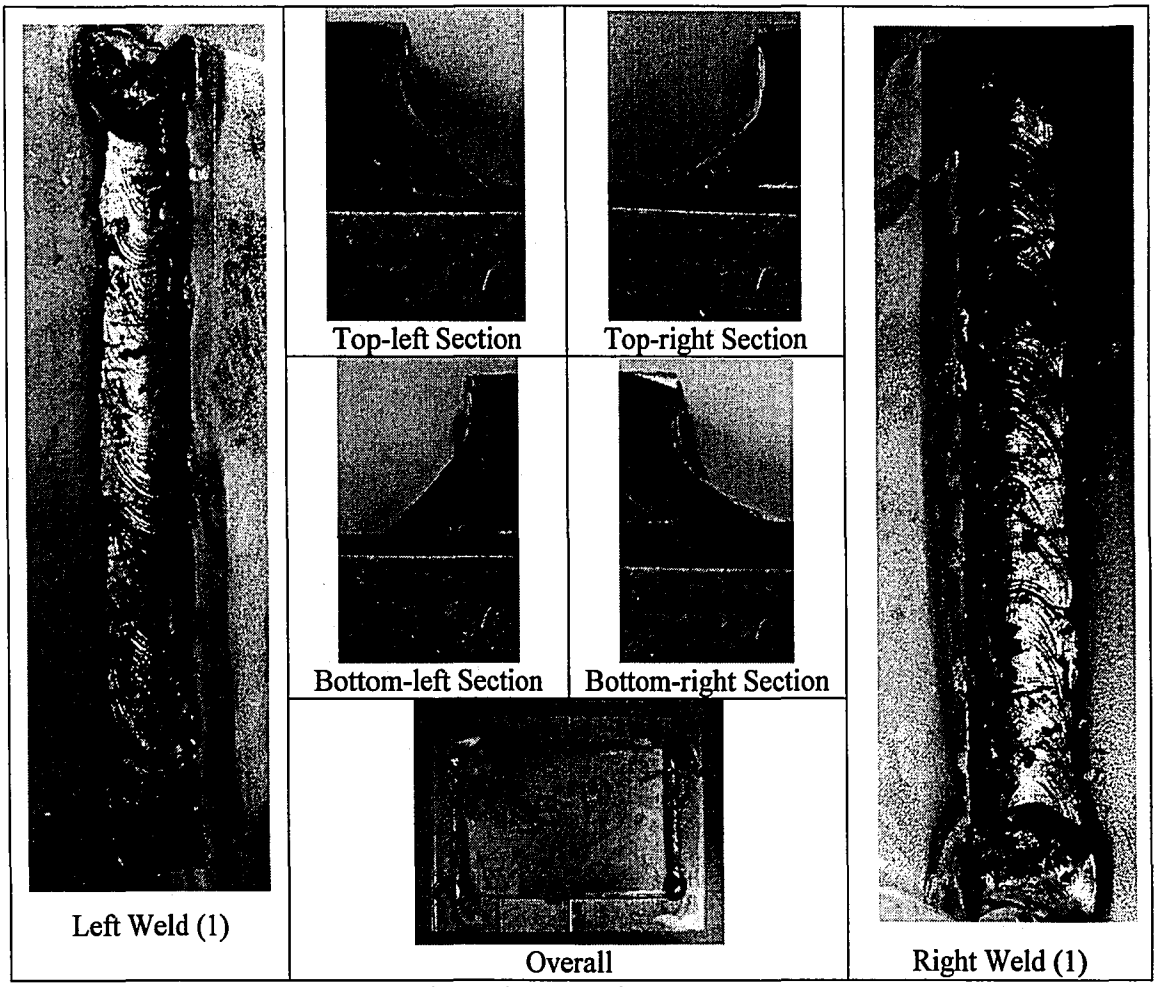

Figure 6.10: Specimen SS-79

6.10.1 Visual Observation Summary

The right weld had edge-melt at its end, while the left weld had an erratic shape and edge-melt and what appeared to be mild undercut along the weld. The top-left profile had a skew to the vertical leg, and the top-right, bottom-right and bottom-left profiles each had a root inclusion (.018-in., .023-in., .026-in.). Additionally, the top-left, top-right, and bottom-left sections had a significant skew to their vertical legs. The top-right, bottom-left, and top-left profiles had a small amount of undercut (.015-in., .015-in., .014-in.). Only the bottom-left section met the 3/16-in. profile requirements. Visibility was severely limited by intense fog in the chamber during welding.

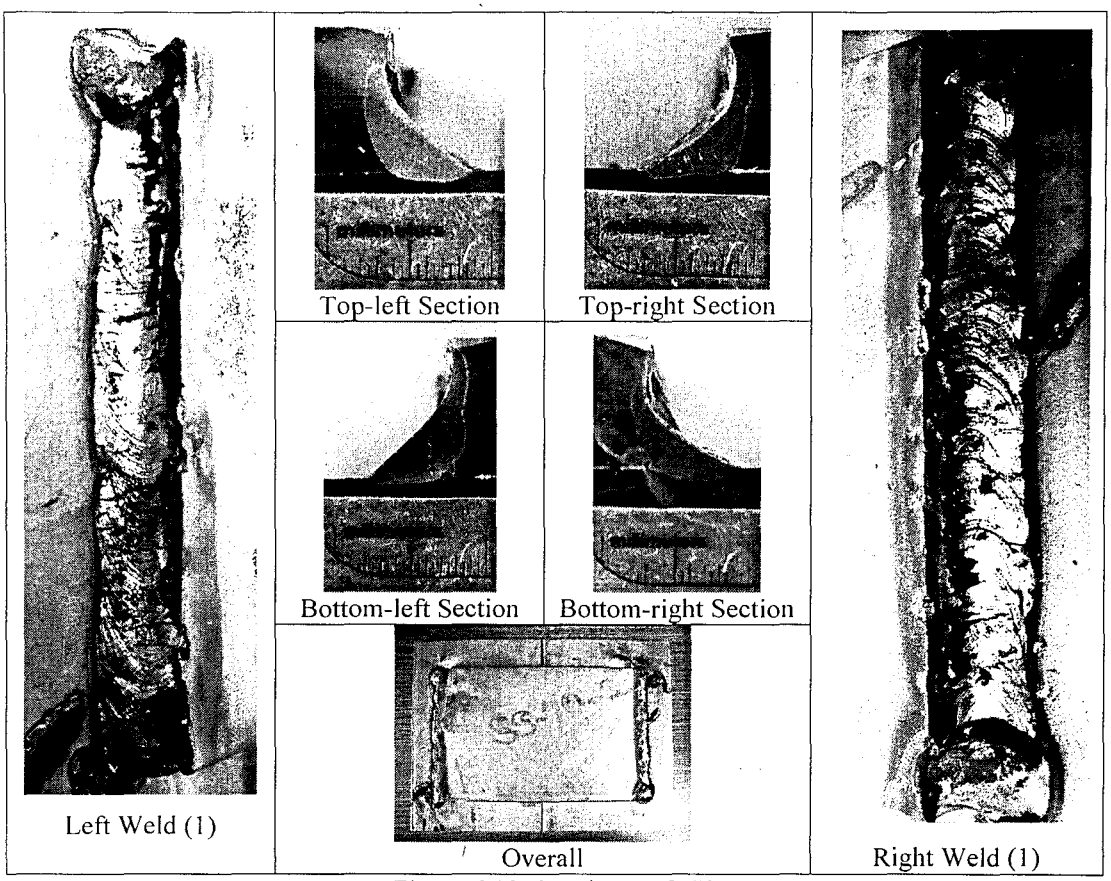

Figure 6.10: Specimen SS-79

6.10.1 Visual Observation Summary

The right weld had edge-melt at its end, while the left weld had an erratic shape and edge-melt and what appeared to be mild undercut along the weld. The top-left profile had a skew to the vertical leg, and the top-right, bottom-right and bottom-left profiles each had a root inclusion (.018-in., .023-in., .026-in.). Additionally, the top-left, top-right, and bottom-left sections had a significant skew to their vertical legs. The top-right, bottom-left, and top-left profiles had a small amount of undercut (.015-in., .015-in., .014-in.). Only the bottom-left section met the 3/16-in. profile requirements. Visibility was severely limited by intense fog in the chamber during welding.

6.11 Specimen SS-82: 32°F, Moderate Humidity, No Wind

This specimen was subjected to conditions summarized in Table 6-10 at the time of welding.

Table 6-10: Environmental Conditions – Specimen SS-82					
Specimen: SS-82	Air Temp.	Concrete Temp.	Steel Temp.	Rel. Humidity	Wind Speed
	°F	°F	°F	%RH	[mph]
Nominal Values	32	32	32	50	0
Measured Values	32.4	45.7	45.5	48.8	0

The welded specimen is shown in Figure 6.11. Photographs of each of the two welds are presented along with an overview photo of the entire specimen. Sections were taken at four locations from the specimen and polished to examine the quality of the weld. These photos are also included.

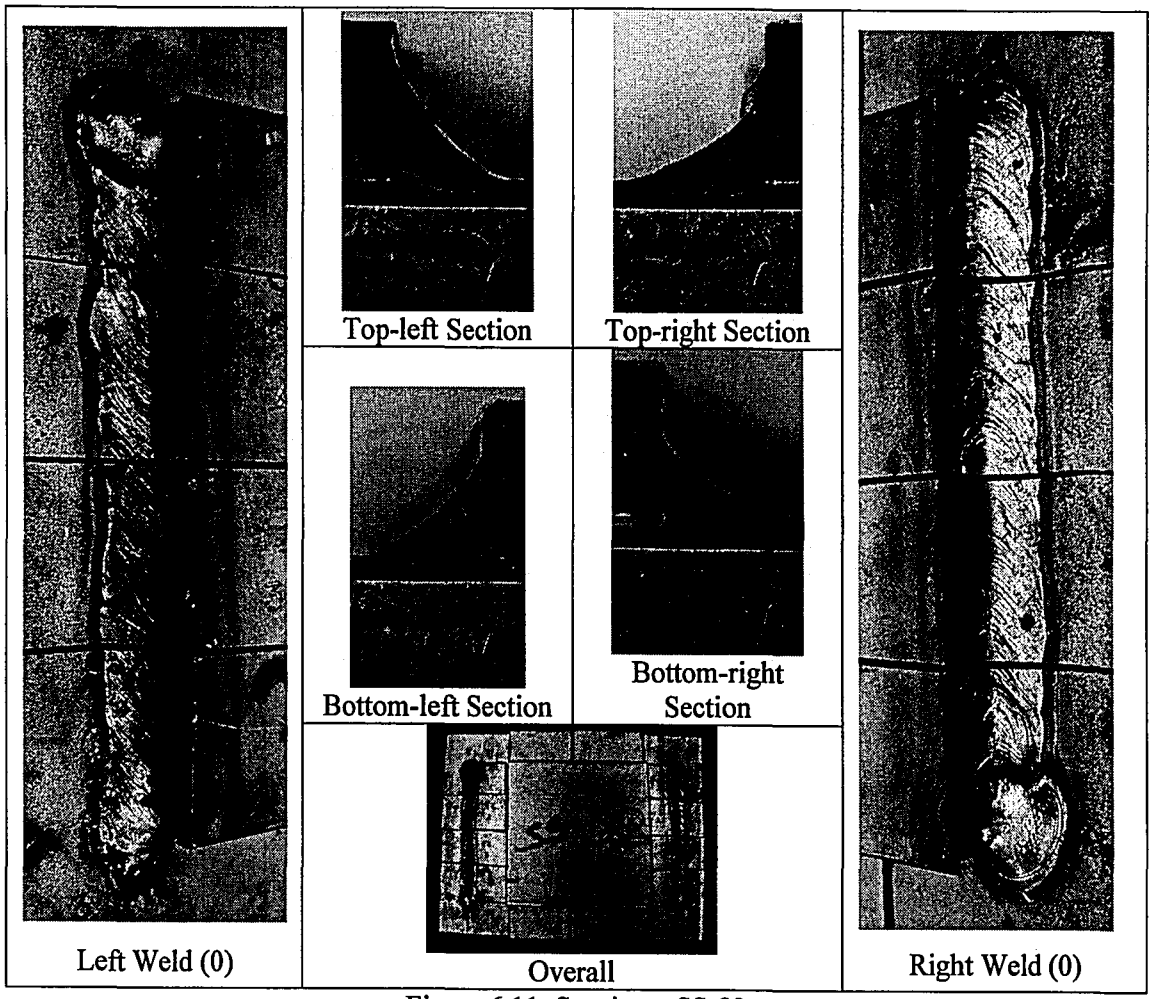

Figure 6.11: Specimen SS-82

6.11.1 Visual Observation Summary

The right weld exhibited no discontinuities, while the left weld had two surface pores (.051-in., .053-in.) at its beginning and edge-melt at its end. The top-right, bottom-right, and bottom-left sections exhibited small inclusions at their roots (.003-in., .008-in., .017-in.). The top-right and bottom-left profiles displayed concavity of profile, but all sections met the 3/16-in. profile requirements.

6.12 Specimen SS-83: 32°F, High Humidity, No Wind

This specimen was subjected to conditions summarized in Table 6-11 at the time of welding.

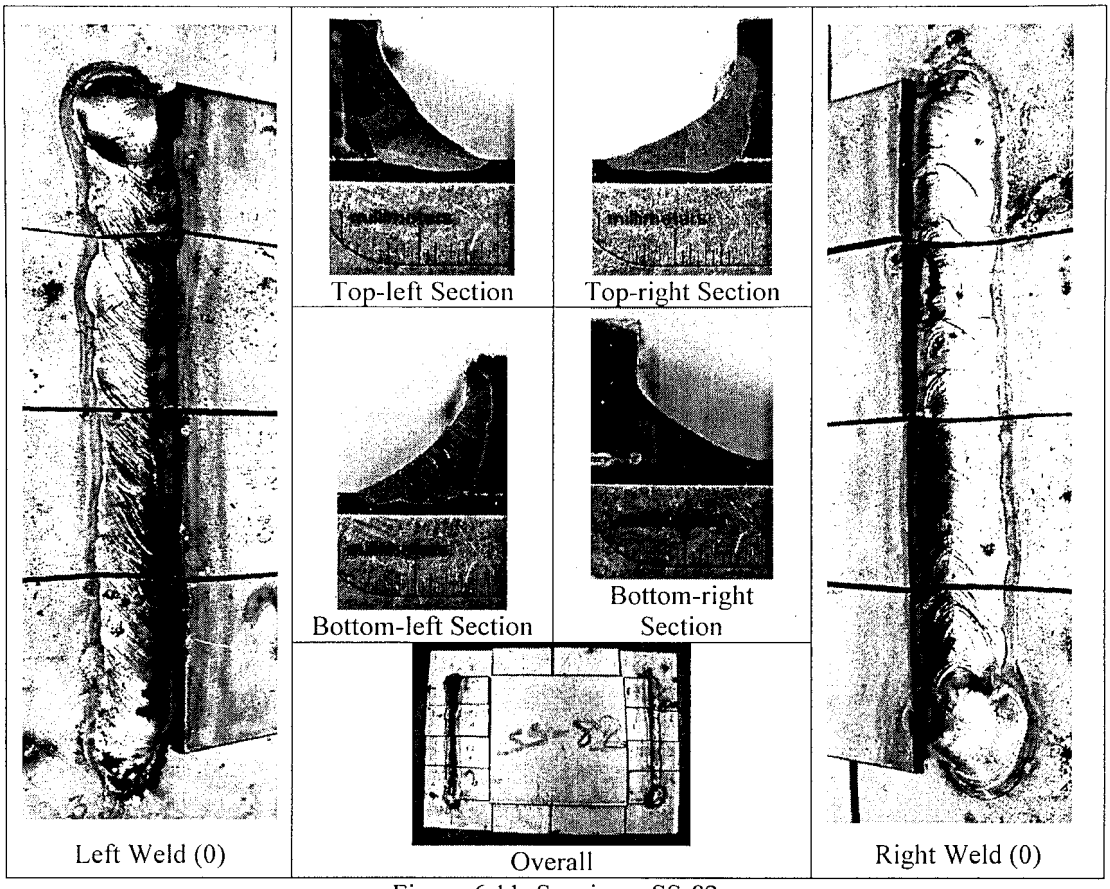

Figure 6.11: Specimen SS-82

6.11.1 Visual Observation Summary

The right weld exhibited no discontinuities, while the left weld had two surface pores (.051-in., .053-in.) at its beginning and edge-melt at its end. The top-right, bottom-right, and bottom-left sections exhibited small inclusions at their roots (.003-in., .008-in., .017-in.). The top-right and bottom-left profiles displayed concavity of profile, but all sections met the 3/16-in. profile requirements.

6.12 Specimen SS-83: 32°F, High Humidity, No Wind

This specimen was subjected to conditions summarized in Table 6-11 at the time of welding.

Table 6-11: Environmental Conditions – Specimen SS-83					
Specimen:SS-83	Air Temp.	Concrete Temp.	Steel Temp.	Rel. Humidity	Wind Speed
	°F	°F	°F	%RH	[mph]
Nominal Values	32	32	32	95	0
Measured Values	31.0	40.6	35.6	100.0	0

The welded specimen is shown in Figure 6.12. Photographs of each of the two welds are presented along with an overview photo of the entire specimen. Sections were taken at four locations from the specimen and polished to examine the quality of the weld. These photos are also included.

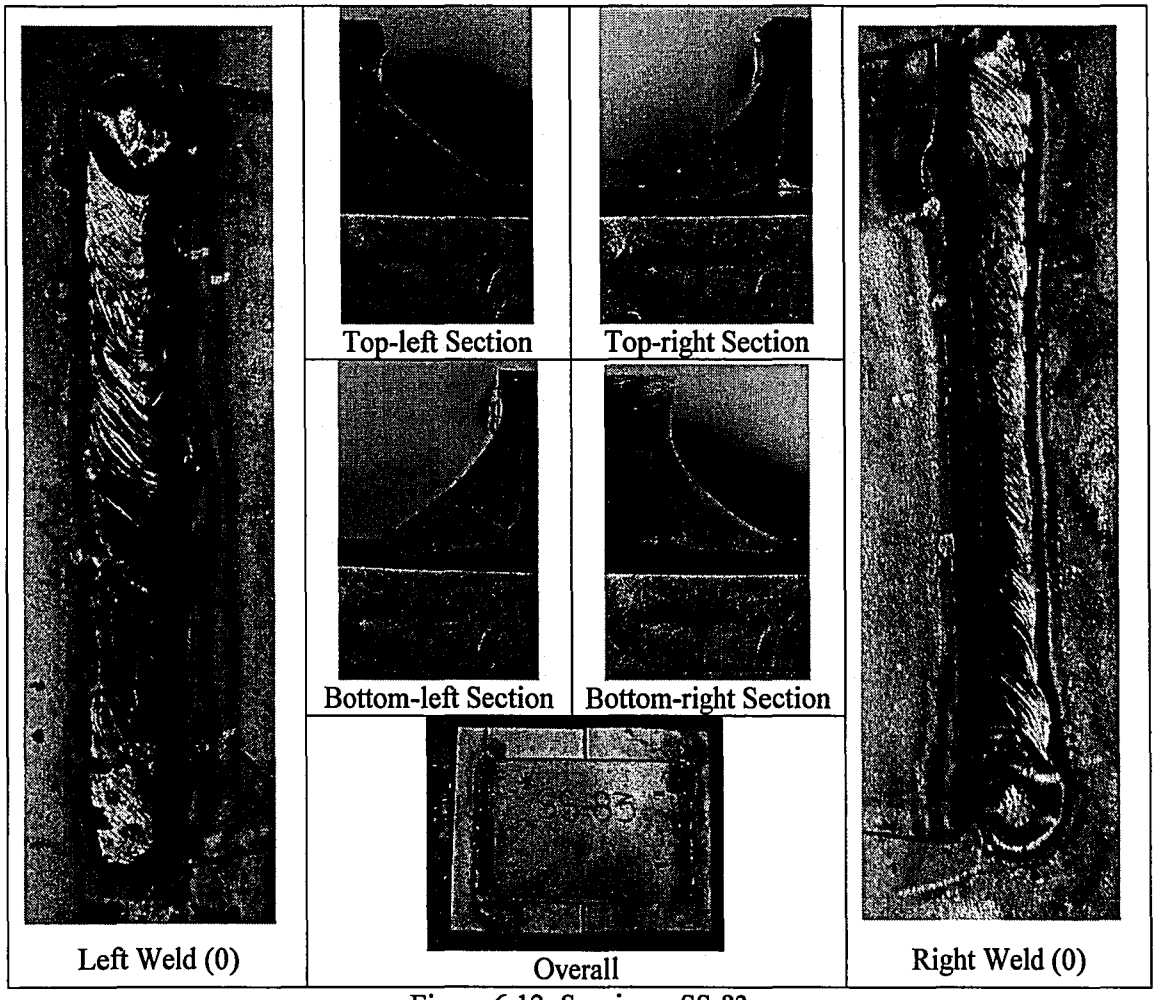

Figure 6.12: Specimen SS-83

Table 6-11: Environmental Conditions – Specimen SS-83					
Specimen:SS-83	Air Temp.	Concrete Temp.	Steel Temp.	Rel. Humidity	Wind Speed
	°F	°F	°F	%RH	[mph]
Nominal Values	32	32	32	95	0
Measured Values	31.0	40.6	35.6	100.0	0

The welded specimen is shown in Figure 6.12. Photographs of each of the two welds are presented along with an overview photo of the entire specimen. Sections were taken at four locations from the specimen and polished to examine the quality of the weld. These photos are also included.

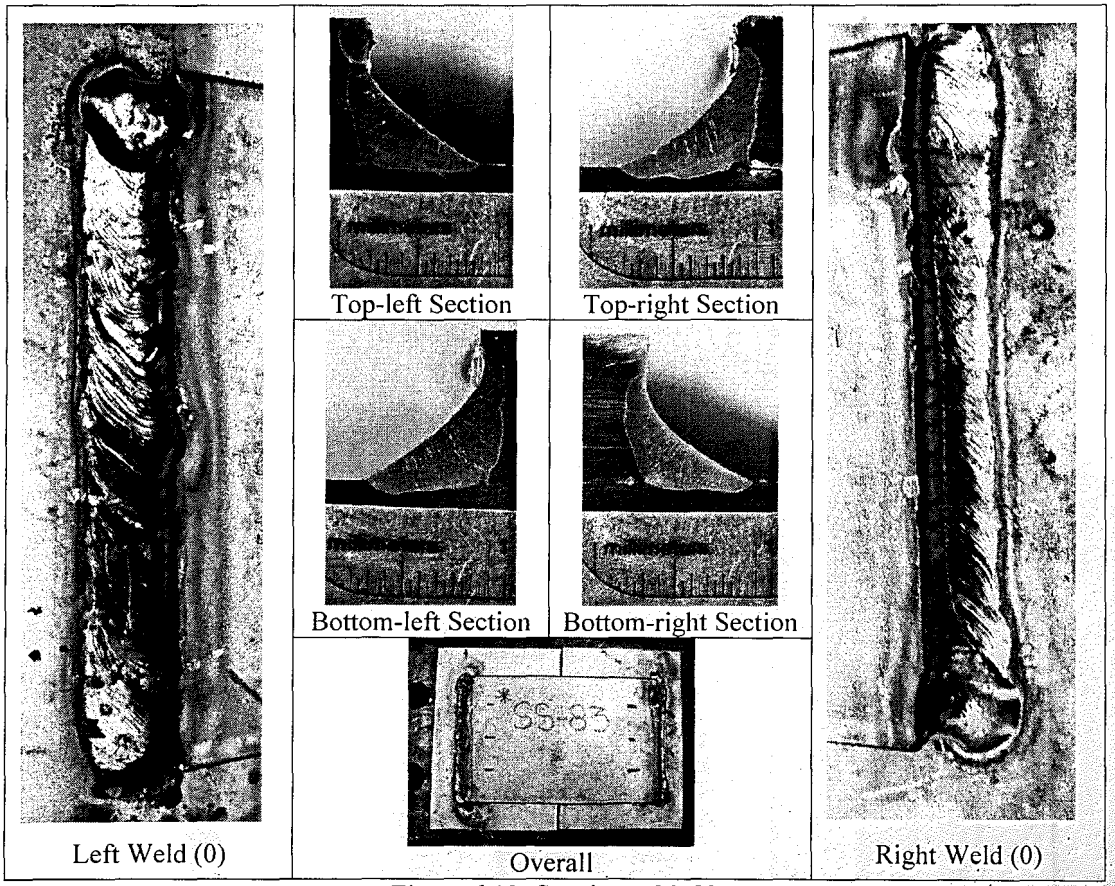

Figure 6.12: Specimen SS-83

6.12.1 Visual Observation Summary

The right and left welds displayed edge-melt at their ends. The top-right profile had a root slag inclusion (.042-in.), and the bottom-left and top-left sections displayed a small amount of undercut (.01-in., .016-in.). The bottom-left and top-left sections also had small root inclusions (.007-in., .016-in.). All four sections met the 3/16-in. profile requirements.

6.13 Specimen SS-84: 32°F, High Humidity, 5 mph Wind

This specimen was subjected to conditions summarized in Table 6-12 at the time of welding.

Table 6-12: Environmental Conditions – Specimen SS-84

Specimen: SS-84	Air Temp.	Concrete Temp.	Steel Temp.	Rel. Humidity	Wind Speed
	°F	°F	°F	%RH	[mph]
Nominal Values	32	32	32	95	5
Measured Values	35.0	43.0	43.4	100.0	5.1

The welded specimen is shown in Figure 6.13. Photographs of each of the two welds are presented along with an overview photo of the entire specimen. Sections were taken at four locations from the specimen and polished to examine the quality of the weld. These photos are also included.

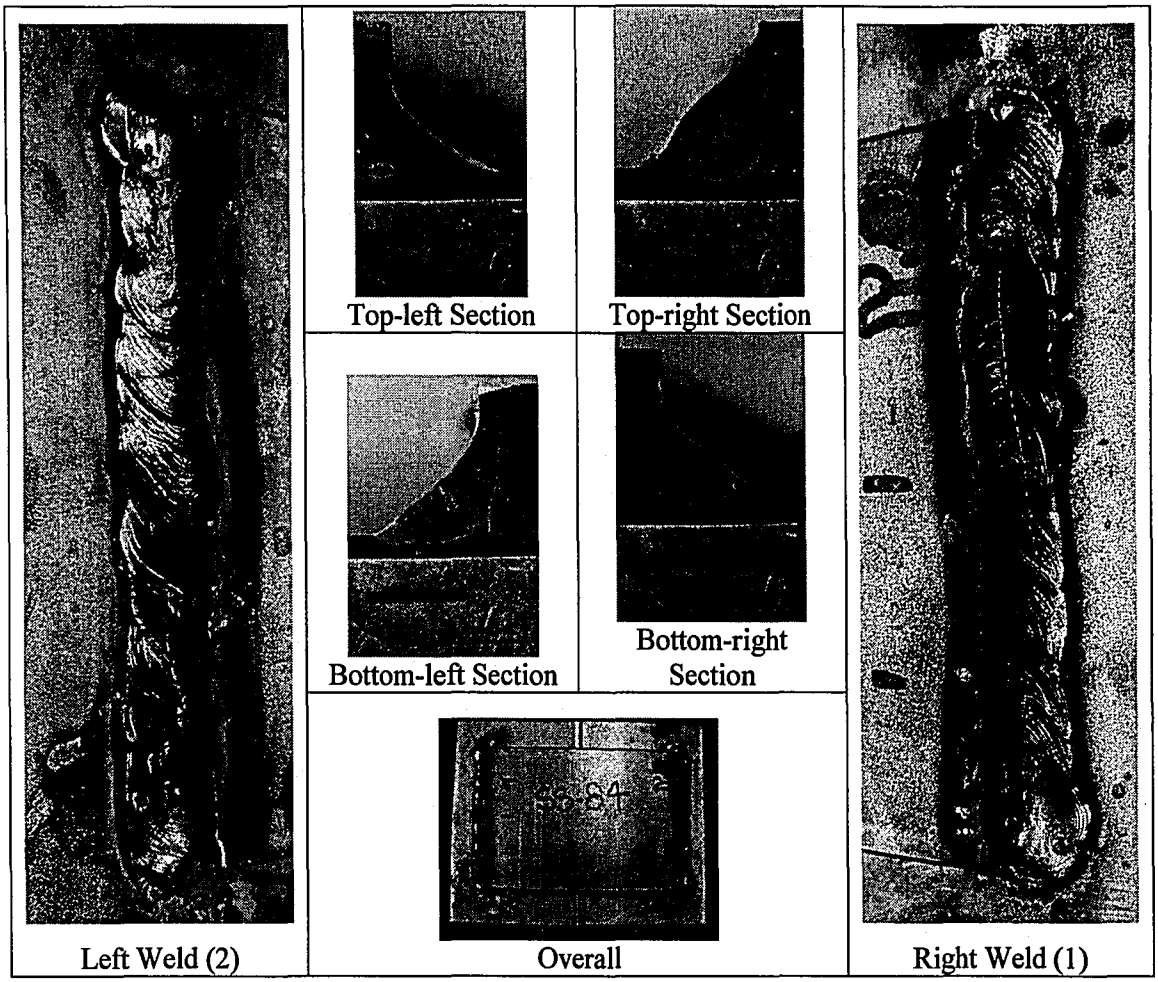

Figure 6.13: Specimen SS-84

6.13.1 Visual Observation Summary

The right and left welds had edge-melt along the length of the welds but had no other observed discontinuities. The top-right profile had a skew toward the vertical leg, and the bottom-left profile had a root slag inclusion (.037-in.). All four sections met the 3/16-in. profile requirements, and the top-right section additionally met the 1/4-in. profile requirements.

6.14 Specimen SS-85: 32°F, High Humidity, 10 mph Wind

This specimen was subjected to conditions summarized in Table 6-13 at the time of welding.

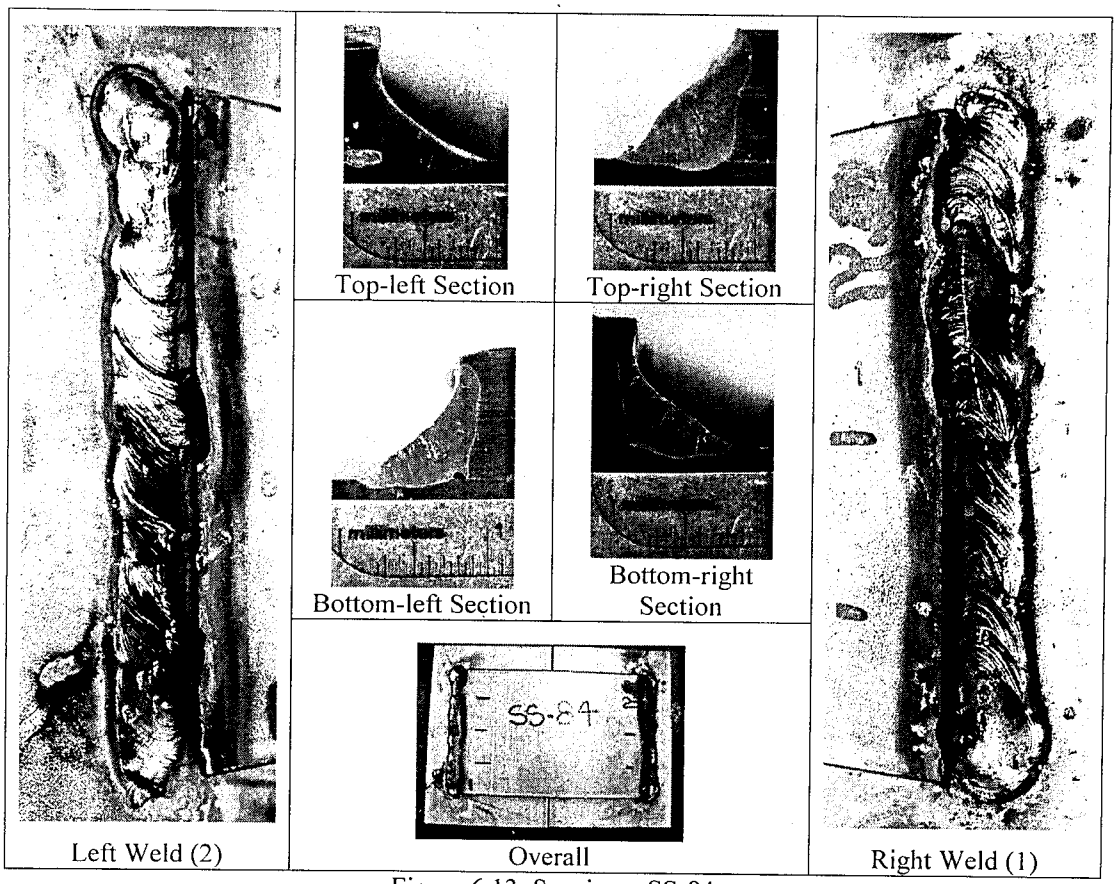

Figure 6.13: Specimen SS-84

6.13.1 Visual Observation Summary

The right and left welds had edge-melt along the length of the welds but had no other observed discontinuities. The top-right profile had a skew toward the vertical leg, and the bottom-left profile had a root slag inclusion (.037-in.). All four sections met the 3/16-in. profile requirements, and the top-right section additionally met the 1/4-in. profile requirements.

6.14 Specimen SS-85: 32°F, High Humidity, 10 mph Wind

This specimen was subjected to conditions summarized in Table 6-13 at the time of welding.

Table 6-13: Environmental Conditions – Specimen SS-85					
Specimen: SS-85	Air Temp.	Concrete Temp.	Steel Temp.	Rel. Humidity	Wind Speed
	°F	°F	°F	%RH	[mph]
Nominal Values	32	32	32	95	10
Measured Values	35.0	39.7	39.8	100.0	10.0

The welded specimen is shown in Figure 6.14. Photographs of each of the two welds are presented along with an overview photo of the entire specimen. Sections were taken at four locations from the specimen and polished to examine the quality of the weld. These photos are also included.

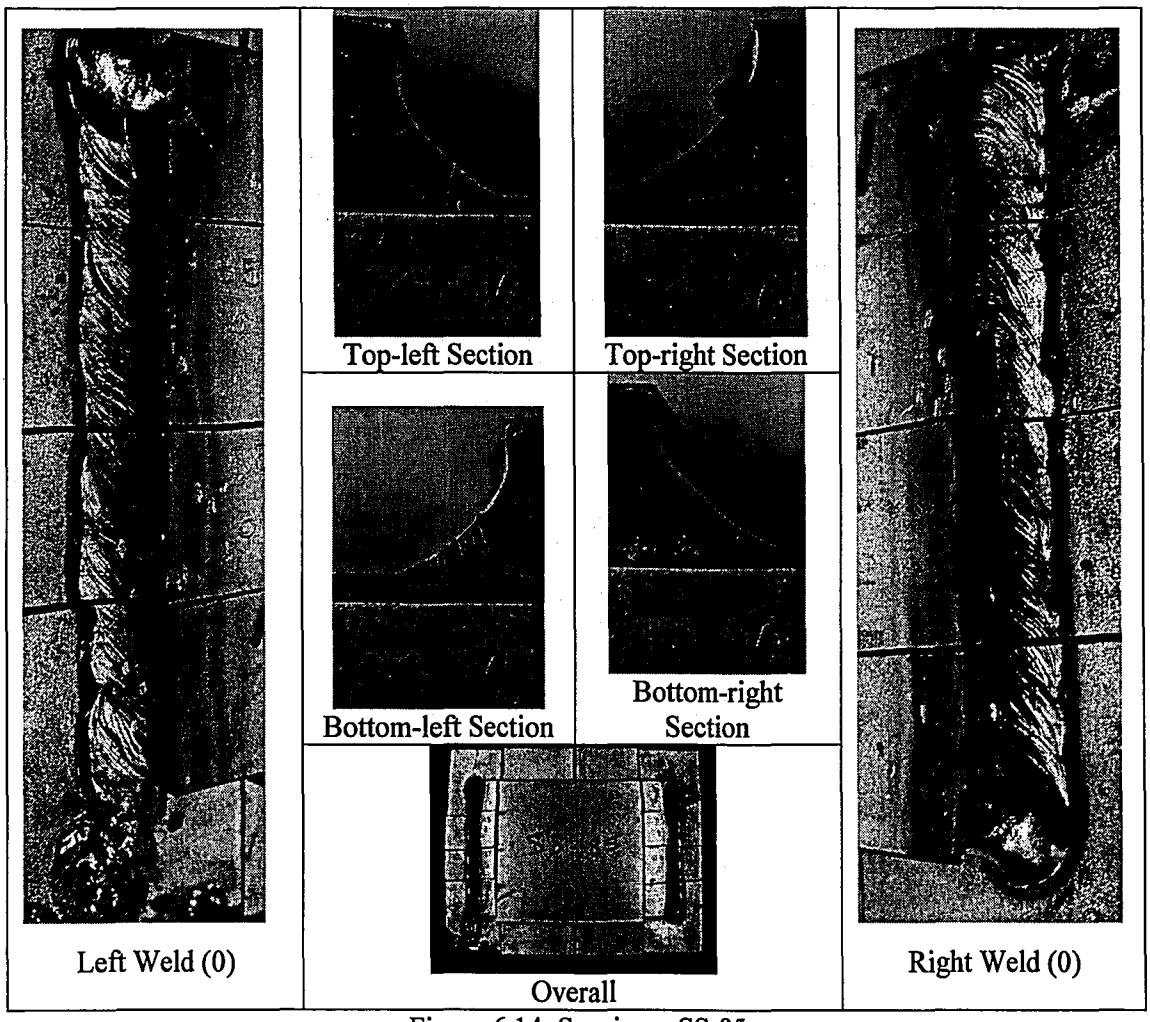

Figure 6.14: Specimen SS-85

Table 6-13: Environmental Conditions – Specimen SS-85					
Specimen: SS-85	Air Temp.	Concrete Temp.	Steel Temp.	Rel. Humidity	Wind Speed
	°F	°F	°F	%RH	[mph]
Nominal Values	32	32	32	95	10
Measured Values	35.0	39.7	39.8	100.0	10.0

The welded specimen is shown in Figure 6.14. Photographs of each of the two welds are presented along with an overview photo of the entire specimen. Sections were taken at four locations from the specimen and polished to examine the quality of the weld. These photos are also included.

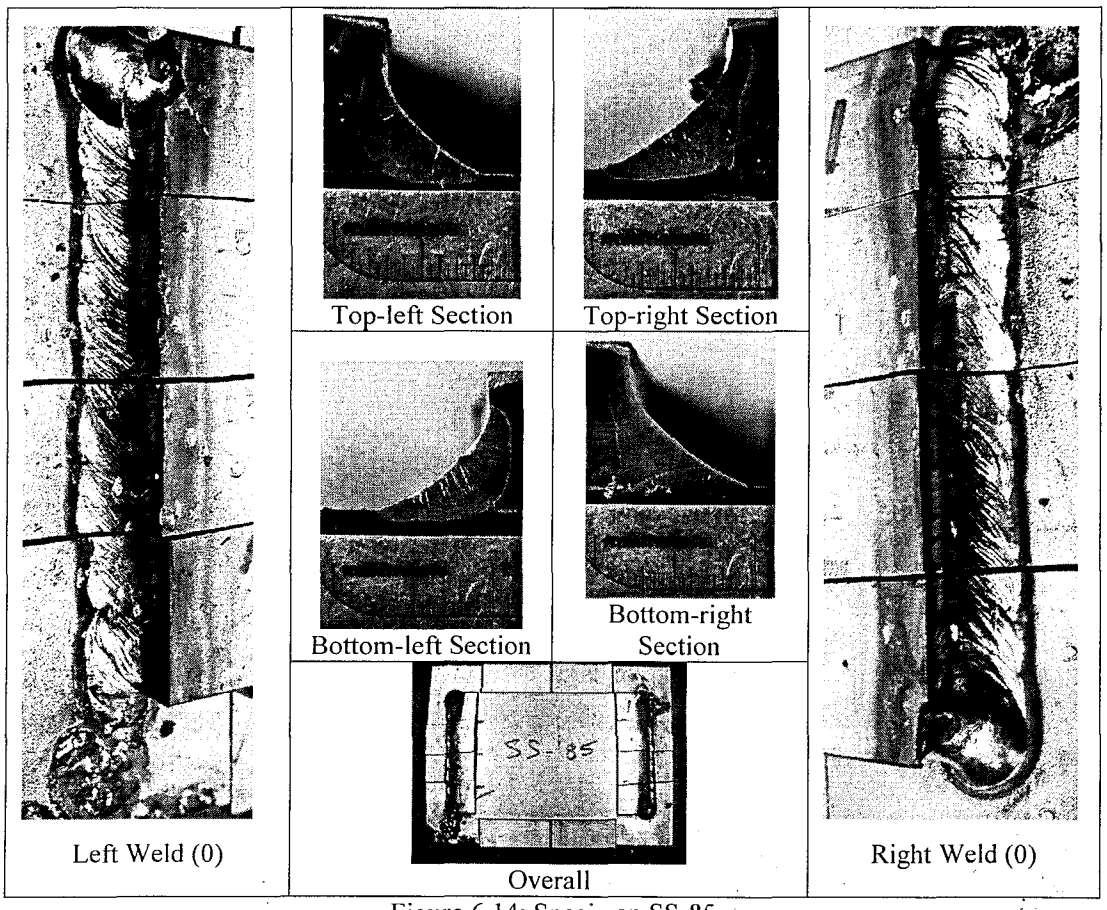

Figure 6.14: Specimen SS-85

6.14.1 Visual Observation Summary

The right and left welds displayed a small amount of edge-melt at their ends, but both welds had no observed surface discontinuities. The only section flaws to be noted were root inclusions in all four sections, with the measurements of their greatest dimension beginning with the top-right section and progressing clockwise being .028-in., .006-in., .011-in., and .009-in.. All sections except the top-left section met the 3/16-in. profile requirements.

6.15 Specimen SS-86: 32°F, High Humidity, 20 mph Wind

This specimen was subjected to conditions summarized in Table 6-14 at the time of welding.

Table 6-14: Environmental Conditions – Specimen SS-86

Specimen: SS-86	Air Temp.	Concrete Temp.	Steel Temp.	Rel. Humidity	Wind Speed
	°F	°F	°F	%RH	[mph]
Nominal Values	32	32	32	95	20
Measured Values	30.7	33.5	37.2	100.0	19.3

The welded specimen is shown in Figure 6.15. Photographs of each of the two welds are presented along with an overview photo of the entire specimen. Sections were taken at four locations from the specimen and polished to examine the quality of the weld. These photos are also included.

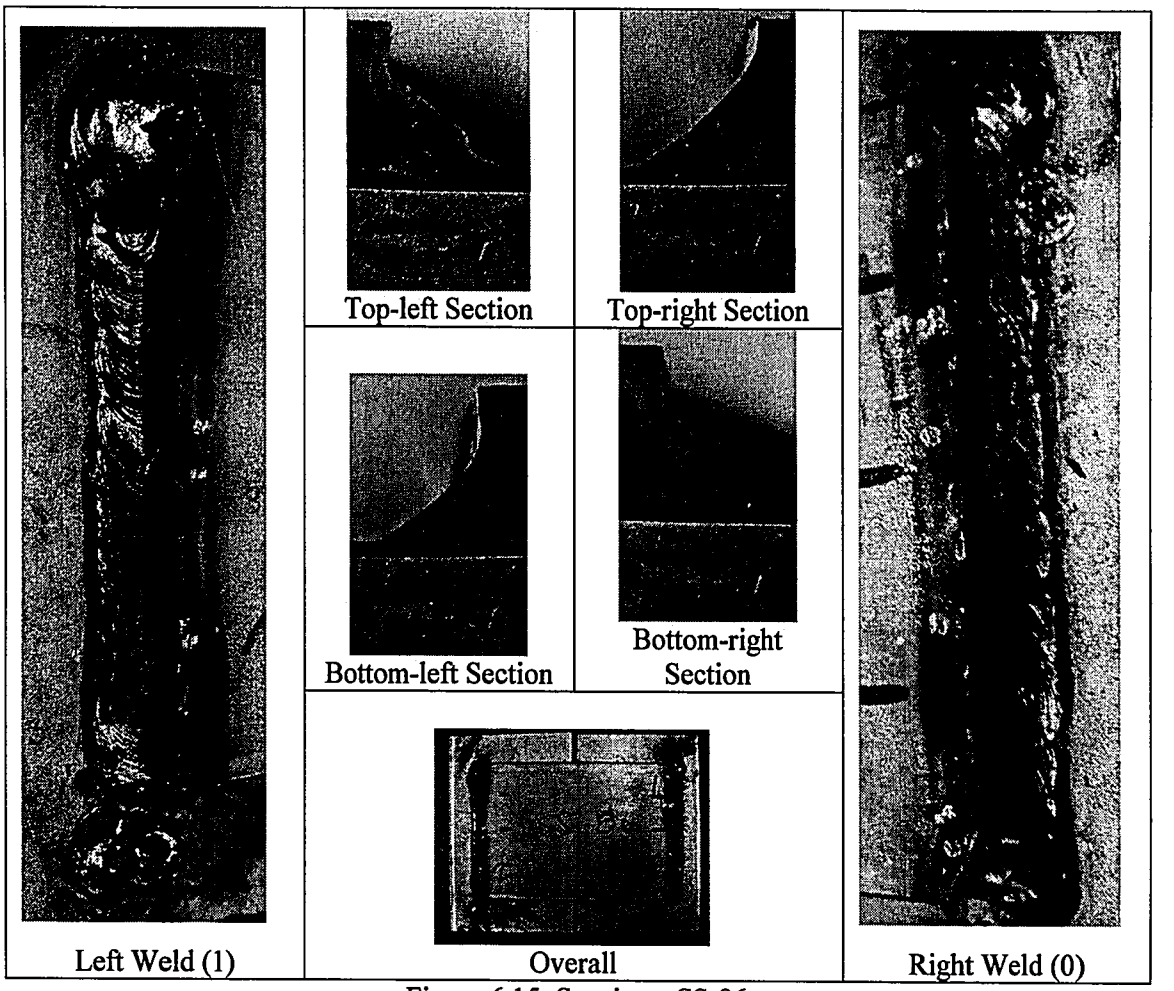

Figure 6.15: Specimen SS-86

6.15.1 Visual Observation Summary

The right weld showed some edge-melt along its length, while the left weld displayed undercut, a small amount of edge-melt, and a small "crater" before the end of the weld. The top-left section had a very unusual profile with two notches on the weld surface as seen in Figure 6.15 and some undercut (.012-in.). The top-right and bottom-left profiles had slag inclusions (.023-in., .027-in.). The bottom-right and top-left sections also contained small root inclusions (.007-in., .013-in.). All four sections met the 3/16-in. profile requirements, and the top-right and top-left profiles met the 1/4-in. profile requirements.

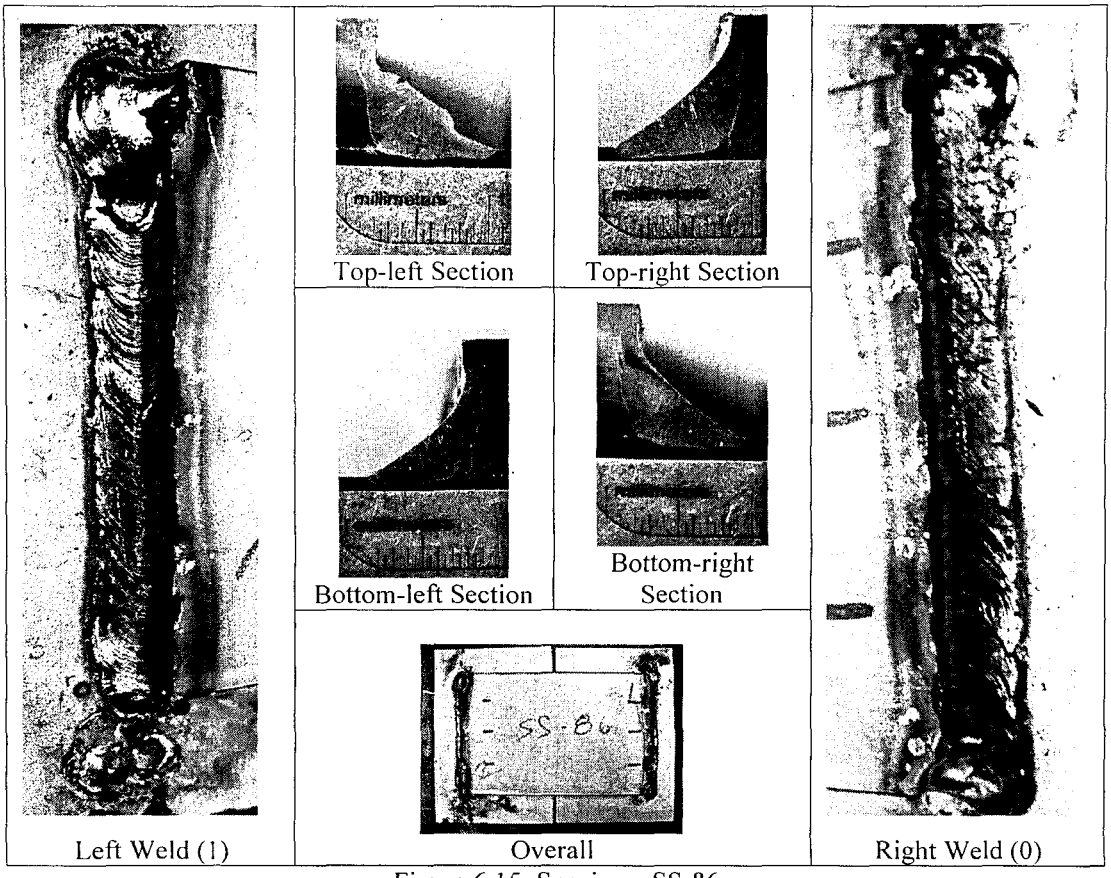

Figure 6.15: Specimen SS-86

6.15.1 Visual Observation Summary

The right weld showed some edge-melt along its length, while the left weld displayed undercut, a small amount of edge-melt, and a small "crater" before the end of the weld. The top-left section had a very unusual profile with two notches on the weld surface as seen in Figure 6.15 and some undercut (.012-in.). The top-right and bottom-left profiles had slag inclusions (.023-in., .027-in.). The bottom-right and top-left sections also contained small root inclusions (.007-in., .013-in.). All four sections met the 3/16-in. profile requirements, and the top-right and top-left profiles met the 1/4-in. profile requirements.

6.16 Specimen SS-87: 32°F, High Humidity, 35 mph Wind

This specimen was subjected to conditions summarized in Table 6-15 at the time of welding.

Table 6-15: Environmental conditions – Specimen SS-87					
Specimen:SS-87	Air Temp.	Concrete Temp.	Steel Temp.	Rel. Humidity	Wind Speed
	°F	°F	°F	%RH	[mph]
Nominal Values	32	32	32	95	35
Measured Values	33.2	34.2	33.8	100.0	33.1

The welded specimen is shown in Figure 6.16. Photographs of each of the two welds are presented along with an overview photo of the entire specimen. Sections were taken at four locations from the specimen and polished to examine the quality of the weld. These photos are also included.

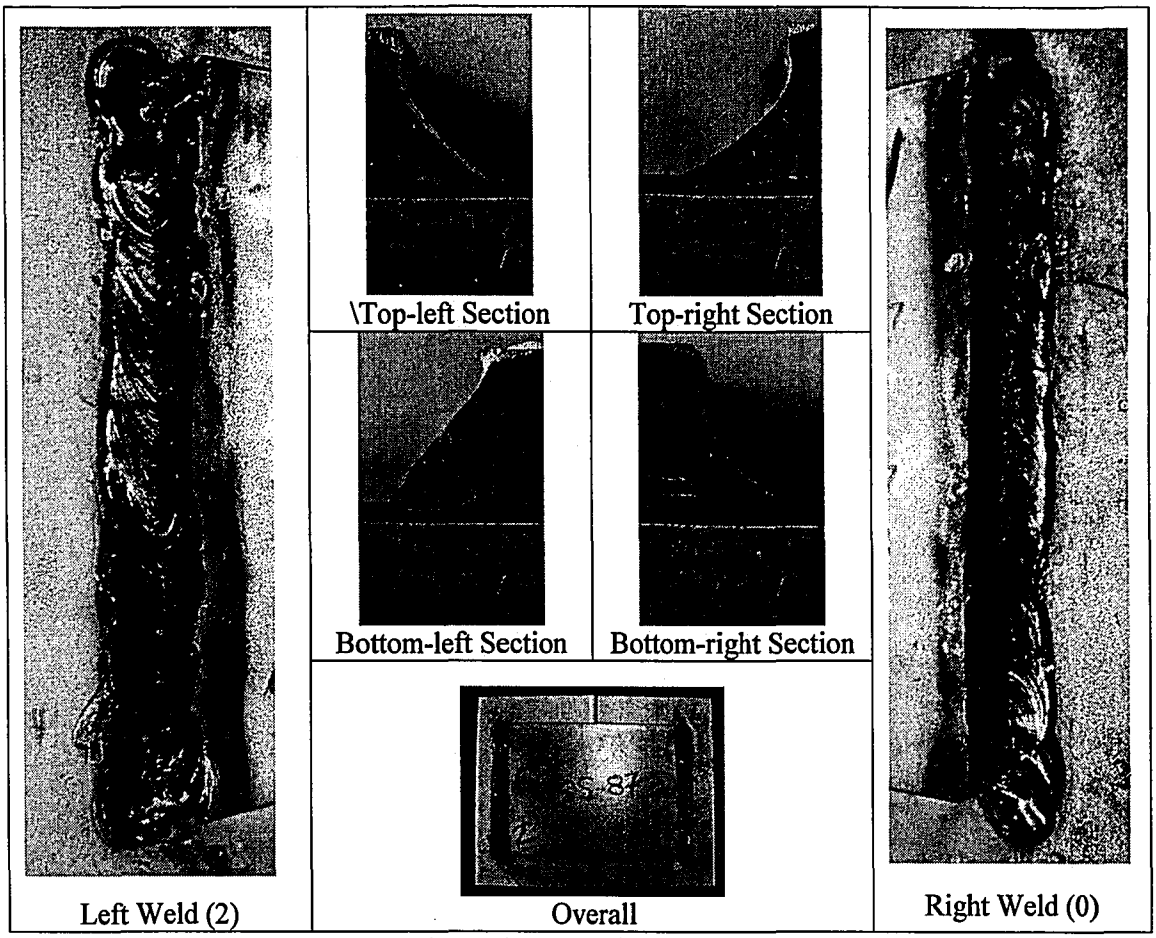

Figure 6.16: Specimen SS-87

6.16.1 Visual Observation Summary

The right weld had edge-melt at its beginning and undercut in the middle portion of the weld. The left weld had a great deal of edge-melt and erratic size changes along the length of the weld. All sections had root inclusions, and their largest dimensions are noted as follows beginning with the top-right section, moving clockwise (.020-in., .023-in., .032-in., .025-in.). All sections except the top-right section had significant skew to the vertical leg. A small amount of undercut was observed in the top-right section (.012-in.). All sections except the bottom-right section met the 3/16-in. profile requirements.

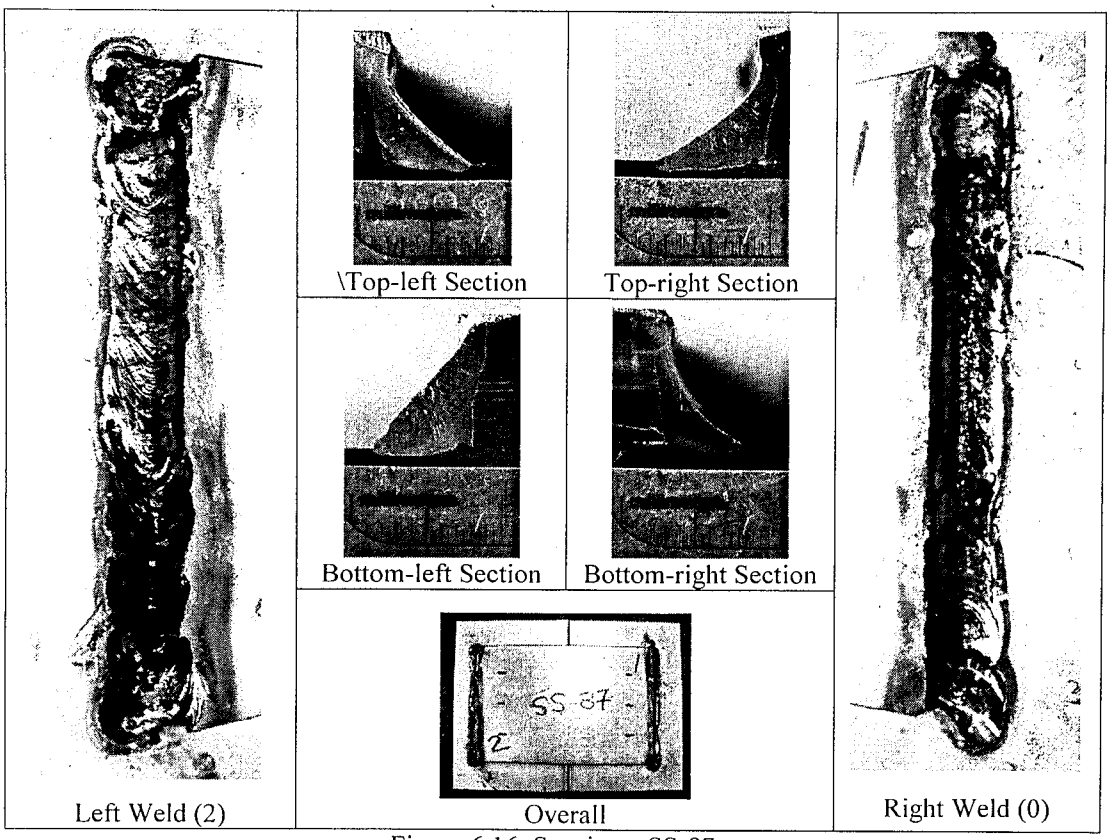

Figure 6.16: Specimen SS-87

6.16.1 Visual Observation Summary

The right weld had edge-melt at its beginning and undercut in the middle portion of the weld. The left weld had a great deal of edge-melt and erratic size changes along the length of the weld. All sections had root inclusions, and their largest dimensions are noted as follows beginning with the top-right section, moving clockwise (.020-in., .023-in., .032-in., .025-in.). All sections except the top-right section had significant skew to the vertical leg. A small amount of undercut was observed in the top-right section (.012-in.). All sections except the bottom-right section met the 3/16-in. profile requirements.

6.17 Specimen SS-88: 32°F, Surface Wet, 15 mph Wind

This specimen was subjected to conditions summarized in Table 6-16 at the time of welding.

Table 6-16: Environmental Conditions – Specimen SS-88					
Specimen: SS-88	Air Temp.	Concrete Temp.	Steel Temp.	Rel. Humidity	Wind Speed
	°F	°F	°F	%RH	[mph]
Nominal Values	32	32	32	Surface Wet	0
Measured	33.2	34.5	35.7	99.9-Surf. Wet	15*

*Note Blower remained on with ~15 mph accidental wind condition

The welded specimen is shown in Figure 6.17. Photographs of each of the two welds are presented along with an overview photo of the entire specimen. Sections were taken at four locations from the specimen and polished to examine the quality of the weld. These photos are also included.

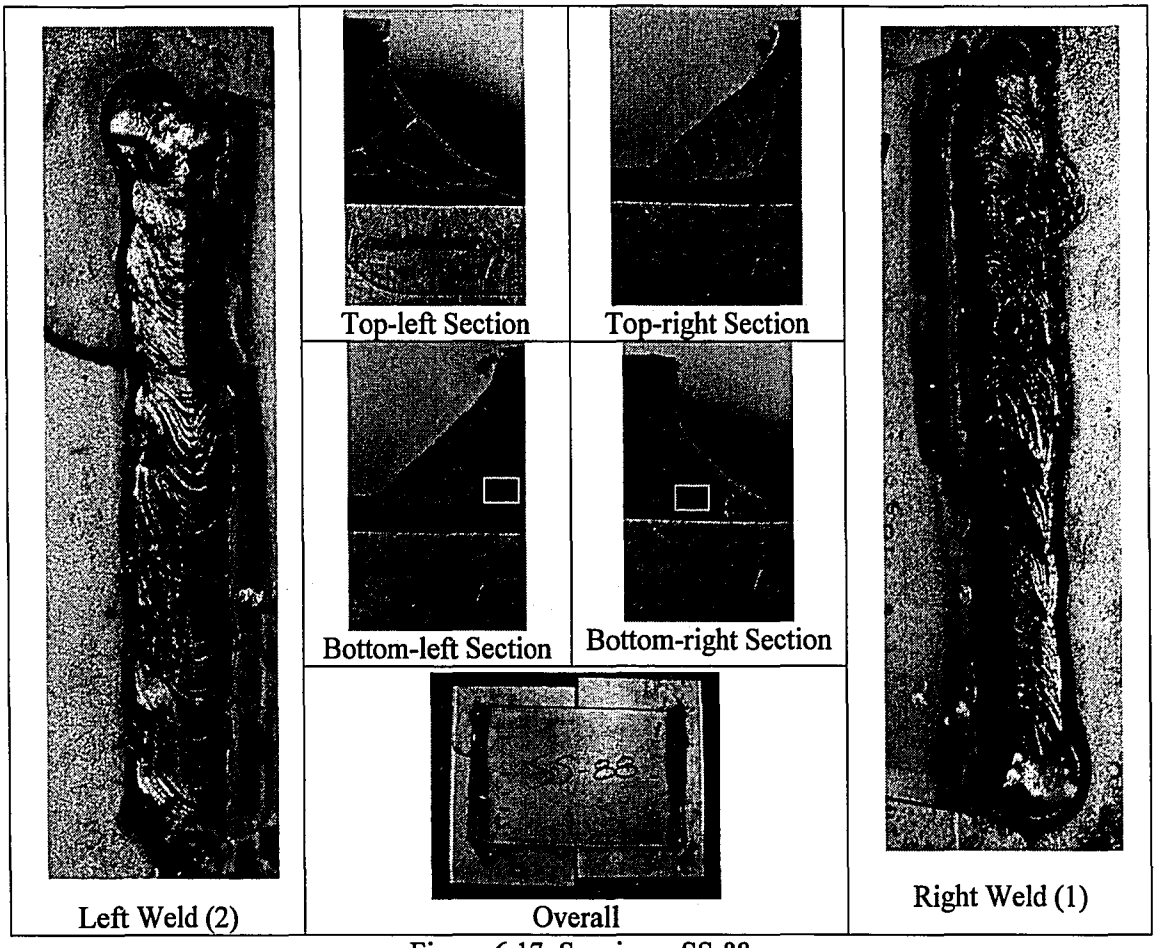

Figure 6.17: Specimen SS-88

6.17.1 Visual Observation Summary

The right and left welds possessed edge-melt along their length, and the left weld displayed some undercut. The top-right and bottom-left profiles had slag inclusions (.024-in., .021-in.) at their roots, and the bottom-right and top-left profiles had a smaller size and had small root inclusions (.006-in., .008-in.). All sections met the 3/16-in. profile requirements.

6.17.2 Microscopy Observation Summary

The bottom-right and bottom-left sections each had small micro-cracks behind the root projecting from the interface between the base plate and cover plate. These sections each possessed a small micro-crack at or behind the root near a root inclusion, shown in Figure 6.18

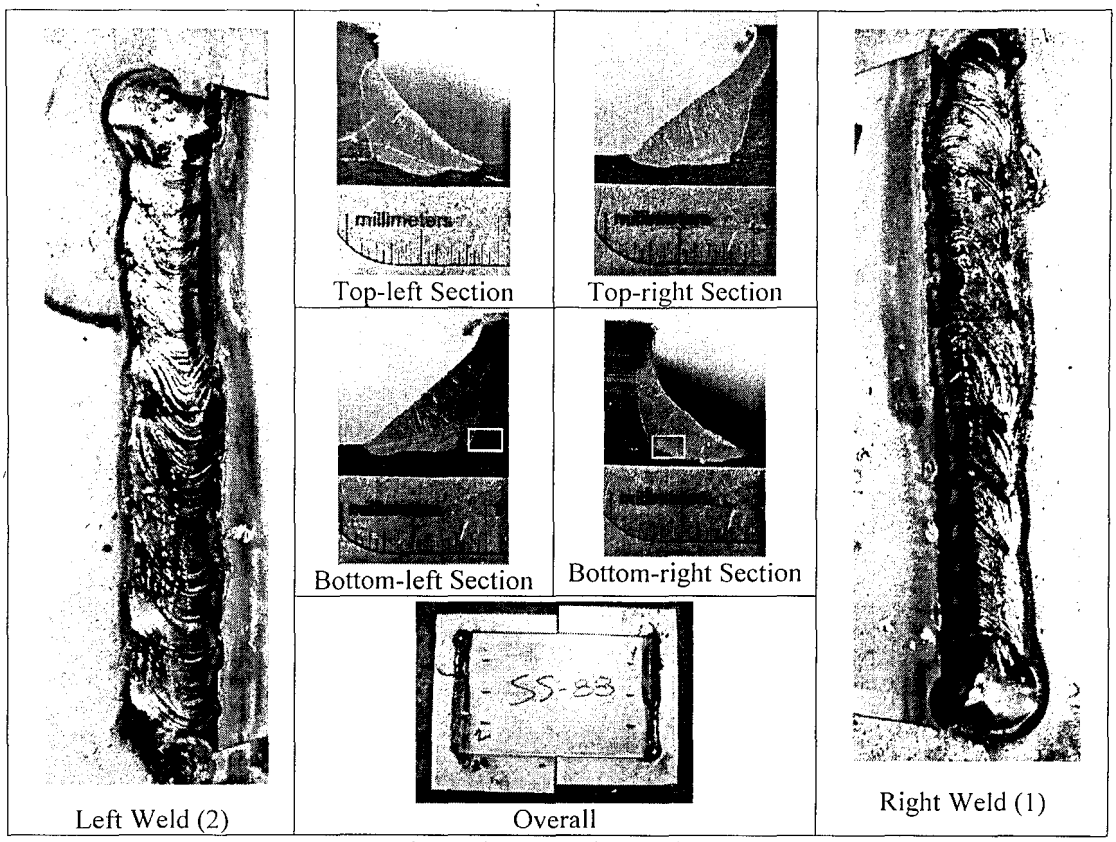

Figure 6.17: Specimen SS-88

6.17.1 Visual Observation Summary

The right and left welds possessed edge-melt along their length, and the left weld displayed some undercut. The top-right and bottom-left profiles had slag inclusions (.024-in., .021-in.) at their roots, and the bottom-right and top-left profiles had a smaller size and had small root inclusions (.006-in., .008-in.). All sections met the 3/16-in. profile requirements.

6.17.2 Microscopy Observation Summary

The bottom-right and bottom-left sections each had small micro-cracks behind the root projecting from the interface between the base plate and cover plate. These sections each possessed a small micro-crack at or behind the root near a root inclusion, shown in Figure 6.18

and Figure 6.19. The micro-cracks protrude from the fusion line and are likely the result of a stress concentration induced at the weld root.

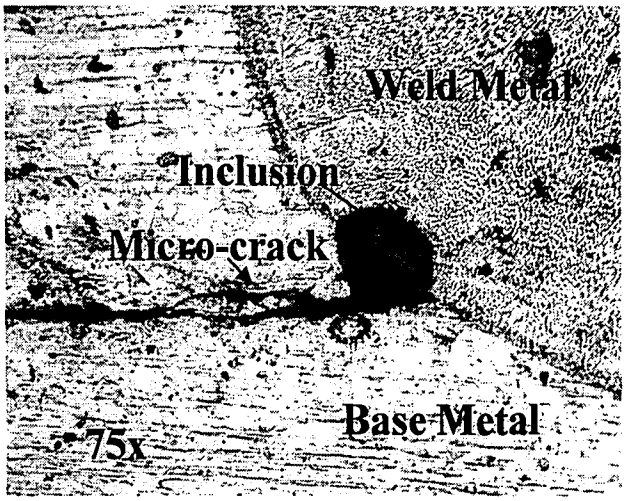

Figure 6.18: Micro-Crack Behind Root of Specimen SS-88, Bottom-right Section

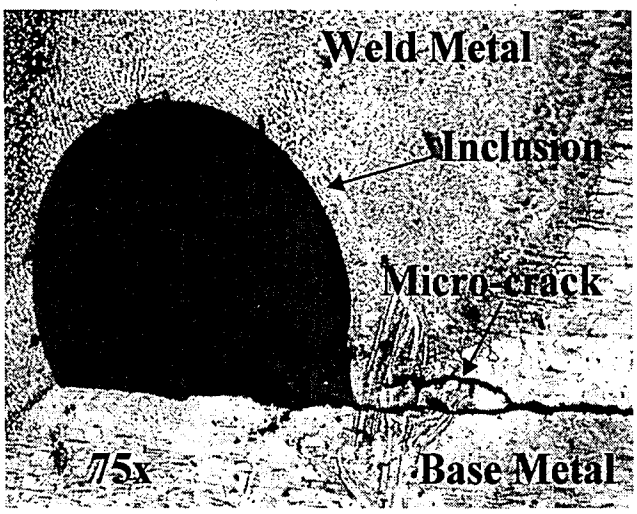

Figure 6.19: Micro-Crack at Root of Specimen SS-88, Bottom-left Section

6.18 Specimen SS-89: -10°F, Low Humidity, No Wind

This specimen was subjected to environmental conditions in the environmental chamber at the time of welding. The specific conditions for the weld are detailed in Table 6-17.

Table 6-17: Environmental Conditions – Specimen SS-89					
Specimen: SS-89	Air Temp.	Concrete Temp.	Steel Temp.	Rel. Humidity	Wind Speed
	°F	°F	°F	%RH	[mph]
Nominal Values	-10	-10	-10	35	0
Measured Values	-10.0	20.6	-4.6	24.7	0

The welded specimen is shown in Figure 6.20. Photographs of each of the two welds are presented along with an overview photo of the entire specimen. Sections were taken at four locations from the specimen and polished to examine the quality of the weld. These photos are also included.

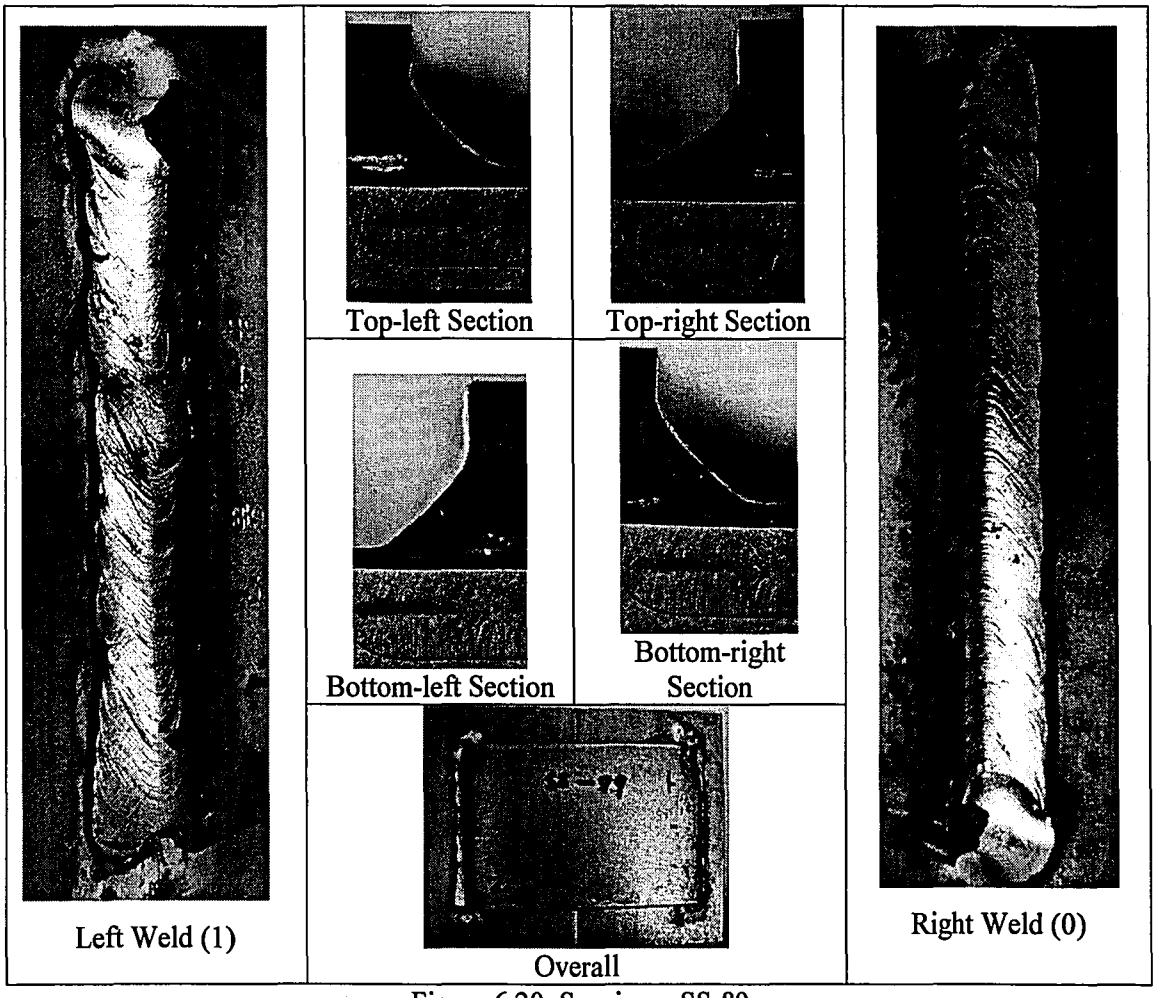

Figure 6.20: Specimen SS-89

Table 6-17: Environmental Conditions – Specimen SS-89					
Specimen: SS-89	Air Temp.	Concrete Temp.	Steel Temp.	Rel. Humidity	Wind Speed
	°F	°F	°F	%RH	[mph]
Nominal Values	-10	-10	-10	35	0
Measured Values	-10.0	20.6	-4.6	24.7	0

The welded specimen is shown in Figure 6.20. Photographs of each of the two welds are presented along with an overview photo of the entire specimen. Sections were taken at four locations from the specimen and polished to examine the quality of the weld. These photos are also included.

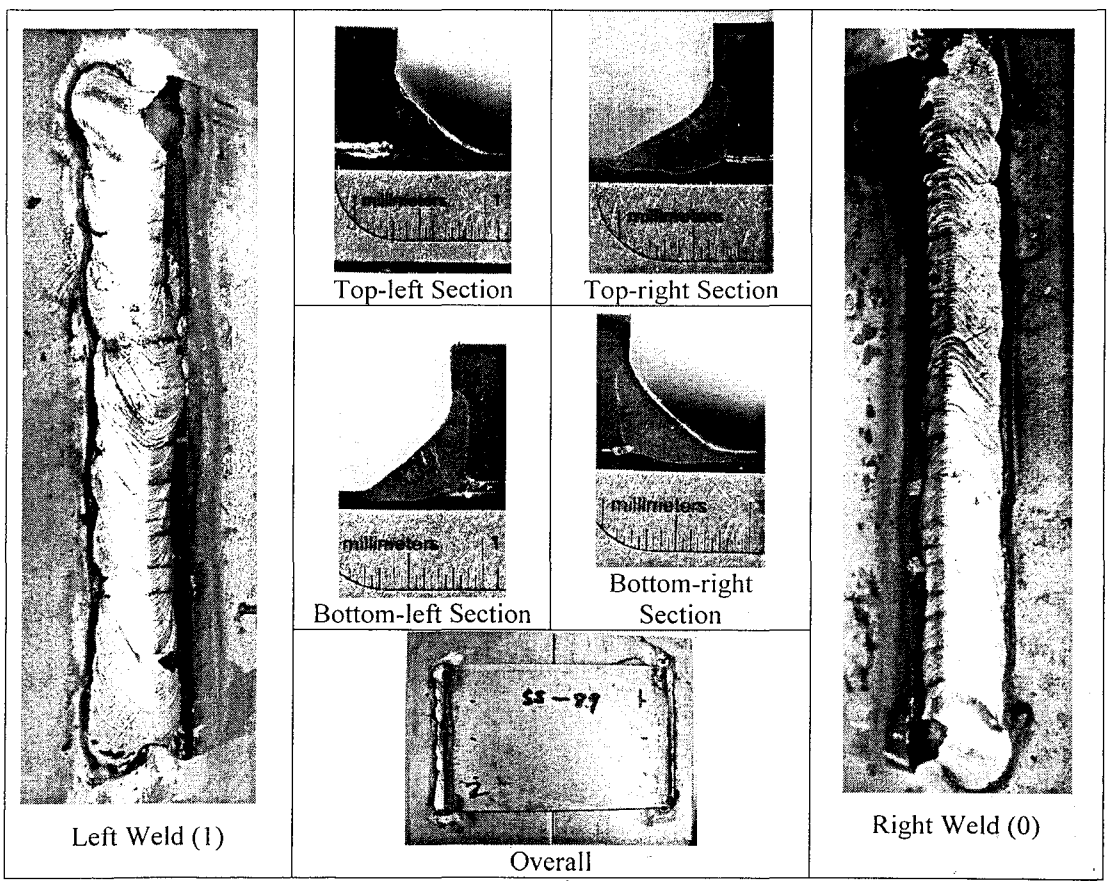

Figure 6.20: Specimen SS-89

6.18.1 Visual Observation Summary

Both welds had a small amount of edge-melt; however, neither of the welds and none of the sections displayed any notable discontinuities except a small amount of undercut (.010-in.) in the top-left section. All sections except the top-right section met the 3/16-in. profile requirements.

6.19 Specimen SS-90: -10°F, Moderate Humidity, No Wind

This specimen was subjected to environmental conditions in the environmental chamber at the time of welding. The specific conditions for the weld are detailed in Table 6-18.

Table 6-18: Environmental Conditions – Specimen SS-90

Specimen: SS-90	Air Temp.	Concrete Temp.	Steel Temp.	Rel. Humidity	Wind Speed
	°F	°F	°F	%RH	[mph]
Nominal Values	-10	-10	-10	50	0
Measured Values	-12.2	5.3	-5.0	49.5	0

The welded specimen is shown in Figure 6.21. Photographs of each of the two welds are presented along with an overview photo of the entire specimen. Sections were taken at four locations from the specimen and polished to examine the quality of the weld. These photos are also included.

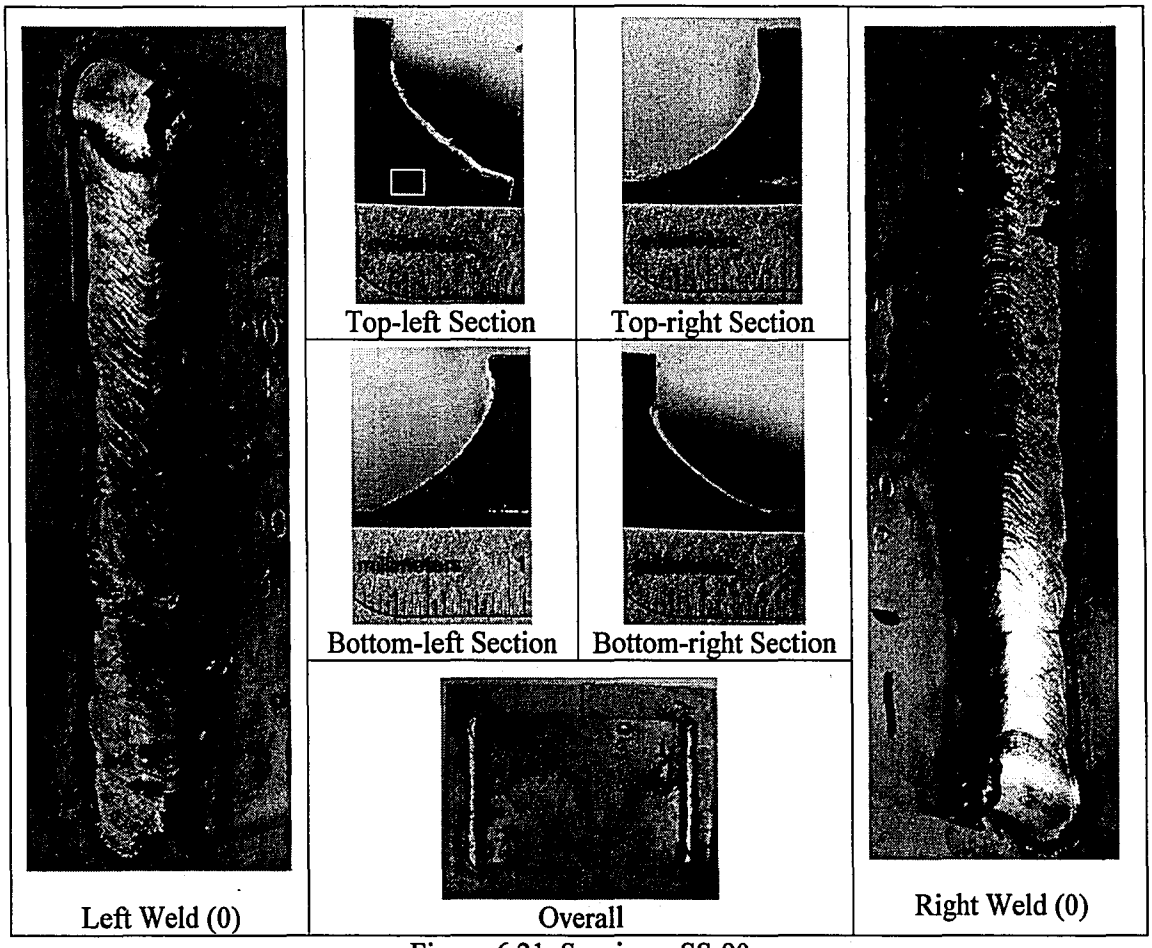

Figure 6.21: Specimen SS-90

6.19.1 Visual Observation Summary

The right weld had some edge-melt at its end but was otherwise free of discontinuities, while the second weld had two surface pores (.054-in., .067-in.) at its beginning and some edge-melt at its end. The bottom-left profile contained a small root inclusion (.009-in.). The bottom-right section exhibited a small amount of undercut (.021-in.). All four sections had rather concave profiles, and the top-right and bottom-right sections did not meet the 3/16-in. profile requirements.

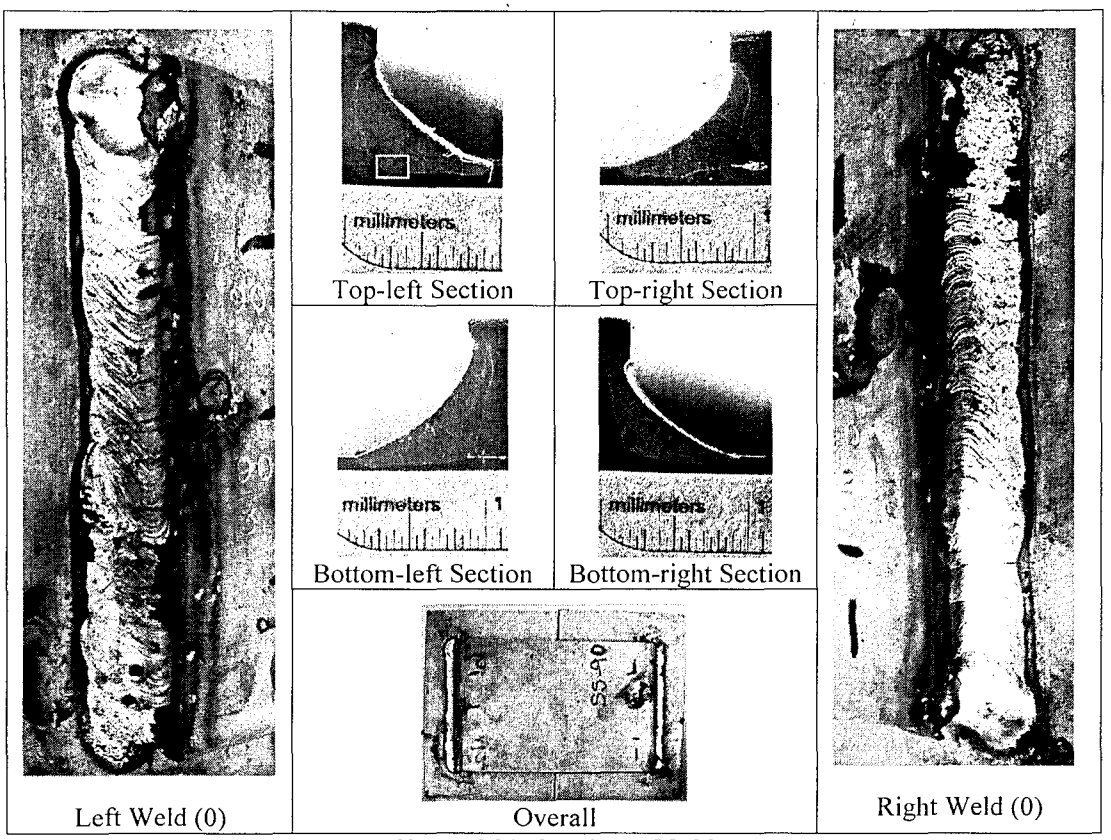

Figure 6.21: Specimen SS-90

6.19.1 Visual Observation Summary

The right weld had some edge-melt at its end but was otherwise free of discontinuities, while the second weld had two surface pores (.054-in., .067-in.) at its beginning and some edge-melt at its end. The bottom-left profile contained a small root inclusion (.009-in.). The bottom-right section exhibited a small amount of undercut (.021-in.). All four sections had rather concave profiles, and the top-right and bottom-right sections did not meet the 3/16-in. profile requirements.

6.19.2 Microscopy Observation Summary

Figure 6.22 depicts what appeared to be micro-cracking that occurred along the interface between the base plate and cover plate behind the root in the top-left section. These micro-cracks were very thin and did not appear to be caused directly by welding, but rather appear to have occurred along the meeting surfaces of the two plates, perhaps through an oxide layer on the plates as the plates were compressed together. The image also shows thousands of small non-metallic inclusions which appeared in many of the stainless steel sections and in some cases were clustered together tightly. In this case, the inclusions are scattered around the root area.

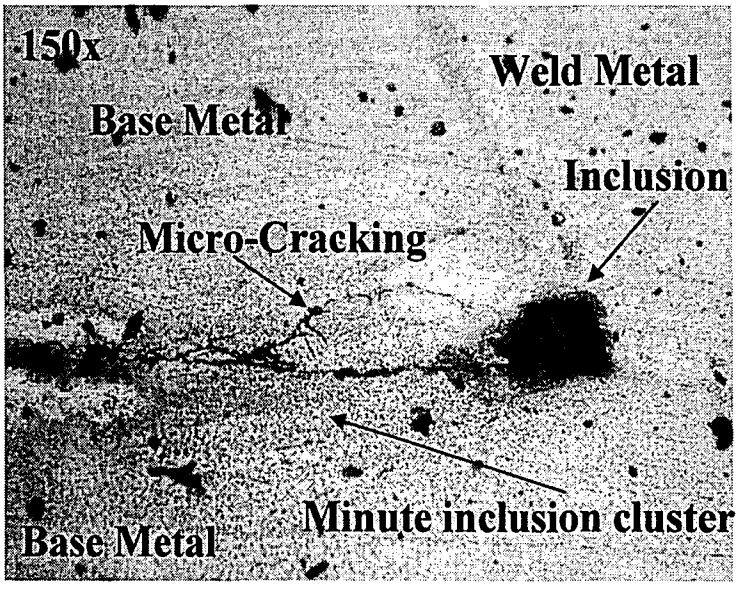

Figure 6.22: Plate Interface Micro-cracking in SS-90, Top-left Section

6.20 Specimen SS-91: -10°F, High Humidity, No Wind

This specimen was subjected to environmental conditions in the environmental chamber at the time of welding. The specific conditions for the weld are detailed in Table 6-19.

Table 6-19: Environmental Conditions – Specimen SS-91					
Specimen: SS-91	Air Temp.	Concrete Temp.	Steel Temp.	Rel. Humidity	Wind Speed
	°F	°F	°F	%RH	[mph]
Nominal Values	-10	-10	-10	95	0
Measured Values	-9.8	1.7	-5.4	100.0	0

The welded specimen is shown in Figure 6.23. Photographs of each of the two welds are presented along with an overview photo of the entire specimen. Sections were taken at four locations from the specimen and polished to examine the quality of the weld. These photos are also included.

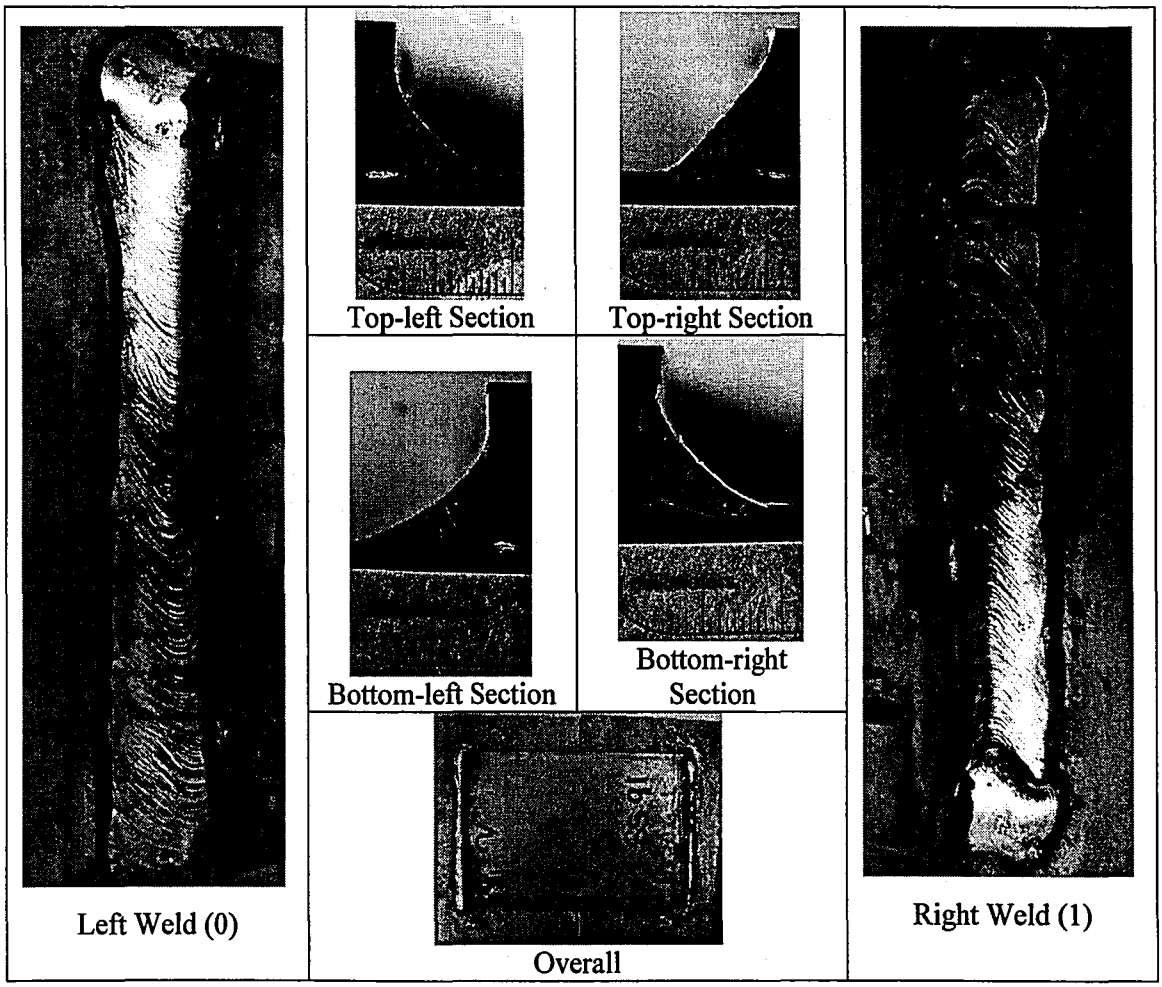

Figure 6.23: Specimen SS-91

Table 6-19: Environmental Conditions – Specimen SS-91					
Specimen: SS-91	Air Temp.	Concrete Temp.	Steel Temp.	Rel. Humidity	Wind Speed
	°F	°F	°F	%RH	[mph]
Nominal Values	-10	-10	-10	95	0
Measured Values	-9.8	1.7	-5.4	100.0	0

The welded specimen is shown in Figure 6.23. Photographs of each of the two welds are presented along with an overview photo of the entire specimen. Sections were taken at four locations from the specimen and polished to examine the quality of the weld. These photos are also included.

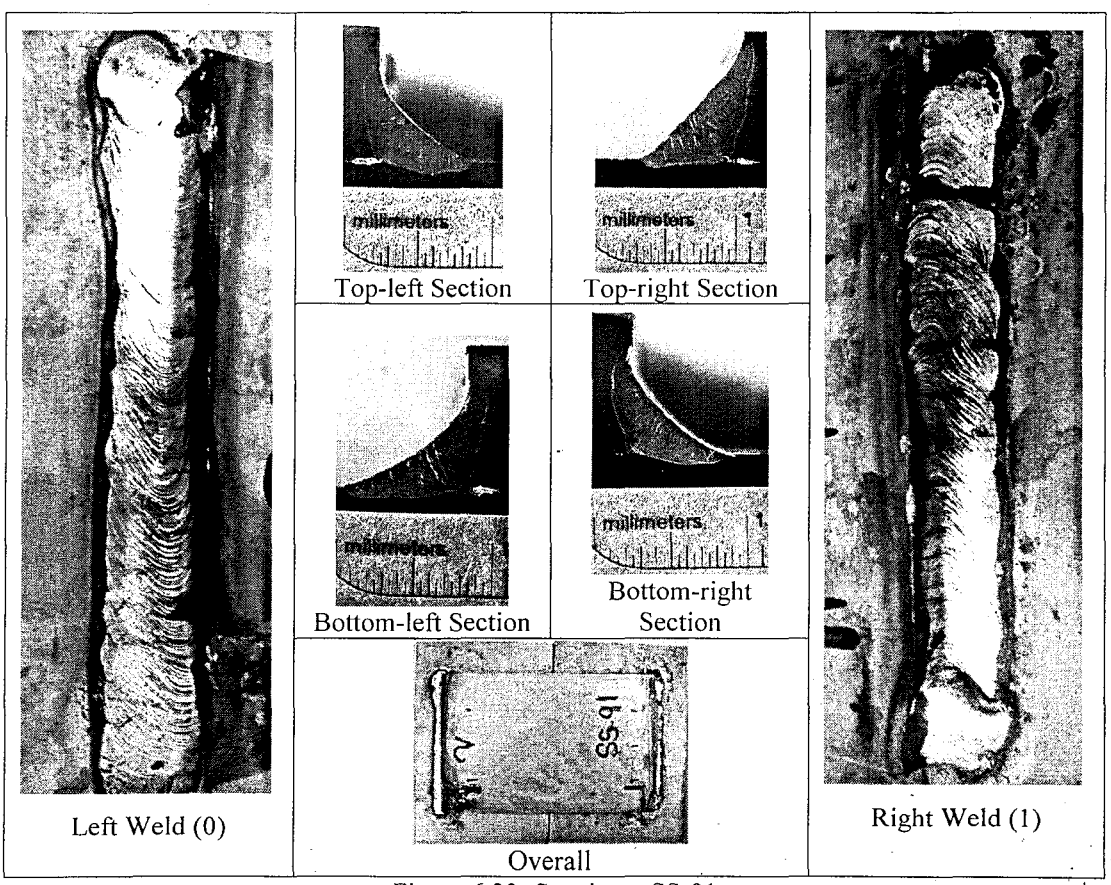

Figure 6.23: Specimen SS-91

6.20.1 Visual Observation Summary

Besides a small amount of edge-melt, the right weld was free of surface discontinuities, and the left weld had one surface pore (.050-in.) at its beginning and edge-melt at its beginning and end. The bottom-right and top-left sections had rather small profiles, and the top-right profile had significant skew to the vertical leg and had a small root slag inclusion (.021-in.). The bottom-left and top-left sections also had small root inclusions (.016-in., .009-in.). The bottom-right section exhibited .012-in. undercut. All four sections met the 3/16-in. profile requirements.

6.21 Specimen SS-92: -10°F, High Humidity, 5 mph Wind

This specimen was subjected to environmental conditions in the environmental chamber at the time of welding. The specific conditions for the weld are detailed in Table 6-20.

Table 6-20: Environmental Conditions – Specimen SS-92

Specimen: SS-92	Air Temp.	Concrete Temp.	Steel Temp.	Rel. Humidity	Wind Speed
	°F	°F	°F	%RH	[mph]
Nominal Values	-10	-10	-10	95	5
Measured Values	-9.8	-1.2	-2.2	95.5	5.5

The welded specimen is shown in Figure 6.24. Photographs of each of the two welds are presented along with an overview photo of the entire specimen. Sections were taken at four locations from the specimen and polished to examine the quality of the weld. These photos are also included.

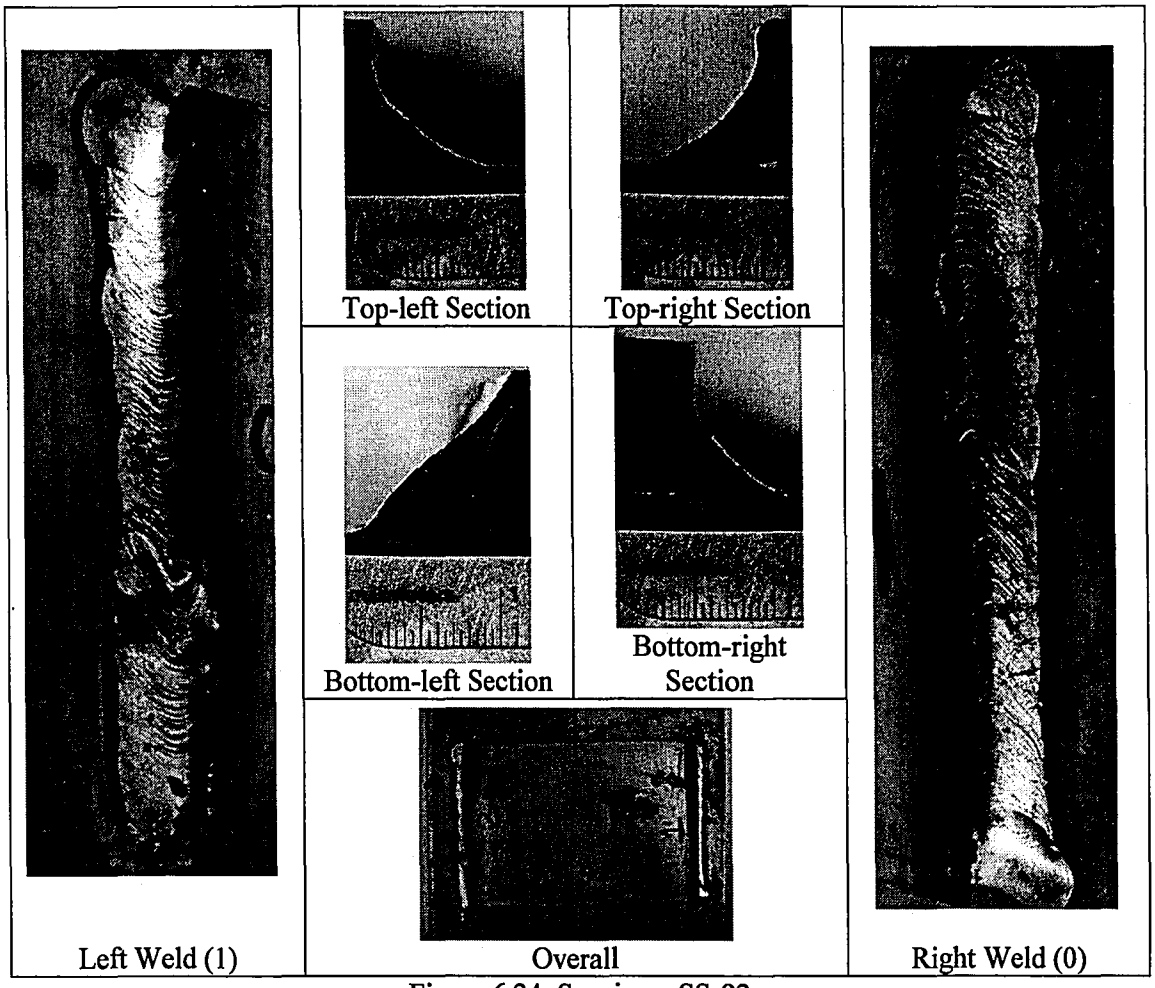

Figure 6.24: Specimen SS-92

6.21.1 Visual Observation Summary

The right weld had some edge-melt at its end, as did the left weld in its middle portion. The top-right section had a root slag inclusion (.021-in.), and the bottom-left section had severe skew toward and curvature in its vertical leg. The bottom-right section was somewhat smaller in size and was the only section of the four which did not meet the 3/16-in. profile requirements.

6.22 Specimen SS-93: -10°F, High Humidity, 10 mph Wind

This specimen was subjected to environmental conditions in the environmental chamber at the time of welding. The specific conditions for the weld are detailed in Table 6-21.

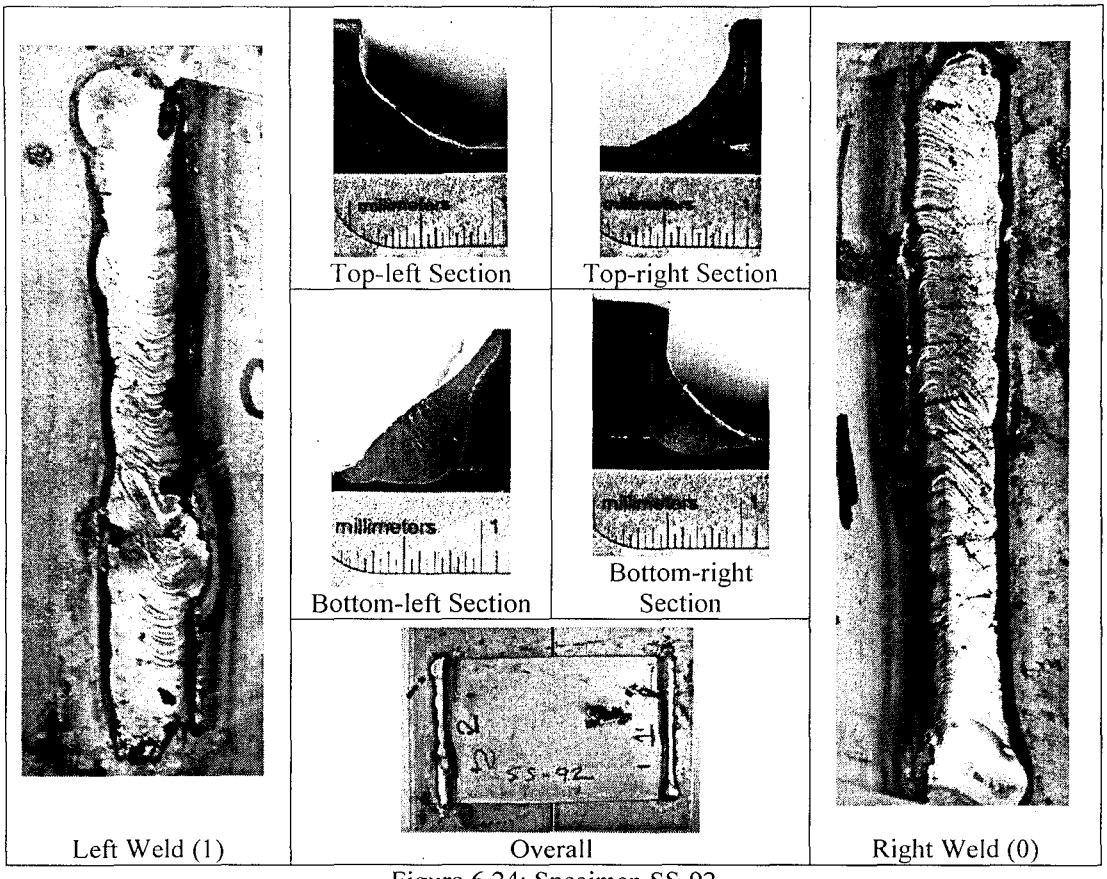

Figure 6.24: Specimen SS-92

6.21.1 Visual Observation Summary

The right weld had some edge-melt at its end, as did the left weld in its middle portion. The top-right section had a root slag inclusion (.021-in.), and the bottom-left section had severe skew toward and curvature in its vertical leg. The bottom-right section was somewhat smaller in size and was the only section of the four which did not meet the 3/16-in. profile requirements.

6.22 Specimen SS-93: -10°F, High Humidity, 10 mph Wind

This specimen was subjected to environmental conditions in the environmental chamber at the time of welding. The specific conditions for the weld are detailed in Table 6-21.

Table 6-21: Environmental Conditions – Specimen SS-93					
Specimen: SS-93	Air Temp.	Concrete Temp.	Steel Temp.	Rel. Humidity	Wind Speed
	°F	°F	°F	%RH	[mph]
Nominal Values	-10	-10	-10	95	10
Measured Values	-10.8	-1.2	-2.4	93	10.0

The welded specimen is shown in Figure 6.25. Photographs of each of the two welds are presented along with an overview photo of the entire specimen. Sections were taken at four locations from the specimen and polished to examine the quality of the weld. These photos are also included.

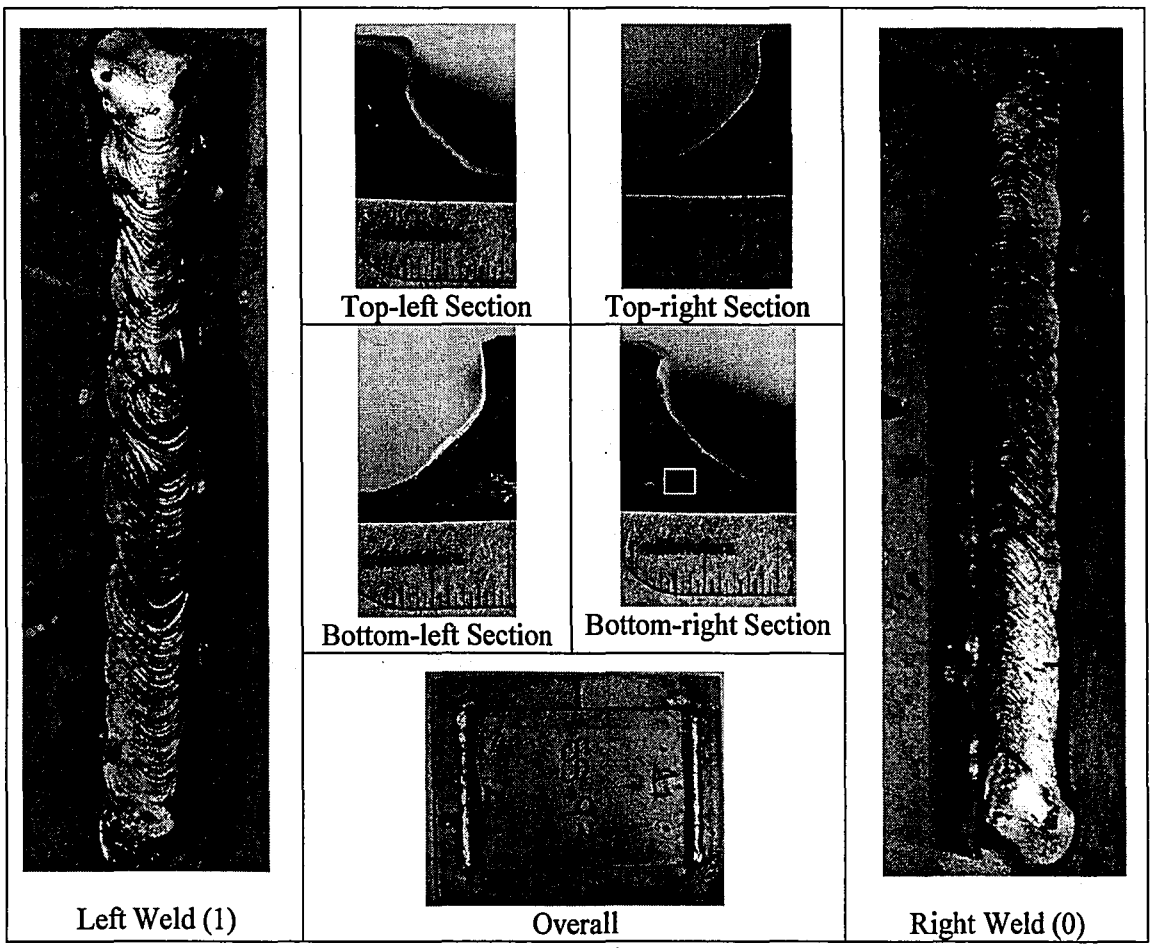

Figure 6.25: Specimen SS-93

Table 6-21: Environmental Conditions – Specimen SS-93					
Specimen: SS-93	Air Temp.	Concrete Temp.	Steel Temp.	Rel. Humidity	Wind Speed
	°F	°F	°F	%RH	[mph]
Nominal Values	-10	-10	-10	95	10
Measured Values	-10.8	-1.2	-2.4	93	10.0

The welded specimen is shown in Figure 6.25. Photographs of each of the two welds are presented along with an overview photo of the entire specimen. Sections were taken at four locations from the specimen and polished to examine the quality of the weld. These photos are also included.

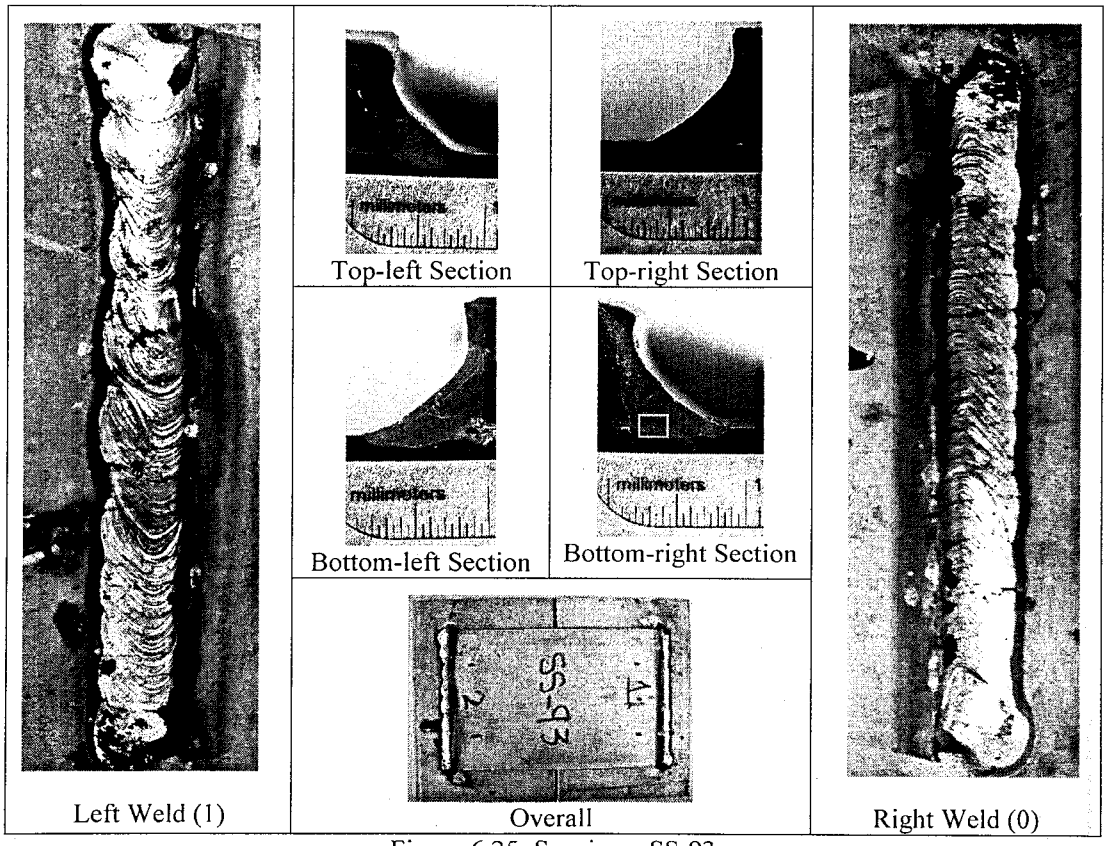

Figure 6.25: Specimen SS-93

6.22.1 Visual Observation Summary

The right weld, with a small amount of edge-melt at its end, had one surface pore (.037-in.) at its beginning, and the left weld had one surface pore (.037-in.) at its beginning and displayed edge-melt along its length. The bottom-right section exhibited .017-in. undercut, although not a sharp notch. The bottom-left profile had a root inclusion (.034-in.), and all sections except the top-left section met the 3/16-in. profile requirements.

6.22.2 Microscopy Observation Summary

A micro-crack can be seen in Figure 6.26 protruding from the plate interface caused by a stress concentration at the root of the weld behind a small root slag inclusion.

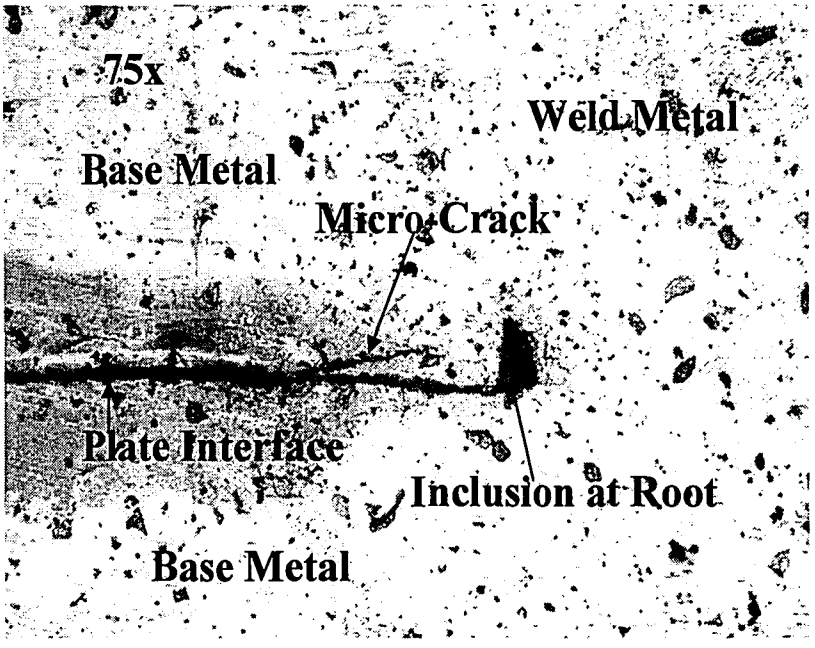

Figure 6.26: Root Micro-crack in Specimen SS-93, Bottom-right Section

6.23 Specimen SS-94: -10°F, High Humidity, 20 mph Wind

This specimen was subjected to environmental conditions in the environmental chamber at the time of welding. The specific conditions for the weld are detailed in Table 6-22.

Table 6-22: Environmental Conditions – Specimen SS-94					
Specimen: SS-94	Air Temp.	Concrete Temp.	Steel Temp.	Rel. Humidity	Wind Speed
	°F	°F	°F	%RH	[mph]
Nominal Values	-10	-10	-10	95	20
Measured Values	-10.0	-2.4	-3.0	100.0	20.6

The welded specimen is shown in Figure 6.27. Photographs of each of the two welds are presented along with an overview photo of the entire specimen. Sections were taken at four locations from the specimen and polished to examine the quality of the weld. These photos are also included.

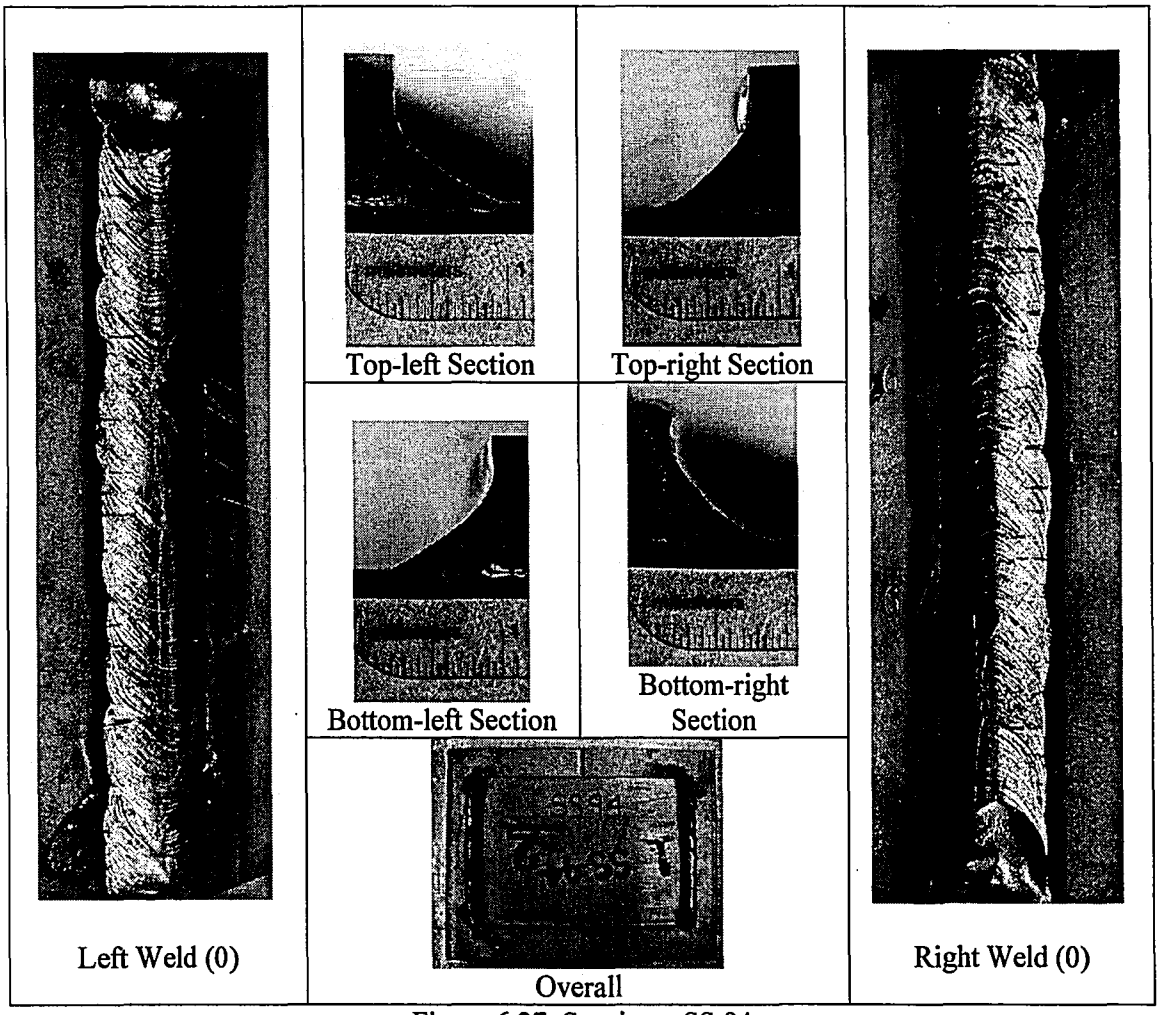

Figure 6.27: Specimen SS-94

Table 6-22: Environmental Conditions – Specimen SS-94					
Specimen: SS-94	Air Temp.	Concrete Temp.	Steel Temp.	Rel. Humidity	Wind Speed
	°F	°F	°F	%RH	[mph]
Nominal Values	-10	-10	-10	95	20
Measured Values	-10.0	-2.4	-3.0	100.0	20.6

The welded specimen is shown in Figure 6.27. Photographs of each of the two welds are presented along with an overview photo of the entire specimen. Sections were taken at four locations from the specimen and polished to examine the quality of the weld. These photos are also included.

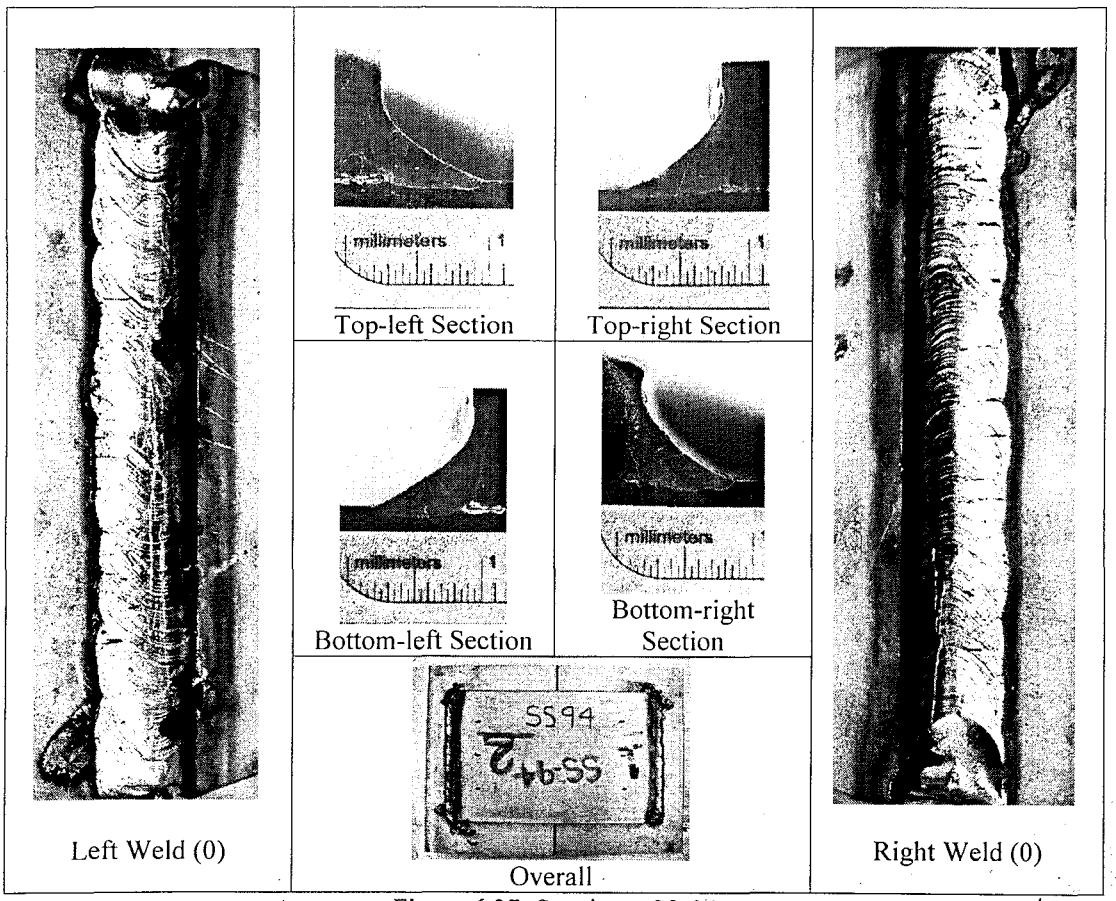

Figure 6.27: Specimen SS-94

6.23.1 Visual Observation Summary

There was a small amount of edge-melt in the case of both welds, and the top-right, bottom-left, and top-left sections each had a root slag inclusion (.010-in., .013-in., .015-in.). The top-left section did not meet 3/16-in. profile requirements.

6.24 Specimen SS-95: -10°F, High Humidity, 35 mph Wind

This specimen was subjected to environmental conditions in the environmental chamber at the time of welding. The specific conditions for the weld are detailed in Table 6-23.

Table 6-23: Environmental Conditions – Specimen SS-95

Specimen: SS-95	Air Temp.	Concrete Temp.	Steel Temp.	Rel. Humidity	Wind Speed
	°F	°F	°F	%RH	[mph]
Nominal Values	-10	-10	-10	95	35
Measured Values	-9.6	4.0	-1.2	100.0	~26-27*

* Due to excessively cold temperatures and high moisture, blower performance was limited to ~27mph.

The welded specimen is shown in Figure 6.28. Photographs of each of the two welds are presented along with an overview photo of the entire specimen. Sections were taken at four locations from the specimen and polished to examine the quality of the weld. These photos are also included.

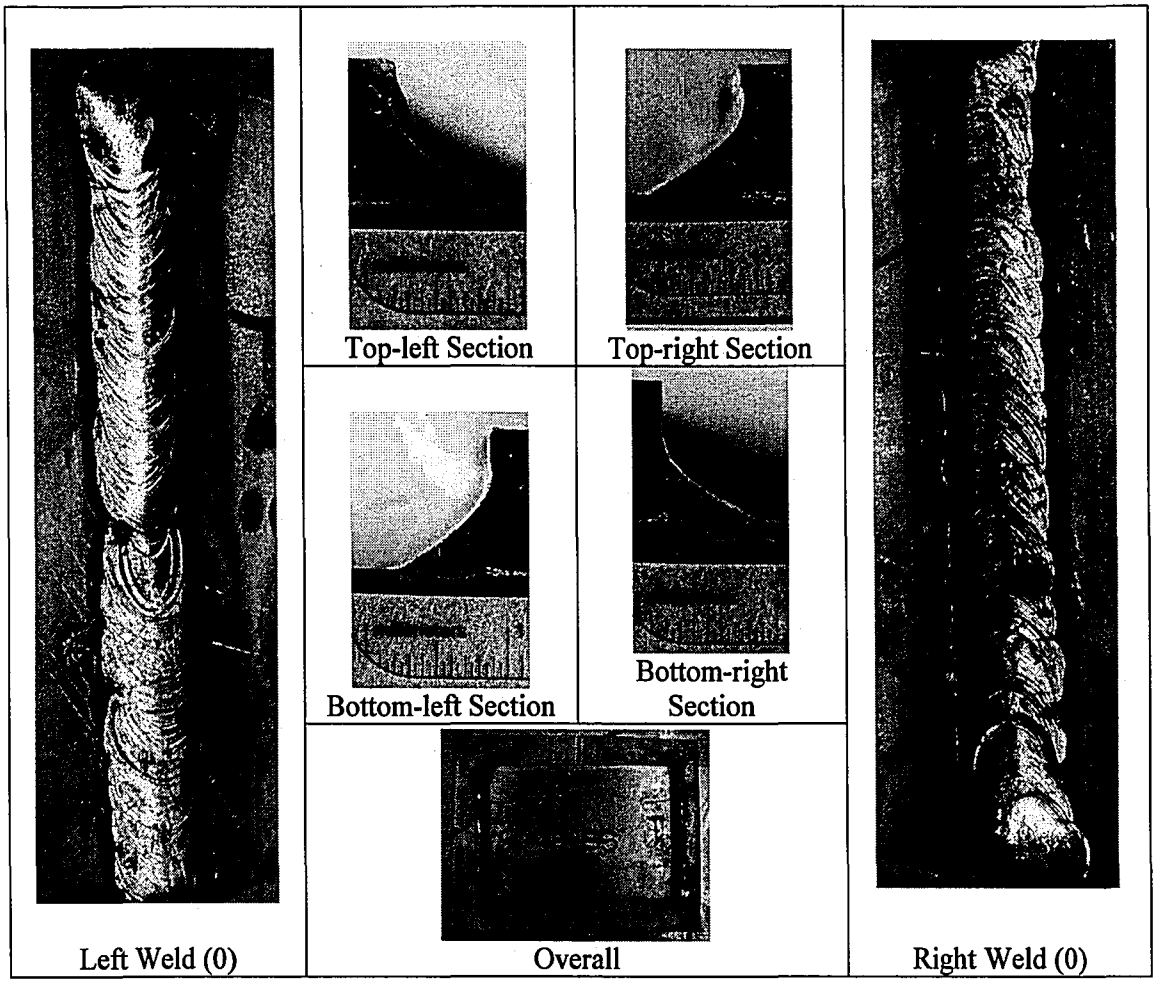

Figure 6.28: Specimen SS-95

6.24.1 Visual Observation Summary

Both welds showed some slight rippling in profile but had no other observed discontinuities. The top-right section had severe skew and curve toward its vertical leg, as well as a root inclusion (.035-in.). The sections were all somewhat concave, with the bottom-right, bottom-left, and top-left section also having root slag inclusions (.019-in., .008-in., .035-in.). Relatively smooth undercut was observed in the top-right and top-left sections (.011-in., .012-in.). All sections except the bottom-right section met the 3/16-in. profile requirements.

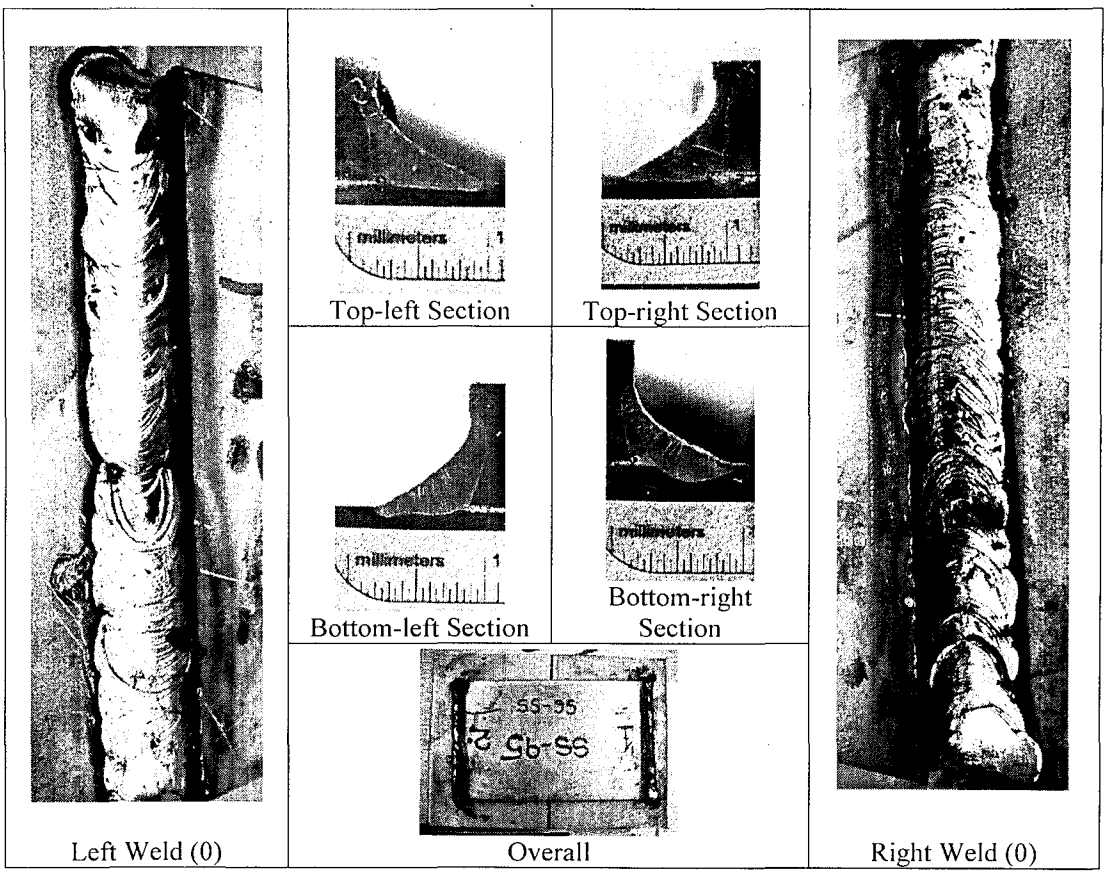

Figure 6.28: Specimen SS-95

6.24.1 Visual Observation Summary

Both welds showed some slight rippling in profile but had no other observed discontinuities. The top-right section had severe skew and curve toward its vertical leg, as well as a root inclusion (.035-in.). The sections were all somewhat concave, with the bottom-right, bottom-left, and top-left section also having root slag inclusions (.019-in., .008-in., .035-in.). Relatively smooth undercut was observed in the top-right and top-left sections (.011-in., .012-in.). All sections except the bottom-right section met the 3/16-in. profile requirements.

6.25 Specimen SS-96: -10°F, Surface Wet, No Wind

This specimen was subjected to environmental conditions in the environmental chamber at the time of welding. The specific conditions for the weld are detailed in Table 6-24.

Table 6-24: Environmental Conditions – Specimen SS-96

Specimen: SS-96	Air Temp.	Concrete Temp.	Steel Temp.	Rel. Humidity	Wind Speed
	°F	°F	°F	%RH	[mph]
Nominal Values	-10	-10	-10	Surface Wet	0
Measured Values	-6.2	5.0	-2.0	99.9/Surf. Wet	0

The welded specimen is shown in Figure 6.29. Photographs of each of the two welds are presented along with an overview photo of the entire specimen. Sections were taken at four locations from the specimen and polished to examine the quality of the weld. These photos are also included.

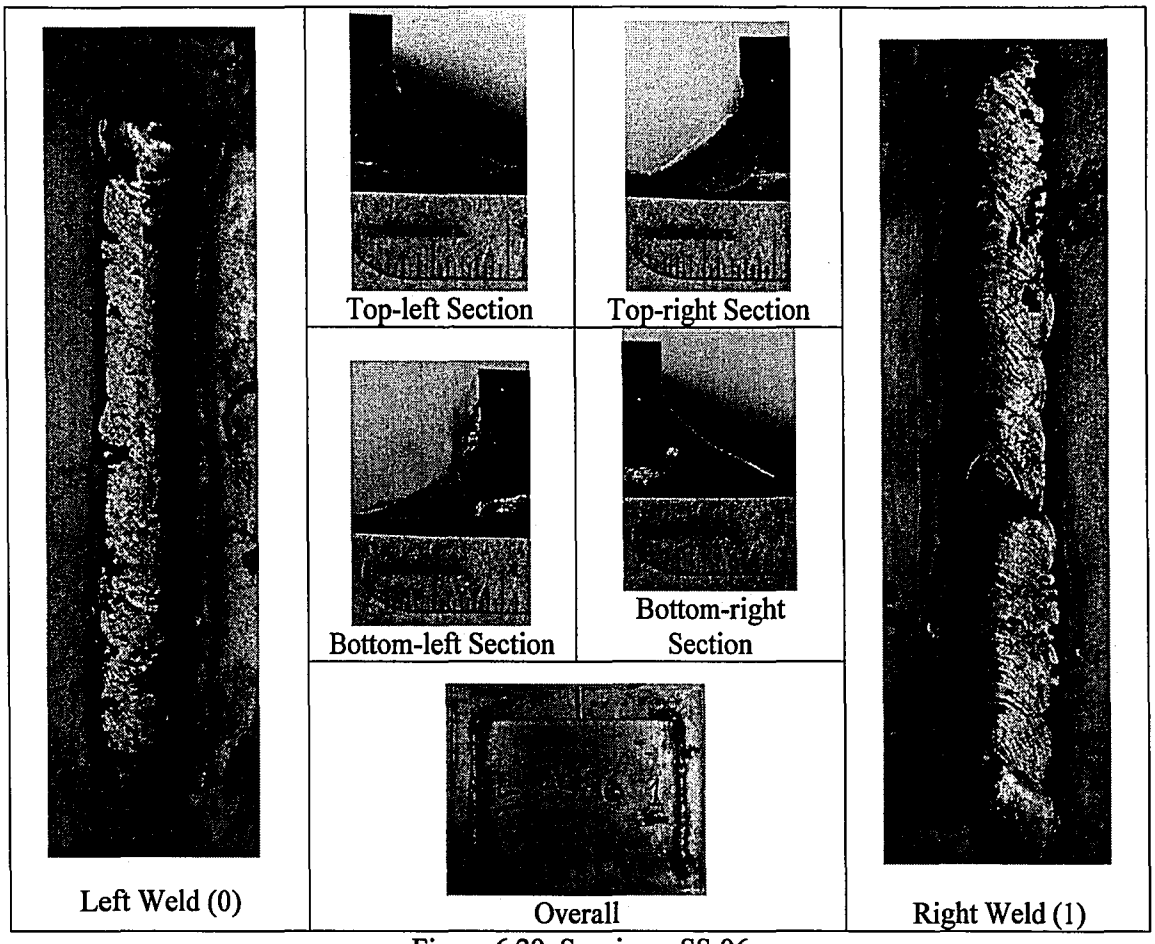

Figure 6.29: Specimen SS-96

6.25.1 Visual Observation Summary

Both welds exhibited significant surface porosity. The right weld had five surface pores along its length (.043-in., .034-in., .046-in., .046-in., .048-in.) and the left weld had four (.047-in., .047-in., .047-in., .066-in.) clumped at its end. In addition, the left weld had some undercut. Two significant slag inclusions (.034-in., .032-in.) were observed in the bottom-right section, and a small root inclusion was observed in the top-left section (.014-in.). The top-right section exhibited undercut in the amount of approximately .016-in. All sections were somewhat concave in nature, and the top-right section did not meet the 3/16-in. profile requirements.

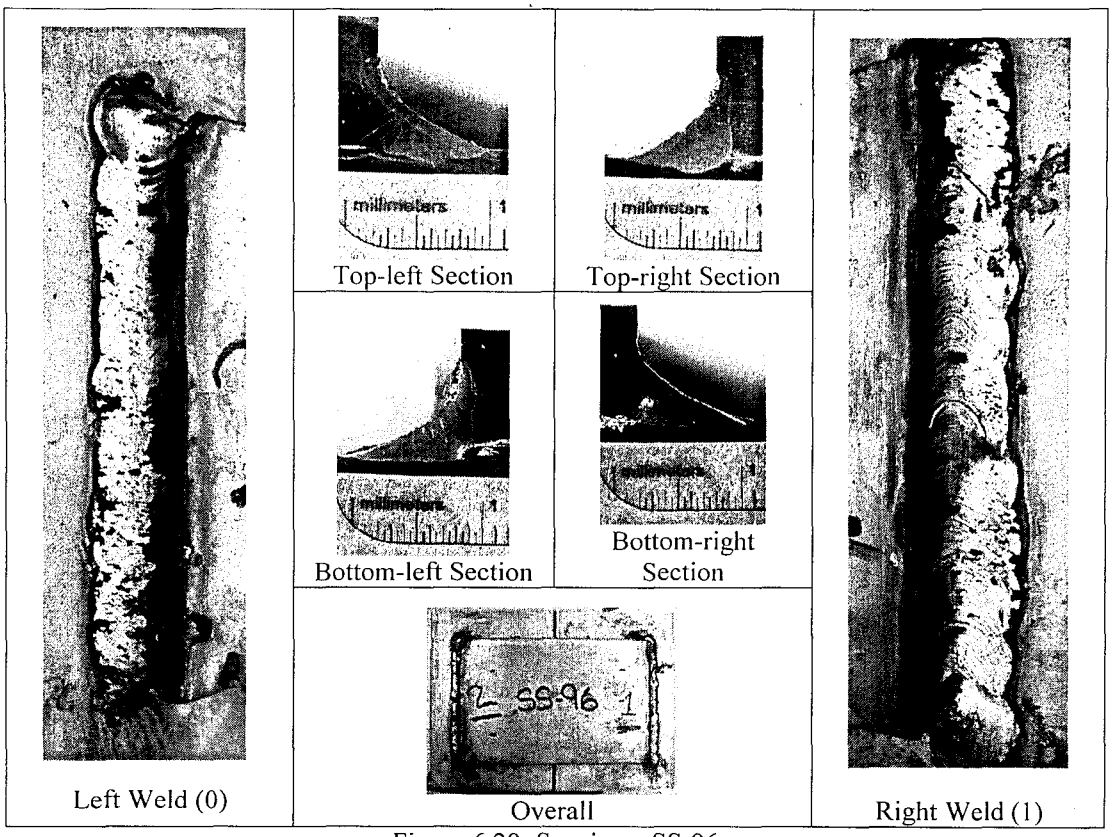

Figure 6.29: Specimen SS-96

6.25.1 Visual Observation Summary

Both welds exhibited significant surface porosity. The right weld had five surface pores along its length (.043-in., .034-in., .046-in., .046-in., .048-in.) and the left weld had four (.047-in., .047-in., .047-in., .066-in.) clumped at its end. In addition, the left weld had some undercut. Two significant slag inclusions (.034-in., .032-in.) were observed in the bottom-right section, and a small root inclusion was observed in the top-left section (.014-in.). The top-right section exhibited undercut in the amount of approximately .016-in. All sections were somewhat concave in nature, and the top-right section did not meet the 3/16-in. profile requirements.

6.26 Specimen SS-4HR(100): Warm, High Humidity, No Wind, 4 hr. electrode exposure

This specimen was subjected to environmental conditions in the environmental chamber at the time of welding. The electrodes were exposed to the chamber's ambient conditions (~95%RH) for approximately four hours prior to welding. The specific conditions for the weld are detailed in Table 6-25.

Table 6-25: Environmental Conditions – Specimen SS-4HR(100)

Specimen: SS-4HR(100)	Air Temp.	Concrete Temp.	Steel Temp.	Rel. Humidity	Wind Speed
	°F	°F	°F	%RH	[mph]
Nominal Values	71	71	71	95	0
Measured Values	71	72	73	96.7	0

The welded specimen is shown in Figure 6.30. Photographs of each of the two welds are presented along with an overview photo of the entire specimen. Sections were taken at four locations from the specimen and polished to examine the quality of the weld. These photos are also included.

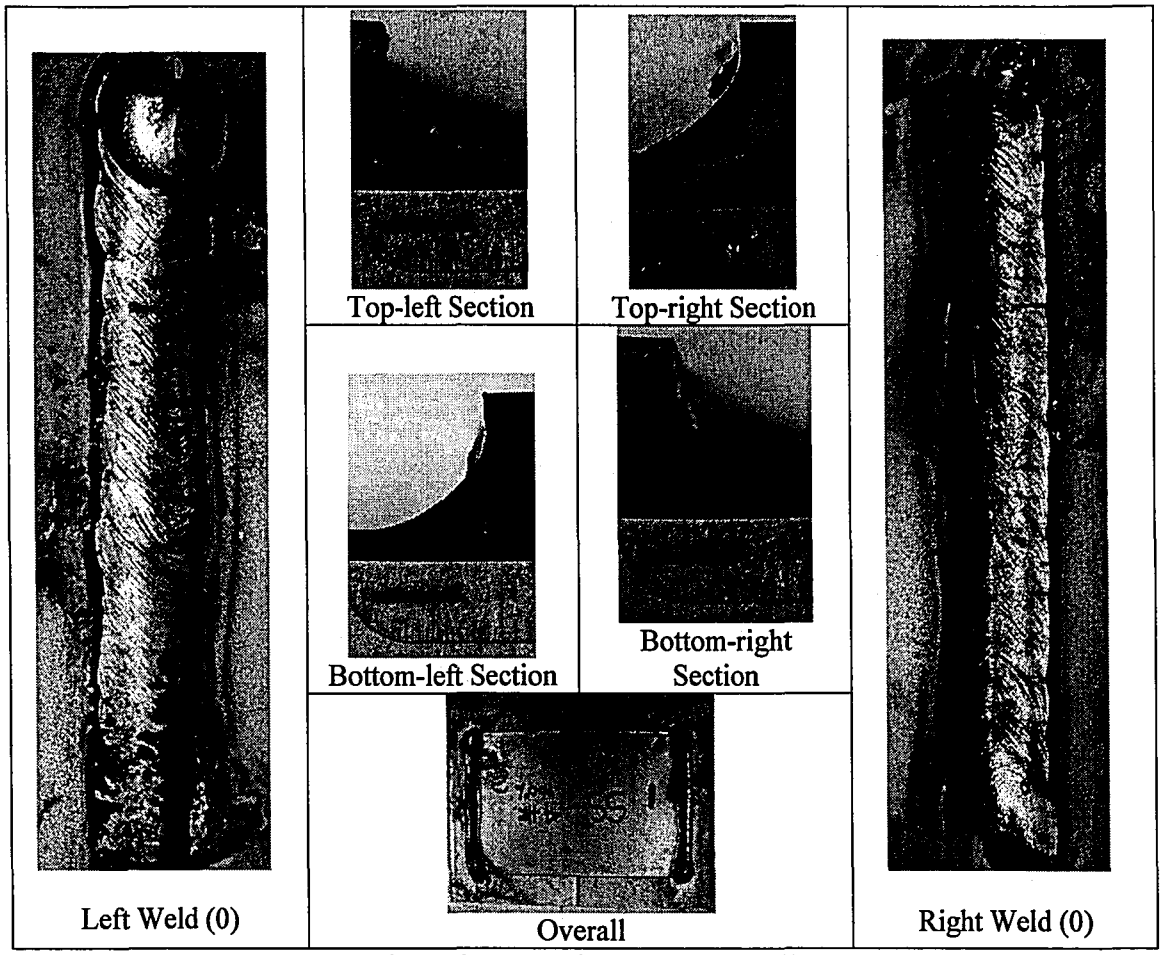

Figure 6.30: Specimen SS-4HR(100)

6.26.1 Visual Observation Summary

The right weld had one surface pore (.043-in.) at its beginning and a small amount of edge-melt at its end, while the left weld had a similarly small amount of edge-melt at its end and one surface pore (.044-in.). The top-right, bottom-left, and top-left sections had small root inclusions (.011-in., .007-in., .025-in.). All sections had a concave profile with a small throat, and all but the bottom-left section met the 3/16-in. profile requirements.

6.27 Specimen SS-(1/4)35: Warm, High Humidity, 35 mph Wind, ¼-in.Profile

This specimen was subjected to environmental conditions in the environmental chamber at the time of welding. The specific conditions for the weld are detailed in Table 6-26. The same 1/8-

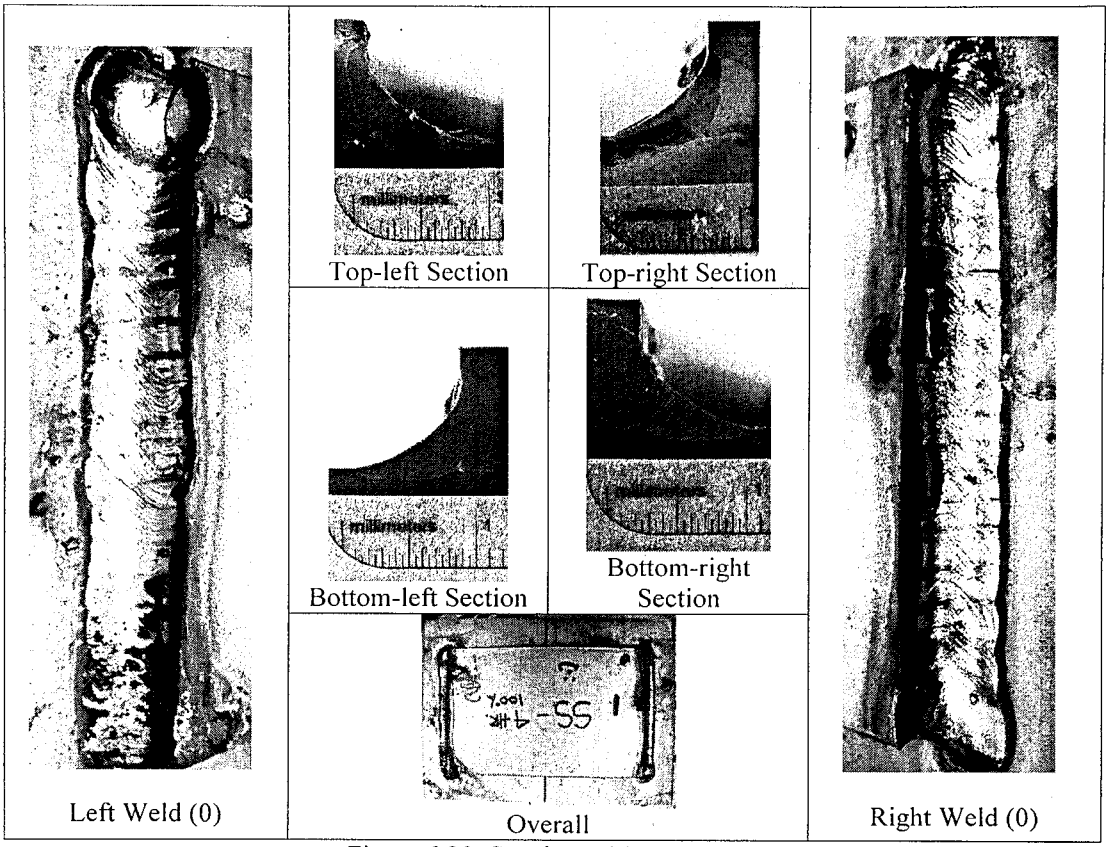

Figure 6.30: Specimen SS-4HR(100)

6.26.1 Visual Observation Summary

The right weld had one surface pore (.043-in.) at its beginning and a small amount of edge-melt at its end, while the left weld had a similarly small amount of edge-melt at its end and one surface pore (.044-in.). The top-right, bottom-left, and top-left sections had small root inclusions (.011-in., .007-in., .025-in.). All sections had a concave profile with a small throat, and all but the bottom-left section met the 3/16-in. profile requirements.

6.27 Specimen SS-(1/4)35: Warm, High Humidity, 35 mph Wind, ¼-in.Profile

This specimen was subjected to environmental conditions in the environmental chamber at the time of welding. The specific conditions for the weld are detailed in Table 6-26. The same 1/8-

in. electrode used for the stainless specimens was used here but travel speed was slowed to attempt to provide a full ¼-in. profile.

Table 6-26: Environmental conditions – Specimen SS-(1/4)35					
Specimen: SS-(1/4)35	Air Temp.	Concrete Temp.	Steel Temp.	Rel. Humidity	Wind Speed
	°F	°F	°F	%RH	[mph]
Nominal Values	71	71	71	95	35
Measured Values	70	72	73	94.6	32

The welded specimen is shown in Figure 6.31. Photographs of each of the two welds are presented along with an overview photo of the entire specimen. Sections were taken at four locations from the specimen and polished to examine the quality of the weld. These photos are also included.

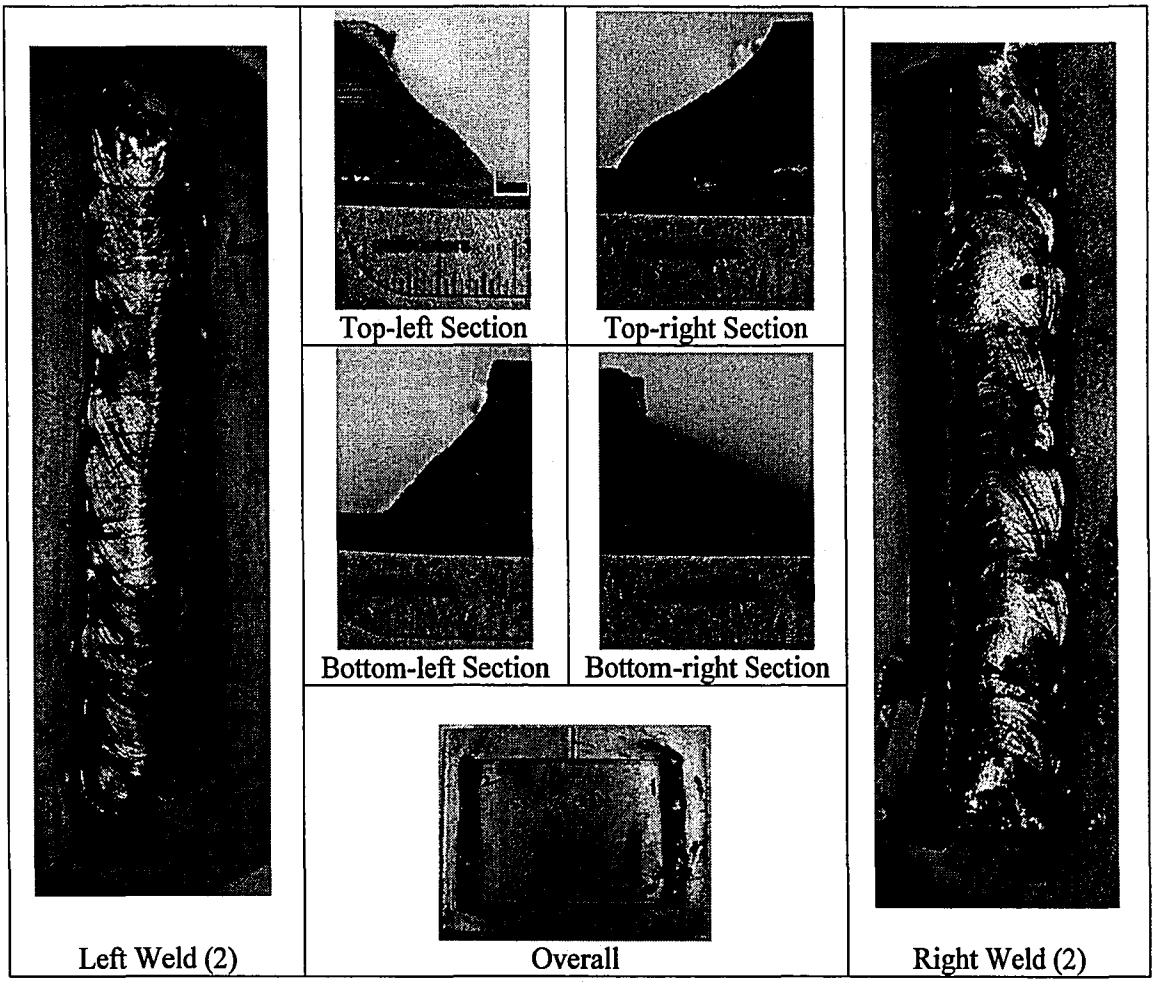

Figure 6.31: Specimen SS-(1/4)35

6.27.1 Visual Observation Summary

Both welds had some edge melt and erratic size changes along their length. The top-right section displayed a relatively large slag inclusion (.106-in.), and deep root penetration. The bottom-left and top-left sections had large slag inclusions (.093-in., .150-in.) at their roots (with a relatively large gap between the base plate and cover plate), and all sections had significant skew toward and curvature in their vertical legs. The bottom-right section had a small inclusion at the root (.027-in.). All sections except the top-right met the 3/16-in. profile requirements, and the bottom-right and bottom-left sections met the 1/4-in. profile requirements. However, due to

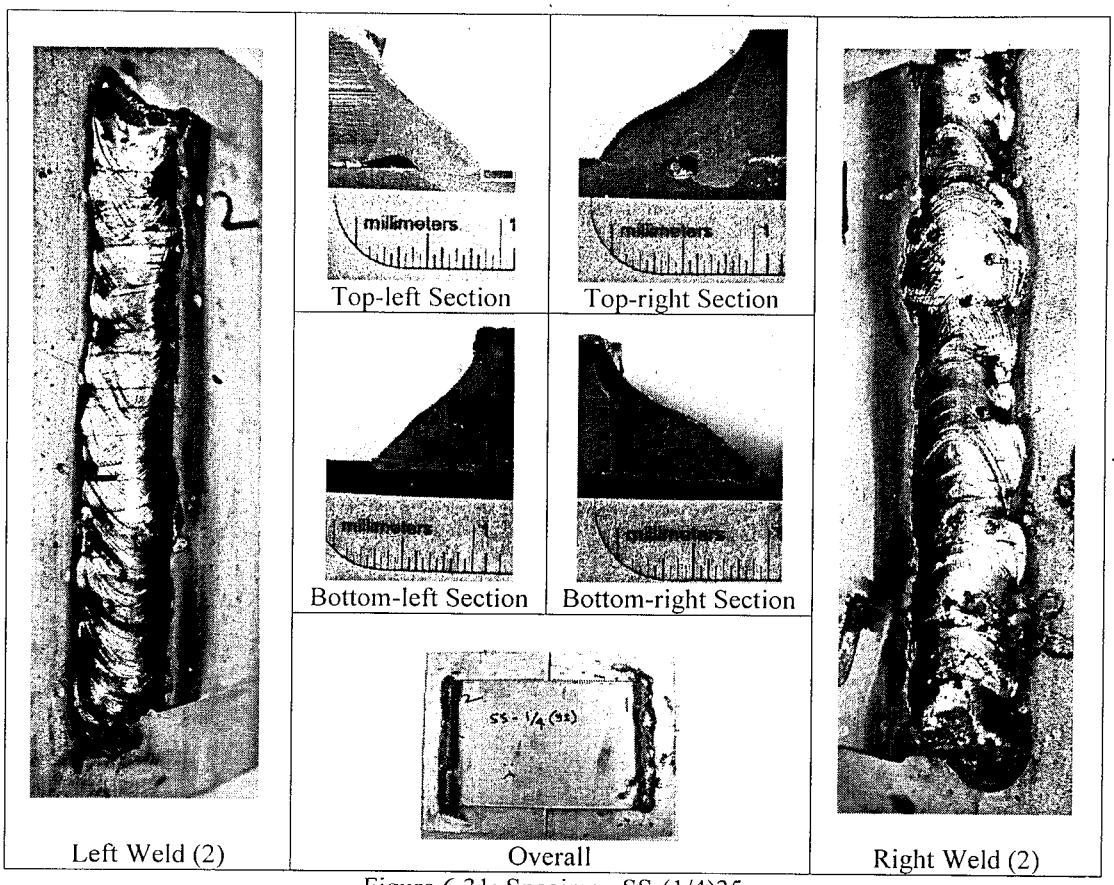

Figure 6.31: Specimen SS-(1/4)35

6.27.1 Visual Observation Summary

Both welds had some edge melt and erratic size changes along their length. The top-right section displayed a relatively large slag inclusion (.106-in.), and deep root penetration. The bottom-left and top-left sections had large slag inclusions (.093-in., .150-in.) at their roots (with a relatively large gap between the base plate and cover plate), and all sections had significant skew toward and curvature in their vertical legs. The bottom-right section had a small inclusion at the root (.027-in.). All sections except the top-right met the 3/16-in. profile requirements, and the bottom-right and bottom-left sections met the 1/4-in. profile requirements. However, due to

extreme curvature and skew, the top-right section did not actually meet the 1/4-in. profile requirements.

6.27.2 Microscopy Observation Summary

Several of the stainless weld cross-sections exhibited thousands of small round-shaped inclusions that often formed clusters, as was the case in the top-left section of Specimen SS-(1/4)35 at the toe of the weld (Figure 6.32). In this case, the minute inclusions formed what appeared to be an arc-shaped line protruding from the toe into the weld metal.

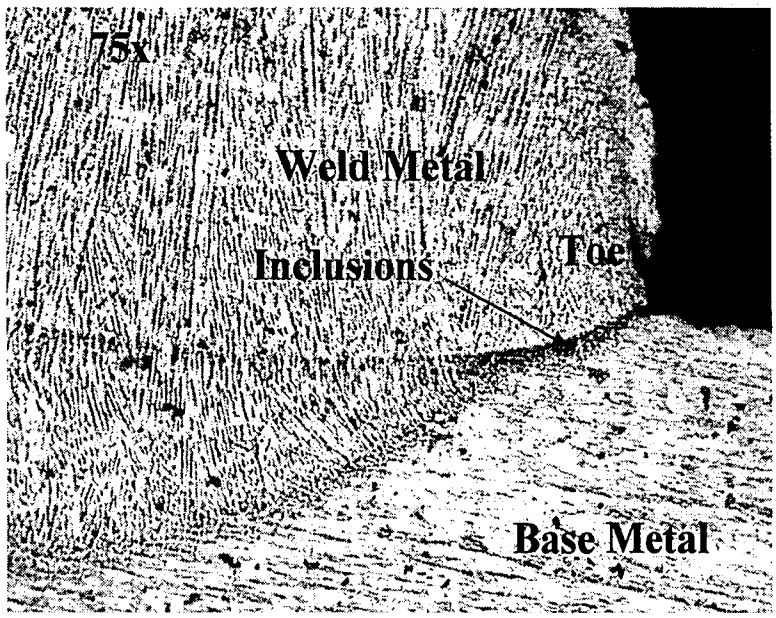

Figure 6.32: Collection of Small Inclusions-Specimen (1/4)35, Top-left Section

6.28 Specimen SS-(1/4)0: Warm, Moderate Humidity, No Wind, ¼-in. Profile

This specimen was subjected to the environmental conditions detailed in Table 6-27 at the time of welding. The same 1/8-in. electrode used for the stainless specimens was used here but travel speed was slowed to attempt to provide a full ¼-in. profile.

Table 6-27: Environmental conditions – Specimen SS-(1/4)0					
Specimen: SS-(1/4)0	Air Temp.	Concrete Temp.	Steel Temp.	Rel. Humidity	Wind Speed
	°F	°F	°F	%RH	[mph]
Nominal Values	71	71	71	50%	0
Measured Values	75	80	78	45.4	0

The welded specimen is shown in Figure 6.33. Photographs of each of the two welds are presented along with an overview photo of the entire specimen. Sections were taken at four locations from the specimen and polished to examine the quality of the weld. These photos are also included.

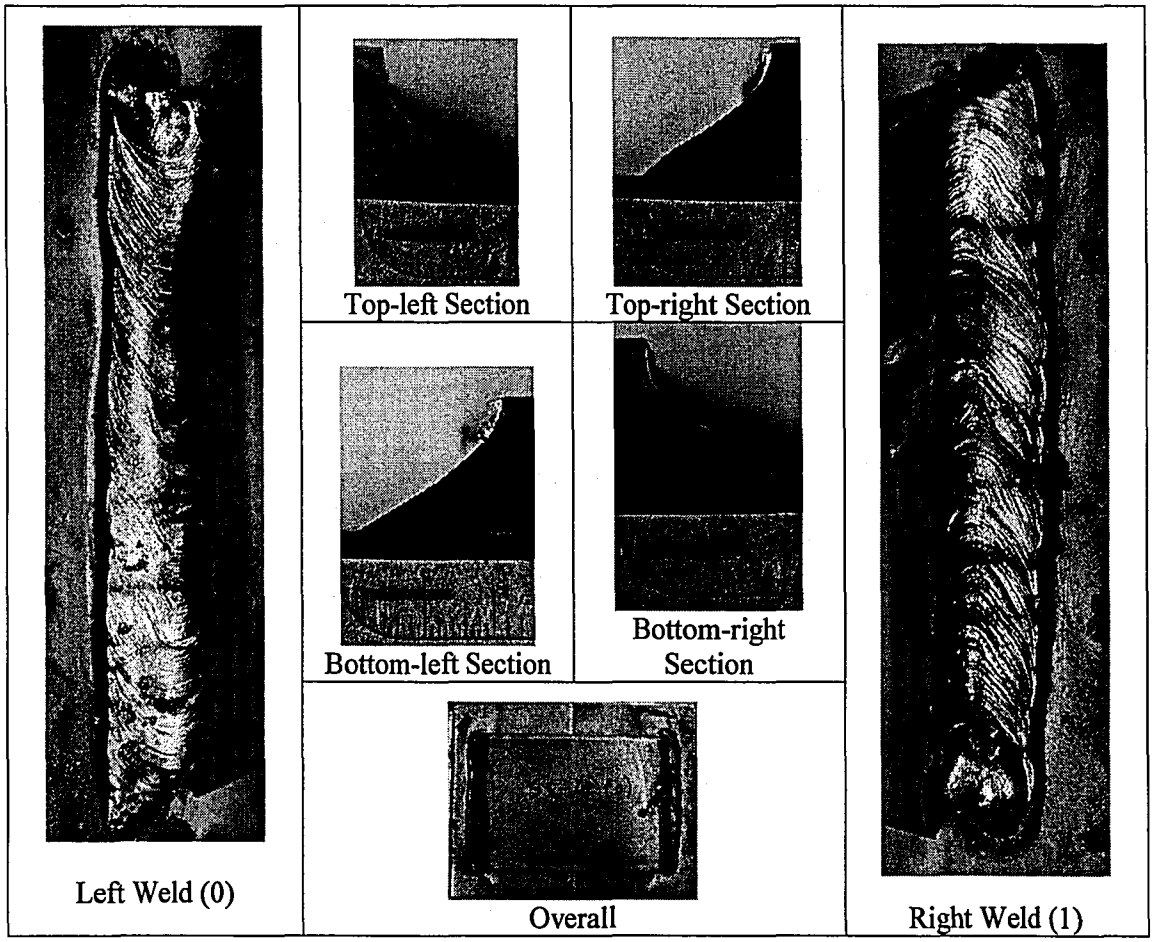

Figure 6.33: Specimen SS-(1/4)0

Table 6-27: Environmental conditions – Specimen SS-(1/4)0					
Specimen: SS-(1/4)0	Air Temp.	Concrete Temp.	Steel Temp.	Rel. Humidity	Wind Speed
	°F	°F	°F	%RH	[mph]
Nominal Values	71	71	71	50%	0
Measured Values	75	80	78	45.4	0

The welded specimen is shown in Figure 6.33. Photographs of each of the two welds are presented along with an overview photo of the entire specimen. Sections were taken at four locations from the specimen and polished to examine the quality of the weld. These photos are also included.

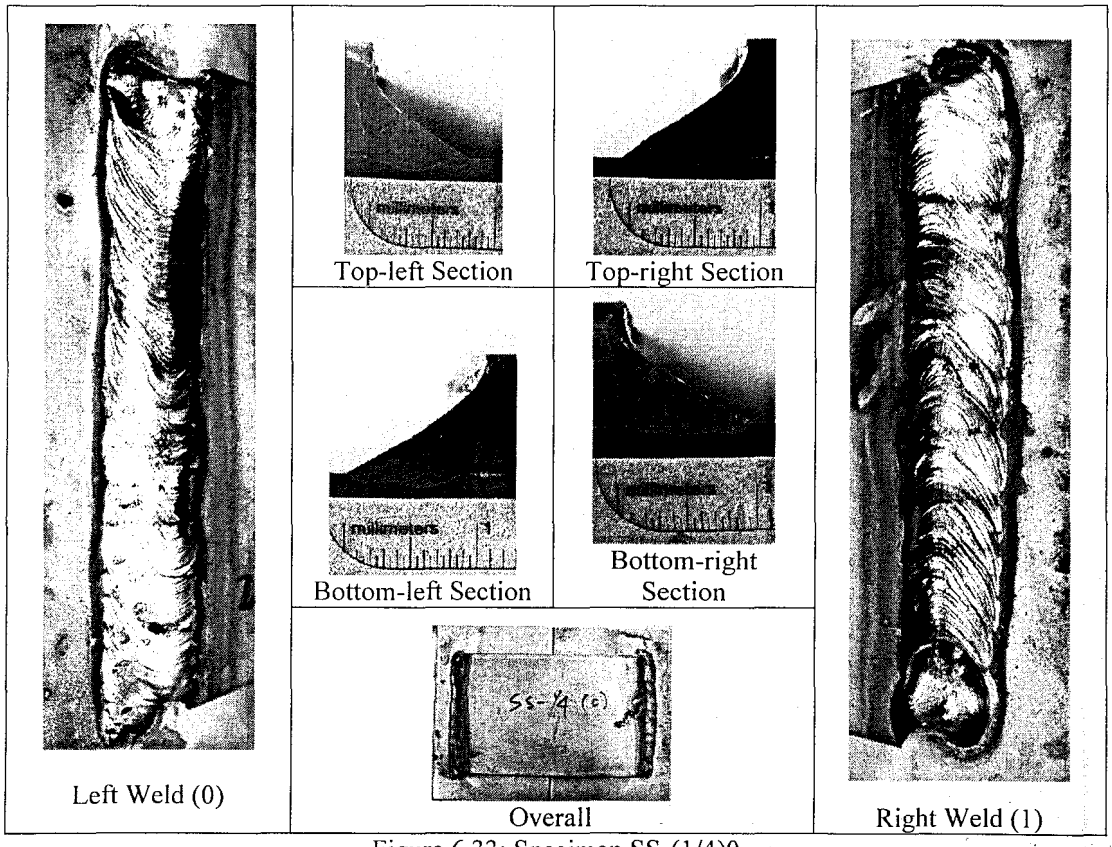

Figure 6.33: Specimen SS-(1/4)0

6.28.1 Visual Observation Summary

The right weld had slight edge-melt along its length but was otherwise free from notable discontinuities. The left weld had one large surface pore at its beginning (.070-in.) and edge-melt along its length. The top-right, bottom-right, and bottom-left profiles exhibited skew to their vertical legs, and all sections had root inclusions, with their largest dimensions listed as follows, beginning with the top-right and moving clockwise (.042-in., .026-in., .031-in., .009-in.). All sections met the 3/16-in. profile requirements, but the bottom-right, bottom-left, and top-left sections did not actually meet the full 1/4-in. profile requirements.

7 Discussion of Phase 1 Results

A discussion of the Phase 1 test results is presented in this chapter. Possible causes of the various observed discontinuities are suggested. The relationships between the environmental parameters and the discontinuities observed are also summarized in graphical form.

7.1 A36 Phase 1 Results

The Phase 1 specimens welded using the moderate carbon A36 plate material exhibited a broad range of discontinuities. The impact of the environmental conditions (temperature, humidity, wind, surface wetness, and electrode condition) on the welds is discussed with respect to profile, undercut, slag inclusions, porosity, incomplete fusion, and cracking. These are the most widely observed discontinuities which have the greatest impact on the quality of the fillet welds in the present study.

7.1.1 Profile Examination

The acceptability of the profiles was determined using measurements of the weld cross-sections as described in Section 2.4.1. If a weld profile had leg lengths which were too short, insufficient throat dimension, or convexity greater than the 1/8-in. limit, it was deemed unacceptable. The weld profiles, in many cases, were widely varying along the length of the welds, but measurements were taken at only the two locations where the sections were cut. As a result, the profile measurements do not follow clear trends with respect to the wind, temperature, or moisture conditions. However, the impact of environmental conditions on overall observations of profile quality and regularity is clearer.

The inspection method used in the study incorporated a high degree of accuracy through the use of photography and scaled measurements of the weld cross-sections. This method is more accurate than the usual measurements with a fillet weld gage. As a consequence, it appears that

the frequency of unacceptable profiles was greater than would be identified in a field inspection. Based on the criteria used, 48% of the sections taken from A36 welds were acceptable, and the remaining 52% failed to meet the acceptability criteria for profile. This high frequency of unacceptable profiles was also a result of the unusual conditions under which the welds were made. The environmental chamber armholes required the welder to weld in an unnatural position without much flexibility of motion, which can be seen in Figure 7.1.

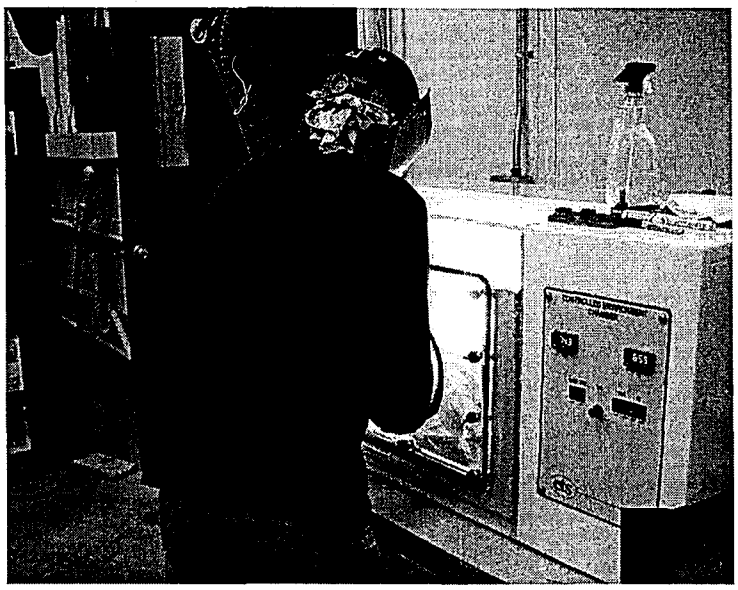

Figure 7.1: Welder Position During Welding Process

The smoke and, in some cases, steam generated by the welding process within the environmental chamber often resulted in poor visibility conditions that were not desirable for welding, coupled with the welder's need to wear a shielded facemask, which further deteriorated visibility when smoke or steam were present. The need for environmental control, however, outweighed the need for a more natural welder position, and the environmental chamber was used because it provided the best means of controlling environmental conditions.

7.1.2 Influence of Wind on Weld Geometry

It was expected that the high wind conditions would have a negative impact on the profile and surface condition of the welds. To compare the weld surface condition and the wind speed, the "profile index" described in Section 3.7.3 was established to quantify the regularity of the weld surface and profile. The profile index is plotted with respect to wind speed for the 14 welds examined in

Figure 7.2

The data in

Figure 7.2 represents three data sets in which temperature and humidity were held constant and wind speed alone was varied. The temperature and humidity for each data set are denoted beside their respective lines of fit. A linear fit is included to show a general trend in the data, but due to the limited amount of data, a mathematical model was not developed. The plot illustrates that higher wind speeds produce poorer profiles.

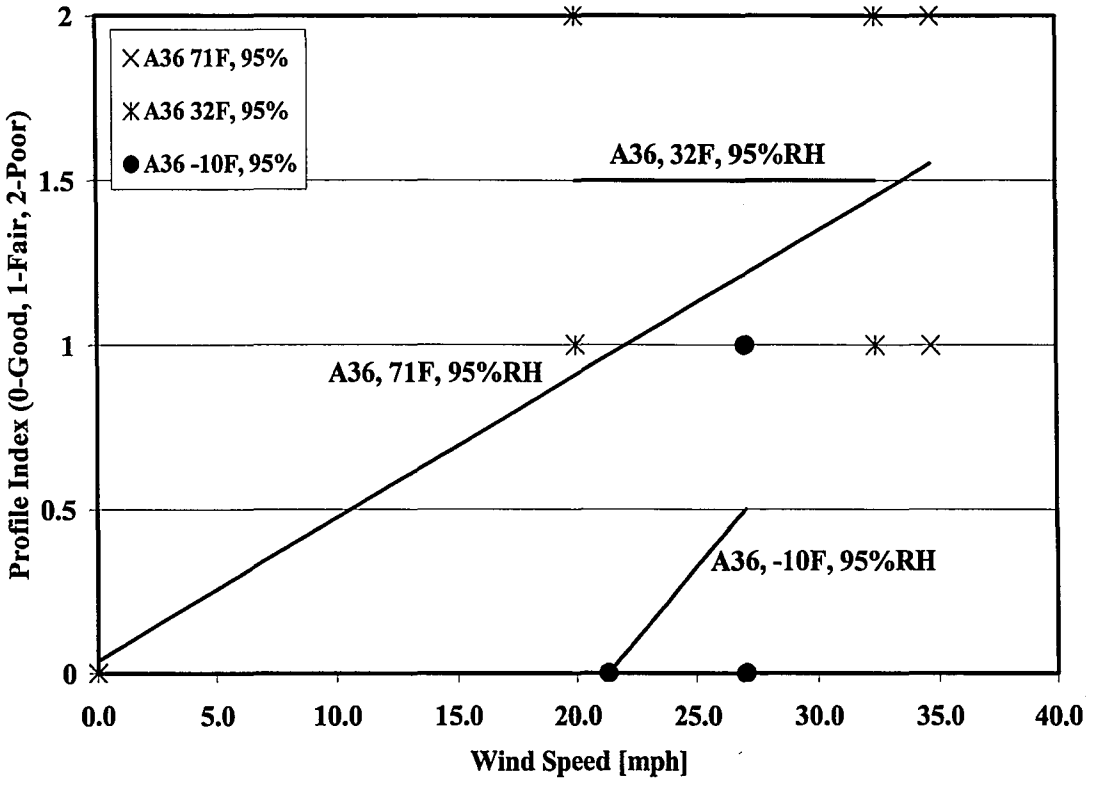

Figure 7.2: Plot of A36 Weld Profile vs. Wind Speed

Examination of the welds suggests that ripples form from the effects of wind on the molten weld pool. In addition, high wind also causes the arc to move erratically. It has been reported[29] in the context of pipeline fabrication that even in cases where internal cracks are present, for example, at the weld root, weld failure can be initiated instead from weld ripples on the weld surface. This underscores the importance of maintaining profile quality.

In all cases, wind was applied perpendicular to the longitudinal axis of the weld. In general, the high wind did not cause any significant concavity in the A36 sections examined. The sensitivity of wind direction on the weld was not examined. Wind in the direction of the welding axis may have a greater effect on the formation of ripples and less of an effect on concavity of the welds. This hypothesis should be verified through additional experimentation.

7.1.3 Undercut

Undercut was measured as the perpendicular distance from the cover plate edge to the deepest point of the notch into the plate edge. AWS D1.1 places a limit of 1/32-in. on undercut. Undercut was only observed in four of the 56 sections (7%) taken from A36 Phase 1 specimens. For one section taken from Specimen 36-8 (78.3°F, 92.4%RH, 0 mph, Surface Wet), the 1/32-in. limit was reached but not exceeded. Undercut formation is largely related to welding technique and was not expected to be impacted by any of the environmental conditions. The results support this hypothesis, as the undercut was not observed for the majority of the weld sections. Severe undercut was observed when welds were made through surface wetness in Specimen 36-8 (78.3°F, 92.4%RH, 0 mph, Surface Wet). The smoke and fog created when welding this specimen hampered the welder's vision of the weld joint. Visibility in the environmental chamber was also poor during the welding of Specimen 36-7 (73.6°F, 97.8%RH, 34.7 mph), in which undercut was also observed. Since undercut is typically caused by incorrect electrode angle, poor weaving technique, excessive current, or too high a travel speed, it is understandable that more severe undercut was observed in the cases where the welder's vision was hampered.

The two sections exhibiting undercut, other than those from the surface wet Specimen 36-8, came from specimens made under high wind speeds. One section from Specimen 36-7, as mentioned above, and one section from Specimen 36-23 (-13.0°F, 100%RH, 27.0 mph) exhibited undercut. From the limited data available, it appears that high wind speed, in addition to creating poor profiles, might contribute to undercut. It is noted that in neither case was the AWS D1.1 limit (1/32-in.) exceeded. The limited data support a general conclusion that high wind speed leads to undercut in fillet welds, however.

7.1.4 Porosity

Porosity was observed and quantified in two ways: (1) surface porosity, or piping porosity which reached the weld surface, was measured as the sum of the diameters of surface pores for a 4-in. long weld, and (2) section porosity was measured as the sum of the diameters of pores in a polished cross-section. The second method examines only two discrete sections of a 4-in. weld, and the likelihood of sectioning through a pore is low. Consequently, the surface porosity is considered to be a better indication of the porosity of a given weld.

It was expected that moisture would have the greatest impact on the occurrence of porosity, as pores are created by the introduction of hydrogen from the dissociation of water during the welding process. Because welds are often made in the field under wet conditions, for example, when welding on plates that have been exposed to rain, it was determined that extra attention should be given to the conditions with surface wetness. In addition to the surface wet condition of Specimen 36-8, six additional tests were conducted that focused on the surface wet condition. For Specimen 36-8, surface wetness was applied by misting the clamped plate assembly at the weld joint prior to welding. For Specimens 36-PC1 to 36-PC6, wetness was applied by wetting the base plate surfaces prior to laying the cover plate on top of the base plates. Once the cover plate was in place, the assembly was further moistened. Water was applied to the surfaces using a misting bottle, and in some cases, pouring liquid water over plates until a pool of water could be seen on plate surfaces.

Two specimens were also fabricated using electrodes exposed to a moist environment for a time duration longer than that allowed by the AWS D1.1 code (9 hours), denoted as Specimens 36-17HR(1) and 36-17HR(2). The moisture in the electrodes resulted from 17 hours of exposure to an environment of roughly 71°F [22°C] and 95% RH. From mass measurements of the moist

electrodes and dry electrodes, the moist electrodes were determined to have collected 4% moisture by weight. AWS D1.1 states, in Section 5.3.2.3, for an alternative atmospheric exposure time of electrodes established by testing, that, "...E70XX or E70XX-X low-hydrogen electrode coverings shall be limited to a maximum moisture content not exceeding 0.4% by weight." The exposure of the electrodes to 17 hours of moist conditions in the environmental control chamber, therefore, produced a moisture content 10 times that allowed by this section of AWS D1.1. This level of moisture in the electrode coating was expected to yield a higher level of porosity than surface wetness as a result of direct introduction of the water into the molten weld pool as the flux coating containing the moisture is consumed during welding.

The total surface porosity of all welds made on A36 plates is plotted in Figure 7.3 against the condition of the plates and electrode used. The area of the light shaded circles in the plot represents the number of occurrences of that level of measured surface porosity. The dark-colored circles with bars represent the average level of surface porosity measured for the indicated plate and electrode condition. A dashed line indicates an interpretation of the AWS D1.1 surface porosity acceptance criteria discussed in this section. The plot includes 24 welds conducted with dry electrodes on a dry surface, 9 welds conducted with dry electrodes on a wet surface, and 4 welds conducted with moist electrodes on a dry surface.

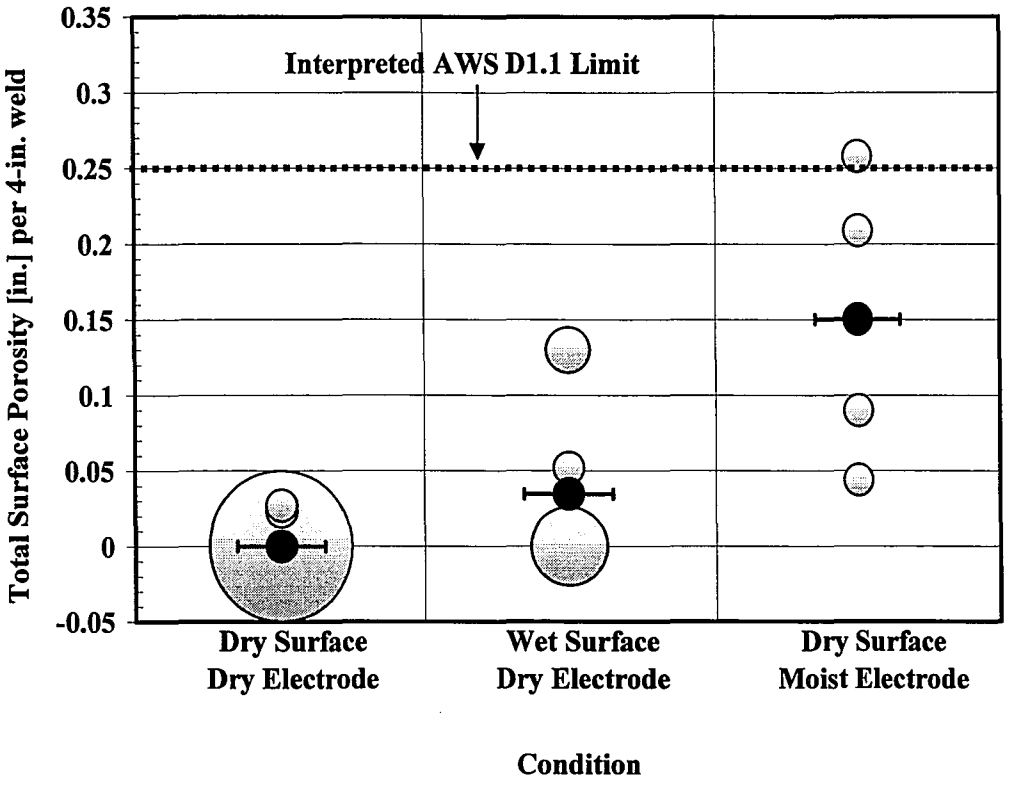

Figure 7.3: Total Surface Porosity vs. Plate and Electrode Condition

The figure shows that the moist electrodes generate the highest level of surface porosity. Interestingly, the surface wet conditions did not generate an appreciable level of surface porosity. The welder observed that the visible surface water was evaporated by the high temperature of the welding arc.

The data on surface porosity is compared in Figure 7.3 to the acceptable level of porosity from AWS D1.1, as discussed in Section 3.7.3. For the case of statically loaded, nontubular connections, the criteria is, "...the sum of the visible piping porosity 1/32 in. [1 mm] or greater in diameter shall not exceed 3/8 in. [10 mm] in any linear inch of weld and shall not exceed 3/4 in. [20 mm] in any 12 in. [300 mm] length of weld." The AWS limits on surface porosity were interpreted for the test specimens by dividing the limit for a 12-in. weld (3/4-in) by 3, resulting in a limit of 1/4-in. in a 4-in. weld. The 1/4-in. in a 4-in. weld length limit represents a

conservative limit for porosity, and it is indicated in Figure 7.3 as a dashed line. All welds satisfy the interpreted AWS D1.1 limit for surface porosity of 1/4-in. in 4-in. of weld, except one weld made with a moist electrode.

Porosity was observed in four cases on section cuts made from the Phase 1 specimens. Three of the four cases were from welds made with moist electrodes, and in one section (from Specimen 36-17HR(1)-72.9°F, 92.0%RH, 0 mph, Moist Electrode) the weld metal cross-sectional area was reduced by 8.74% from porosity. The cross-section porosity of this section exceeded the 5% threshold above which static tensile properties might be affected, according to the discussion of Section 2.4.5 and the studies cited there. This section came from a specimen made with a moist electrode. None of the four sections with porosity had porosity that exceeded the AWS macroetch specimen limit of 1/4-in. of accumulated dimensions of porosity, as discussed in Section 3.7.3. The macroetch test specimen for this criterion is based on a larger 5/16-in. weld.

The results indicate that surface wetness does not appear to generate surface porosity at an unacceptable level, while moist electrodes generated higher but still acceptable (for static loading) levels of porosity. Radiographic examination might, however, further reveal that subsurface pores were generated, some of which were observed in the cross-sectioning process as discussed above. Furthermore, cold cracking is related to the presence of hydrogen and therefore moisture should be avoided. For these reasons, it is recommended that electrodes should be used according to manufacturer guidelines and AWS D1.1 requirements, and surface wetness, whenever practically possible, should be eliminated using a preheating torch. This preheating does not necessarily need to bring the plates to AWS D1.1 prescribed temperatures but should drive off moisture on plate surfaces prior to welding. In cases where preheat is not practical, wetness should be removed by wiping the surface dry with a cloth.

7.1.5 Slag Inclusions

Slag inclusions were measured on each cross-section on which they were found. The inclusions are irregular in shape, so the largest dimension of an inclusion was used to quantify its size. The measurement technique used is consistent with that used to quantify slag inclusions in AWS D1.1. The sum of all the inclusion lengths on each section was recorded. Slag inclusions impact weld strength in proportion to their projected area on the cross-section on which they are found. As discussed in Section 3.7.3, inclusions have been shown to produce stress concentrations less than those produced by pores, regardless of the material comprising the inclusion, although sharp-edged or aligned inclusions could have a greater impact on strength.

Slag inclusions were widely observed in the A36 specimens. It was expected that cold temperatures might increase the presence of slag inclusions in the welds by increasing the solidification rate. This trend was not observed in the test data.

A positive correlation was observed in the total dimension of slag inclusions per cross-section and the wind speed. Figure 7.4 shows this correlation by plotting the sum of the largest dimensions of the slag inclusions on a section (total cross section slag) versus the wind speed. Linear trends of the three data series conducted at 95% relative humidity and three different temperatures (-10°F, 32°F and 71°F) are presented. The 32°F condition (representing 8 sections examined) has the highest correlation followed by the 71°F condition (12 conditions examined). The -10°F condition (8 sections examined) shows no correlation; however, this may be attributed to the limited number of samples examined. The acceptability for an AWS D1.1 macroetch specimen is 1/4-in accumulated maximum dimensions of slag on a 5/16-in. weld, and this threshold is well above the upper bound of the ordinate of Figure 7.4, indicated by the dotted line with upward arrows on the figure.

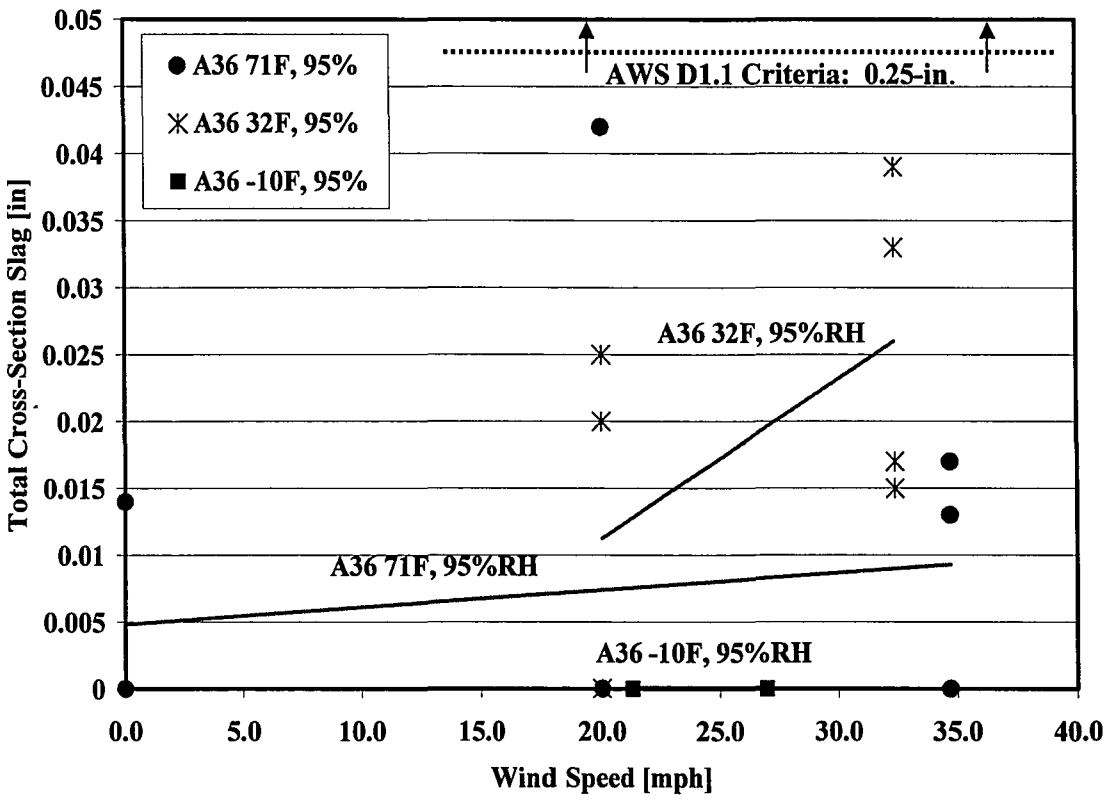

Figure 7.4: Total Cross Section Slag vs. Wind Speed

The majority of the slag was observed at the root of the weld. It is hypothesized that this may be due to one of three effects of wind speed. At high wind speeds, negative pressure may produce suction at the root of the joint, trapping slag. At high wind speeds, the slag may be forced ahead of the weld pool, causing entrapment of slag under the advancing weld bead. At high wind speeds, the welding arc stability decreases, and erratic arc behavior could result in more slag inclusions. Regardless of the cause, the sizes of the inclusions are well below a level (~5% cross-sectional area) that would have an impact on weld strength and are below the AWS D1.1 limit for a 5/16-in. weld, meaning they are conservatively acceptable for a 1/4-in. weld cross-section.

Slag inclusions, in some cases, resulted in local micro-crack formation. Microscopic evaluation of the region around the inclusion indicated that connecting micro-cracks can form between inclusions, an example of which is shown in Figure 7.5.

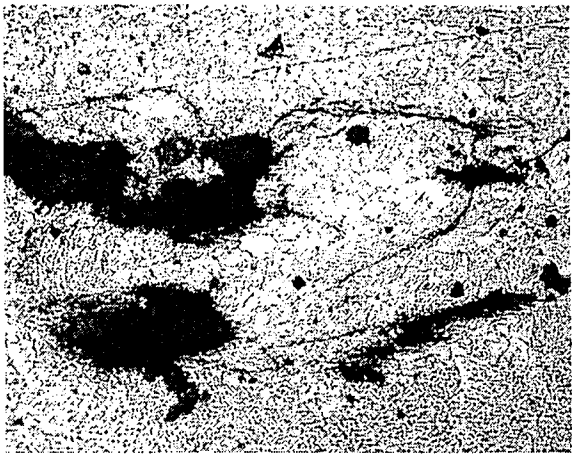

Figure 7.5: Micro-Cracks Connecting Slag in Specimen 36-14

The micro-crack formation is most likely due to the stress concentration which is created by the inclusion. It is uncertain whether the micro-cracks formed due to the inclusions or if preexisting micro-cracks propagated to the inclusions. Regardless, it is observed that even small slag inclusions produce stress risers which can lead to micro-cracking. This issue will be further discussed in Section 7.1.7.

It is noted that to simulate more critical field welding conditions, the existing mill scale or rust was not removed for the specimens prior to welding. In some cases, the amount of mill scale can be substantial, and as a general practice it should be removed by cleaning the plate surfaces to be welded to lower the likelihood of inclusions.

7.1.6 Incomplete Fusion

There were 10 examples of incomplete fusion in sections taken from the A36 Phase 1 specimens. The maximum length of a non-fused segment was approximately 3/64-in, and the

incomplete fusion was observed in sections taken from welds made under high and low temperatures, high and low wind speeds, dry plate surfaces and wet plate surfaces, and moderate and high carbon steel plates. An image of incomplete fusion is presented in Figure 7.6.

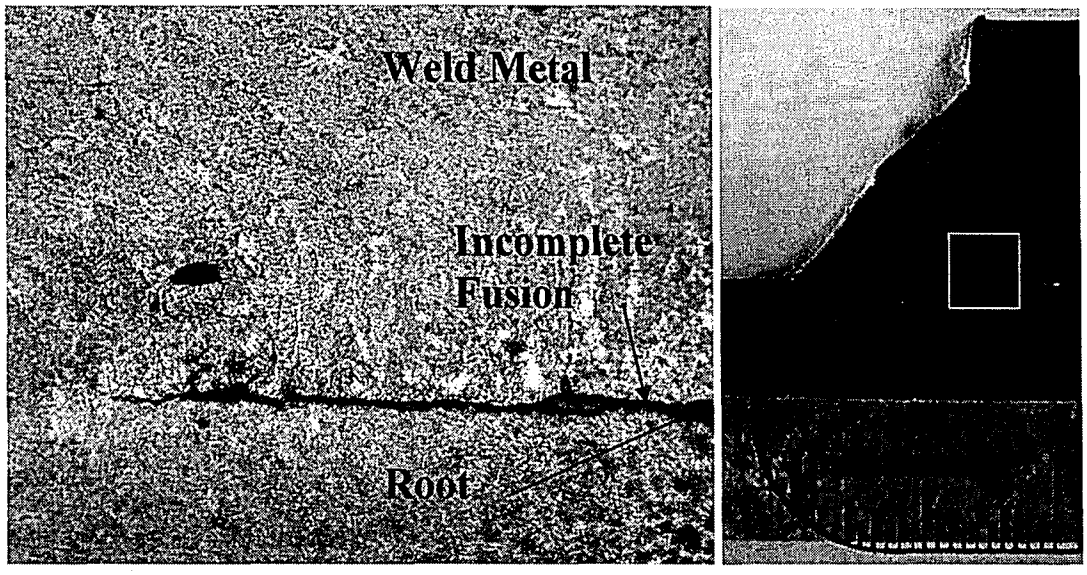

Figure 7.6: Example of Incomplete Fusion in Specimen 36-22

From the results observed, there does not appear to be any correlation between incomplete fusion and environmental conditions. It is possible that the observed incomplete fusion was due to excessive oxides on the plate surfaces which was not removed in order to simulate critical field welding conditions.

7.1.7 Weld Cracking

Visual inspection of the exposed surfaces of completed welds did not reveal any cracks in welds made under any of the environmental conditions considered in the study. Following visual inspection, the welds were sectioned and examined using an optical microscope. Crack-like discontinuities on the order of 1/64-in. to 1/16-in. were found near the root or toe of the weld metal. The part of the weld cross section with the greatest hardness is the coarse-grained HAZ,

incomplete fusion was observed in sections taken from welds made under high and low temperatures, high and low wind speeds, dry plate surfaces and wet plate surfaces, and moderate and high carbon steel plates. An image of incomplete fusion is presented in Figure 7.6.

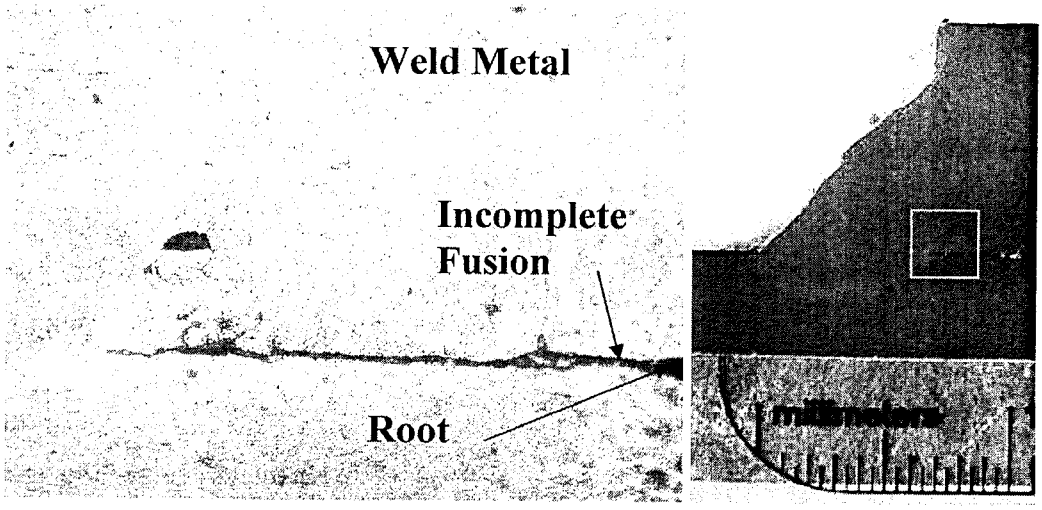

Figure 7.6: Example of Incomplete Fusion in Specimen 36-22

From the results observed, there does not appear to be any correlation between incomplete fusion and environmental conditions. It is possible that the observed incomplete fusion was due to excessive oxides on the plate surfaces which was not removed in order to simulate critical field welding conditions.

7.1.7 Weld Cracking

Visual inspection of the exposed surfaces of completed welds did not reveal any cracks in welds made under any of the environmental conditions considered in the study. Following visual inspection, the welds were sectioned and examined using an optical microscope. Crack-like discontinuities on the order of 1/64-in. to 1/16-in. were found near the root or toe of the weld metal. The part of the weld cross section with the greatest hardness is the coarse-grained HAZ,

the narrow region of the HAZ that borders the weld metal. Crack-like discontinuities were observed adjacent to this region, and cracks were also observed at discontinuities where stress concentrations existed.

As discussed in Section 3.7.3, no cracking of any kind is permitted according to AWS D1.1 because the high level of stress concentration at crack tips can result in premature weld failure. However, as discussed in Section 2.4.6, AWS D1.1 does not prescribe a microscopic examination of cross-sections for cracks. Crack-like discontinuities which would not be detected through simple visual inspection as prescribed in the AWS D1.1 code are termed micro-cracks. The largest crack length for a micro-crack is approximately 1/32-in., and cracks longer than 1/32-in. are termed "cracks".

Root micro-cracking was observed in 15 sections taken from Phase 1 specimens, including 2 sections taken from the porosity-check specimen PC-6. The root micro-cracks were observed in the following: 1 section from 36-1 (72°F, 41%RH, 0 mph wind), 2 sections from 36-8 (78.3°F, Surface Wet, 0 mph wind), 1 section from 36-14 (39°F, 75.5%RH, 20.0 mph wind), 1 section from 36-22 (-5°F, 99.9%RH, 21.3 mph wind), 2 sections from 36-23 (-13°F, 100%RH, 27.0 mph wind, delayed removal), 1 section from 36-17HR(1) (72.9°F, moist electrode, 0 mph wind), 2 sections from 36-C1 (-6°F, 100%RH, 0 mph wind, high carbon plate), 3 sections from 36-C2 (-4°F, 66.7%RH, 0 mph wind, high carbon plate, delayed removal), and 2 sections from 36-PC6 (74.2°F, surface wet, 0 mph wind).

The occurrence of root micro-cracking in the above specimens was *not correlated to specific* temperatures, restraint, wind, or moisture conditions. The observed root micro-cracking was widespread among specimens with no apparent correlation to any specific environmental conditions. The relatively high frequency of root micro-cracks may be a result of the careful

evaluation and high magnification used to microscopically examine the cross-sections. No cracks were observed on weld surfaces prior to destructive evaluation. Micro-cracks were identified only after sectioning, polishing and observing with a magnification of 75x or greater under an optical microscope.

The only root or toe crack detectable by visual examination (that is, with a length longer than approximately 1/32-in.) was the vertical root crack found in Specimen 36-7 (73.6°F, 97.8%RH, 34.7 mph wind), which is depicted in Figure 7.7. The length of the crack is approximately 1/16-in. Because the crack formed along the boundary between the HAZ and weld metal and formed vertically as opposed to the typical 45 degree inclination of hot cracks at the weld root, it is most-likely a cold crack. During cooling, hydrogen may have pooled in the areas of the discontinuities shown in Figure 7.7 and caused higher local hardnesses resulting in propagation of the crack. Furthermore, the stress concentrations caused by the discontinuities near the crack may have contributed to its propagation.

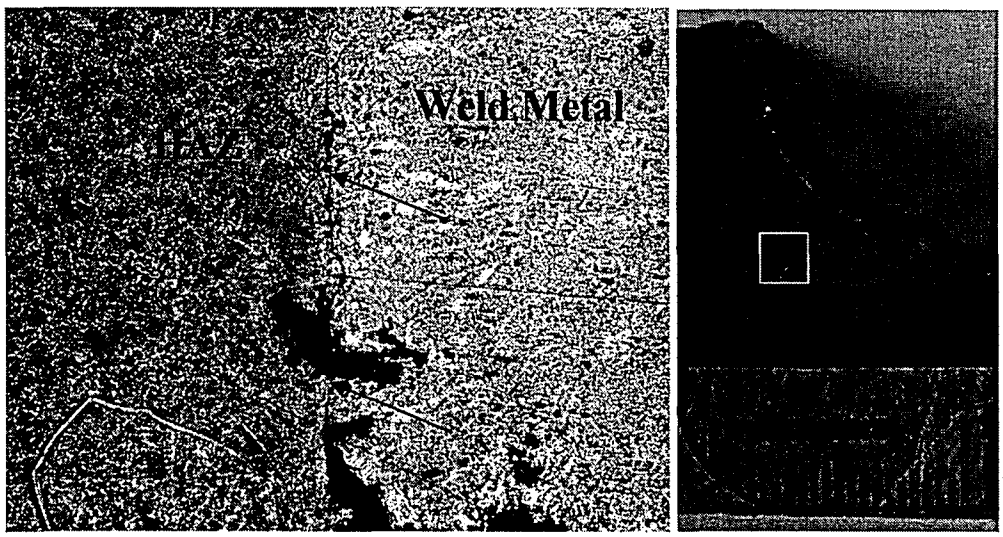

Figure 7.7: Vertical Root Crack in Specimen 36-7

evaluation and high magnification used to microscopically examine the cross-sections. No cracks were observed on weld surfaces prior to destructive evaluation. Micro-cracks were identified only after sectioning, polishing and observing with a magnification of 75x or greater under an optical microscope.

The only root or toe crack detectable by visual examination (that is, with a length longer than approximately 1/32-in.) was the vertical root crack found in Specimen 36-7 (73.6°F, 97.8%RH, 34.7 mph wind), which is depicted in Figure 7.7. The length of the crack is approximately 1/16-in. Because the crack formed along the boundary between the HAZ and weld metal and formed vertically as opposed to the typical 45 degree inclination of hot cracks at the weld root, it is most-likely a cold crack. During cooling, hydrogen may have pooled in the areas of the discontinuities shown in Figure 7.7 and caused higher local hardnesses resulting in propagation of the crack. Furthermore, the stress concentrations caused by the discontinuities near the crack may have contributed to its propagation.

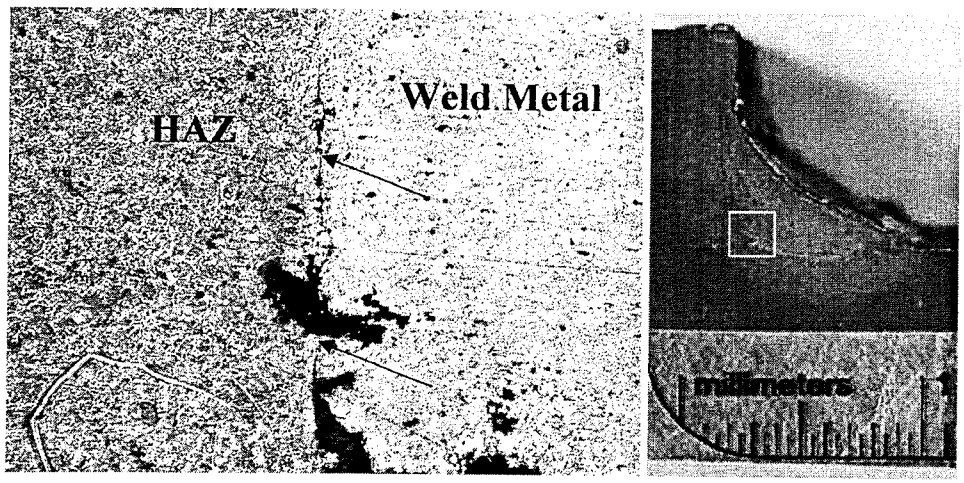

Figure 7.7: Vertical Root Crack in Specimen 36-7

To investigate the issue of hardness and its relationship to cracking, a sample of weld sections were measured to determine their hardness in locations throughout the weld metal and HAZ, as described in Section 4.18. One of the major contributors to cracking, a susceptible microstructure, is largely related to the carbon content and carbon equivalent of the steel. It would be expected that the higher carbon content and carbon equivalent of the steel plates used in Specimens 36-C1 and 36-C2 would result in a harder HAZ with a greater likelihood of cracking. The results of the hardness testing, shown in Figure 4.47, show that the higher carbon specimens did have a higher hardness than the welds made on moderate carbon steel plate. The increase in hardness, however, was minimal (10% higher peak hardness for high carbon steel specimens versus moderate carbon specimens). This is likely a result of using thin plate (3/8-in.), since a thicker plate would provide a more rapid cooling rate due to its greater thermal mass, and higher cooling rates tend to produce more martensite in the HAZ. In addition, a thicker plate would provide greater restraint to the weld shrinkage, further contributing to cracking.

Two specimens, 36-C1 (-6.0°F, 100%RH, 0 mph) and 36-C2 (-4.0°F, 66.7%RH, 0 mph) were welded using high carbon A36 steel, and 5 of the 8 sections from these two specimens were observed to have root or toe micro-cracks. It is possible that micro-cracks formed in areas where the cooling rate was sufficient to form martensite locally, while the hardness measurements discussed above were taken at a location of lower hardness. Three of the four of the sections taken from Specimen 36-C2 exhibited some form of micro-cracking. These micro-cracks may have been influenced by residual stresses which developed as the specimen was restrained in the concrete block for at least 24 hours prior to removal. The condition of high carbon content in the base metal and a high level of restraint often leads to cracking. The potential for cracking would be further increased if hydrogen were introduced as a result of

moisture on the plates or in the electrode. This worst case of high carbon A36 steel, restraint, and the presence of added moisture was not studied. The uncertainty of the carbon level in the plates being welded in precast applications should be considered when interpreting the results of the study.

The sensitivity of crack formation to surface wetness on crack formation was examined in Specimen 36-PC6. This specimen was fabricated with surface water present at a temperature of 74.2°F, a humidity of 17.6%RH and under a 0 mph wind condition. The specimen was restrained for 24 hours in the concrete test block prior to removal. Four sections were taken from the specimen, and two of them were observed to have micro-cracks. One of the sections had micro-cracks through a slag inclusion near the root. Another section had root micro-cracks, as well as two toe micro-cracks. While it is difficult to make general conclusions from these four sections taken from a single specimen, it appears that the wetness may have an impact on the potential for micro-cracking. This is a reason for not welding through surface wetness, as the introduction of hydrogen from the moisture can result in increased potential for cold cracking (hydrogen-assisted cracking).

The formation of micro-cracking occurred to a greater extent where discontinuities such as inclusions existed. These local discontinuities generate stress concentrations resulting in a micro-crack forming through the inclusion, an example of which is seen in Figure 7.5. Therefore, slag inclusions, even if the inclusions are small and acceptable according to AWS, can indirectly contribute to local micro-cracks. The same is true for other discontinuities, such as porosity or undercut, which can serve as initiation points for cracks or contribute to their formation.

Restraint contributed to the formation of micro-cracks. Only a few specimens were fully restrained for a period of 24 hours in the concrete block. Several specimens were fabricated and removed within 3-5 minutes of welding. A selection of specimens, usually the most critical cases welded on a given day, were left overnight in the fixture. This delayed removal from the fixture restrained thermal shrinkage strains as the welds cooled. Cracks can form as a result of this restraint, especially in the toe area at the HAZ boundary, where shrinkage strains are high. It was, in fact, observed that toe micro-cracks were more likely to form in restrained specimens than unrestrained specimens.

Four of the fourteen Phase 1 A36 specimens examined were restrained for 24 hours or more. There were only two observations of toe micro-cracks in the A36 specimens, but these sections both came from specimens which were restrained. Specimen 36-15 (31.0°F, 100%RH, 32.4 mph wind) and 36-PC6 (74.2°F, 17.6%RH. 0 mph wind, surface wet) were the two specimens exhibiting a toe micro-crack in a polished cross-section.

7.2 A36 Galvanized Phase 1 Results

Four galvanized A36 steel specimens were evaluated. They include:

1. Specimen 36G-25: Base Condition (71°F, 50%RH, Low Wind)
2. Specimen 36G-33(1): 32°F, Low Humidity, Low Wind
3. Specimen 36G-33(2): 32°F, Low Humidity, Low Wind
4. Specimen 36G-17HR: Warm, High Humidity, Low Wind, 17 hr. electrode exposure

The number of galvanized specimens was limited due to excessive amounts of zinc oxide fumes generated during welding through the zinc galvanization. Within the environmental chamber, the smoke developed so densely and rapidly during welding that visibility was obscured,

preventing the creation of a sound weld. To overcome the poor visibility, a ventilation system was utilized to remove the smoke during welding. This required the side door of the chamber to be open during welding, which limited control of the environmental conditions. The "base" condition specimen was welded using the ventilation system in the chamber in order to determine if a satisfactory weld could be produced without removing the zinc coating. Upon examination, this specimen proved satisfactory in terms of weld quality, and it was determined that a number of specimens would be welded outdoors where adequate ventilation could be provided. Welds were made under prevailing ambient conditions which are noted for each specimen. The smoke produced by welding through the zinc coating on the plate is illustrated in Figure 7.8.

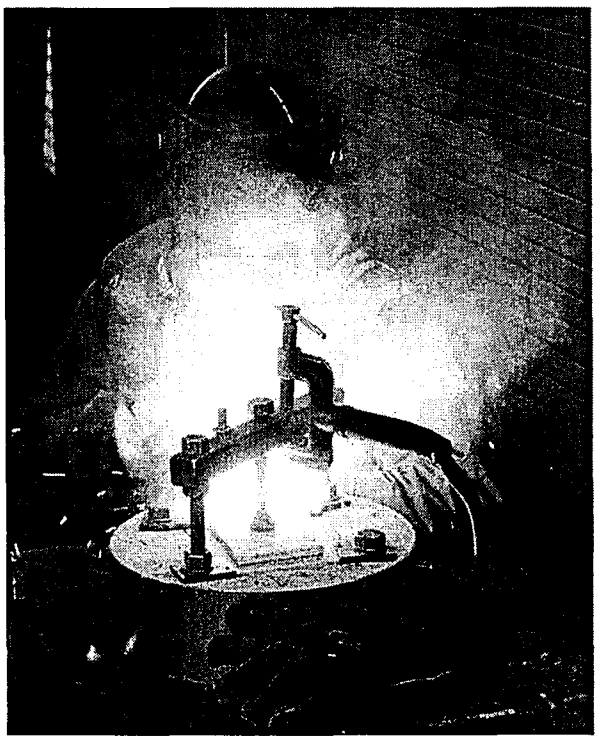

Figure 7.8: Outdoor Welding of Galvanized Steel

Two welds were carried out under the ambient outdoor environmental conditions typical of winter conditions in Pennsylvania. The conditions at the time of welding were approximately 37°F, 30% RH, 0 mph. Two specimens were welded at this time to compare results between the two welds and because the conditions outdoors were sufficiently cold to replicate a set of conditions from the test matrix.

To assess the effect of moist electrodes on the galvanized steel, a specimen was welded using E7018-H4R electrodes which had been exposed to a moist environment for a period of approximately 17 hours, resulting in electrode moisture content of approximately 4.0% by weight. One section taken from this specimen contained a toe crack, and a large hot crack was found at the root of another section, which is further discussed subsequently in this section.

The profiles of the welds made through the galvanized coating tended to have a higher rate of unacceptability than those welded on non-galvanized carbon steel in the study. 14 out of the 16 sections examined, or 87.5%, of the sections failed to meet the profile acceptability criteria described in Section 3.7.3, as compared to 52% of uncoated steel welds. This may be a function of poorer arc stability as a result of welding through the zinc coating.

The welds made through galvanization appeared to be free from porosity both on the weld surfaces and in cross-sections. Only one of the 16 sections exhibited a slag inclusion, and it was of a very small size (0.008-in.). Two of the sections exhibited undercut, and one of the examples of undercut was measured to be approximately 1/32-in., the limit set forth in AWS D1.1. The relative lack of discontinuities in the sections examined indicates that welding through the galvanization may not have a great impact on porosity or slag inclusions. Due to the small sample size, further study into the practice of welding through galvanization and more

thorough non-destructive evaluation (NDE) of such welds is necessary before making such a conclusion.

One problem that arises from welding the galvanized plates is that the plate gap between the base plates and the cover plate appears to promote micro-crack formation at the root of the weld. Because the hot-dip galvanized coating is irregular and creates a plate surface that is not smooth, large plate gaps result. This poor fit between plates produces inclusions or incomplete fusion at the root which can lead to hot micro-cracks like those shown in Figure 7.9 and Figure 7.10.

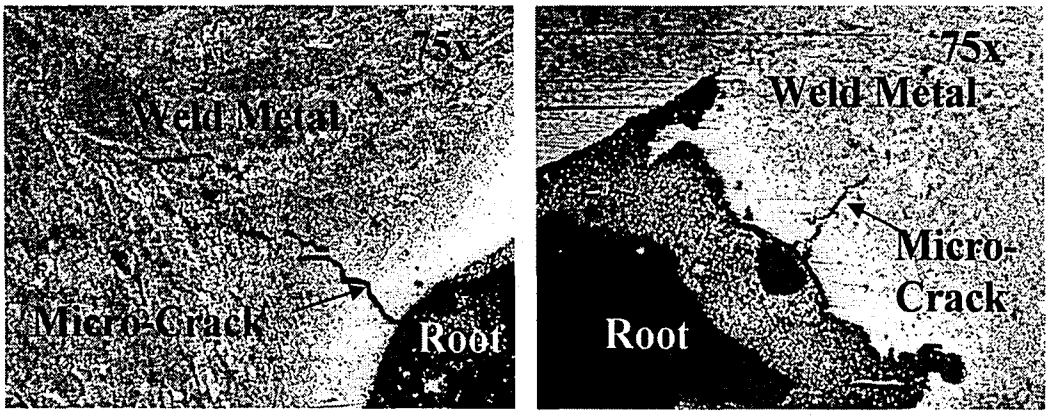

Figure 7.9: Root Gap Micro-cracks in Galvanized Specimens

The only crack that was detected by visual examination unaided by microscopy is the solidification crack found protruding from the root of a section taken from Specimen 36G-17HR (77.3°F, wet electrode, 4 mph wind). The crack, shown in Figure 7.10, is approximately 5/64-in. in length and protrudes from the root of the weld at a 45 degree angle, which suggests that it is a solidification crack caused by restraint of the cooling weld metal surrounding the root area, which cools last in the solidification process.

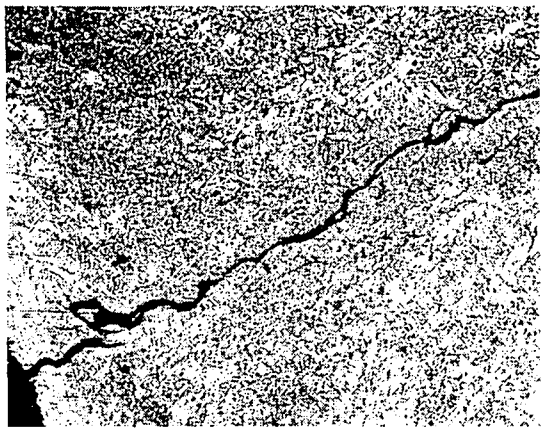

Figure 7.10: Solidification Crack in Specimen 36G-17HR

7.3 Type 304 Stainless Steel Phase 1 Results

The welds produced with the Type 304 Stainless Steel base metal proved to be less sensitive to environmental conditions compared to the welds made with carbon steel. Stainless welds, however, exhibited the same discontinuities as those made on carbon steel, including: profile irregularities, undercut, porosity, slag inclusions, and cracking.

7.3.1 Profile

The profiles of the welds were nearly all concave, and sized at 3/16-in. as a result of the undersized electrode used for the welds, which was a 1/8-in. diameter E308-16 rod. The profile index described in Section 3.7.3 is plotted in Figure 7.11 against wind speed for welds made on stainless steel plate. The three data sets (each representing 20 cross-sections) correspond to data over which temperature and humidity were held constant and wind speed was independently varied from 0 mph to 35 mph. The temperature and humidity for each data set are noted beside their respective lines of fit, which are provided to depict a general trend in data. Comparing Figure 7.11 to the similar figure for the welds made on A36 steel (

Figure 7.2), it can be seen that the weld profile is generally better for the stainless steel welds. It is noted that in the case of the welds made at roughly -10°F [-23°F] and 95% humidity, the profile appears to have improved with elevated wind speeds. However, additional tests are needed to assess this unexpected result, which may be due to an insufficient number of tests.

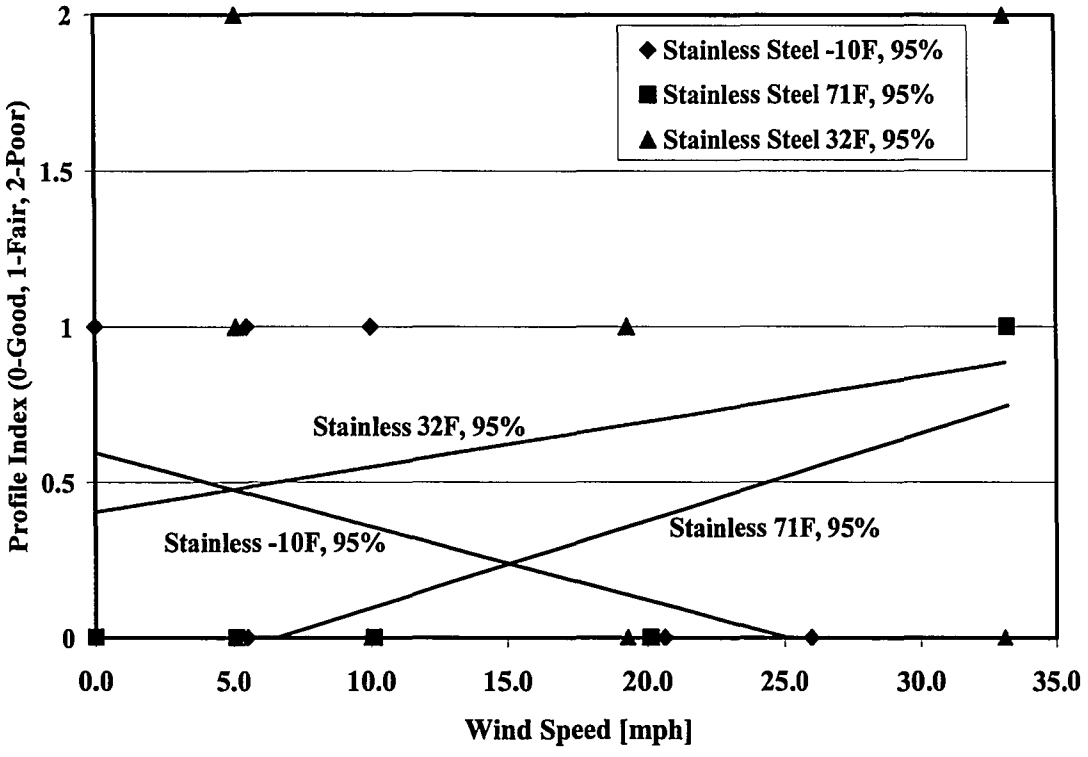

Figure 7.11: Stainless Steel Bead Profile vs. Wind Speed

7.3.2 Undercut

Undercut was observed in 16% of the sections taken from specimens made with type 304 stainless steel plate. The undercut was, in most cases, not deep or sharp in nature. None of the 16 occurrences of undercut were greater than the 1/32-in. AWS acceptability limit. Some examples of undercut observed in stainless steel specimens are shown in Figure 7.12. The relative smooth and shallow nature of the undercut is noted, as discussed above.

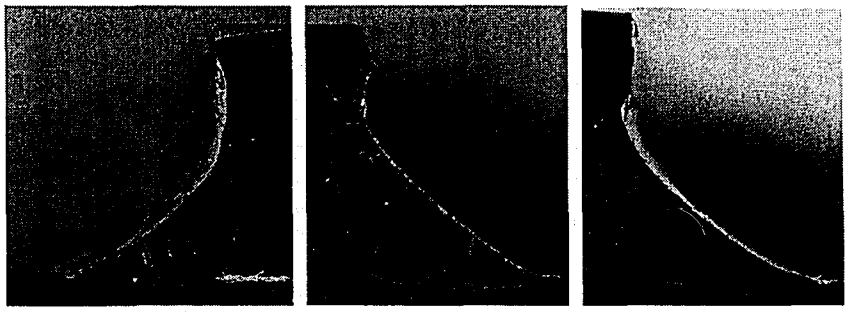

Figure 7.12: Examples of Undercut in Stainless Steel Specimens

7.3.3 Porosity

Porosity was observed on the surfaces of welds made under a wide range of environmental conditions. 13 of the 50, or 26%, of the welds made on stainless steel exhibited surface porosity. This frequency of surface porosity is higher than that of the A36 welds.

The maximum accumulated dimension of porosity in any weld was 0.217-in. from Specimen SS-96 (-2.0°F, 99.9%RH, 0 mph wind), made through surface wetness. The other weld of Specimen SS-96 exhibited similar surface porosity, with a sum of pore diameters of 0.207-in. The interpreted AWS limit for surface porosity, discussed in Section 7.1.4, is 1/4-in. in a 4-in. weld, meaning the observed level of porosity is below the acceptability limit. This level of porosity in the welds made through surface wetness is somewhat greater than the results for A36 steel. This may indicate that plate surface moisture has a greater impact on stainless steel plates or stainless steel weld metal. However, an extensive study of surface wetness was not carried out on stainless steel plates and a more extensive study to determine the effect of surface moisture on porosity in stainless steel welds is needed.

7.3.4 Slag Inclusions

Slag inclusions were observed in many of the sections taken from the stainless steel specimens. In fact, 62 of the 100 sections examined exhibited at least one inclusion. The presence and size

of inclusions tended to increase with wind speed, as was the case for A36 sections. This is illustrated in

Figure 7.13, which plots the total size of slag inclusions in 60 cross-sections (20 cross sections for each data set) against the wind speed which they were made under, while the temperature and humidity were held constant for each data set, as noted above the linear lines of fit. The acceptability limit for an AWS D1.1 macroetch specimen is 1/4-in accumulated maximum dimensions of slag on a 5/16-in. weld, and this limit is well above the upper bound of the ordinate of Figure 7.4, as indicated by the dotted line with upward arrows on the figure.

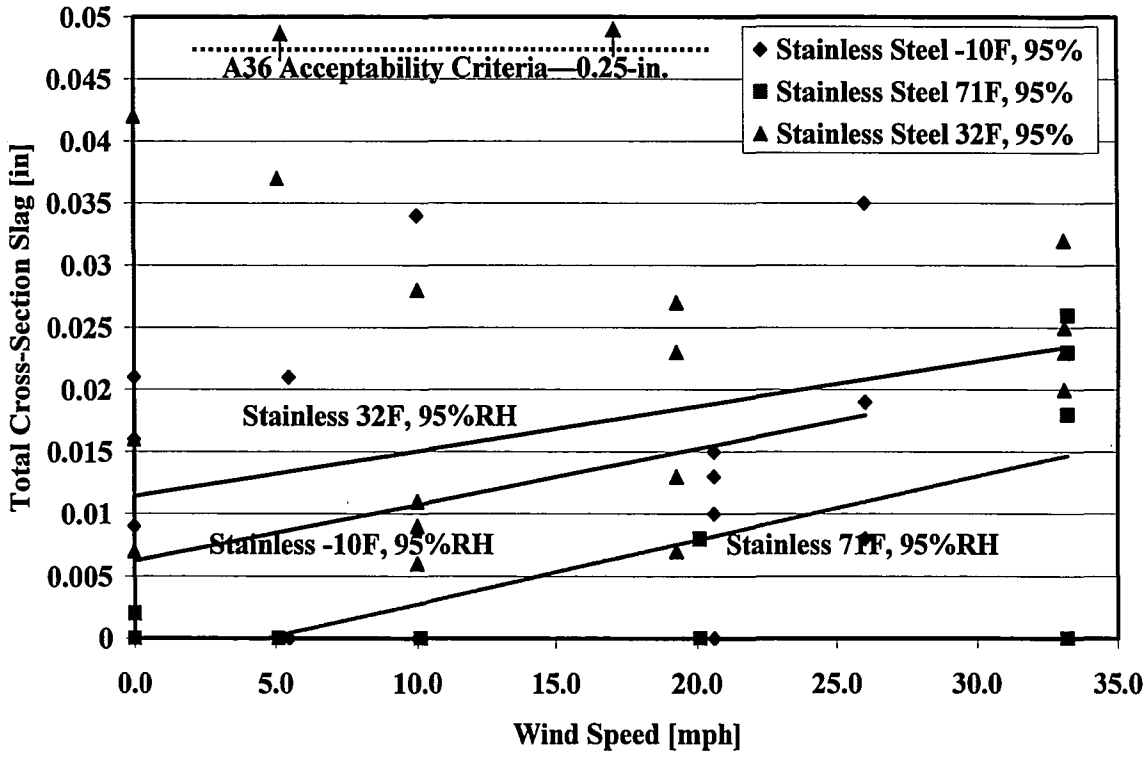

Figure 7.13: Plot of Total Cross Section Slag vs. Wind Speed

7.3.5 Crack-like Discontinuities

Type 304 stainless steel has an austenitic microstructure and is not susceptible to the moisture-related cracking that can occur in carbon steel welds because the microstructure does not permit

martensite formation when cooling takes place.[30] Weld metal, or solidification cracking can occur at elevated temperatures while the weld metal solidifies, and these cracks form between grain boundaries. Solidification cracking is more likely in microstructures that are fully austenitic as compared to those which contain some ferrite. For this reason, filler metal selection is important, as it can add a small percentage of ferrite to the microstructure, as in the case of using the Type 308 electrode on Type 304 Stainless Steel.[30]

Five micro-cracks were observed in the 100 stainless steel sections that were studied. One of these micro-cracks, in Specimen SS-75 (77.0°F, 100%RH, 0 mph wind), was found near the weld surface in the weld metal, and is likely a solidification crack. The remaining four were interestingly found in locations similar to one another, branching from the non-fused plate interface immediately behind the weld root. The micro-cracks do not appear to have any correlation with environmental parameters, as they occurred in warm and cold temperatures and under moderate wind and no wind conditions.

8 Phase 2 Results and Discussion

Destructive strength tests were conducted on welds made on A36 steel plate which had no galvanization. Five combinations of environmental conditions were chosen which were expected to model "base" conditions and several more critical conditions. The conditions examined and the materials used are tabulated in Table 3-4 and are repeated in Table 8-1. This chapter compares the measured and predicted strengths of each strength test specimen and describes the condition of the welds and the post-test fracture surfaces.

The five A36 steel specimens listed in Table 8-1 were loaded until failure as shown in Figure 8.1. The tests were conducted at a quasi-static rate of approximately 9.2 kips/minute. The specimens were loaded until a complete loss in load carrying capacity occurred. The maximum load at failure for each specimen was recorded, and the sections were examined to identify the failure mode. All failures occurred in the weld metal. The failure was characterized by yielding and significant plastic deformation in the weld region followed by fracture on a plane inclined approximately 30-45 degrees from the base plate. Typical failure modes are illustrated in throughout this chapter for each specimen tested. Fracture surfaces were examined under an optical microscope to determine whether any discontinuities were present which may have influenced the ultimate strength of the specimen.

Table 8-1: Phase 2 Test Matrix

ID	Base Material	Temp. [°F]	Relative Humidity %RH	Wind Speed [mph]	Electrode Condition	Plate Surface Condition
T-1	ASTM A36 (Orig.)	84	15.4	0	AWS D1.1*	Dry
T-2	ASTM A36 High Carbon(2)	77.9	26.4	0	AWS D1.1*	Dry
T-3	ASTM A36 High Carbon(2)	-15.4	73	0	AWS D1.1*	Dry
T-4	ASTM A36 High Carbon(1)	72	32.3	0	AWS D1.1*	Wet**
T-5	ASTM A36 High Carbon(2)	72.7	19.3	0	AWS D1.1*	Wet**

*AWS D1.1 indicates proper storage of electrodes according to AWS D1.1 specifications.
** Wet indicates intentional application of liquid moisture to thoroughly wet all plate surfaces.

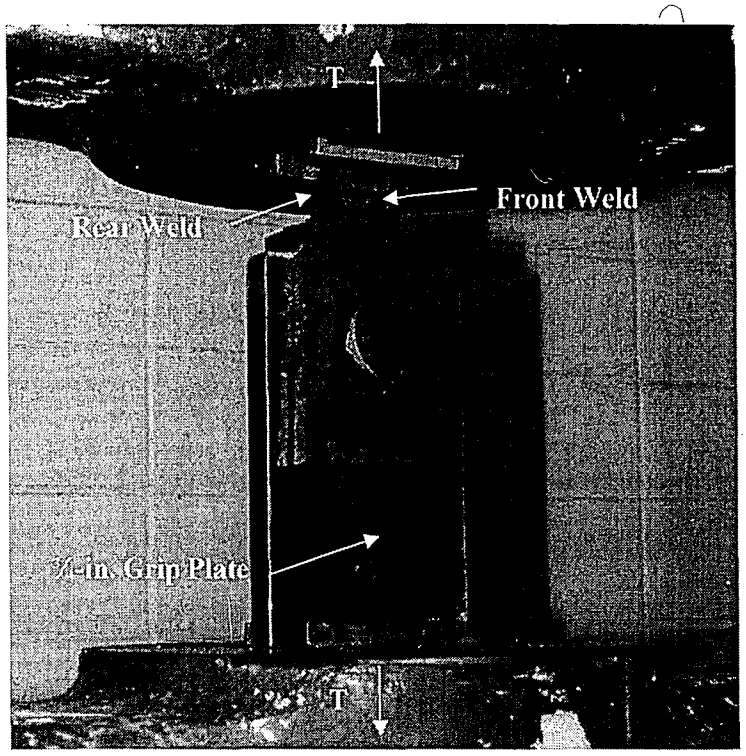

Figure 8.1: Phase 2 Specimen in Testing Machine

8.1 Strength

The strength of each weld, P, was predicted using the AISC equation for the strength of a fillet weld loaded in transverse tension as shown in Equation 5.[28] The predicted strength was computed with the nominal electrode tensile strength and with the measured electrode tensile strength. For both cases, the minimum measured throat dimension and weld length were used.

$$P = 0.6F \cdot T \cdot 2l \cdot 1.5 \qquad \text{Equation 5}$$

In Equation 7, F represents the ultimate tensile stress [ksi] of the weld metal. Two values of weld strength, P, were calculated using two values for F: (1) the nominal weld metal ultimate tensile stress, F_{nom}, or 70 ksi, and (2) the ultimate tensile stress estimated from hardness measurements, F_{est}. The minimum throat dimension, T, and, weld length, l, were measured for each weld. Since the weld length is 1-in. for a single weld and the specimen shown in Figure

8.1 has two welds, a multiplier of 2 is included in the formulation for the weld strength of the complete specimen. The factor of 1.5 is included to account for loading in transverse shear, as opposed to longitudinal shear, which the AISC equation for weld strength in shear loading is based upon.

To estimate the in-situ ultimate tensile stress of the weld metal, Rockwell B hardness measurements were taken on each specimen tested. These measurements were taken from the discarded portion of the weld after creating the tensile specimen, as illustrated in Figure 8.2. The ultimate tensile stress was estimated from the Rockwell B hardness using a standard correlation.[16] A minimum of four hardness measurements were taken and averaged for each specimen. The average value was used to estimate the ultimate tensile stress of the weld metal. The hardness measurements, ultimate tensile strength, and length and throat dimensions for all of the test specimens are presented below in Table 8-2.

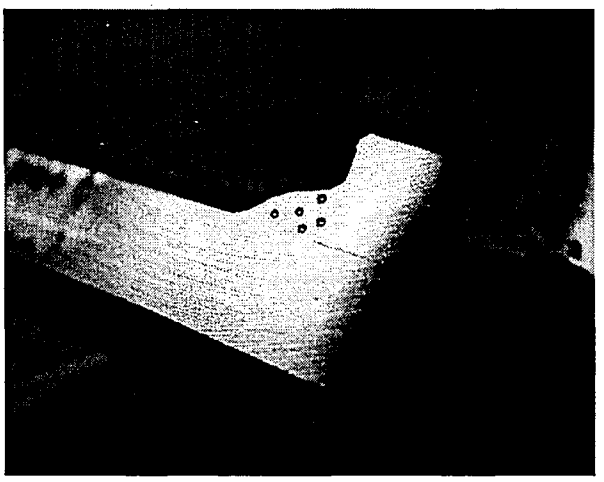

Figure 8.2: Rockwell B Hardness Indentations on Test Specimen Weld Cross-Section

The two strength predictions were compared to the strength measured from destructive testing. The measured strength was taken directly from the maximum measured load. As previously discussed, the specimens included two 1.0-in. long welds. In all cases one weld failed prior to

the other due to slight variations in size. After the first failure, the load dropped and the other weld continued to yield and eventually fractured. The two predicted strengths, namely P_{nom}, based on F_{nom}, and P_{est}, based on F_{est}, and measured strengths are presented in Table 8-3. Also presented in Table 8-3 are the ratios of the measured strengths to values of the P_{nom} and P_{est} values.

Table 8-2: Phase 2 Measured Properties

ID	Minimum Throat [in.]	Average Hardness [Rockwell B]	Ultimate Tensile Stress, F_{est} [ksi]	Minimum Weld Length [in.]
T-1	0.186	92.0	92.0	1.000
T-2	0.215	89.7	88.7	0.992
T-3	0.244	87.1	84.2	1.053
T-4	0.195	90.4	89.4	1.013
T-5	0.215	87.9	85.8	0.972

From the data in the Table 8-3, it is observed that the measured strength exceeded the predicted strength based on the nominal weld metal ultimate tensile stress by 30% on average. When the estimated weld metal ultimate tensile stress was used to calculate the predicted strength, the AISC formulation provided an accurate prediction of the specimen strength. In each case, the P_{est} is within 10% of the measured failure load. Based on these results, the shear strength of the fillet welds was not compromised by any of the environmental conditions examined. Furthermore, the AISC formulations for strength provide a conservative estimate of strength in all cases when nominal ultimate tensile stress of the filler metal was used (P_{nom}).

Table 8-3: Phase 2 Failure Loads

ID	P_{nom} (based on F_{nom}) [kips]	P_{est} (based on F_{est}) [kips]	Measured Strength [kips]	Ratio Measured/Pred. 1	Ratio Measured/Pred. 2
T-1	23.44	30.80	33.10	1.41	1.07
T-2	26.87	34.05	33.80	1.26	0.99
T-3	32.37	38.94	42.80	1.32	1.10
T-4	24.82	31.71	30.20	1.22	0.95
T-5	26.33	32.27	35.05	1.33	1.09

8.2 Specimen Detailed Examination

A post-test investigation of each strength test specimen is presented in this section, along with images and descriptions of the fracture surfaces of each specimen. A discussion of discontinuities observed on the fracture surfaces and their potential contribution to the failure are also discussed.

8.2.1 Specimen T-1 (Low Carbon – Typical Environmental Conditions)

Specimen T-1 was made using moderate carbon A36 steel plate material. The steel temperature at welding was 84°F, and the relatively humidity and wind speed were 15.4% RH and 0 mph, respectively. The weld was free from surface discontinuities and was regular in size along its length. This weld served as the base case since it was not welded under any adverse conditions, and it was made on moderate carbon steel.

In the strength test, both welds failed simultaneously; the failed specimen is shown in Figure 8.3.

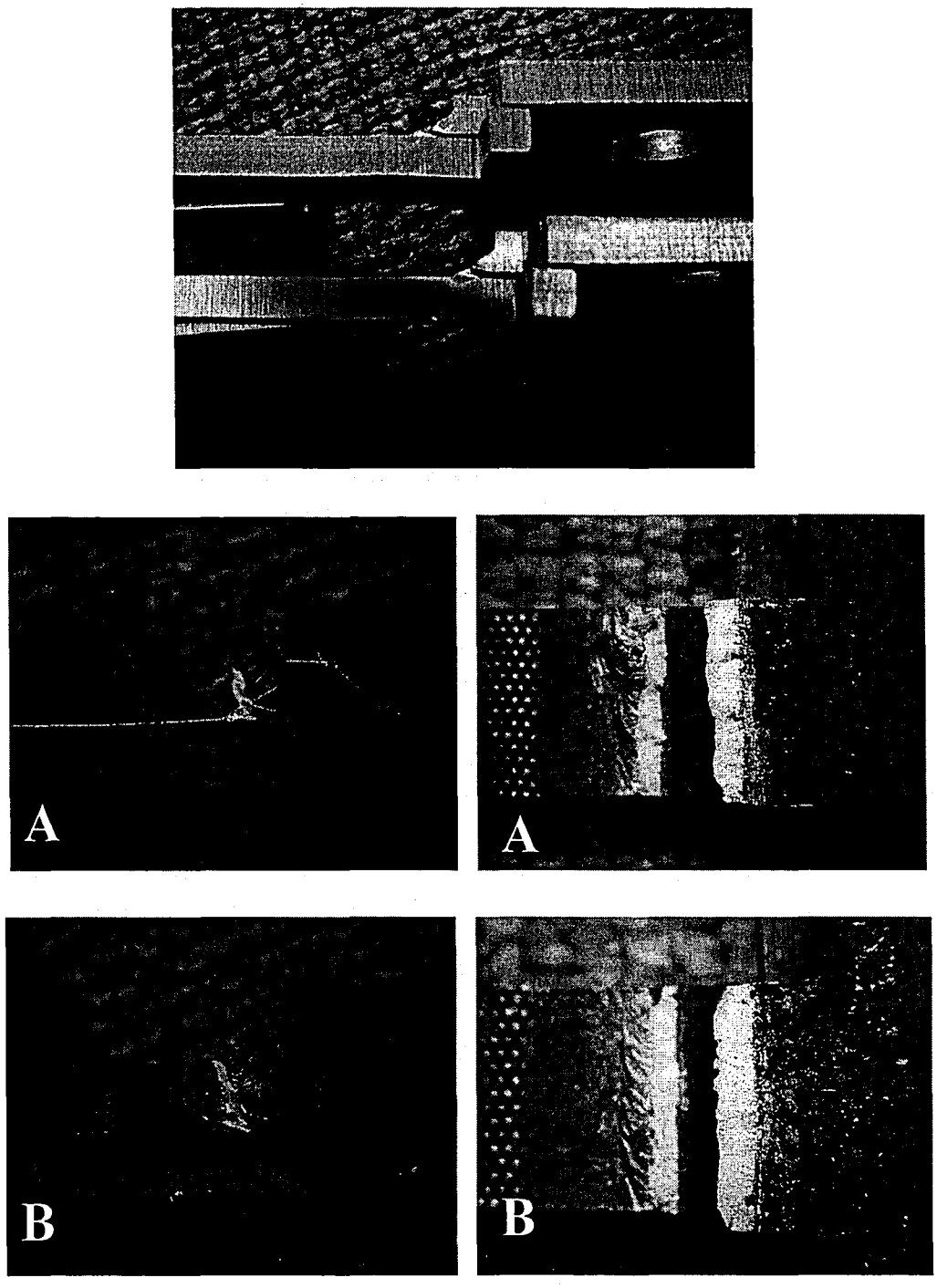

Figure 8.3: Specimen T-1 Failure Surfaces

As can be seen from the images of Figure 8.3, the failure occurred through the weld metal of both welds. The measured failure load was 33.1 kips. The P_{est} was 30.80 kips, and the ratio of measured strength to P_{est} was 1.07.

The fracture surfaces were examined under an optical microscope to investigate the presence of discontinuities on the fracture surface. Fracture surface A in Figure 8.3 has two pores along its root, as well as two slag inclusions. Fracture surface B contains sections of two or three small pores, as well as several small voids which had been filled with slag inclusions prior to fracture. These discontinuities appear to have had no significant effect on the weld strength, and the strength was accurately predicted using the measured weld metal tensile strength and conservatively predicted using the nominal weld metal strength.

8.2.2 Specimen T-2 (High Carbon – Typical Environmental Conditions)

Specimen T-2 was made using high carbon A36 steel plate material from the second heat of high carbon A36 steel plate, with a carbon equivalent of 0.397. The steel temperature at welding was 77.9°F, and the relatively humidity and wind speed were 26.4% RH and 0 mph, respectively. The weld is shown in Figure 8.4. The weld is free from surface discontinuities and relatively regular in throat dimension along its length.

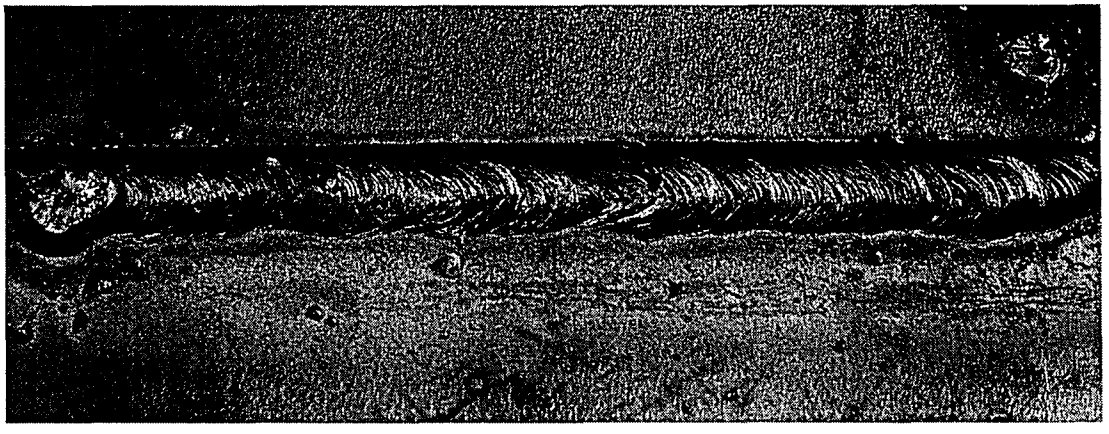

Figure 8.4: Weld for Specimen T-2

Two sections were polished from the discarded portions of the weld after the strength test specimen was made. These sections are shown in Figure 8.5.

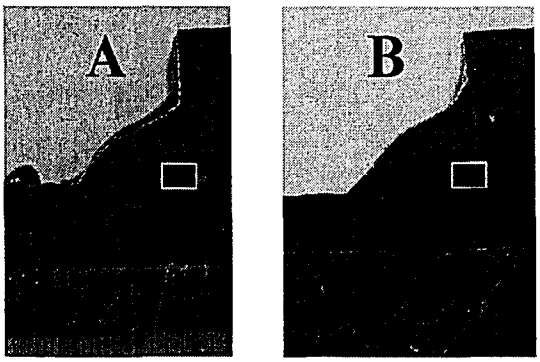

Figure 8.5: Polished Sections from Specimen T-2

Both sections shown in Figure 8.5 are free from slag inclusions and porosity. A vertical root micro-crack, however, was observed in section A, and a segment of incomplete fusion was observed at the root of the section B. The vertical micro-crack, depicted in Figure 8.6, protrudes from the root of the weld along the boundary between weld metal and the HAZ and may be related to the higher carbon content of the steel. The length of the vertical crack is on the order of 1/32-in, the micro-crack length limit. The non-fused segment of section B is shown in Figure 8.7.

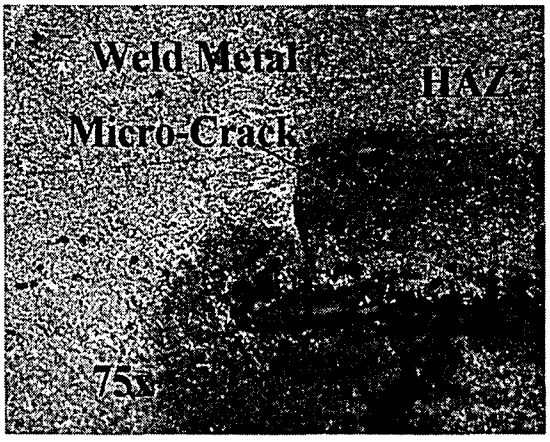

Figure 8.6: Vertical Root Micro-Crack in T-2 Weld at Root-Section A

Two sections were polished from the discarded portions of the weld after the strength test specimen was made. These sections are shown in Figure 8.5.

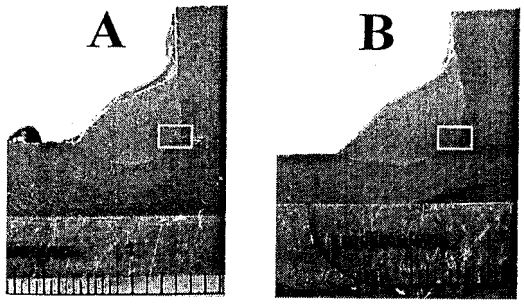

Figure 8.5: Polished Sections from Specimen T-2

Both sections shown in Figure 8.5 are free from slag inclusions and porosity. A vertical root micro-crack, however, was observed in section A, and a segment of incomplete fusion was observed at the root of the section B. The vertical micro-crack, depicted in Figure 8.6, protrudes from the root of the weld along the boundary between weld metal and the HAZ and may be related to the higher carbon content of the steel. The length of the vertical crack is on the order of 1/32-in, the micro-crack length limit. The non-fused segment of section B is shown in Figure 8.7.

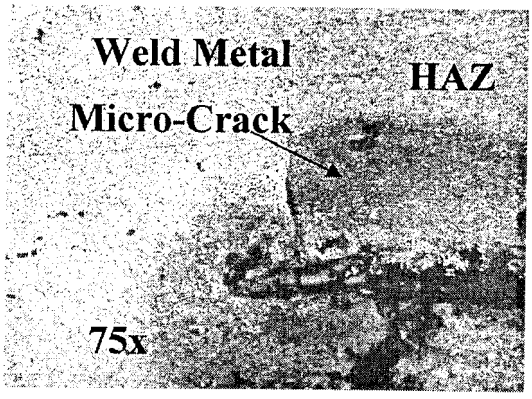

Figure 8.6: Vertical Root Micro-Crack in T-2 Weld at Root-Section A

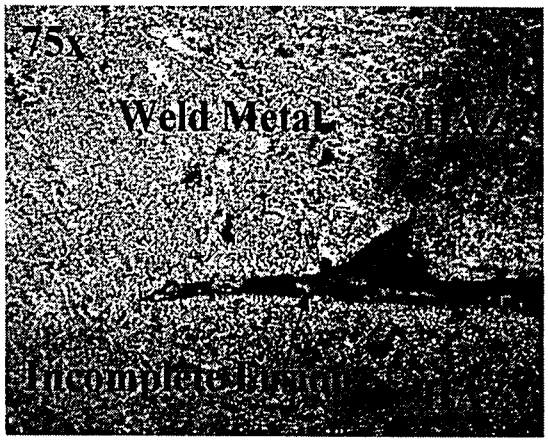

Figure 8.7: Incomplete Fusion in T-2 Weld-Section B

The failure surfaces for Specimen T-2 are shown in Figure 8.8.

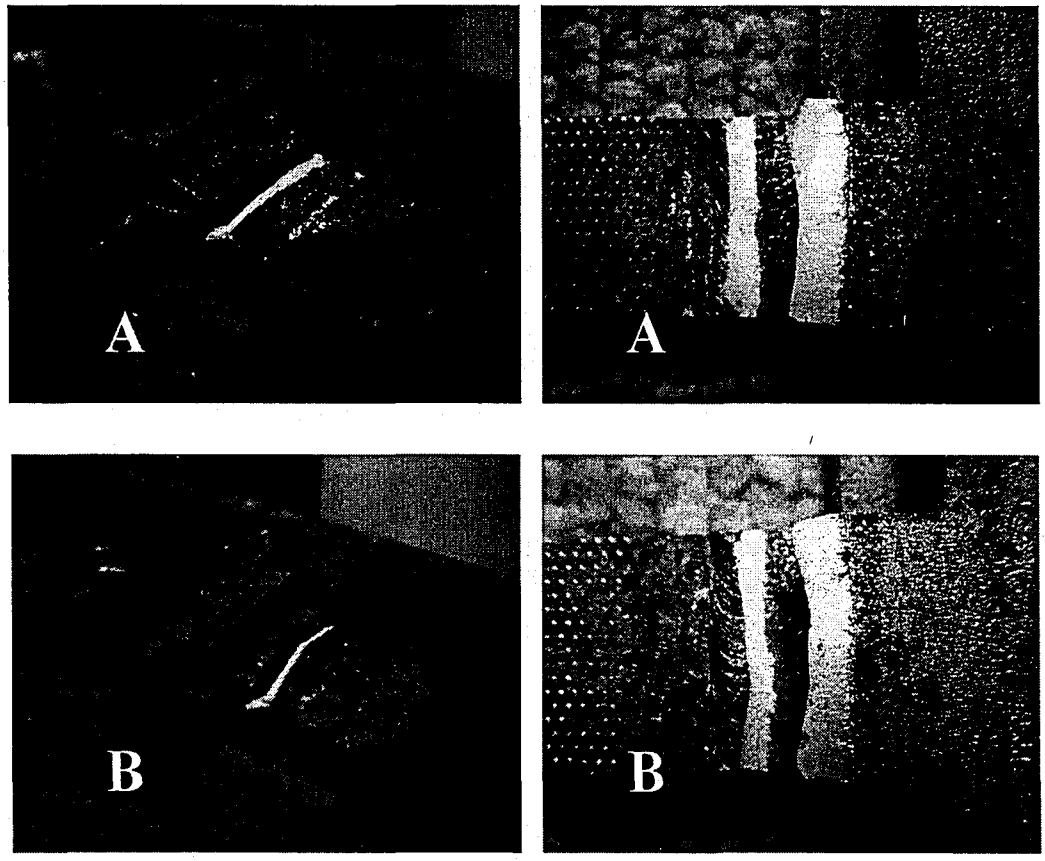

Figure 8.8: Specimen T-2 Fracture Surfaces

The failure occurred through the weld metal, and the measured strength was 33.8 kips. The P_{est} was 34.05 kips, and the ratio of measured strength to P_{est} was 0.99. The strength was accurately predicted when using the measured ultimate tensile stress of the weld metal. The strength was conservatively predicted when using the nominal weld metal strength.

Fracture surface A, shown in Figure 8.8, has one pore along the weld root and some small voids which had been occupied by slag inclusions. Fracture surface B has two small pores and several voids along the root, as well. The failure surfaces did not occur through the crack or incomplete fusion presented above from the cross-sections, so the discontinuities observed in the cross-sections did not appear to reduce the ultimate strength of the specimen.

8.2.3 Specimen T-3 (High Carbon – Cold)

Specimen T-3 was made using high carbon A36 stel plate material from the second heat of high carbon A36 steel plate, with a carbon equivalent of .397. The steel temperature at welding was -15.4°F, and the relatively humidity and wind speed were 73% RH and 0 mph, respectively. The weld is shown in Figure 8.9, and there is an unacceptable weld region near the center of the weld based on its profile. This region of the weld is a stop/start locations that occurred because the welder terminated the weld due to poor visibility from smoke accumulation. The weld was restarted from the opposite end and met the previously terminated weld bead at this central location. This region of the weld did not impact the validity of the test, since the right-hand portion of the weld was used to predict the strength of the specimen, and the portion of the specimen taken from the left side of the weld was able to support at least as much load as the smaller weld from the right side since it was oversized. As a result, the failure load was based only on the more uniform weld segment from the right side of the weld.

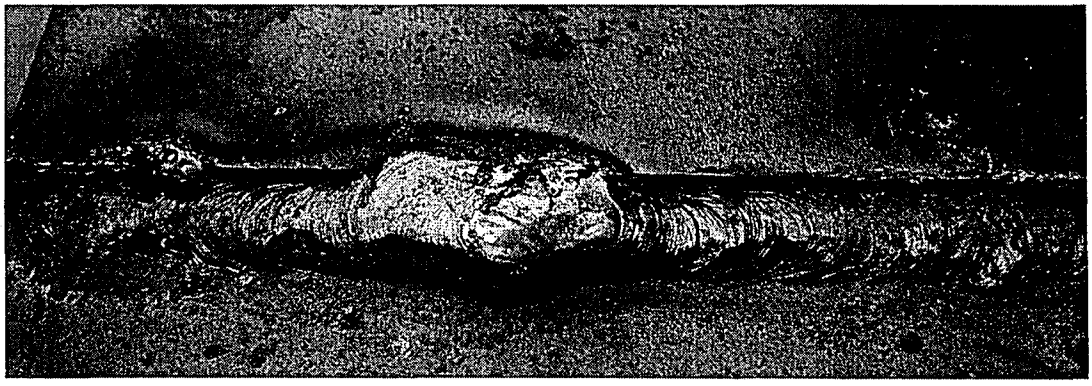

Figure 8.9: Weld for Specimen T-3

Two sections were polished from the discarded portions of the weld after the strength test specimen was made. These sections are shown below in Figure 8.10.

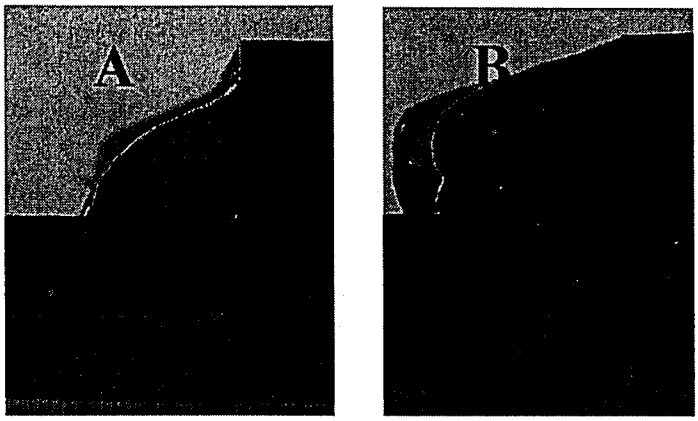

Figure 8.10: Polished Sections from Specimen T-3

Section A has a root inclusion and exhibits minor convexity, section B, taken from the oversized weld region, has extreme convexity and is unacceptable according to AWS D1.1 profile requirements. There were no cracks found in the section A; however, the section B has a small non-fused segment at the root, some slag and connecting micro-cracks at the root, and some slag and connecting micro-cracks at the toe, depicted in Figure 8.11 and Figure 8.12.

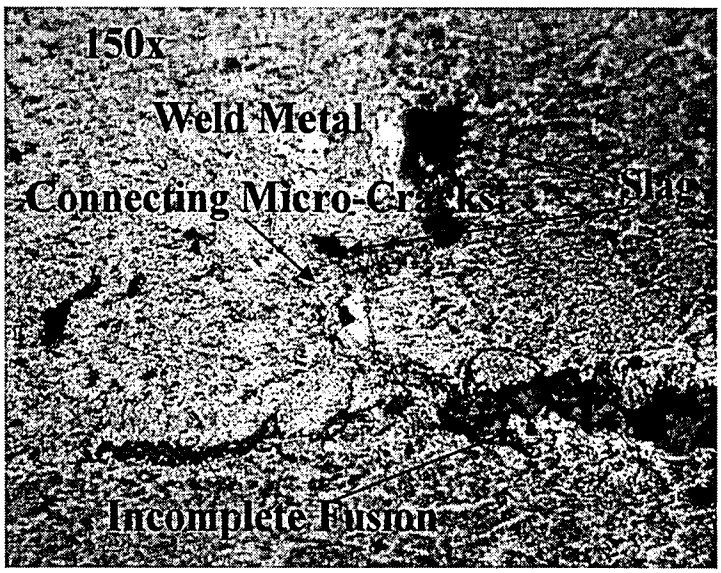

Figure 8.11: Root of Specimen T-3, Section B

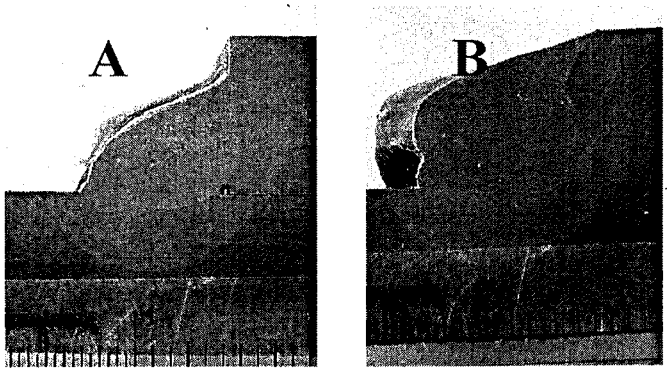

Figure 8.10: Polished Sections from Specimen T-3

Section A has a root inclusion and exhibits minor convexity, section B, taken from the oversized weld region, has extreme convexity and is unacceptable according to AWS D1.1 profile requirements. There were no cracks found in the section A; however, the section B has a small non-fused segment at the root, some slag and connecting micro-cracks at the root, and some slag and connecting micro-cracks at the toe, depicted in Figure 8.11 and Figure 8.12.

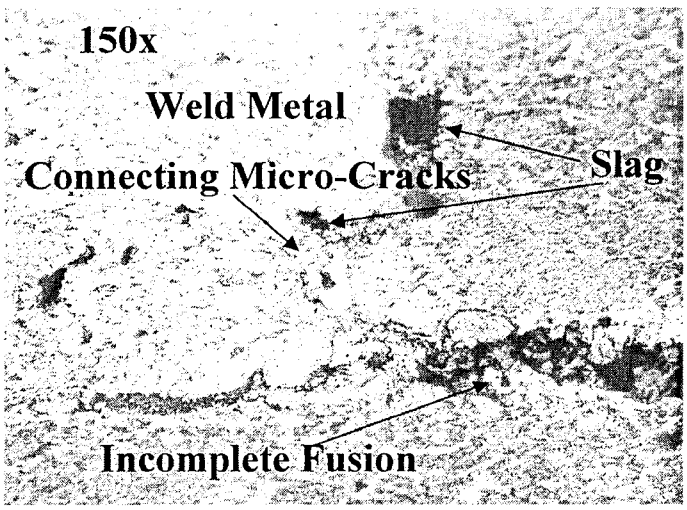

Figure 8.11: Root of Specimen T-3, Section B

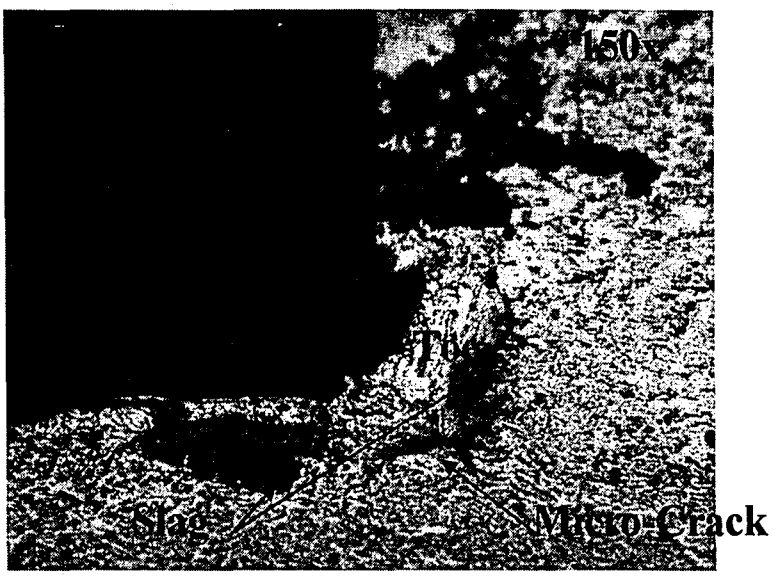

Figure 8.12: Toe Inclusions and Micro-cracking in Specimen T-3, Section B

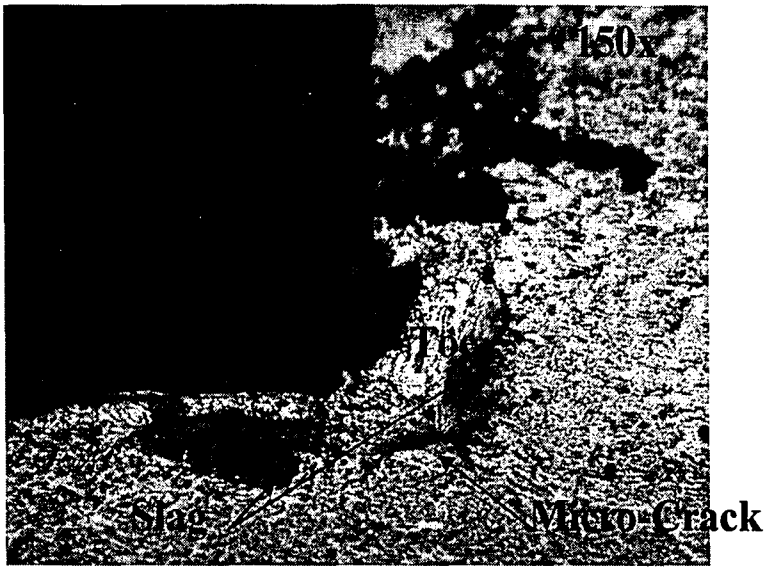

Figure 8.12: Toe Inclusions and Micro-cracking in Specimen T-3, Section B

The fractured specimen and fracture surfaces are shown in Figure 8.13.

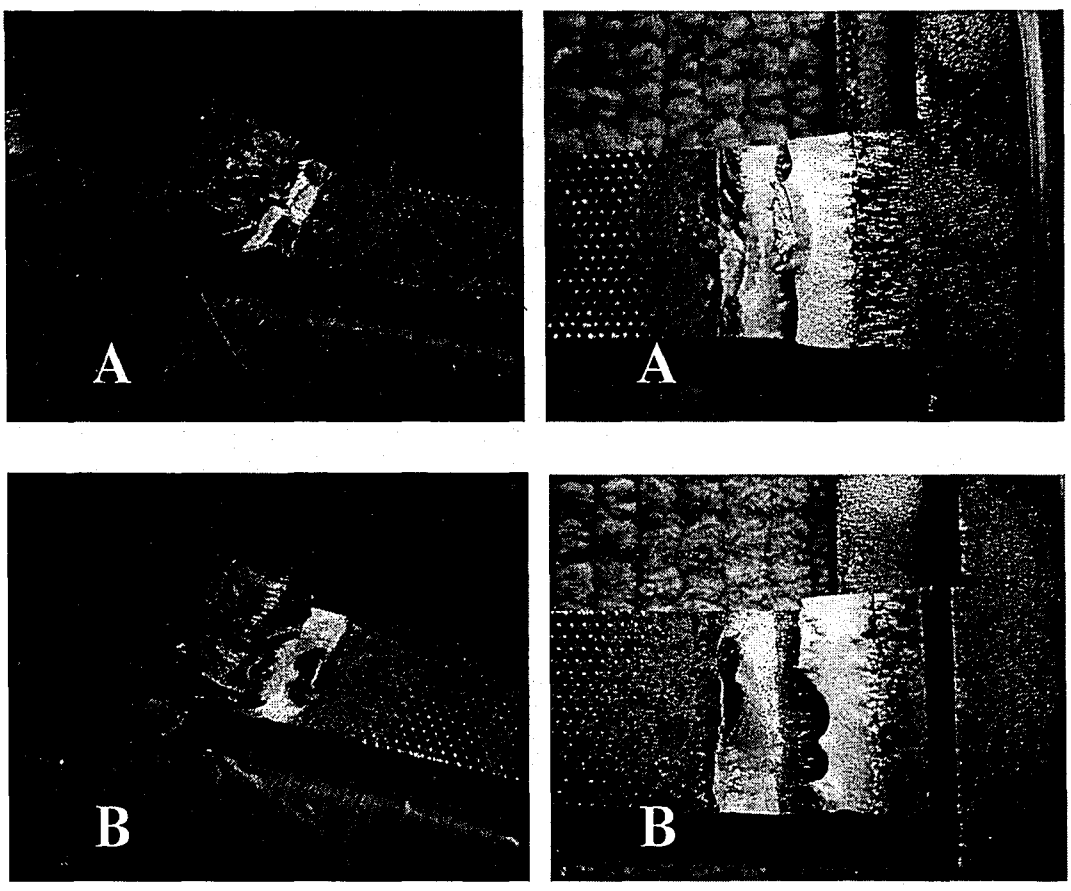

Figure 8.13: Specimen T-3 Fracture Surfaces

The failure occurred through the weld metal of both welds, and the measured strength was 42.8 kips, while the P_{est} was 38.94 kips. The ratio of the measured strength to P_{est} was 1.10.

Fracture surface A has five pores along its root and several voids previously occupied by slag inclusions, as well. There are two large slag inclusions along the root of fracture surface B. The irregularity of the fracture surface shape is due to the changes in the throat dimension along the weld length and occurs along the shear plane that provides the least resistance.

Fracture surface B, shown in Figure 8.13, was further examined under a scanning electron microscope (SEM) to investigate a discontinuity in the right side of the fracture surface as seen

in Figure 8.14, which is a photograph of the fracture surface being examined under the SEM. Figure 8.15, Figure 8.16, and Figure 8.17 show progressive zoom into the initial area of interest, revealing the characteristic dark (filled), cracked area that is a cluster of slag inclusions.

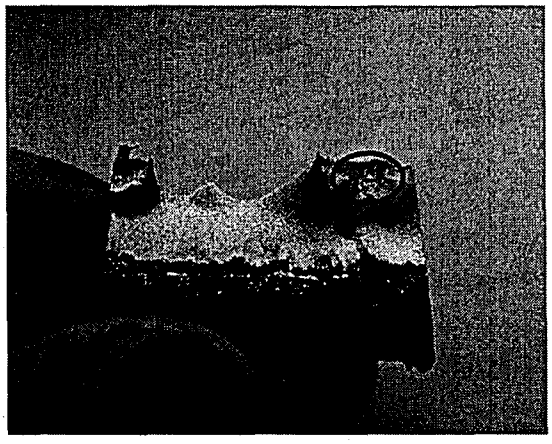

Figure 8.14: Fracture Surface B—T-3

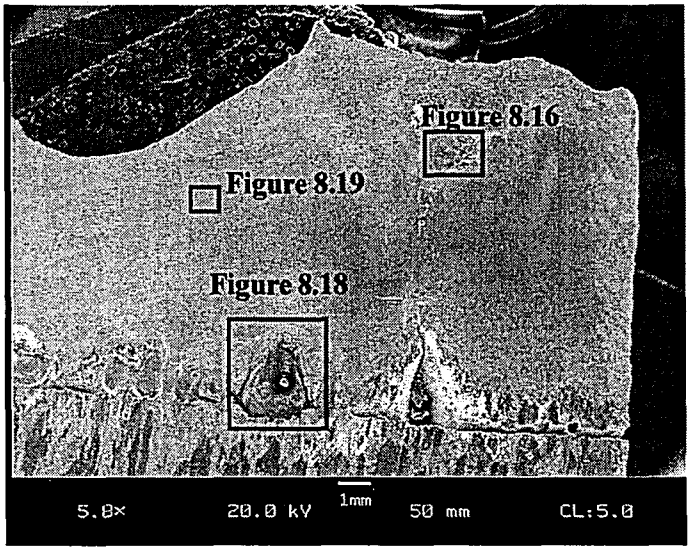

Figure 8.15 SEM Overview (5.8x) of Fracture Surface B—T-3

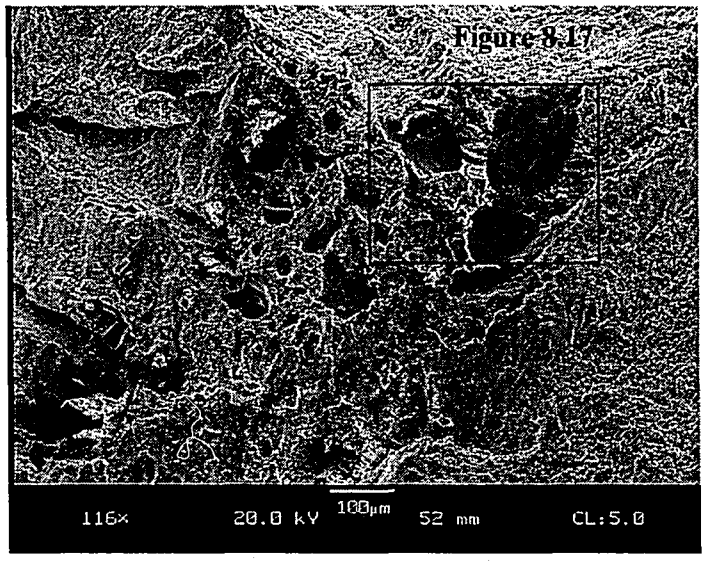

Figure 8.16: SEM Image (116x) of Discontinuity Area—T-3

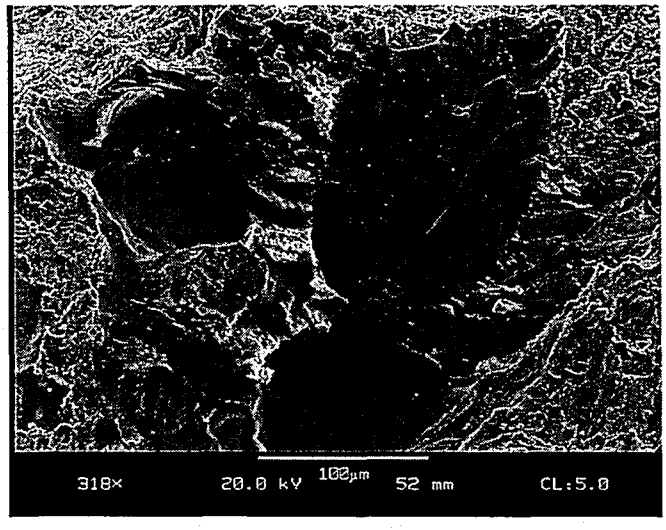

Figure 8.17: SEM Image (318x) of Slag Inclusions—T-3

Two additional images were taken with the SEM on this fracture surface. Figure 8.18 shows what appears to be a slag inclusion embedded at the root of the weld along the fracture surface. Figure 8.19 shows a typical ductile shear fracture surface at high magnification, taken from the area indicted with a yellow box and corresponding label in Figure 8.15. The figure shows regions shaped like elongated ovals, each of which surrounds a small inclusion, appearing as a

white dot in the image. The image also shows microvoids in the weld metal which elongated and coalesced under shear loading as the weld metal deformed plastically to form this ductile shear fracture surface. These small slag inclusions around which microvoids formed are well below a size that would have any impact on weld strength and are only viewable at a level of magnification such as that in the SEM image.

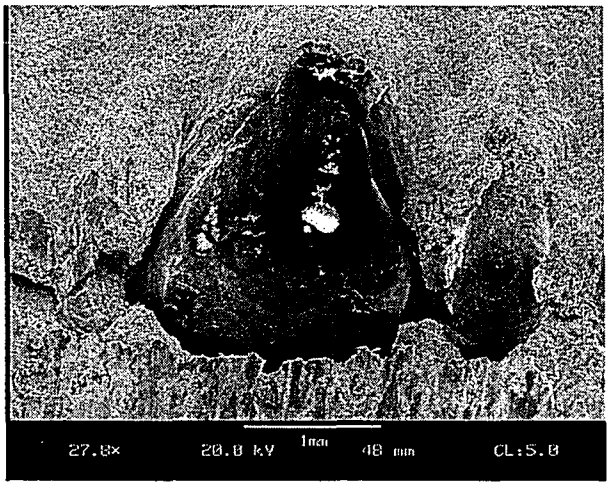

Figure 8.18: SEM Image (27.8x) of Large Inclusion—T-3

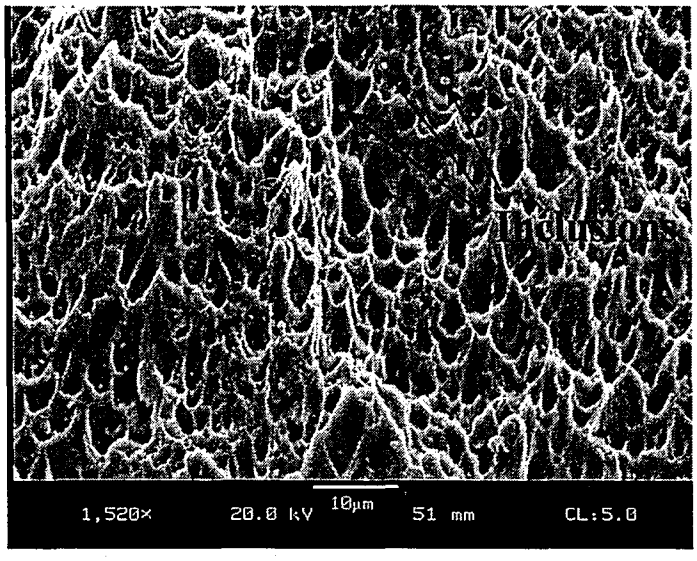

Figure 8.19: SEM Image (1,520x) of Ductile Shear Fracture Surface

The flaws observed on the fracture surface and the small cracks observed on the cross sections did not appear to reduce the load carrying capacity of the weld, as the ratio of the measured strength to the P_{est} was 1.10.

8.2.4 Specimen T-4 (High Carbon – Wet)

Specimen T-4 was made using high carbon A36 steel plate material from the first heat of high carbon A36 steel plate with a carbon equivalent of 0.425. The steel temperature at welding was 72˚F, and the relative humidity and wind speed were 32.3% RH and 0 mph, respectively. The plate surfaces were thoroughly wet prior to welding. The weld is shown in Figure 8.28, and the weld surface has deep ripples and an irregular throat dimension due to poor visibility as steam was generated during welding.

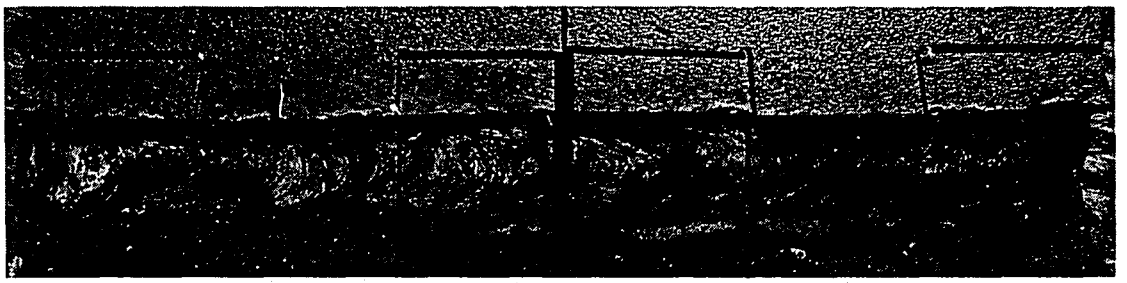

Figure 8.20: Weld for Specimen T-4

Two sections were polished from the discarded portions of the weld after the specimen was made. These are shown in Figure 8.21.

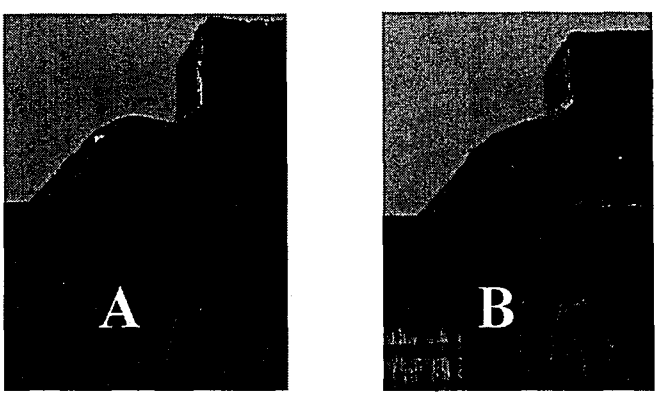

Figure 8.21: Polished Sections from Specimen T-4

Section A has two small slag inclusions in the weld metal near the root. Section B has no slag inclusions or porosity, but there is a non-fused segment at the root of section B. Both sections exhibit convexity in their profiles, which may be a result of welding through the surface wetness. The surface moisture may have impacted the non-uniformity of the weld pool, causing ripples and geometry changes, or the steam generated by welding through surface moisture may have reduced the welder's vision of the weld to the extent that the profile was negatively impacted.

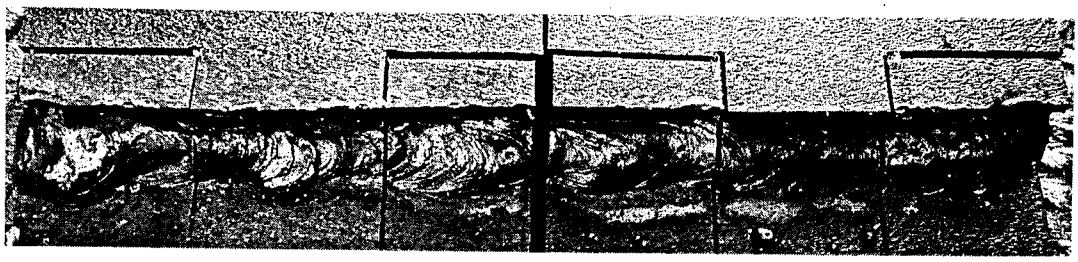

Figure 8.20: Weld for Specimen T-4

Two sections were polished from the discarded portions of the weld after the specimen was made. These are shown in Figure 8.21.

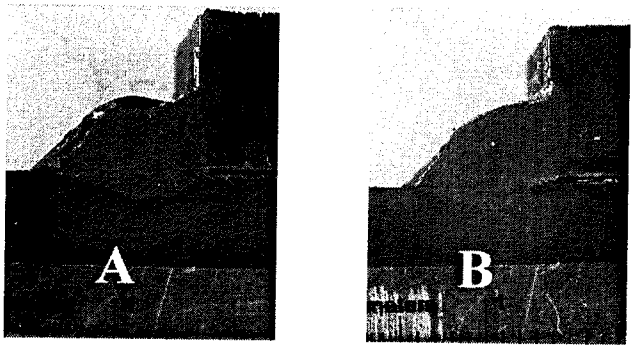

Figure 8.21: Polished Sections from Specimen T-4

Section A has two small slag inclusions in the weld metal near the root. Section B has no slag inclusions or porosity, but there is a non-fused segment at the root of section B. Both sections exhibit convexity in their profiles, which may be a result of welding through the surface wetness. The surface moisture may have impacted the non-uniformity of the weld pool, causing ripples and geometry changes, or the steam generated by welding through surface moisture may have reduced the welder's vision of the weld to the extent that the profile was negatively impacted.

The failed specimen and fracture surfaces are shown in Figure 8.8.

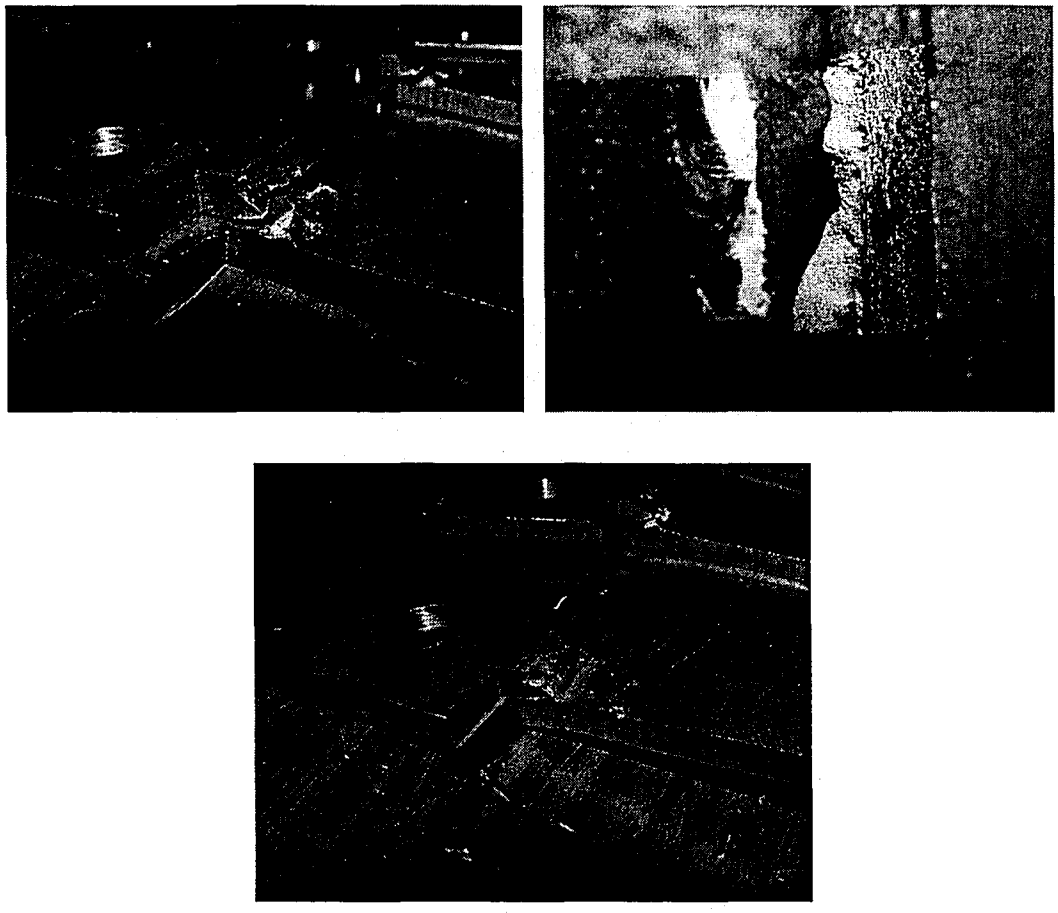

Figure 8.22: Post-test Specimen T-4

Failure occurred in one weld at a measured load of 30.2 kips. The P_{est} of the specimen was 31.71 kips, so the ratio of measured strength to P_{est} was 0.95.

Only one of the welds failed during the test, and this single fracture surface included two pores and two slag inclusions. Because this specimen failed at the lowest ratio of actual to predicted load, and because there was a small discontinuity of interest on the fracture surface which was, the failed weld was observed under the SEM. The surface examined is shown in Figure 8.23.

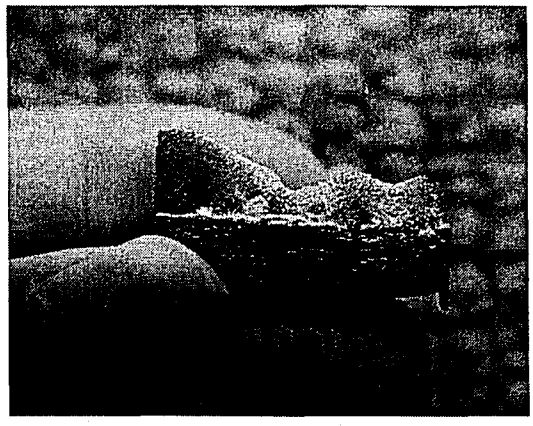

Figure 8.23: Fracture Surface—T-4

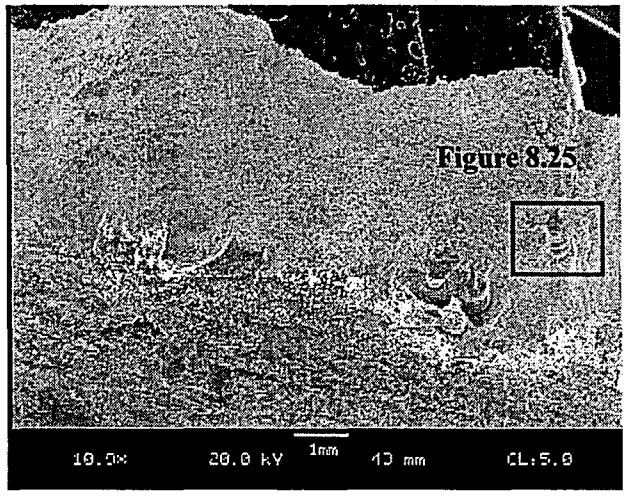

Figure 8.24: SEM Image (10x) of Right Side Fracture Surface—T-4

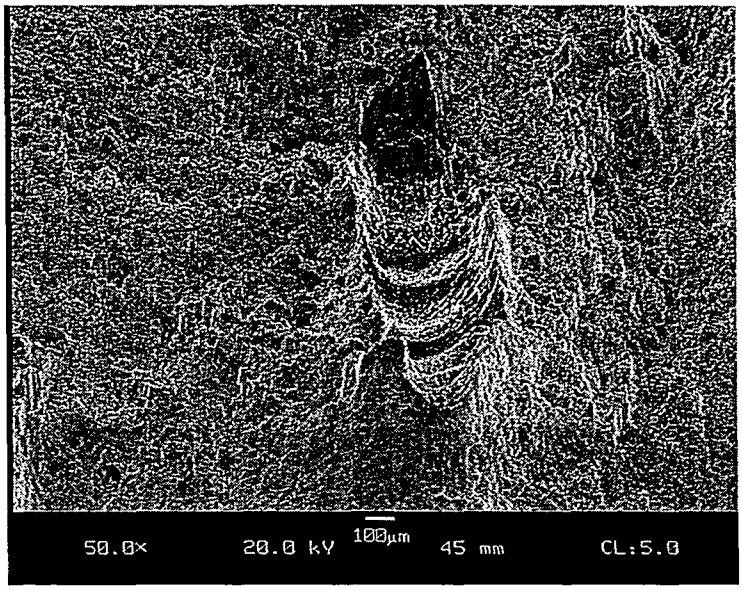

Figure 8.25: SEM Image (50x) of Piping Porosity—T-4

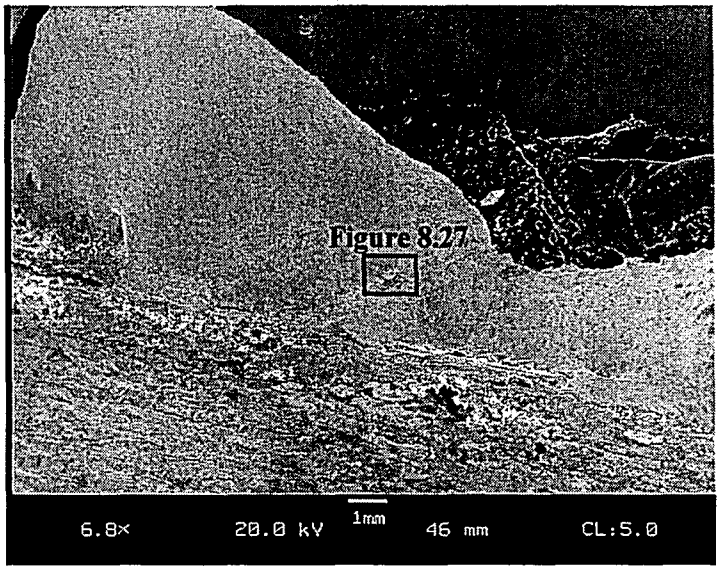

Figure 8.26: SEM Image (6.8x) of Left Side Fracture Surface—T-4

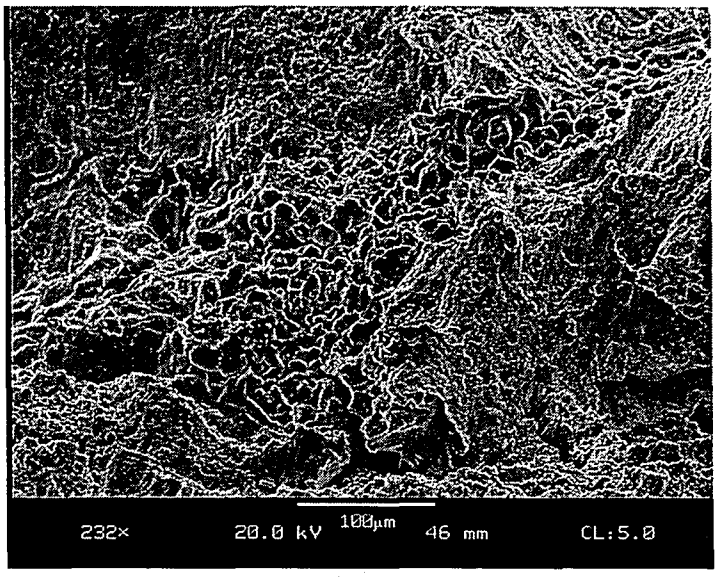

Figure 8.27: SEM Image (232x) of Discontinuity—T-4

Figure 8.24 and Figure 8.25 depict an example of piping porosity, or an elongated pore which forms because of a large amount of gas being entrapped during solidification.[31] Figure 8.26 and Figure 8.27 show a linear discontinuity from the central portion of the fracture surface. The discontinuity appears to be some form of dendrite growth in a void area on the fracture surface. Dendrites are crystalline formations resulting from the solidification of the weld metal. There do not appear to be any gross discontinuities which would have significantly reduced the weld strength, although this specimen, as previously noted, failed at the lowest ratio of measured strength to P_{est}. The profile was irregular with regard to the throat dimension along the length of the weld, and this may have contributed to a reduced load carrying capacity. The ratio of measured to predicted load, however, was 0.95, indicating the strength prediction was within 5% of the measured load when using the measured weld metal ultimate tensile stress. The P_{est} might have been over-predicted as a result of measurement techniques used to quantify the throat dimension, as discussed in Section 8.3.

8.2.5 Specimen T-5 (High Carbon – Wet)

Specimen T-5 was made using high carbon A36 steel plate material from the second heat of high carbon A36 plate material with a carbon equivalent of .397. The steel temperature at welding was 72.7°F, and the relative humidity and wind speed were 19.3% RH, and 0 mph, respectively. The plate surfaces were thoroughly wet prior to welding, as illustrated in Figure 8.28. The weld is shown in Figure 8.29 and is irregular with respect to profile and throat dimension. There are several abrupt changes in weld size along the length of the weld, which were likely influenced by the presence of the surface wetness or poor welder vision due to steam created during welding.

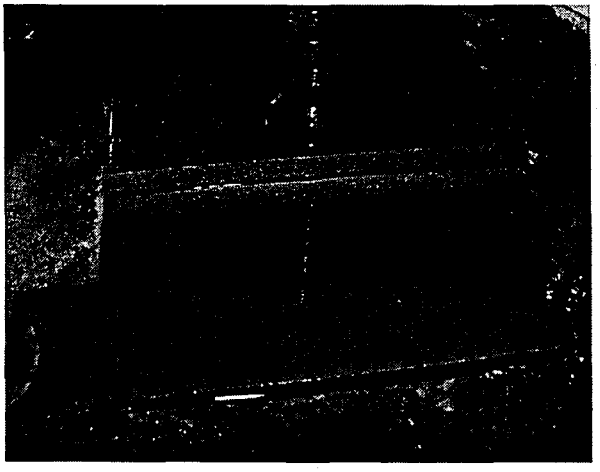

Figure 8.28: Wet Specimen T-5 prior to welding

Figure 8.29: Weld—Specimen T-5

Two sections were polished from the discarded portions of the weld after the strength test specimen had been made. These are shown below in Figure 8.30.

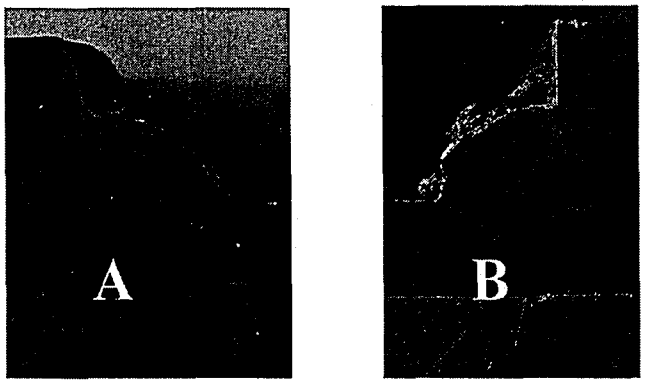

Figure 8.30: Polished Sections from Specimen T-5

Section A has three slag inclusions, and it also has a vertical crack with a length on the order of 1/16-in. and small non-fused segment at its root (Figure 8.31). Additionally, there is a micro-crack in the HAZ of section A, seen in Figure 8.32, which shows the micro-crack located in the HAZ. This micro-crack is perhaps related to the introduction of moisture into the weld through surface wetness which may have contributed to cracking in the hardened HAZ. Section B has a convex profile and no notable discontinuities.

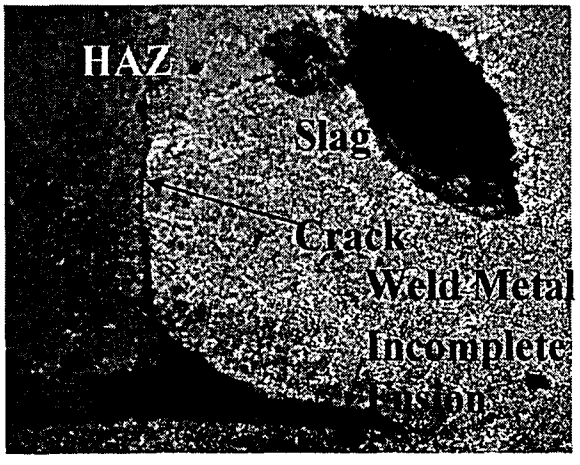

Figure 8.31: Vertical Crack, Non-fused Root- Specimen T-5, Section A

Two sections were polished from the discarded portions of the weld after the strength test specimen had been made. These are shown below in Figure 8.30.

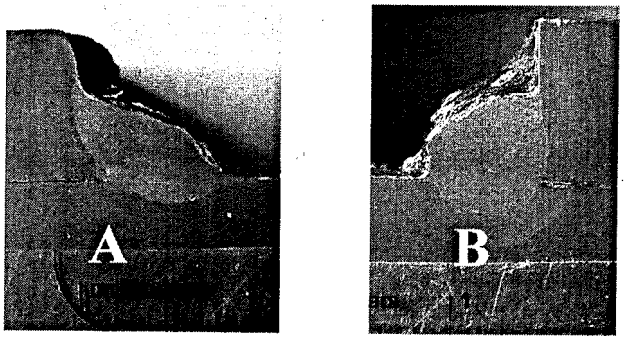

Figure 8.30: Polished Sections from Specimen T-5

Section A has three slag inclusions, and it also has a vertical crack with a length on the order of 1/16-in. and small non-fused segment at its root (Figure 8.31). Additionally, there is a micro-crack in the HAZ of section A, seen in Figure 8.32, which shows the micro-crack located in the HAZ. This micro-crack is perhaps related to the introduction of moisture into the weld through surface wetness which may have contributed to cracking in the hardened HAZ. Section B has a convex profile and no notable discontinuities.

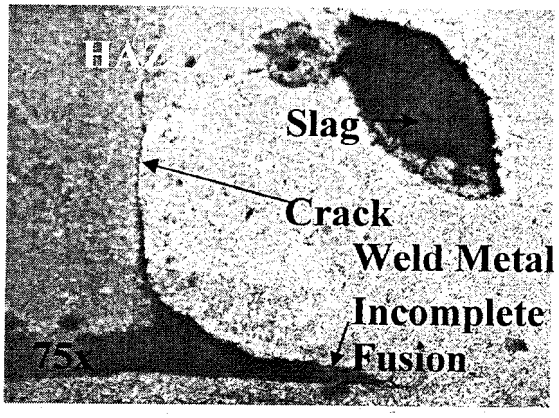

Figure 8.31: Vertical Crack, Non-fused Root- Specimen T-5, Section A

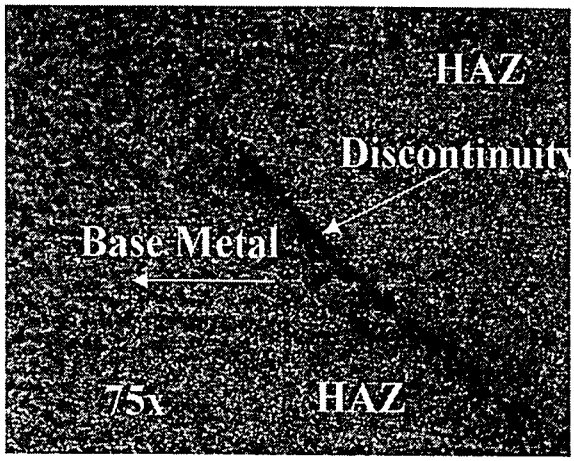

Figure 8.32: HAZ Discontinuity in Specimen T-5, Section A

The failed specimen is shown in Figure 8.33.

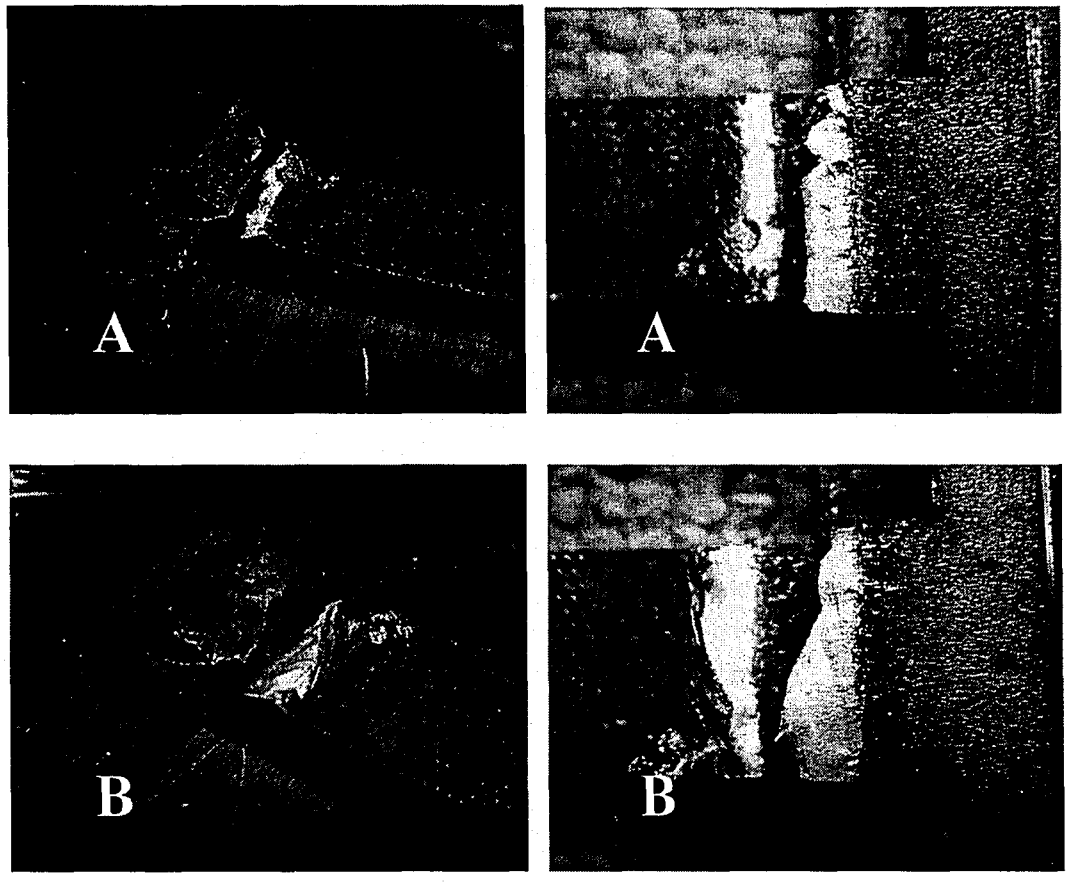

Figure 8.33: Specimen T-5 Failure Surfaces

The fracture occurred through the weld metal of both welds, and the measured strength was 35.05 kips. The P_{est} was 32.27 kips, and the ratio of the measured strength to P_{est} was 1.09.

Fracture surface B in Figure 8.33 has a very irregular geometry, which is a result of the varying throat dimension along its length. Because the throat dimension varied, the fracture surface did not occur through a single plane.

Failure surface A in Figure 8.33 has roughly 12 pores along its root and throughout the fracture surface, including two long parallel piping pores shown in greater detail in Figure 8.34.

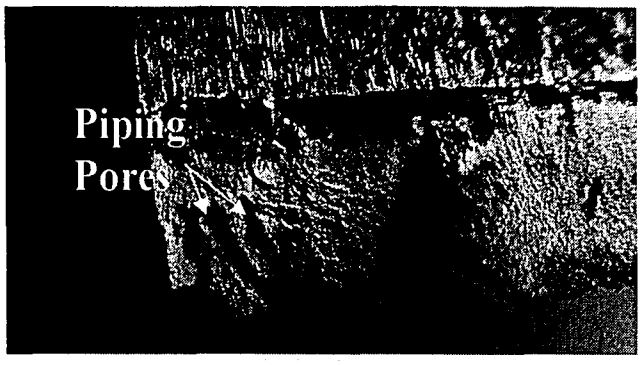

Figure 8.34: Piping Pores in Specimen T-5-Surface A

The bottom fracture surface of Figure 8.33, Surface B, has five pores and several additional voids which had been occupied by slag inclusions. The high number of pores is likely related to the application of surface wetness to the plates prior to welding.

The significant amount of porosity resulting from the surface wet conditions did not appear to have reduced the strength of the weld significantly since the measured failure load was approximately 9% larger than the predicted failure load. The strength prediction using the estimated weld metal ultimate tensile stress was accurate to within 9%.

8.3 Discussion of Test Results

The strength of the fillet welds were accurately predicted using the AISC strength equation (Equation 5) for fillet welds loaded in transverse shear. As discussed, the equation provided an accurate estimate of strength when the estimated weld metal ultimate tensile stress and weld dimensions were used. When the nominal weld metal ultimate tensile stress was used with the measured dimensions, the equation provided a very conservative estimate of capacity. Weld metal compositions are developed to meet minimum tensile stress requirements over a range of electrode sizes and resulting weld deposit sizes. Smaller welds will exhibit higher ultimate

tensile stress as compared to larger welds. The weld metal ultimate tensile stress of a small fillet weld is therefore significantly higher than the nominal weld metal ultimate tensile stress.

The variation in the ratio of measured strength to P_{est} among the specimens is likely a function of material variations and of the technique used to measure the throat dimension of the specimens. The throat dimension was taken as the minimum throat dimension of the weld metal, measured using a digital caliper on a cross section of a discarded portion of weld from the tested specimen. In the case of specimens T-4 and T-5, the throat dimension had a greater variation along the one inch weld length, and the minimum throats measured at each end of the weld were averaged to obtain the "minimum" throat dimension for the calculation of the predicted strengths. However, the failure surfaces were not simple planes through the weld metal at the minimum throat dimension, but were rather three-dimensional failure surfaces that were affected by changes in profile along the one inch weld length. The relative differences in the ratio of measured-to-predicted strength between specimens do not, however, appear to be related to loss of strength from the discontinuities observed on the fracture surfaces.

The failure loads calculated using nominal weld metal ultimate tensile stress were conservative for all measured specimen failure loads. The level of conservatism ranged from 22% to 41%, and this would be further increased by the use of the strength reduction factor, φ, from the LRFD method of design, which is 0.75 when calculating the design strength of fillet welds.[28] The weld shear strength would range from 1.62 to 1.88 times greater than the factored nominal strength based on the AISC equation, the nominal weld metal ultimate tensile stress, and the measured weld throat dimensions and lengths, and the strength reduction factor, as seen in Table 8-4.

Table 8-4: Phase 2 Results Comparison to AISC Code					
ID	P_{nom} (based on F_{nom}) [kips]	Factored Design Capacity (φP_{nom}) [kips]	Measured Failure Load [kips]	Ratio Measured / P_{nom}	Ratio Measured / φP_{nom}
T-1	23.44	17.58	33.10	1.41	1.88
T-2	26.87	20.15	33.80	1.26	1.68
T-3	32.37	24.28	42.80	1.32	1.76
T-4	24.82	18.62	30.20	1.22	1.62
T-5	26.33	19.75	35.05	1.33	1.77

9 Findings and Conclusions

The findings and conclusions of the investigation are presented in this chapter. The findings of the study are organized according to the three types of base metal plates used in the welding study, and additional findings are given based on the strength tests. Finally, conclusions related to each of the environmental conditions evaluated in the test program are given.

The findings and conclusions are limited by the scope of the research study and should not be extended outside the ranges of the variables that were examined. The study included:

- 1/4-in fillet welds made with the SMAW process on A36 steel.
- Low hydrogen (E7018-H4R) electrodes for weld made on A36 steel.
- 3/16-in. fillet welds made with the SMAW process for welds made on type 304 stainless steel.
- E308-16 electrodes for welds made on type 304 stainless steel.
- Plate thicknesses equal to or less than 3/8-in.
- Plate sizes typical of precast connections on the order of 4-in. x 6in.
- Statically loaded conditions.

9.1 Findings for Welds on A36 Steel

The findings with regard to welds made on the non-galvanized A36 Steel are:

- Higher wind speeds tend to produce poorer weld profiles.
- Higher wind speeds increase the presence and severity of slag inclusions, but the slag inclusions do not exceed AWS acceptability limits.

- Undercut was observed in several specimens but does not appear to be correlated strongly with a specific environmental parameter. All observed undercut was within the AWS limit of 1/32-in.

- Porosity increases when the electrodes are exposed to a moist environment beyond the AWS D1.1 code limit (a 9 hour limit on exposure to a moist environment).

- Surface porosity was not significantly increased by welding through surface wetness. This does not imply that the practice of welding through surface wetness results in sound welds. Welding through surface wetness has the *potential* to increase micro-cracking and create visible cracking and should be further investigated. Furthermore, substantial subsurface porosity was observed in the case of the surface wet Phase 2 specimen, T-5. This level of porosity did not reduce the strength of the specimen, but the presence of subsurface pores was not investigated for this specimen using the sectioning procedure because the specimen was subjected to strength testing.

- Micro-cracking was widely observed and was more prevalent in specimens welded using higher carbon plate material. The presence of micro-cracks in A36 steel specimens was not correlated with environmental conditions.

- Extended restraint of plates resulted in micro-cracks at the toe of a few welds. Depending on the loading conditions, these micro-cracks could propagate.

9.2 Findings for Welds on A36 Galvanized Steel

The findings with regard to welds made on galvanized A36 steel are:

- The profiles of welds made on galvanized A36 steel tend to have a higher rate of unacceptability, possibly due to arc instability and poor welder vision caused by smoke generated when welding through the zinc coating.
- Poor fit-up of plates as a result of the rough galvanized surface can contribute to root cracks where large plate gaps exist.
- Micro-cracking was observed more often for galvanized specimens as compared to non-galvanized specimens.
- Very few discontinuities were observed in the sections of welds made on galvanized A36 steel, indicating that the galvanized coating does not cause a significant increase in porosity or slag inclusions.

9.3 Findings for Welds on Type 304 Stainless Steel

The findings with regard to the welds made on Type 304 stainless steel are:

- The profiles of welds made on stainless steel plate, although concave, are generally of higher quality and uniformity than those made on carbon steel plate.
- Surface porosity was more widely observed in welds made on stainless steel plate than on carbon steel plate, but this porosity was at an acceptable level.
- Few micro-cracks were observed in stainless steel specimens, and the micro-cracking behavior does not appear to be correlated with any environmental parameter.

9.4 Findings from Phase 2 Tests

Findings from the destructive tensile test conducted in Phase 2 are:

- The transverse shear strength of fillet welds made with the SMAW process is accurately predicted using the AISC formulation, using an estimate of the actual ultimate tensile stress of the weld metal, as approximated using Rockwell B hardness testing.
- Discontinuities of the size and shape observed in the specimens did not have a significant impact on the weld strength.
- Failure loads predicted using the AISC codified expression for fillet weld strength are conservative based on the failure loads measured in the study. This is attributed to the higher ultimate tensile stress of the weld metal compared to the nominal weld metal ultimate tensile stress used in the codified expression.

9.5 Conclusions

The following conclusions are derived from the results of both phases of testing and relate to the impact of environmental conditions on the quality of welds simulating the welds used in precast construction.

- **Humidity**-Ambient humidity did not appear to be correlated with the presence of weld discontinuities. High humidity increases the presence of hydrogen in the vicinity of the weld; however, it was not found to impact the quality of the welds. The exposure of electrodes to humid conditions, however, did impact weld quality, increasing the potential for porosity and cracking. The guidelines and restrictions set out in AWS D1.1 should be closely followed.
- **Surface Wetness**-Welds made on surface wet plates did not exhibit a greater amount of surface porosity. The moisture appeared to be driven away from the weld joint as the weld was deposited. A thorough investigation of subsurface

porosity on these welds was not made. Welding through surface wetness also has the *potential* to increase micro-cracking and create visible cracking and should be further investigated. The impact of moisture in the form of falling rain entering the weld pool was not studied, and this condition should be examined further. Until such research is performed, it is recommended that welding not be performed when the weld pool is subject to falling precipitation and, whenever possible, that surface moisture be eliminated from the plate surfaces before welding.

- **Temperature**-Cold temperatures were examined and found to have no impact on porosity or slag inclusions. Cold temperatures have a tendency to increase cooling rates which increase the propensity for high hardness and crack formation. The hardness levels measured in the specimens, however, were below a level that would increase the propensity for cracking. Micro-cracks were observed in welds made over a variety of temperatures and are perhaps more sensitive to base metal composition, restraint, and hydrogen present than the ambient temperature during welding.

- **Wind**-High wind had a negative impact on the profile and surface geometry of the welds and tended to increase the presence of slag inclusions. The amount of slag included, however, was below AWS limits. In addition, successful SMAW welds were made in wind up to 35 mph. If the correct weld profile and good weld surface conditions can be achieved by a welder in a high wind condition, than welding should be permitted. The resulting profile must be verified in accordance with the details set forth in AWS D1.1.

- **Strength**-The welds which were tested in strength performed adequately and predictably. There was no appreciable reduction in strength for welds exhibiting discontinuities of the type and severity seen in the first phase of testing and examination. Design codes are conservative with regard to their prediction of strength for 1/4-in. fillet field welds made with the SMAW process.

10 Recommendations

The research study examined field welded connections used in precast concrete construction. Recommendations for allowable welding practice are presented in this chapter, but it is noted that the following recommendations are limited by the scope of the research study and should not be extended outside of the range of the variables that were examined. The study included:

- 1/4-in fillet welds made with the SMAW process on A36 steel.
- Low hydrogen (E7018-H4R) electrodes for welds made on A36 steel.
- 3/16-in. fillet welds made with the SMAW process on Type 304 stainless steel.
- E308-16 electrodes for welds made on type 304 stainless steel.
- Plate thicknesses equal to or less than 3/8-in.
- Plate sizes typical of precast connections on the order of 4-in. x 6in.
- Statically loaded conditions.

10.1 Recommendations for Welding on A36 Steel Plates in Precast Concrete Construction

Based on the results presented in this report, ¼-in. fillet welds made on 3/8-in. thick A36 plate using E7018-H4R electrodes can be performed under any of the following environmental conditions as long as the welder is able to create a weld meeting the AWS profile requirements. The allowable environmental conditions include:

- In wind up to 35MPH in the vicinity of the weld.
- In an ambient temperature of 0°F and above without preheat.
- In high humidity conditions up to 100% relative humidity.

SMAW electrodes should be stored, handled, and used in accordance with the manufacturer guidelines and AWS D1.1 requirements. Failure to follow these requirements may result in excess porosity and crack formation in the weld. Welding through surface wetness has the *potential* to increase micro-cracking and subsurface porosity and create visible cracking and should be further investigated. It is not recommended to perform welds when water from precipitation can enter the weld pool without further investigation.

All of these conditions will have a direct impact on the welder and may decrease his/her ability to successfully deposit a weld. Furthermore, skill level varies between welders; therefore it is imperative that the welder operate within their abilities. This may require the fabrication of a wind shield or covered structure in certain environmental conditions.

10.2 Recommendations for Welding on A36 Galvanized Steel Plates During Precast Concrete Construction

Based on the limited results obtained in the study with respect to galvanized welds, it is not recommended that field welds be made through galvanized coatings on A36 plate. A higher potential for micro-cracking was found to be present in galvanized welds, and one significant macro-crack was observed in a galvanized specimen. As a result of the impact galvanization has on profile and cracking, no recommendation is made in this study for welding through hot-dip galvanized coatings. Further studies should be conducted with a focus on galvanized plate with proper safety precautions taken. Until further studies are completed, it is recommended that the procedures suggested by the American Galvanizers Association be followed; namely, the removal of galvanizing 1-in. to 4-in. away from the weld joint prior to welding.

10.3 Recommendations for Welding on Type 304 Stainless Steel Plate During Precast Concrete Construction

Based on the results presented in this report, 3/16-in. fillet welds made on 3/8-in. thick type 304 stainless steel plate using E308-16 electrodes can be performed under any of the following environmental conditions as long as the welder is able to create a weld meeting the AWS profile requirements. The allowable environmental conditions include:

- In wind up to 35MPH in the vicinity of the weld.
- In an ambient temperature of 0°F and above without preheat.
- In high humidity conditions up to 100% relative humidity.

Electrodes should be stored, handled, and used in accordance with the manufacturer guidelines and AWS D1.6 requirements. Failure to abide by these requirements may result in excess porosity in the welds. A recommendation cannot be made regarding welding through surface wetness on stainless steel plates until the issue is further investigated.

All of these conditions will have a direct impact on the welder and may decrease his/her ability to successfully deposit a weld. Furthermore, skill level varies between welders; therefore it is imperative that the welder operate within their abilities. This may require the fabrication of a wind shield or covered structure in certain environmental conditions.

10.4 Recommendations for Future Work

The results presented in this study are the product of a very broad investigation of the impact of environmental conditions on weld quality and strength. In addition to the many combinations of environmental parameters investigated, moist electrodes were also tested. Additional variability was introduced as a result of the necessity to weld in a controlled environmental

chamber, which resulted in visibility problems under certain conditions. Furthermore, the process of welding itself is highly dependent on the welder, and variability between welds was necessarily introduced as a result of using a human welder as opposed to a machine-welding process, which was not possible within a controlled environmental chamber.

As a result of the broad extent of the study, it is recommended that additional, narrowly focused studies be carried out on a few specific issues in order to generate a larger data set for a given condition. The data from focused studies would allow for statistical analysis and more quantitative conclusions. This was difficult to achieve with the data from the current study as a result of the number of variables investigated.

Some of the issues which deserve further investigation include:

- the impact of surface wetness and falling water from precipitation on the cracking and porosity of welds made on carbon steels and stainless steels
- the impact of wind and moisture on arc stability in the SMAW process
- welding methods for galvanized steel which might reduce the excessive costs associated with grinding zinc coatings away but could be proven to produce sound welds safely
- investigation of the impact of specific discontinuities on the strength of welds made with the SMAW process in a larger strength test matrix
- the use of radiographic and other advanced NDE techniques to more thoroughly study overall weld quality when welds are exposed to temperature, wind, and moisture extremes.

11 References

[1] National Climatic Data Center, "Lowest Temperature of Record," Northeast Regional Climate Center, Cornell University, 2000.

[2] National Climatic Data Center. "Average Relative Humidity," Northeast Regional Climate Center, Cornell University, 2000.

[3] National Climatic Data Center. "Average Wind Speed," Northeast Regional Climate Center, Cornell University, 2000.

[4] AWS D1 Committee on Structural Welding. 2006. *Structural Welding Code—Steel (ANSI/AWS D1.1/D1.1M:2006)*. Miami, FL: AWS.

[5] AWS Committee on Structural Welding. 1999. *Structural Welding Code—Stainless Steel(ANSI/AWS D1.6:1999)*. Miami, FL: AWS.

[6] American Petroleum Institute (API), *Welded Steel Tanks for Oil Storage, 7th ed.* American Petroleum Institute, Washington, D.C. 1980.

[7] Sperko Engineering Services, Inc., *Welding Galvanized Steel—Safely,* 1999.

[8] PCI Industry Handbook Committee. *PCI Design Handbook, 6th ed.* Precast/Prestressed Concrete Institute, Chicago, IL, 2004.

[9] The Lincoln Electric Company, *The Procedure Handbook of Arc Welding, 14th ed.* Cleveland, Ohio, 1999.

[10] Precast/Prestressed Concrete Institute, *Design and Typical Details of Connections for Precast and Prestressed Concrete, Second ed.*, MNL-123-88, Chicago, IL, 1988.

[11] American Welding Society, *Safety and Fact Health Sheet No. 25-Metal Fume Fever,* AWS, January 2002.

[12] American Galvanizers Association. *Welding and Hot-Dip Galvanizing,* Englewood, CO, 2002.

[13] Bland, Jay, and AWS Technical Department., *Welding Zinc-Coated Steel(AWS WZC/D19.0-72),* American Welding Society, Miami, FL, 1972.

[14] Precast/Prestressed Concrete Institute., "Survey Results on the Use of Galvanizing for Precast Concrete Structures," *PCI Journal*, pp. 106-110, July-August, 2006.

[15] TWI World Centre for Materials Joining Technology, *"A general review of geometric shape imperfections-types and causes,"* TWI Ltd., 2003. < http://www.twi.co.uk/j32k/protected/band_3/jk67.html>.

[16] Conner, Leonard P. 1987. *Welding Handbook: Welding Technology, Eighth Edition,* Vol. 1. Miami, FL: American Welding Society.

[17] Lundin, C.D. *Fundamentals of Weld Discontinuities and Their Significance.* Welding Research Council, Bulletin 295, New York, NY. June 1984.

[18] Masi, O. and Erra, A., "Weld Radiography Correlation Between Defects and Static and Fatigue Strength," *Met. It.,* **45** (8), 273-83, Aug. 1953. In Italian.

[19] Kihara, H., Tuda, Y. Watanabe, M., and Ishii, Y., "Non-Destructive Testing of Welds and their Strength," *Soc. Naval Arch. Jpn.,* **7** (1960).

[20] Ishii, Y., Kihara, H., and Tuda, Y., "On the Relation Between the Non-Destructive Testing Information of Steel Welds and their Mechanical Strength," *J. Non-Destr. Test. (Japan),* **16** (8) (1967). IIW Doc XIII-466-67.

[21] Green, W.L., Hamad, M.F., and McCauley, R.B., "The Effects of Porosity on Mild-Steel Welds," *Welding Journal Supplement,* **37** (5), 206s-209s, May 1958.

[22] Bradley, J.W. and McCauley, R.B., "The Effects of Porosity in Quenched and Tempered Steel," *Welding Journal Supplement,* **43** (9), 4086s-14s, Sept. 1964.

[23] Stephanov, A.A. and Kurkin, S.A., "Effects of Pores in Longitudinal Welds on the Strength of Thin-Walled Cylindrical Vessels Made of SP-28 Steel," *Svar. Proizv.,* **18** (7), 25-27, July 1971.

[24] Norrish, J. and Moore, D.C., "Porosity in Arc Welds and its Effect on Mechanical Properties," Significance of Weld Defects, Proc. Of 2nd Conf., May 1968—Welding Institute.

[25] Lundin, C.D. *The Significance of Weld Discontinuities-A Review of Current Literature.* Welding Research Council Bulletin 222, WRC.

[26] TWI World Centre for Materials Joining Technology, *"Defects-hydrogen cracks in steel-identification,"* TWI Ltd., 2006. < http://www.twi.co.uk/j32k/protected/band_3/jk45.html>.

[27] American Society for Testing and Materials. *Annual Book of ASTM Standards 2000: Section One-Iron and Steel Products, Volume 01.04-Steel: Structural, Reinforcing, Pressure Vessel, Railway.* ASTM. West Conshohocken, PA. 2000.

[28] AISC Committee on Manuals and Textbooks. *Steel Construction Manual,* Thirteenth Edition. American Institute of Steel Construction, Inc. 2005.

[29] Lowenburg, A. L., Norris, E.B., and Whiting, A.R., "Evaluation of Discontinuities in Pipeline Weld Joints—Summary Report No. 1," Pres. Ves. Res. Comm. Of WRC, Nov. 15, 1968.

[30] TWI World Centre for Materials Joining Technology, *Weldability of Materials,* TWI Ltd., 2004. <http://www.twi.co.uk/j32k/protected/band_3/jk20.html>.

[31] TWI World Centre for Materials Joining Technology, *Defects/Imperfections in Welds-Porosity,,* TWI Ltd., 2004. < http://www.twi.co.uk/j32k/protected/band_3/jk42.html>.

12 Vita

Jason A. Zimpfer was born on June 17. 1985 in Allentown, Pennsylvania. He is the son of Keith and Linda Zimpfer. Jason is married to Kelly L. Zimpfer, who graduated from Messiah College in May 2006. Jason earned his Bachelor of Science degree in Civil Engineering at Lehigh University in Bethlehem, Pennsylvania in May 2006. Jason was the recipient of the John B. Carson Prize in Civil Engineering in the class of 2006 at Lehigh University. After receiving his undergraduate degree, Jason began a year of graduate studies through the Presidential Scholar program at Lehigh University to pursue a Master of Science degree in Structural Engineering. Jason will receive his degree in September 2007. After graduation, Jason and his wife plan to travel to Zambia for a year and a half of teaching and mission work. Upon return to the United States, Jason plans to pursue a career in structural engineering with a design firm in the Northeast.

END OF TITLE